# RUSSIAN TECHNOLOGICAL JOURNAL

РОССИЙСКИЙ ТЕХНОЛОГИЧЕСКИЙ ЖУРНАЛ



Information systems.
Computer sciences.
Issues of information security

Multiple robots (robotic centers) and systems. Remote sensing and non-destructive testing

Modern radio engineering and telecommunication systems

Micro- and nanoelectronics. Condensed matter physics

Analytical instrument engineering and technology

Mathematical modeling

Economics of knowledge-intensive and high-tech enterprises and industries. Management in organizational systems

Product quality management. Standardization

Philosophical foundations of technology and society





# RUSSIAN TECHNOLOGICAL JOURNAL

### РОССИЙСКИЙ ТЕХНОЛОГИЧЕСКИЙ ЖУРНАЛ

- Information systems. Computer sciences. Issues of information security
- Multiple robots (robotic centers) and systems. Remote sensing and non-destructive testing
- Modern radio engineering and telecommunication systems
- Micro- and nanoelectronics. Condensed matter physics
- Analytical instrument engineering and technology
- Mathematical modeling
- Economics of knowledge-intensive and high-tech enterprises and industries.
   Management in organizational systems
- Product quality management.
   Standardization
- Philosophical foundations of technology and society

- Информационные системы. Информатика. Проблемы информационной безопасности
- Роботизированные комплексы и системы.
   Технологии дистанционного зондирования и неразрушающего контроля
- Современные радиотехнические и телекоммуникационные системы
- Микро- и наноэлектроника. Физика конденсированного состояния
- Аналитическое приборостроение и технологии
- Математическое моделирование
- Экономика наукоемких и высокотехнологичных предприятий и производств.
   Управление в организационных системах
- Управление качеством продукции.
   Стандартизация
- Мировоззренческие основы технологии и общества

Russian Technological Journal 2023, Vol. 11, No. 3

Russian Technological Journal 2023, Tom 11, № 3

https://www.rtj-mirea.ru



## Russian Technological Journal 2023, Vol. 11, No. 3

Publication date May 31, 2023.

The peer-reviewed scientific and technical journal highlights the issues of complex development of radio engineering, telecommunication and information systems, electronics and informatics, as well as the results of fundamental and applied interdisciplinary researches, technological and economical developments aimed at the development and improvement of the modern technological base.

Periodicity: bimonthly.

The journal was founded in December 2013. The titles were «Herald of MSTU MIREA» until 2016 (ISSN 2313-5026) and «Rossiiskii tekhnologicheskii zhurnal» from January 2016 until July 2021 (ISSN 2500-316X).

#### Founder and Publisher:

Federal State Budget Educational Institution of Higher Education «MIREA – Russian Technological University» 78, Vernadskogo pr., Moscow, 119454 Russia.

The journal is included into the List of peer-reviewed science press of the State Commission for Academic Degrees and Titles of Russian Federation. The Journal is included in Russian State Library (RSL), Russian Science Citation Index, eLibrary, Socionet, Directory of Open Access Journals (DOAJ), Directory of Open Access Scholarly Resources (ROAD), Google Scholar, Ulrich's International Periodicals Directory.

### **Editor-in-Chief:**

Alexander S. Sigov, Academician at the Russian Academy of Sciences, Dr. Sci. (Phys.—Math.), Professor, President of MIREA – Russian Technological University (RTU MIREA), Moscow, Russia.

Scopus Author ID 35557510600, ResearcherID L-4103-2017, sigov@mirea.ru.

### **Editorial staff:**

Managing Editor Cand. Sci. (Eng.) Galina D. Seredina Scientific Editor Dr. Sci. (Eng.), Prof. Gennady V. Kulikov Executive Editor Anna S. Alekseenko Darya V. Trofimova

86, Vernadskogo pr., Moscow, 119571 Russia. Phone: +7 (499) 600-80-80 (#31288). E-mail: seredina@mirea.ru.

The registration number ΠИ № ФС 77 - 81733 was issued in August 19, 2021 by the Federal Service for Supervision of Communications, Information Technology, and Mass Media of Russia.

The subscription index of Pressa Rossii: 79641.

## Russian Technological Journal 2023, Tom 11, № 3

Дата опубликования 31 мая 2023 г.

Научно-технический рецензируемый журнал освещает вопросы комплексного развития радиотехнических, телекоммуникационных и информационных систем, электроники и информатики, а также результаты фундаментальных и прикладных междисциплинарных исследований, технологических и организационно-экономических разработок, направленных на развитие и совершенствование современной технологической базы.

Периодичность: один раз в два месяца. Журнал основан в декабре 2013 года. До 2016 г. издавался под названием «Вестник МГТУ МИРЭА» (ISSN 2313-5026), а с января 2016 г. по июль 2021 г. под названием «Российский технологический журнал» (ISSN 2500-316X).

### Учредитель и издатель:

федеральное государственное бюджетное образовательное учреждение высшего образования «МИРЭА – Российский технологический университет» 119454, РФ, г. Москва, пр-т Вернадского, д. 78.

Журнал входит в Перечень ведущих рецензируемых научных журналов ВАК РФ, в которых должны быть опубликованы основные научные результаты диссертаций на соискание ученой степени кандидата наук и доктора наук, индексируется в РГБ, РИНЦ, eLibrary, Coционет, Directory of Open Access Journals (DOAJ), Directory of Open Access Scholarly Resources (ROAD), Google Scholar, Ulrich's International Periodicals Directory.

### Главный редактор:

Сигов Александр Сергеевич, академик РАН, доктор физ.-мат. наук, профессор, президент ФГБОУ ВО МИРЭА – Российский технологический университет (РТУ МИРЭА), Москва, Россия. Scopus Author ID 35557510600, ResearcherID L-4103-2017, sigov@mirea.ru.

### Редакция:

Зав. редакцией к.т.н. Г.Д. Середина Научный редактор д.т.н., проф. Г.В. Куликов Выпускающий редактор А.С. Алексеенко Технический редактор Д.В. Трофимова 119571, г. Москва, пр-т Вернадского, 86, оф. Л-119.

Тел.: +7 (499) 600-80-80 (#31288). E-mail: seredina@mirea.ru.

Регистрационный номер и дата принятия решения о регистрации СМИ ПИ № ФС 77 - 81733 от 19.08.2021 г. СМИ зарегистрировано Федеральной службой по надзору в сфере связи, информационных технологий и массовых коммуникаций (Роскомнадзор).

Индекс по объединенному каталогу «Пресса России» 79641.

### **Editorial Board**

Dr. Sci. (Eng.), Professor, Rector of RTU MIREA, Moscow, Russia. Scopus Author ID Stanislav A. Kudzh 56521711400, ResearcherID AAG-1319-2019, https://orcid.org/0000-0003-1407-2788, rector@mirea.ru Habilitated Doctor of Sciences, Professor, Vice-Rector of Vilnius University, Vilnius, Lithuania. **Juras Banys** 

Scopus Author ID 7003687871, juras.banys@ff.vu.lt

Academician at the Russian Academy of Sciences (RAS), Dr. Sci. (Phys.-Math.), Professor, Vladimir B. Betelin Supervisor of Scientific Research Institute for System Analysis, RAS, Moscow, Russia. Scopus

Author ID 6504159562, ResearcherID J-7375-2017, betelin@niisi.msk.ru

Dr. Sci. (Phys.-Math.), Senior Research Fellow, Department of Chemistry and 4D LABS, Simon Alexei A. Bokov Fraser University, Vancouver, British Columbia, Canada. Scopus Author ID 35564490800, ResearcherID C-6924-2008, http://orcid.org/0000-0003-1126-3378, abokov@sfu.ca

Dr. Sci. (Phys.-Math.), Professor, Head of the Laboratory of Neutron Research, A.F. loffe Sergey B. Vakhrushev Physico-Technical Institute of the RAS, Department of Physical Electronics of St. Petersburg Polytechnic University, St. Petersburg, Russia. Scopus Author ID 7004228594, ResearcherID

A-9855-2011, http://orcid.org/0000-0003-4867-1404, s.vakhrushev@mail.ioffe.ru

Yury V. Gulyaev Academician at the RAS, Dr. Sci. (Phys.-Math.), Professor, Supervisor of V.A. Kotelnikov Institute of Radio Engineering and Electronics of the RAS, Moscow, Russia. Scopus Author ID

35562581800, gulyaev@cplire.ru

Dr. Sci. (Eng.), Professor, Head of the Department of Intelligent Technologies and Systems, **Dmitry O. Zhukov** RTU MIREA, Moscow, Russia. Scopus Author ID 57189660218, zhukov do@mirea.ru

PhD (Phys.-Math.), Professor, Radboud University, Nijmegen, Netherlands, Scopus Author ID

Alexey V. Kimel 6602091848, ResearcherID D-5112-2012, a.kimel@science.ru.nl

Dr. Sci. (Phys.-Math.), Professor, Surgut State University, Surgut, Russia. Scopus Author Sergey O. Kramarov ID 56638328000, ResearcherID E-9333-2016, https://orcid.org/0000-0003-3743-6513,

mavoo@yandex.ru

Academician at the RAS, Dr. Sci. (Eng.), Director of V.A. Trapeznikov Institute of Control **Dmitry A. Novikov** Sciences, Moscow, Russia. Scopus Author ID 7102213403, ResearcherID Q-9677-2019,

https://orcid.org/0000-0002-9314-3304, novikov@ipu.ru

Philippe Pernod Dr. Sci. (Electronics), Professor, Dean of Research of Centrale Lille, Villeneuve-d'Ascq, France,

Scopus Author ID 7003429648, philippe.pernod@ec-lille.fr

Dr. Sci. (Eng.), Professor, Director of the Institute of Artificial Intelligence, RTU MIREA, Mikhail P. Romanov Moscow, Russia. Scopus Author ID 14046079000, https://orcid.org/0000-0003-3353-9945,

m romanov@mirea.ru

Viktor P. Savinykh Academician at the RAS, Dr. Sci. (Eng.), Professor, President of Moscow State University of

Geodesy and Cartography, Moscow, Russia. Scopus Author ID 56412838700, vp@miigaik.ru

Professor, Dr. Sci. (Phys.-Math.), Director of Institute for Information Transmission Problems Andrei N. Sobolevski (Kharkevich Institute), Moscow, Russia. Scopus Author ID 7004013625, ResearcherID

D-9361-2012, http://orcid.org/0000-0002-3082-5113, sobolevski@iitp.ru

Li Da Xu Academician at the European Academy of Sciences, Russian Academy of Engineering

(formerly, USSR Academy of Engineering), and Armenian Academy of Engineering, Dr. Sci. (Systems Science), Professor and Eminent Scholar in Information Technology and Decision Sciences, Old Dominion University, Norfolk, VA, the United States of America. Scopus Author

ID 13408889400, https://orcid.org/0000-0002-5954-5115, lxu@odu.edu

Yury S. Kharin Academician at the National Academy of Sciences of Belarus, Dr. Sci. (Phys.-Math.), Professor, Director of the Institute of Applied Problems of Mathematics and Informatics of the Belarusian

State University, Minsk, Belarus. Scopus Author ID 6603832008, http://orcid.org/0000-0003-

4226-2546, kharin@bsu.by

Yuri A. Chaplygin Academician at the RAS, Dr. Sci. (Eng.), Professor, Member of the Departments of

Nanotechnology and Information Technology of the RAS, President of the National Research University of Electronic Technology (MIET), Moscow, Russia. Scopus Author ID 6603797878,

ResearcherID B-3188-2016, president@miet.ru

Cand. Sci. (Econ.), Deputy Minister of Industry and Trade of the Russian Federation, Ministry of Vasilii V. Shpak Industry and Trade of the Russian Federation, Moscow, Russia; Associate Professor, National

Research University of Electronic Technology (MIET), Moscow, Russia, mishinevaiv@minprom.gov.ru

### Редакционная коллегия

Кудж

Станислав Алексеевич

Банис

Юрас Йонович

Бетелин

Владимир Борисович

Боков

Алексей Алексеевич

Вахрушев Сергей Борисович

Гуляев Юрий Васильевич

Жуков Дмитрий Олегович

Кимель Алексей Вольдемарович

Крамаров Сергей Олегович

Новиков Дмитрий Александрович

Перно Филипп

Романов Михаил Петрович

Савиных Виктор Петрович

Соболевский Андрей Николаевич

Сюй Ли Да

Харин Юрий Семенович

Чаплыгин Юрий Александрович

Шпак Василий Викторович д.т.н., профессор, ректор РТУ МИРЭА, Москва, Россия. Scopus Author ID 56521711400, ResearcherID AAG-1319-2019, https://orcid.org/0000-0003-1407-2788, rector@mirea.ru

хабилитированный доктор наук, профессор, проректор Вильнюсского университета, Вильнюс, Литва. Scopus Author ID 7003687871, juras.banys@ff.vu.lt

академик Российской академии наук (РАН), д.ф.-м.н., профессор, научный руководитель Федерального научного центра «Научно-исследовательский институт системных исследований» РАН, Москва, Россия. Scopus Author ID 6504159562, ResearcherID J-7375-2017, betelin@niisi.msk.ru

д.ф.-м.н., старший научный сотрудник, химический факультет и 4D LABS, Университет Саймона Фрейзера, Ванкувер, Британская Колумбия, Канада. Scopus Author ID 35564490800, ResearcherID C-6924-2008, http://orcid.org/0000-0003-1126-3378, abokov@sfu.ca

д.ф.-м.н., профессор, заведующий лабораторией нейтронных исследований Физикотехнического института им. А.Ф. Иоффе РАН, профессор кафедры Физической электроники СПбГПУ, Санкт-Петербург, Россия. Scopus Author ID 7004228594, Researcher ID A-9855-2011, http://orcid.org/0000-0003-4867-1404, s.vakhrushev@mail.ioffe.ru

академик РАН, д.ф.-м.н., профессор, научный руководитель Института радиотехники и электроники им. В.А. Котельникова РАН, Москва, Россия. Scopus Author ID 35562581800, gulyaev@cplire.ru

д.т.н., профессор, заведующий кафедрой интеллектуальных технологий и систем РТУ МИРЭА, Москва, Россия. Scopus Author ID 57189660218, zhukov\_do@mirea.ru

к.ф.-м.н., профессор, Университет Радбауд, г. Наймеген, Нидерланды. Scopus Author ID 6602091848, ResearcherID D-5112-2012, a.kimel@science.ru.nl

д.ф.-м.н., профессор, Сургутский государственный университет, Сургут, Россия. Scopus Author ID 56638328000, ResearcherID E-9333-2016, https://orcid.org/0000-0003-3743-6513, mavoo@yandex.ru

академик РАН, д.т.н., директор Института проблем управления им. В.А. Трапезникова РАН, Москва, Россия. Scopus Author ID 7102213403, ResearcherID Q-9677-2019, https://orcid.org/0000-0002-9314-3304, novikov@ipu.ru

Dr. Sci. (Electronics), профессор, Центральная Школа г. Лилль, Франция. Scopus Author ID 7003429648, philippe.pernod@ec-lille.fr

д.т.н., профессор, директор Института искусственного интеллекта РТУ МИРЭА, Москва, Россия. Scopus Author ID 14046079000, https://orcid.org/0000-0003-3353-9945, m romanov@mirea.ru

академик РАН, Дважды Герой Советского Союза, д.т.н., профессор, президент Московского государственного университета геодезии и картографии, Москва, Россия. Scopus Author ID 56412838700, vp@miigaik.ru

д.ф.-м.н., директор Института проблем передачи информации им. А.А. Харкевича, Москва, Россия. Scopus Author ID 7004013625, ResearcherID D-9361-2012, http://orcid.org/0000-0002-3082-5113, sobolevski@iitp.ru

академик Европейской академии наук, Российской инженерной академии и Инженерной академии Армении, Dr. Sci. (Systems Science), профессор, Университет Олд Доминион, Норфолк, Соединенные Штаты Америки. Scopus Author ID 13408889400, https://orcid.org/0000-0002-5954-5115, lxu@odu.edu

академик Национальной академии наук Беларуси, д.ф.-м.н., профессор, директор НИИ прикладных проблем математики и информатики Белорусского государственного университета, Минск, Беларусь. Scopus Author ID 6603832008, http://orcid.org/0000-0003-4226-2546, kharin@bsu.by

академик РАН, д.т.н., профессор, член Отделения нанотехнологий и информационных технологий РАН, президент Института микроприборов и систем управления им. Л.Н. Преснухина НИУ «МИЭТ», Москва, Россия. Scopus Author ID 6603797878, ResearcherID B-3188-2016, president@miet.ru

к.э.н., зам. министра промышленности и торговли Российской Федерации, Министерство промышленности и торговли РФ, Москва, Россия; доцент, Институт микроприборов и систем управления им. Л.Н. Преснухина НИУ «МИЭТ», Москва, Россия, mishinevaiv@minprom.gov.ru

### **Contents**

### Information systems. Computer sciences. Issues of information security

- Alexander S. Albychev, Stanislav A. Kudzh
- 7 Development of a research environment for the operational and computational architecture of central bank digital currency software
- Sergey O. Kramarov, Oleg R. Popov, Ismail E. Dzhariev, Egor A. Petrov Dynamics of link formation in networks structured on the basis of predictive terms

### Modern radio engineering and telecommunication systems

Gennady V. Kulikov, Xuan Khang Dang, Alexey G. Kulikov

Effect of synchronization system errors on the reception noise immunity of amplitude-phase shift keyed signals

### Micro- and nanoelectronics. Condensed matter physics

- Vladislav R. Bilyk, Kirill A. Brekhov, Mikhail B. Agranat, Elena D. Mishina Dispersion of optical constants of Si:PbGeO crystal in the terahertz range
  - Stanislav I. Sovetov, Sergey F. Tyurin
- 46 Method for synthesizing a logic element that implements several functions simultaneously

### **Mathematical modeling**

Alexander E. Alexandrov, Sergey P. Borisov, Ludmila V. Bunina, Sergey S. Bikovsky,

- 56 *Irina V. Stepanova, Andrey P. Titov*Statistical model for assessing the reliability of non-destructive testing systems by solving inverse problems
  - Eduard M. Kartashov
- **70** Developing generalized model representations of thermal shock for local non-equilibrium heat transfer processes
- Ivan G. Lebo
   Mathematical modeling of experiments on the interaction of a high-power ultraviolet laser pulse with condensed targets

### Philosophical foundations of technology and society

Nadezhda I. Chernova, Ekaterina A. Ivanova, Nadezhda B. Bogush,

104 Nataliya V. Katakhova

Technology for determining non-humanities university students' cognitive-andpsychological characteristics

### Содержание

### **Информационные системы. Информатика. Проблемы информационной** безопасности

А.С. Албычев, С.А. Кудж

**7** Среда исследований операционно-вычислительной архитектуры информационного обеспечения цифровой валюты центрального банка

С.О. Крамаров, О.Р. Попов, И.Э. Джариев, Е.А. Петров

**17** Динамика формирования связей в сетях, структурированных на основе прогностических терминов

### Современные радиотехнические и телекоммуникационные системы

Г.В. Куликов, С.Х. Данг, А.Г. Куликов

Влияние погрешностей системы синхронизации на помехоустойчивость приема сигналов с амплитудно-фазовой манипуляцией

### Микро- и наноэлектроника. Физика конденсированного состояния

В.Р. Билык, К.А. Брехов, М.Б. Агранат, Е.Д. Мишина

**38** Дисперсия оптических характеристик кристалла Si:PbGeO в терагерцовом диапазоне

С.И. Советов, С.Ф. Тюрин

**46** Метод синтеза логического элемента, реализующего несколько функций одновременно

### Математическое моделирование

А.Е. Александров, С.П. Борисов, Л.В. Бунина, С.С. Быковский,

И.В. Статистическая модель оценки надежности систем неразрушающего контроля на основе решения обратных задач

Э.М. Карташов

**70** Развитие обобщенных модельных представлений теплового удара для локально-неравновесных процессов переноса теплоты

И.Г. Лебо

Численное моделирование экспериментов по взаимодействию мощных ультрафиолетовых лазерных импульсов с конденсированными мишенями

### Мировоззренческие основы технологии и общества

Nadezhda I. Chernova, Ekaterina A. Ivanova, Nadezhda B. Bogush,

Nataliya V. Katakhova
Technology for determining non-humanities university students' cognitive-and-psychological characteristics

### Information systems. Computer sciences. Issues of information security Информационные системы. Информатика. Проблемы информационной безопасности

UDC 004 https://doi.org/10.32362/2500-316X-2023-11-3-7-16



### RESEARCH ARTICLE

### Development of a research environment for the operational and computational architecture of central bank digital currency software

Alexander S. Albychev <sup>1, 2, @</sup>, Stanislav A. Kudzh <sup>2</sup>

- <sup>1</sup> The Federal Treasury of the Ministry of Finance of the Russian Federation, Moscow, 101000 Russia
- <sup>2</sup> MIREA Russian Technological University, Moscow, 119454 Russia

### **Abstract**

**Objectives.** The development and implementation of information and computing architecture and information support for a state central bank digital currency (CBDC) is based on the selection of a software and hardware platform, including technologies and methods for supporting interaction between the elements of the computing complex. The implementation of CBDC technologies significantly depends both on the operational and computing architecture, as well as on the technological characteristics of the means for implementing digital currency information support, which determines the need to develop an appropriate research environment. Thus, the present study sets out to develop an infrastructure for the experimental research environment of the operational and computing architecture used to provide information support for the CBDC.

**Methods.** Digital technologies required for forming an CBDC implementation stack are under development in many countries of the world. The basis for the formation of a software and hardware complex for providing CBDC information support is comprised of theoretical and experimental studies into contemporary digital transaction management tools.

**Results.** The main architectural and technological components that make up the CBDC operational and computing environment comprise operational and computing architectures, blockchain technologies, consensus algorithms, and various forms of digital currencies. Five CBDC operational and computing architecture options are presented. Information models of interaction between the participants in transactions of the central bank digital currency were studied with the aim of establishing the effects of an architectural solution to the characteristics of the computing complex used to provide information support. Features of various digital currencies in the form of accounts and tokens were analyzed.

**Conclusions.** A research environment infrastructure for the CBDC operational and computing information support architecture has been developed. The prerequisites for a comprehensive analysis of the technological characteristics of the CBDC operational and computing environment are set out along with a comparison of operational and computing architecture variants. As a result of the analysis, a summary list of the characteristics of the studied architectures is drawn up. This provides for selecting the optimal operational and computing architecture depending on the requirements imposed on the CBDC.

**Keywords:** digital currency, central bank digital currency, blockchain, consensus algorithm, digital currency architecture

<sup>&</sup>lt;sup>®</sup> Corresponding author, e-mail: albychev@mirea.ru

• Submitted: 20.03.2023 • Revised: 14.04.2023 • Accepted: 20.04.2023

**For citation:** Albychev A.S., Kudzh S.A. Development of a research environment for the operational and computational architecture of central bank digital currency software. *Russ. Technol. J.* 2023;11(3):7–16. https://doi.org/10.32362/2500-316X-2023-11-3-7-16

Financial disclosure: The authors have no a financial or property interest in any material or method mentioned.

The authors declare no conflicts of interest.

### НАУЧНАЯ СТАТЬЯ

# Среда исследований операционно-вычислительной архитектуры информационного обеспечения цифровой валюты центрального банка

А.С. Албычев <sup>1, 2, @</sup>, С.А. Кудж <sup>2</sup>

### Резюме

**Цели.** Внедрение и разработка информационно-вычислительной архитектуры и информационного обеспечения цифровой валюты центрального банка (ЦВЦБ) страны основываются на выборе программно-аппаратной платформы, включая технологии и способы взаимодействия элементов вычислительного комплекса. Внедрение технологий ЦВЦБ существенно зависит как от операционно-вычислительной архитектуры, так и от технологических характеристик конкретной реализации информационного обеспечения цифровой валюты, что определяет необходимость разработки соответствующей среды исследований. Цель статьи – разработка инфраструктуры среды экспериментальных исследований операционно-вычислительной архитектуры информационного обеспечения ЦВЦБ.

**Методы.** Развитие цифровых технологий не сформировало стек реализации ЦВЦБ, а комплекс технологических реализаций находится в разработке во многих странах мира. Основой для формирования программно-аппаратного комплекса информационного обеспечения являются теоретические и экспериментальные исследования современных инструментов цифрового управления транзакциями.

**Результаты.** Рассмотрены архитектурные и технологические компоненты, составляющие операционновычислительную среду цифровой валюты центрального банка: операционно-вычислительные архитектуры, блокчейн-технологии, алгоритмы консенсуса, формы представления цифровых валют. Представлено 5 вариантов операционно-вычислительных архитектур ЦВЦБ. Проведено исследование информационных моделей взаимодействия участников транзакций ЦВЦБ, направленных на установление степени влияния архитектурного решения на характеристики вычислительного комплекса информационного обеспечения. Проанализированы особенности цифровых валют в форме аккаунтов и токенов.

**Выводы.** Разработана инфраструктура среды исследований операционно-вычислительной архитектуры информационного обеспечения ЦВЦБ. Созданы предпосылки для комплексного анализа технологических характеристик операционно-вычислительной среды ЦВЦБ. Проведен анализ вариантов операционно-вычислительных архитектур. В результате анализа сформирован сводный перечень характеристик приведенных архитектур. В зависимости от требований, предъявляемых к ЦВЦБ, на основе этого перечня может быть выбрана наиболее адекватная операционно-вычислительная архитектура.

<sup>1</sup> Федеральное казначейство Министерства финансов Российской Федерации, Москва, 101000 Россия

<sup>&</sup>lt;sup>2</sup> МИРЭА – Российский технологический университет, Москва, 119454 Россия

<sup>&</sup>lt;sup>®</sup> Автор для переписки, e-mail: albychev@mirea.ru

**Ключевые слова:** цифровая валюта, цифровая валюта центрального банка, блокчейн, алгоритм консенсуса, архитектура цифровой валюты

• Поступила: 20.03.2023 • Доработана: 14.04.2023 • Принята к опубликованию: 20.04.2023

**Для цитирования:** Албычев А.С., Кудж С.А. Среда исследований операционно-вычислительной архитектуры информационного обеспечения цифровой валюты центрального банка. *Russ. Technol. J.* 2023;11(3):7–16. https://doi.org/10.32362/2500-316X-2023-11-3-7-16

**Прозрачность финансовой деятельности:** Авторы не имеют финансовой заинтересованности в представленных материалах или методах.

Авторы заявляют об отсутствии конфликта интересов.

### INTRODUCTION

The development of modern financial, electronic payment, digital currency and blockchain technologies [1] has led to the prospect of sovereign states issuing digital currencies. Central bank digital currencies (CBDCs) are under consideration by a number of states as a new form of monetary representation alongside existing currencies [2, 3]. Such digital currencies, which are managed by a state central bank (CB), are issued in a 1:1 ratio to the national currency.

CBDC research focuses on various aspects of digital currencies [3, 4]. Some studies consider performance issues associated with technological support for digital currencies [5–7], i.e., the ability to process a certain number of financial transactions in a period of time. Others focus on the reliability of data storage [3, 7, 8], security against unauthorized digital currency transactions [4, 7, 9], as well as privacy [7, 9, 10], as among the key characteristics of a CBDC.

Blockchain technologies [5, 11] are used in digital currencies to ensure the authenticity of transaction history. Meanwhile, consensus algorithms [7, 12, 13] are required to prevent the unscrupulous behavior of one or more participants in the blockchain network. In other words, in the absence of a single source of trustworthy information, there is a need for a consensus algorithm to avoid this.

As a rule, studies explore two ways of the digital currency storing data: accounts and tokens [8, 9, 14–16]. The first form of data storage implies that the account owner has some number reflecting the current account balance; here, financial transactions consist of changing the corresponding number in the participants of the transaction. Although tokens are described in less detail, in general they can be represented as a bundle of a unique token identifier and denomination. Each token is assigned a current owner, for example, using a unique owner identifier. Financial transactions in this case consist of changing the unique owner ID for one or more tokens.

Studies [7, 14, 17] have noted that one of the main issues in the development of CBDC is the choice of operational and computational architecture. An operational and computational architecture describes the participants of the system that ensures the functioning

of a digital currency, as well as the connections between them. Some researchers use a different, broader term—CBDC design [5, 18]—which includes, among other things, details of the digital currency realization. When choosing the operational and computational architecture, it is important to consider both organizational requirements, such as the Know Your Customer (KYC) principle [6, 14, 19], along with the various technical aspects.

The aim of the article is to develop the infrastructure of the research environment of the operational and computational architecture of the information support of the central bank digital currency.

## 1. VARIANTS OF CBCD OPERATIONAL-COMPUTING ARCHITECTURE IMPLEMENTATION

Let us consider the variants of operational and computational architectures used to ensure the functioning of CBDC in terms of their advantages and disadvantages.

### 1.1. Centralized two-level architecture

As the simplest option in terms of architecture, we can consider a centralized two-level architecture, where the only organization that ensures the functioning of CBDC will be the CB (Fig. 1).

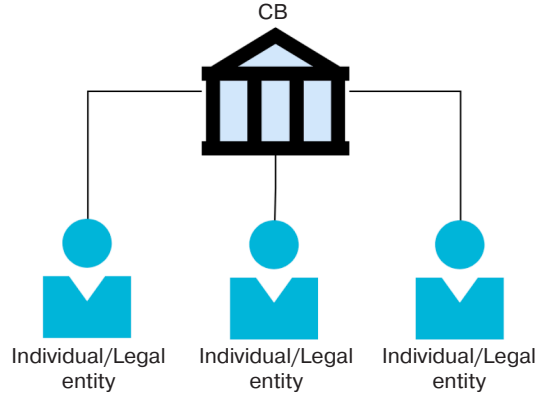


Fig. 1. Diagram of a centralized two-level CBDC architecture

In such a CBDC implementation variant, the only source of reliable information on the movement and ownership of funds is the CB, which also carries out all technological support. The CB performs both the issuance of digital currency and the processing of transactions. The advantages of this option include:

- 1) ease of implementation, since there is no need to coordinate the work of several organizations;
- 2) minimization of delays in transactions due to the absence of intermediaries;
- 3) the CB has a real-time access to all data.

However, this operational and computational architecture has significant disadvantages:

- 1) all technical support for CBDC must be provided by a single issuer—the CB;
- 2) organizational support of CBDC is also fully entrusted to the CB (e.g., compliance with the KYC principle).

With such an operational and computational architecture, the reliability of data storage and security can be provided with different quality levels depending on the implementation of the technological support of the data center.

#### 1.2. Centralized three-level architecture

By supplementing the two-level architecture with an intermediate link in the form of private banks, a three-level architecture is formed. Private banks can help to to reduce the organizational burden on CB by ensuring compliance with the KYC principle. A scheme of the three-level architecture is shown in Fig. 2.

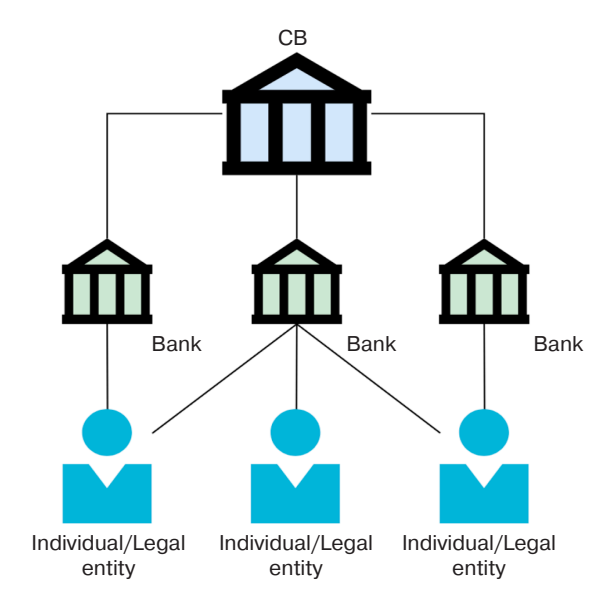


**Fig. 2.** Diagram of the centralized three-level architecture of CBDC

The advantages of this architecture are:

1) ease of implementation, since data storage and transaction execution are provided by the CB;

- 2) organizational support (compliance with the KYC principle) is distributed among the private banks;
- 3) the CB has a real-time access to all data;
- 4) the CB provides banks with a single tool for transactions.

The main disadvantage of this architecture is that all technical support for CBDC must be provided by a single issuer, i.e., the CB.

As in the two-level architecture, reliability of data storage and security in this case is also highly dependent on the Central Bank.

### 1.3. Four-level architecture with a single CBDC operator

In the article [7], several operational and computational architectures are proposed, one of which consists in transferring the technological support for the operation of the CBDC to a separate organization—the CBDC operator. The diagram in Fig. 3 shows the connection between the elements of the architecture.

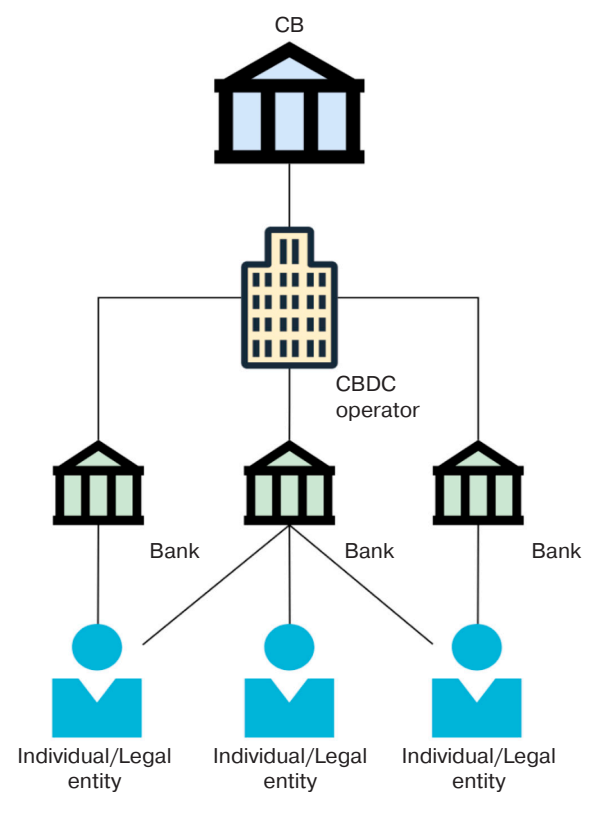


**Fig. 3.** Diagram of the four-level architecture with a single operator of CBDC

In many ways, this operational and computational architecture is similar to the three-tiered centralized architecture. However, the division of responsibility between the CBDC operator, CB and private banks offers the following additional advantages:

1) the resource-intensive task of transaction execution is ensured by the CBDC operator;

- 2) organizational support (compliance with the KYC principle) is distributed among the private banks;
- 3) CBDC operator provides banks with a single tool for transactions.

However, the disadvantages of such a four-level architecture are significant:

- 1) CB does not have access to all data in real time; a separate API is required to access transaction history;
- 2) all transaction data is under the control of one organization;
- 3) all technical support for CBDC must be provided by a single provider—the CBDC operator.

The listed disadvantages suggest that a monopoly on transaction processing may lead to unfair use of the CBDC system. In addition, as in the case of the centralized architectures described, the issue of scaling the transaction processing system becomes the task of one organization.

## 1.4. Four-level architecture with segmentation between several CBDC operators

The four-level architecture involving several CBDC operators (Fig. 4), also proposed in [7], solves a number of problems associated with the data monopoly: a single point of failure of the system is eliminated, along with an increase in scalability. This is achieved by segmenting the CBDC data.

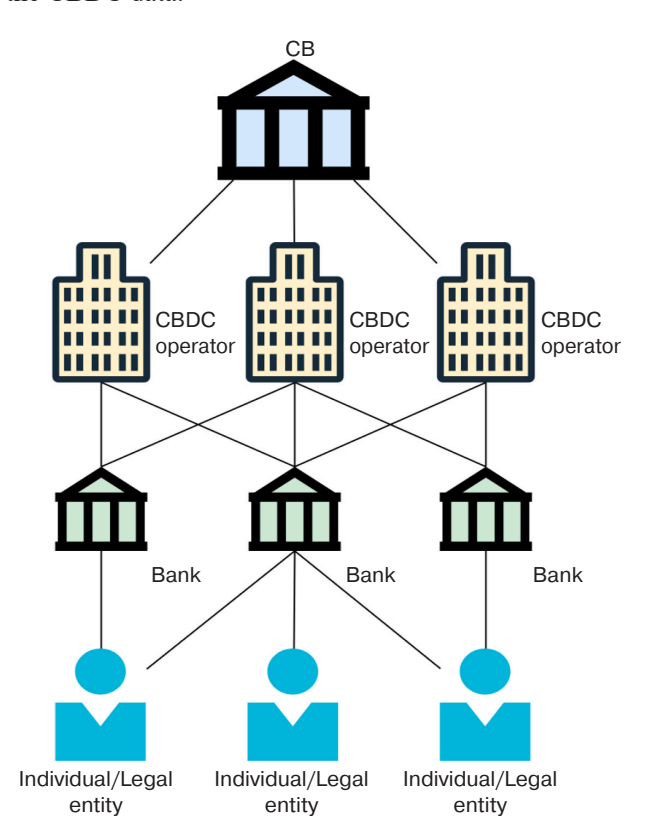


**Fig. 4.** Diagram of the four-level architecture with segmentation between several CBDC operators

The advantages of this architecture are as follows:

- 1) organizational support (compliance with the KYC principle) is distributed among the private banks;
- computational workload of transaction processing is distributed among several CBDC operators.
   The disadvantages include:
- 1) difficulty in accessing transaction history on the part of the CB due to CBDC data segmentation;
- increasing complexity of transactions processing related to the involvement of two or more operators;
- more complicated logistics of interaction between banks and operators due to the use of many-to-many communication.

Although there is no single point of failure, each segment in this architecture is the responsibility of only one organization; however, in the event of a failure, transaction data can be lost. It is also possible for an operator to unfairly use the CBDC system, although the scope is limited to a single segment.

## 1.5. Four-level architecture with segmentation and replication between several CBDC operators

In order to eliminate the disadvantages of an operational and computational architecture with segmentation, a refinement involving data replication between CBDC operators is proposed. As shown in Fig. 5, each segment must be replicated between multiple operators. Executing the transaction would require a consensus between the CBDC operators owning the segment. In such a case, the consensus algorithm can be flexibly selected to suit security and performance preferences.

The more CBDC operators are involved in the operation of a single segment, the higher the reliability of the system, but also the higher the redundancy of the stored data. The more CBDC operators are involved in transaction processing to ensure consensus, the more resistant the system is to unfair actions on the part of operators. However, at the same time the performance decreases.

The operating and computing architecture under consideration has the following advantages:

- 1) organizational support (compliance with the KYC principle) is distributed among the private banks;
- 2) computational workload of transaction processing is distributed among several CBDC operators;
- 3) operator disconnection does not lead to loss of data or availability of CBDC service;
- 4) availability of consensus algorithm when performing transactions allows operators to mutually verify results in order to avoid unfair actions.

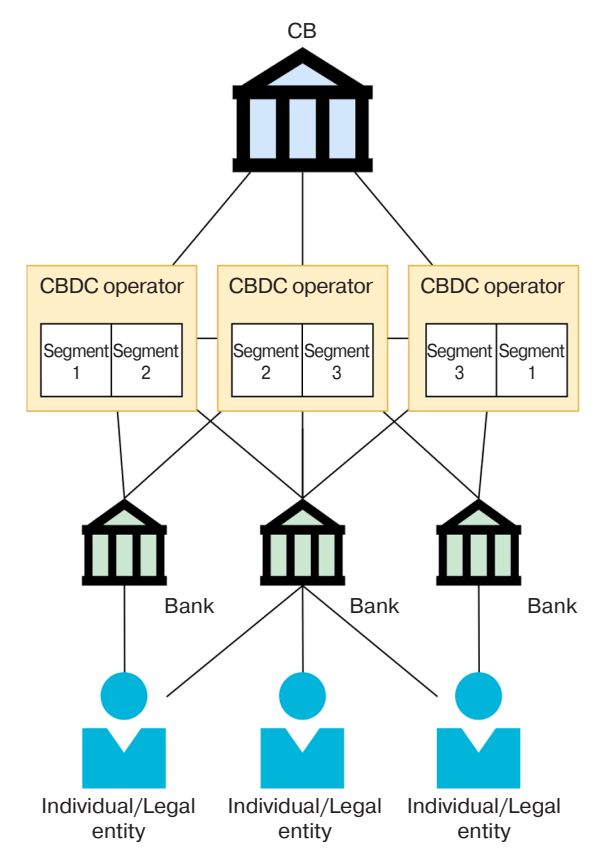


Fig. 5. Diagram of the four-level architecture with segmentation and replication between the several CBDC operators

The operating and computing architecture has a number of disadvantages:

- difficult access to transaction history for CB due to its segmentation;
- 2) icreasing complexity of transactions related processing to the involvement of two or more operators;
- 3) more complicated logistics of interaction between banks and operators because of the use of many-tomany communication;
- 4) increased resource intensity of transaction processing and increase of the total volume of stored data due to redundancy.

### 2. RESEARCH ENVIRONMENT INFRASTRUCTURE

In order to solve this problem, we will develop a research environment infrastructure using virtualization technologies [20].

The blockchain network will include several organizations, each organization having one or more nodes [21]. Then the total amount of CPU, RAM, and disk space required for the experiment can be calculated by the formula:

$$R_{\text{total}} = \sum_{i=1}^{O} \sum_{j=1}^{N_i} (R_{ij}R_{\text{h}} + R_{\text{c}}),$$

where O is the number of organizations;  $N_i$  is the number of nodes in ith organization;  $R_{ij}$  is the amount of resource required for the jth node in the ith organization to function;  $R_{\rm h}$  is the resource overhead for hypervisor operation, proportional to the allocated resource;  $R_{\rm c}$  is the resource overhead for hypervisor operation required to keep the node running regardless of the amount of resource allocated to it.

Thus, assuming that the amount of RAM required by the nodes is invariant and equal to 2,  $R_{\rm h}=0$ , and  $R_{\rm c}=0.2$ , 22 GB of RAM will be required to maintain a CBDC model containing four organizations (one with 4 nodes and the other three with 2 nodes each).

In the case of a digital currency implementation in the form of accounts, the transactions themselves (without considering the computational complexity of the consensus algorithm) have a computational complexity of O(1), since changes of one or two scalar values are trivial operations. However, when implementing digital currencies in the form of tokens, transactions can have greater computational complexity.

Both forms of digital currency representation can be considered in terms of financial transaction transparency for regulatory authorities. If the history of transactions is stored, as in the case of accounts with numerical representation of the balance, it can be extremely difficult to trace the ways of transferring a certain amount of money. It is problematic to reliably distinguish the fact of targeted funds expenditure from other funds if they are passed through a single account. On the contrary, with tokens, when each monetary unit has its own unique identifier, the transaction history reflects the transfer of a particular monetary unit from one owner to another. Thus, it is possible to implement a mechanism to identify misuse of funds.

In order to carry out research on the technological parameters of the information support of the data center, an infrastructure for the research environment using *VMWare ESXi*<sup>1</sup> was developed.

The tools used are:

- modified version of *Repexlab*<sup>2</sup> for work with *VMWare ESXi*;
- plug-in *vagrant-vmware-esxi*<sup>3</sup>;
- utility program ovftool<sup>4</sup>;
- system *Ansible*<sup>5</sup>;
- monitor atop<sup>6</sup>.

<sup>&</sup>lt;sup>1</sup> https://www.vmware.com/products/esxi-and-esx.html. Accessed March 17, 2023.

https://github.com/rnd-student-lab/repexlab. Accessed March 17, 2023.

<sup>&</sup>lt;sup>3</sup> https://github.com/josenk/vagrant-vmware-esxi. Accessed March 17, 2023.

<sup>&</sup>lt;sup>4</sup> https://developer.vmware.com/web/tool/4.4.0/ovf. Accessed March 17, 2023.

<sup>&</sup>lt;sup>5</sup> https://www.ansible.com/. Accessed March 17, 2023.

<sup>&</sup>lt;sup>6</sup> https://www.atoptool.nl/. Accessed March 17, 2023.

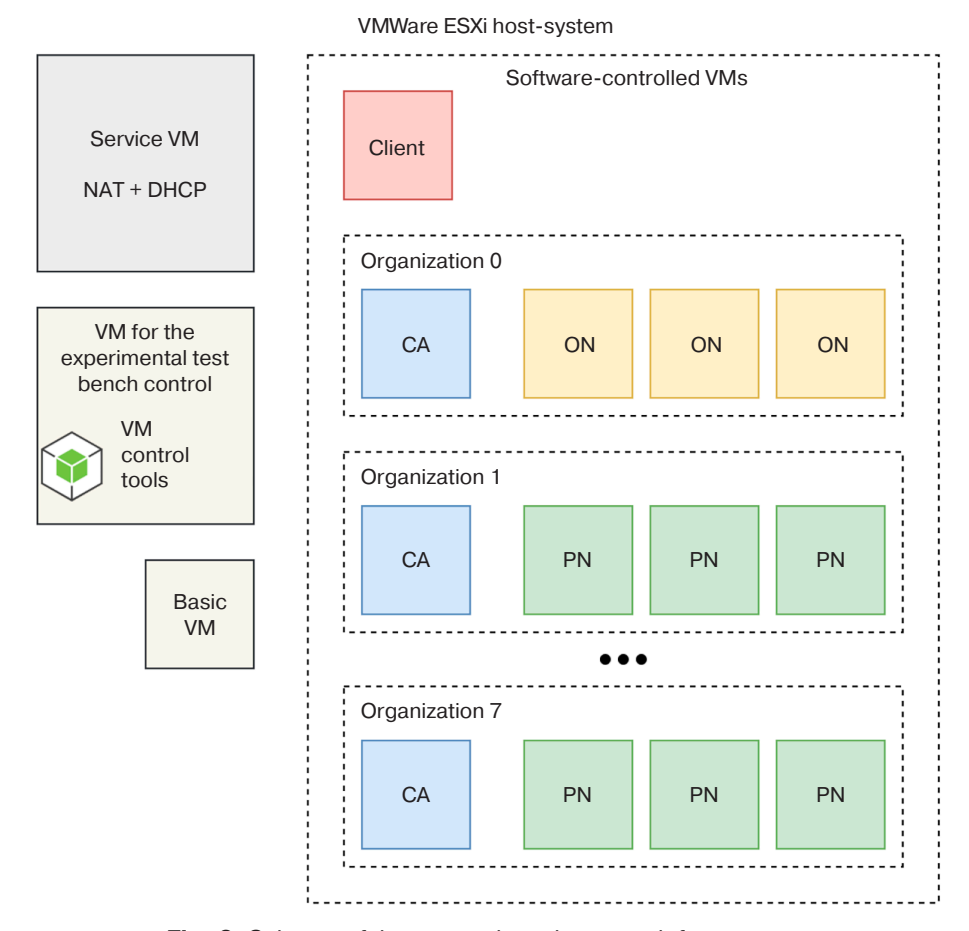


**Fig. 6.** Scheme of the research environment infrastructure (NAT—network address translation; DHCP— dynamic host configuration protocol; CA—certification authority; ON—orderer node; PN—peer node)

The general configuration diagram is shown in Fig. 6. The experiment management toolkit was hosted on a dedicated virtual machine (VM). The service VM was used to configure the NAT network and DHCP service, assigning IP addresses according to the MAC addresses of the software-managed VMs. A pre-configured VM was used (in Fig. 6, the Base VM), which was subsequently cloned to create and configure the software-managed VMs. When all 33 software-managed VMs were started and provisioned, the central processing unit (CPU) load from the installed monitoring system appeared to be acceptable, as shown in Fig. 7.

## 3. ANALYSIS OF THE OPERATIONAL COMPUTING ARCHITECTURES CHARACTERISTICS

A number of properties characterizing the considered operational and computational architectures are shown in the table. On their basis, a selection of the architecture most adequate to the requirements for the CBDC can be made.

The application of consensus algorithms becomes expedient when a segment is located at several CBDC

operators. Regardless of the form of presentation of the CBDC, the design should determine the acceptable number of operators per segment, which implies experimental research. This requires the development of an experimental-research environment for the operation of the CBDC model.

### **CONCLUSIONS**

A review of the architectural and technological components that make up a CBDC has been carried out. The main operational and computational CBDC architecture variants, which differ in their essential characteristics, are compared. A consolidated list of characteristics of the given operational and computational architectures formed as a result of the analysis is drawn up. On the basis of this list, the most adequate operational-computing architecture depending on the CBDC requirements can be selected. The discussion has been mainly focused on the forms of representation of digital currencies and their impact on the properties of digital currencies. While storing digital currencies in the form of accounts may be less resource-intensive than storage in the form of tokens, the history of digital

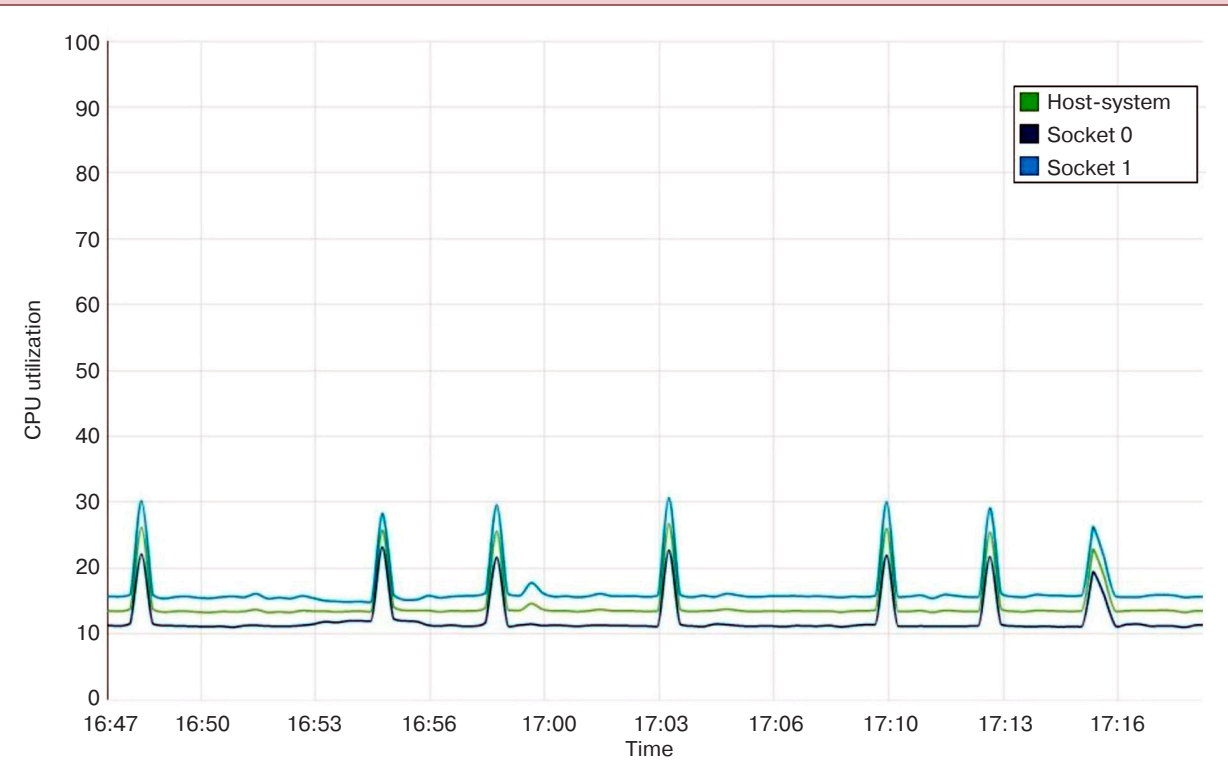


Fig. 7. CPU resource utilization after provisioning of VMs under VMWare ESXi hypervisor

**Table.** Characteristics of operational computer architectures

Characteristic	A1	A2	A3	A4	A5
Technological infrastructure for storing the entire volume of data is provided by CB	+	+	_	_	_
Technological infrastructure for processing the entire volume of transactions is provided by CB	+	+	_	_	_
Technological infrastructure for storing all data is provided by the operator	_	_	+	+	+
Technological infrastructure for processing the entire volume of transactions is provided by the operator	_	_	+	+	+
Technological infrastructure is distributed and scaled horizontally among several operators	_	_	_	+	+
KYC principle is carried out by CB	+	_	_	_	_
KYC principle is carried out by private banks	_	+	+	+	+
The system will retain partial functionality when one operator's services are disconnected	-	-	_	+	+
The system will remain fully operational when one operator's services are disconnected	_	_	_	_	+
The system will retain partial functionality when CB services are disconnected	_	_	+	+	+
The system will remain fully operational when CB services are disconnected	_	_	+	_	_
CB has real-time access to all data	+	+	_	_	_
Operators verify the results of transaction processing	_	_	_	_	+
Data backup with independent operators	_	_	_	_	+
No cross-segment transactions	+	+	+	_	_
CB provides a platform for individuals/legal entities	+	-	_	_	_
CB provides a platform for banks	+	+	_	_	_
CB provides a platform for operator(s)	_	_	+	+	+
Operator(s) provide(s) a platform for banks	_	_	+	+	+
Private banks provide a platform for individuals/legal entities	_	+	+	+	+

Note: A1—centralized two-level architecture; A2—centralized three-level architecture; A3—four-level architecture with a single CBDC operator; A4—four-LEVEL architecture with segmentation between several CBDC operators; A5—four-level architecture with segmentation and replication among several CBDC operators.

currency transactions in the form of tokens provides a more convenient tool for auditing.

The infrastructure of the research environment for the operational and computational architecture used to provide CBDC information support has been developed, on which basis prerequisites for a comprehensive analysis of technological characteristics of the operational and computational environment of CBDC can be identified. Further research should be focused on the choice of technological support for the development of the experimental and research environment, including experimental and analytical evaluation of the dependence of the characteristics of CBDC on the consensus algorithm used, the form of presentation of the digital currency, and various other parameters.

**Authors' contribution.** All authors equally contributed to the research work.

### **REFERENCES**

- 1. Allen F., Gu X., Jagtiani J. Fintech, cryptocurrencies, and CBDC: Financial structural transformation in China. *J. Int. Money Finance*. 2022;124(3–4):102625. https://doi.org/10.1016/j.jimonfin.2022.102625
- Wang Y.-R., Ma C.-Q., Ren Y.-S. A model for CBDC audits based on blockchain technology: Learning from the DCEP. Res. Int. Bus. Financ. 2022;63(3):101781. https://doi.org/10.1016/j.ribaf.2022.101781
- 3. Choi K.J., Henry R., Lehar A., Reardon J., Safavi-Naini R. A proposal for a Canadian CBDC. *SSRN Electron. J.* 2021. https://doi.org/10.2139/ssrn.3786426
- Chu Y., Lee J., Kim S., Kim H., Yoon Y., Chung H. Review of offline payment function of CBDC considering security requirements. *Appl. Sci.* 2022;12(9):4488. https:// doi.org/10.3390/app12094488
- Zhang T., Huang Z. Blockchain and central bank digital currency. *ICT Express*. 2022;8(2):264–270. https://doi. org/10.1016/j.icte.2021.09.014
- Tsai W.-T., Zhao Z., Zhang C., Yu L., Deng E. A multichain model for CBDC. In: 2018 5th International Conference on Dependable Systems and Their Applications (DSA). Dalian, China: IEEE; 2018. P. 25–34. https://doi.org/10.1109/DSA.2018.00016
- Jin S.Y., Xia Y. CEV Framework: A central bank digital currency evaluation and verification framework with a focus on consensus algorithms and operating architectures. *IEEE Access*. 2022;10:63698–63714. https://doi.org/10.1109/ACCESS.2022.3183092
- Opare E.A., Kim K. A compendium of practices for central bank digital currencies for multinational financial infrastructures. *IEEE Access*. 2020;8:110810–110847. https://doi.org/10.1109/ACCESS.2020.3001970
- 9. Lee Y., Son B., Park S., Lee J., Jang H. A survey on security and privacy in blockchain-based central bank digital currencies. *J. Internet Serv. Inform. Secur.* 2021;11(3): 16–29. https://doi.org/10.22667/JISIS.2021.08.31.016
- Ballaschk D., Paulick J. The public, the private and the secret: Thoughts on privacy in central bank digital currencies. *Journal of Payments Strategy & Systems*. 2021;15(3):277–286. Available from URL: https://www. bundesbank.de/resource/blob/880792/7f4b5efd53026f 51a9f53b176859e715/mL/digital-currencies-ballaschkpaulick-data.pdf

- 11. Monrat A.A., Schelén O., Andersson K. A survey of blockchain from the perspectives of applications, challenges, and opportunities. *IEEE Access*. 2019;7: 117134–117151. https://doi.org/10.1109/ACCESS.2019. 2936094
- Hang L., Kim D.-H. Optimal blockchain network constructionmethodology based on analysis of configurable components for enhancing Hyperledger Fabric performance. *Blockchain: Res. Appl.* 2021;2(1):100009. https://doi.org/10.1016/j.bcra.2021.100009
- 13. Lashkari B., Musilek P. A comprehensive review of blockchain consensus mechanisms. *IEEE Access*. 2021;9:43620–43652. https://doi.org/10.1109/ACCESS.2021.3065880
- 14. Auer R., Böhme R. The technology of retail central bank digital currency. *BIS Quarterly Review*. 2020. Available from URL: https://papers.ssrn.com/sol3/papers.cfm?abstract id=3561198
- Ozili P.K. Central bank digital currency research around the world: a review of literature. *J. Money Launder.* Control. 2022;26(2):215–226. https://doi.org/10.1108/ JMLC-11-2021-0126
- Bordo M.D., Levin A.T. Central bank digital currency and the future of monetary policy. *NBER Working Paper Series*. 2017; Working Paper 23711. https://doi.org/10.3386/w23711
- Zhang J., Tian R., Cao Y., Yuan X., Yu Z., Yan X., et al. A hybrid model for central bank digital currency based on blockchain. *IEEE Access*. 2021;9:53589–53601. https://doi.org/10.1109/ACCESS.2021.3071033
- Allen S., Čapkun S., Eyal I., Fanti G., Ford B.A., Grimmelmann J., et al. Design choices for central bank digital currency: Policy and technical considerations. NBER Working Paper Series. 2020; Working Paper 27634. https://doi.org/10.3386/w27634
- Chaum D., Grothoff C., Moser T. How to issue a central bank digital currency. SNB Working Papers. 2021;3. 38 p. https://doi.org/10.2139/ssrn.3965032
- Netto M.A.S., Menon S., Vieira H.V., Costa L.T., de Oliveira F.M., Saad R., et al. Evaluating load generation in virtualized environments for software performance testing. In: 2011 IEEE International Symposium on Parallel and Distributed Processing Workshops and Phd Forum. 2011. P. 993–1000. https://doi.org/10.1109/ IPDPS.2011.244

 Albychev A.S., Ilin D.Y., Nikulchev E.V., Magomedov S.G. Development of a methodology for experimental studies of technologies for central bank digital currencies. *Vestnik of RSREU*. 2022;82:136–146 (in Russ.). https://doi.org/10.21667/1995-4565-2022-82-136-146

### About the authors

**Alexander S. Albychev,** Deputy Head of the Federal Treasury, The Ministry of Finance of the Russian Federation (6/1, Bol'shoi Zlatoustinskii per., Moscow, 101000 Russia); Head of the State Financial Technologies Department, Institute for Cybersecurity and Digital Technologies, MIREA – Russian Technological University (78, Vernadskogo pr., Moscow, 119454 Russia). E-mail: albychev@mirea.ru. https://orcid.org/0000-0001-9632-7806

**Stanislav A. Kudzh,** Dr. Sci. (Eng.), Professor, Rector, MIREA – Russian Technological University (78, Vernadskogo pr., Moscow, 119454 Russia). E-mail: rector@mirea.ru. Scopus Author ID 56521711400. https://orcid.org/0000-0003-1407-2788

### Об авторах

**Албычев Александр Сергеевич,** заместитель руководителя, Федеральное казначейство Министерства финансов Российской Федерации (101000, Россия, Москва, Большой Златоустинский пер., д. 6, стр. 1); заведующий кафедрой «Государственные финансовые технологии» Института кибербезопасности и цифровых технологий ФГБОУ ВО «МИРЭА – Российский технологический университет» (119454, Россия, Москва, пр-т Вернадского, д. 78). E-mail: albychev@mirea.ru. https://orcid.org/0000-0001-9632-7806

**Кудж Станислав Алексеевич,** д.т.н., профессор, ректор ФГБОУ ВО «МИРЭА – Российский технологический университет» (119454, Россия, Москва, пр-т Вернадского, д. 78). E-mail: rector@mirea.ru. Scopus Author ID 56521711400. https://orcid.org/0000-0003-1407-2788

Translated from Russian into English by Lyudmila O. Bychkova Edited for English language and spelling by Thomas A. Beavitt Information systems. Computer sciences. Issues of information security Информационные системы. Информатика. Проблемы информационной безопасности

UDC 001.18:004.94:008.2 https://doi.org/10.32362/2500-316X-2023-11-3-17-29



### RESEARCH ARTICLE

# Dynamics of link formation in networks structured on the basis of predictive terms

Sergey O. Kramarov <sup>1, 2</sup>, Oleg R. Popov <sup>3, @</sup>, Ismail E. Dzhariev <sup>2</sup>, Egor A. Petrov <sup>2</sup>

- <sup>1</sup> MIREA Russian Technological University, Moscow, 119454 Russia
- <sup>2</sup> Surgut State University, Surgut, 628408 Russia
- <sup>3</sup> Southern Federal University, Rostov-on-Don, 344006 Russia

### Abstract

**Objectives.** In order to model and analyze the information conductivity of complex networks having an irregular structure, it is possible to use percolation theory methods known in solid-state physics to quantify how close the given network is to a percolation transition, and thus to form a prediction model. Thus, the object of the study comprises international information networks structured on the basis of dictionaries of model predictive terms thematically related to cutting-edge information technologies.

**Methods.** An algorithmic approach is applied to establish the sequence of combining the necessary operations for automated processing of textual information by the internal algorithms of specialized databases, software environments and shells providing for their integration during data transmission. This approach comprises the stages of constructing a terminological model of the subject area in the Scopus bibliographic database, then processing texts in natural language with the output of a visual map of the scientific landscape of the subject area in the *VOSviewer* program, and then collecting the extended data of parameters characterizing the dynamics of the formation of links of the scientific terminological network in the *Pajek* software environment.

**Results.** Visual cluster analysis of the range of 645–3364 terms in the 2004–2021 dynamics of the memory and data storage technologies category, which are integrated into a total of 23 clusters, revealed active cluster formation in the field of the term *quantum memory*. On this basis, allowing qualitative conclusions are drawn concerning the local dynamics of the scientific landscape. The exploratory data analysis carried out in the *STATISTICA* software package indicates the correlation of the behavior of the introduced *MADSTA* keyword integrator with basic terms including periods of extremes, confirming the correctness of the choice of the methodology for detailing the study by year.

**Conclusions.** A basis is established for the formation of a set of basic parameters required for an extensive computational modeling of a cluster formation in the semantic field of the scientific texts, especially in relation to simulations of the formation of the largest component of the network and percolation transitions.

**Keywords:** information network, algorithm, database, term, cluster, visualization, mapping, dynamics, network analysis

<sup>&</sup>lt;sup>®</sup> Corresponding author, e-mail: cs41825@aaanet.ru

• Submitted: 11.08.2022 • Revised: 01.11.2022 • Accepted: 02.03.2023

For citation: Kramarov S.O., Popov O.R., Dzhariev I.E., Petrov E.A. Dynamics of link formation in networks structured on the basis of predictive terms. *Russ. Technol. J.* 2023;11(3):17–29. https://doi.org/10.32362/2500-316X-2023-11-3-17-29

Financial disclosure: The authors have no a financial or property interest in any material or method mentioned.

The authors declare no conflicts of interest.

### НАУЧНАЯ СТАТЬЯ

# Динамика формирования связей в сетях, структурированных на основе прогностических терминов

С.О. Крамаров <sup>1, 2</sup>, О.Р. Попов <sup>3, @</sup>, И.Э. Джариев <sup>2</sup>, Е.А. Петров <sup>2</sup>

### Резюме

**Цели.** Для моделирования и анализа информационной проводимости сложных сетей с нерегулярной структурой возможно применение известных в физике твердого тела методов теории перколяции, позволяющих количественно оценить, насколько данная сеть близка к перколяционному переходу, и тем самым сформировать модель прогнозирования. Объектом исследования выступают международные информационные сети, структурированные на основе словарей модельных прогностических терминов, тематически относящихся к перспективным информационным технологиям.

**Методы.** Применен алгоритмический подход, согласно которому задается последовательность комбинирования необходимых операций по автоматизированной обработке текстовой информации внутренними алгоритмами специализированных баз данных (БД), программных сред и оболочек, предусматривающих их интеграцию при передаче данных. Данный подход, в частности, включает этапы построения терминологической модели предметной области в библиографической БД Scopus, затем обработку текстов на естественном языке с выводом визуальной карты научного ландшафта предметной области в программе *VOSviewer* и далее – сбор расширенных данных параметров, характеризующих динамику формирования связей научной терминологической сети в программной среде *Pajek*.

**Результаты.** Визуальный кластерный анализ, составляющий в динамике 2004–2021 гг. диапазон 645–3364 термов категории «Технологии памяти и хранения данных», интегрированных суммарно в 23 кластера, выявил активное кластерообразование в области терма «quantum memory» (квантовая память), позволяющее делать качественные выводы о локальной динамике научного ландшафта. Проведенный в программном пакете *STATISTICA* разведочный анализ данных свидетельствует о корреляции поведения введенного интегратора ключевых слов MADSTA с базовыми термами, включая периоды экстремумов, что подтверждает правильность выбора методики детализации исследования по годам.

<sup>1</sup> МИРЭА – Российский технологический университет, Москва, 119454 Россия

<sup>&</sup>lt;sup>2</sup> Сургутский государственный университет, Сургут, 628408 Россия

<sup>&</sup>lt;sup>3</sup> Южный федеральный университет, Ростов-на-Дону, 344006 Россия

<sup>&</sup>lt;sup>®</sup> Автор для переписки, e-mail: cs41825@aaanet.ru

**Выводы.** Заложена основа для формирования комплекса базовых параметров, необходимых при обширном вычислительном моделировании кластерообразования в семантическом поле научных текстов, особенно в отношении симуляций формирования наибольшего компонента сети и перколяционных переходов.

**Ключевые слова:** информационная сеть, алгоритм, база данных, термин, кластер, визуализация, картирование, динамика, сетевой анализ

• Поступила: 11.08.2022 • Доработана: 01.11.2022 • Принята к опубликованию: 02.03.2023

**Для цитирования:** Крамаров С.О., Попов О.Р., Джариев И.Э., Петров Е.А. Динамика формирования связей в сетях, структурированных на основе прогностических терминов. *Russ. Technol. J.* 2023;11(3):17–29. https://doi.org/10.32362/2500-316X-2023-11-3-17-29

**Прозрачность финансовой деятельности:** Авторы не имеют финансовой заинтересованности в представленных материалах или методах.

Авторы заявляют об отсутствии конфликта интересов.

### INTRODUCTION

The study of information dissemination in social networks with a random topology is an urgent task for the optimization of the modern sociotechnical systems, which is confirmed by the undiminished interest in the problems of social network analysis (SNA) [1–3].

A distinct category of complex networks, along with social and biological networks, is comprised by information networks, also called "knowledge networks." An example is the citation networks between scientific publications, whose structure quite accurately reflects the structure of the information stored in its vertices (articles), which defines the terminology "information network."

When applied to an analysis of the relationships between classes of words in the thesaurus, an information network can also be seen in conceptual terms, representing the structure of language, or perhaps even the mental constructs language represents [4].

To model and analyze the information processes occurring in the networks with an irregular structure, it is possible to apply percolation methods [5] known in solid-state physics.

Percolation, which is derived from Latin (percolare), means "leakage, seepage." For a long time, this simple probabilistic model was the ideal basic model used in physics to demonstrate phase transitions and critical phenomena. As a mathematical object, it was first considered in the classic work of Broadbent and Hammersley in 1957 [6], in which the term as well as geometric and probabilistic concepts were introduced.

Methods for solving various theoretical and applied problems over the last decades have brought new insights into the mathematical study of percolation [7]. Although the penetration of a fluid inside a porous stone, the spreading of an epidemic or the dissemination of the information in a social network seemingly have nothing in common, all three aspects converge in mathematics to comprise an additive component [7–9].

Regardless of the physical nature and the model of the system, percolation theory in its most general form addresses questions concerning the probability that there is an open path from 0 to infinity (or whether there is an infinite cluster of connected pores or nodes). Thus, the problem is reduced to finding an answer to the question whether such paths exist for a given probability p. The theory is mainly concerned with the existence of such a cluster and its structure with respect to the filling probability p.

To mathematically describe this criticality, it is necessary to define a percolation model. As an example, we selected the simplest model represented by an infinite two-dimensional (or square) grid. The intersection points of the lines are called nodes (graph vertices), while the lines themselves are called links (graph edges). There are two grid models: permeability of links and permeability of nodes.

In the first model, each link is mathematically occupied with probability p or free with probability 1-p. The occupied links then connect the nodes into clusters. This model can be used to simulate the process of liquid penetration inside a porous stone and epidemic propagation.

In the node percolation model, we occupy not a link, but each node with probability p, leaving it free with probability 1 - p. In general, link percolation is considered less general than node percolation due to the possibility of reformulating link percolation as node percolation on another grid, but not *vice versa*.

Percolation theory mainly focuses on the appearance of an infinite cluster with increasing probability p. To characterize this phenomenon, one typically takes the size of a giant cluster S, which is defined as:

$$S = \lim_{N \to \infty} \frac{S_1}{N},\tag{1}$$

where N is the system size (total number of nodes);  $S_1$  is the number of nodes in the largest cluster.

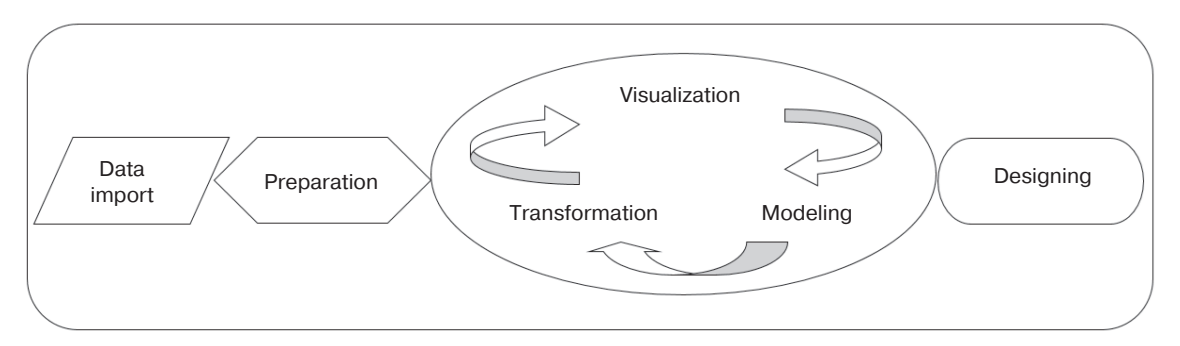


Fig. 1. Science data scientific project implementation algorithm diagram [11]

As the probability p increases, there must exist a critical  $p_S$ , called the percolation threshold or critical point, above which a non-zero value of S can be found. This determines the percolation transition of the system with respect to the control parameter p, while S is the corresponding parameter of order.

To describe the features of finite clusters, the distribution of clusters by size can also be used:

$$p_S = \frac{m_S}{\sum_S m_S},\tag{2}$$

where  $m_S$  is the number of clusters with size S.

Models have now been constructed for threedimensional and higher grid dimensions or for other percolation conditions.

Extensive computational modeling of social networks, both on classical 2D-regular grids and for higher-dimensional networks, has yielded results confirming the mapping of the phase of transient behavior characterized by the largest component in the proposed non-consensus opinion model with the well-known physical problem of seepage in incompressible fluids [9].

The use of computational modeling methods of random networks with a large number of links has led to analytical solutions, such as the construction of stochastic models describing the dynamics of node state changes and percolation transitions that predict the dynamics of social network behavior [2].

By analogy with social networks, we believe that a properly constructed research methodology will allow us to quantify how close the information network is to the threshold of percolation, and thus form a model for its prediction.

In this regard, it makes sense to apply mapping and network analysis techniques to study the patterns that affect the percolation threshold in information dissemination and clustering in networks structured on the basis of dictionaries of model predictive terms extracted from network resources and thesauruses, as well as scientometric and bibliographic databases.

In the article [10], the priority importance of information and communication technologies (ICT) and the field of information sciences was substantiated under the conditions of convergent tendencies of "joint" interdisciplinary links in the development of complex geoinformation systems. This position determined the main choice of the subject area for the present study.

### **TOOLS AND METHODS**

The basic toolkit of the stages of the scientific project associated with the processing of large amounts of information comprised of science data is shown in Fig. 1. The main mechanism of knowledge generation for the final design lies in a large central block, including data visualization and modeling. Analysis of the obtained knowledge at each step will require their transformation and optimization, including narrowing the range of observations of interest, calculation of a set of summary statistics, average values, etc.

The algorithmic approach seeks to maximize the objectivity of the search and the speed with which it allows a user to delve into a given subject area of research.

The basic steps and tools for implementing the empirical part of the algorithm are considered in [12]. A variant modified to solve current research problems consists of the following iterations:

- 1) formation of a terminological model of the subject domain based on a matrix defining the system maturity level (SML) of self-organizing intelligent systems;
- 2) formation of algorithmic queries of the Scopus<sup>1</sup> bibliographic database by a special formula and output the data in .csv format for further processing and analysis in software tools;
- 3) preprocessing, vectorization, clustering of the obtained terminological database by internal algorithms of *VOSviewer*<sup>2</sup> software environment;
- 4) primary visual analysis of intra- and inter-cluster interactions by *VOSviewer* program's basic interfaces by years and terms;

<sup>&</sup>lt;sup>1</sup> https://www.scopus.com/. Accessed March 01, 2022.

<sup>&</sup>lt;sup>2</sup> https://www.vosviewer.com/. Accessed March 22, 2022.

- 5) a detailed study of the parameters of scientific terminology network links by clusters in the dynamics of development with the help of algorithms of the *Pajek*<sup>3</sup> software product;
- 6) data processing and visualizing the dynamic relationships of term network parameters in the *STATISTICA*<sup>4</sup> environment.

There are several ways to achieve this goal. The initial stage of this work is the formation of a terminological model of the subject domain, on the basis of which the database for further research is formed.

The basis for the selection of a given pattern of keywords is the method of calculating the SML matrix of self-organizing intelligent systems (IS) [13], allowing the maturity index of the IS to be quantified. The SML indicator, which is applied at the system level, represents a maturity index from 0 to 1.

In the framework of this study, level 4 of a sociotechnical system maturity is of interest, which has the maturity index range 0.60–0.80, and can be described as follows: "the predicted technologies do not go beyond research and some prototyping, and the requirements of socioeconomic adaptation of the new technologies can be developed by reaching a compromise between communities" [13].

In order to determine the basic structures of the subject domain by the expert method, four categories of promising trends in the development of ICT corresponding to the fourth level of the SML matrix were identified:

- 1) human-computer interfaces;
- 2) computing engineering;
- 3) memory and data storage technologies;
- 4) electronics and communications.

The present study proposes an approach based on the extraction of stable keyword patterns by analyzing the corpora of the subject-oriented texts, including not only stationary databases of scientometric and bibliometric information, but also using dynamic network thesauruses, one of which is represented by the network encyclopedia Wikipedia<sup>5</sup> [14].

At the same time, the desired level of reliability of the obtained information can be increased by forming a combined algorithm of the term extraction. This algorithm allows a multilevel selection based on an extended expert environment using the internal services of Wikipedia at the first stage, while, at the second stage, scientifically reliable algorithmic ways of providing information from highly authoritative qualitative research databases, such as Scopus and Web of Science<sup>6</sup>, are used [15].

The extended terminological basis is obtained by processing the initial sets of basic keywords obtained by expert method in the bibliographic database Scopus using a special formula. The extracted useful database for the study falls within the dynamic range of 645–3364 terms, including related publications in which their joint inclusion occurs.

In [16], the main computational methods leading to an automatic mode of knowledge discovery in publications are classified in detail, including distributive semantic modeling. In addition to term-level modeling analysis, analysis at the level of the dissemination topic—so-called thematic modeling allows a deeper understanding of the information dissemination process. In the aspect of information retrieval and filtering, two generative models are widely used: probabilistic latent semantic analysis (PLSA) and, more commonly, latent Dirichlet allocation, which, in turn, is a generalization of PLSA.

Recently, a fundamentally different and more universal approach to thematic models based on network modeling has been proposed: the stochastic block model [17].

However, the use of these methods for analyzing scientific literature is rare [16–18].

Based on the study of programs for visualization and mapping of science and technology as the primary tool for thematic cluster analysis and visualization of the data obtained, the software package *VOSviewer* was selected. This tool is freely available and well integrated with bibliographic databases, including Scopus [19, 20].

VOSviewer's internal algorithms provide vectorization, normalization, term-document matrix construction, bibliometric mapping and initial clustering of text data, dynamically changing in the context of the assigned research tasks.

The maps generated by *VOSviewer* include various items that can include publications, researchers, or terms. *VOSviewer* maps the strength of a reference reflecting the number of publications in which two terms occur together (in the case of a matching occurrence reference).

For each pair of items i and j, VOSviewer requires as input the similarity  $s_{ij}$  ( $s_{ij} > 0$ ). To determine the similarity between items, the frequency of matching is typically determined using a similarity measure. Different types of similarity measures can be applied: strength of association, Jaccard index, Pearson correlation, cosine measure.

In *VOSviewer*, the similarity  $s_{ij}$  is calculated using the association force *AS* defined in the equation:

$$AS_{ij} = \frac{s_{ij}}{s_i s_j},\tag{3}$$

where  $s_i$  is the similarity of the element of the *i*th component;  $s_i$  is the similarity of the element of the *j*th

<sup>&</sup>lt;sup>3</sup> http://mrvar.fdv.uni-lj.si/pajek/. Accessed April 03, 2022.

<sup>&</sup>lt;sup>4</sup> https://www.statistica.com/en/. Accessed June 15, 2022.

<sup>&</sup>lt;sup>5</sup> https://www.wikipedia.org/. Accessed March 15, 2022.

<sup>&</sup>lt;sup>6</sup> http://www.webofknowledge.com/. Accessed March 04, 2022.

component;  $s_{ij}$  is the similarity of the pair. All the listed quantities have the dimensionality equal to one.

After calculating the similarity between the elements, a special technique for their mapping is applied [16]. *VOSviewer* determines the location of elements on the map by minimizing the function:

$$V(x_1,...,x_n) = \sum_{i < j} s_{ij} \|x_i - x_j\|^2,$$
 (4)

where  $x_i$ ,  $x_j$  are locations of nodes i and j in two-dimensional space; n is the number of the nodes in the grid;  $||x_i - x_j||$  are the Euclidean distances between nodes i and j, provided that:

$$\frac{2}{n(n-1)} \sum_{i < j} s_{ij} \left\| x_i - x_j \right\| = 1.$$
 (5)

Consequently, the idea of *VOSviewer* is to minimize the weighted sum of the squares of distances between all pairs of elements. The squared distance between the pair of elements is weighted as the similarity between the elements.

As a result, a complex associated structure of the network under study is formed, whose nodes and terms are calculated by the weight of different elements according to three basic criteria: degree of nodes, as well as the distance and strength of links between nodes; here, the size of nodes depends on the weight of a particular term.

Particular attention should be paid to the dynamics of the formation of the so-called largest or giant component of the network. A classic example of a discrete probability distribution is the Poisson distribution model of random numbers. Based on this, Erdős and Rényi [21] proposed an extremely simple network model, which they called a random graph. It was shown that a random graph has an important property, which can be called a phase transition to a state when a large fraction of all vertices are connected together into one giant component.

Using the Poisson distribution, the heuristic argument [4] can be used to calculate the expected size of the giant component of random networks. Suppose u is a part of vertices of the network which do not belong to the giant component. Therefore, the probability that a vertex does not belong to the giant component is also equal to the probability that none of the network neighbors of the vertex belongs to the giant component, i.e.,  $u^k$ , where k is the degree of the vertex.

After applying the averaging procedure, the expression for the probability of the Poisson distribution of degrees  $p_k$  in the self-consistency relation for u within a large graph size can be represented as follows:

$$u = \sum_{k=0}^{\infty} p_k u^k = e^{-z} \sum_{k=0}^{\infty} \frac{(zu)^k}{k!} = e^{z(u-1)},$$
 (6)

where e is the Eulerian number; k is the degree of a vertex; z is the average degree of all vertices N of the network.

The fraction S of the network occupied by the giant component is S = 1 - u. By averaging the expression for the random graph model of Erdős and Rényi by the probability of the Poisson distribution of degrees, we obtain the following self-consistency relation within the large size of the graph:

$$S = 1 - e^{-zS}. (7)$$

The appearance of the giant component indicates a phase (percolation) transition at the point z=1, where the divergence of the mean size  $\langle s \rangle$  of the non-giant components also occurs when studying the behavior of the random graph. If z < 1, the only non-negative solution of this equation is S=0, while if z > 1, there exists also a nonzero solution which determines the size of the giant component.

The tasks of general network analysis are performed by the *Pajek* software. This software environment based on large network visualization graphs offers many different efficient (sub-quadratic) network analysis algorithms [22].

From a bibliometric point of view, the methods offered by *Pajek* include clustering and main path analysis. The software is used not only to reveal the global structure of knowledge networks, but also to operationalize and measure the stability of the resulting network models [23]. An important feature of *Pajek* is its close connection to *VOSviewer*, which allows direct two-way communication between these network environments, as well as exporting data in formats of widely used other external tools, including programming language R, *Statistical Package for the Social Sciences* (*SSPS*) and *Excel* [22].

The most fundamental approaches to the study of knowledge networks are related to basic descriptive statistics of the network structure, such as measuring the number and size of components in the network, as well as calculating various measures of centrality (degree, closeness, betweenness). From the point of view of the tasks set in this paper, these latter characteristics of network interactions are effectively computed in *Pajek*.

The universal integrated system *STATISTICA* was used as a software package for statistical analysis. When properly used, the system saves the user from routine calculations by clearly displaying the results of cluster analysis [24], leaving the specialist to interpret the results

and formulate conclusions. At the same time, it provides cues, which are important for the implementation of functions of data analysis, data management and visualization. In terms of implementing iterations of the algorithm of this study, the system is integrated with *Excel*.

### **RESULTS AND DISCUSSION**

The data obtained from the bibliographic database Scopus are taken from the first year of publications, in which the occurrence of each of the keywords in the articles exceeds the lower threshold of 10 articles, and is inclusive up to 2021. The bibliographic data are detailed by year for mapping and primary visual analysis of clusters. In our case, the overall time range of the study covers the period from 1978 to 2021.

As part of the objectives of this research phase, the memory and data storage technologies category was selected as the basis for the selection of the established keywords.

In order to analyze the behavior of the trend, four keywords were selected from the terminology model: phase-change memory, patterned media, quantum memory, DNA digital data storage. From the resulting database the different dates of the initial inclusion of the terms follow.

In this regard, the Scopus query formula was optimized. For example, the database of publications for the keyword *quantum memory*, limited to the year 1978, was specified by the formula: TITLE (quantumANDmemory) AND (LIMIT-TO (PUBYEAR, 1978)).

Full bibliographic descriptions of extracted publications were automatically downloaded in .csv

format for the further processing and analysis in software tools, including a total of 33 information fields for each record.

It should be noted that in the context of the issues we are considering, text data from the TITLE and ABSTRACT fields of the database of uploaded documents was used. These fields are selected in *VOSviewer* automatically when loading the source document.

In order to understand the clearer structure of the network in the *VOSviewer* environment, an additional parameter, which implements the network integration of the specified keywords, with the name *memory and data storage technologies all (MADSTA)*, was introduced. The timing of the introduction of this integrator is related to the period of active research phase since inclusion of the fourth keyword *DNA digital data storage*, i.e., from 2004 to 2021.

In the above time interval, the comparative visual analysis of the obtained range of 645-3364 terms integrated into a total of 23 clusters shown in Fig. 2 presents a well-defined clustering dynamic around the terms quantum memory, phase-change memory. At the same time, the noticeable activation of research by 2021 in the area of the term DNA digital data storage pushed the term patterned media to the periphery of the scientific landscape. At the same time, the formation of a new cluster associated with the term *post-quantum* cryptography is clearly visualized near the quantum memory area. This can be explained by the fact that many cryptographers are now actively developing new algorithms for quantum key search [25] in order to prepare for a future time when quantum computing is likely to present a security threat.

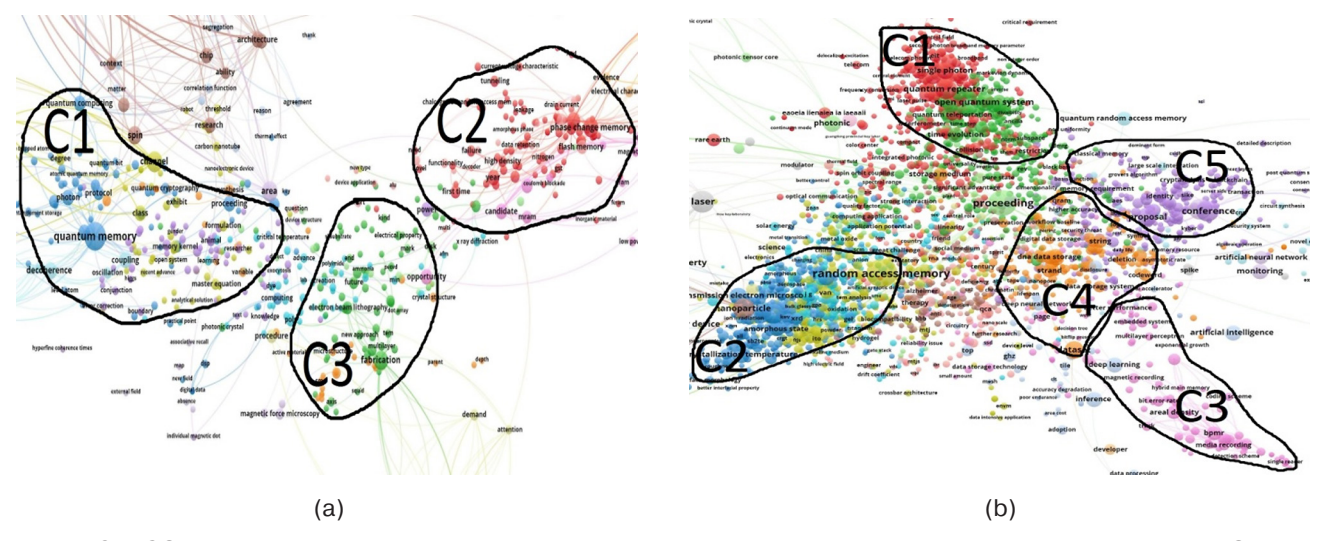


**Fig. 2.** VOSviewer visualization map showing the dynamics of data clustering for the keyword integrator MADSTA, marked clusters in the area of quantum memory (C1), phase-change memory (C2), patterned media (C3), DNA digital data storage (C4), post-quantum cryptography (C5):

(a) the beginning of the period 2004; (b) the end of the period 2021

For the further analysis of clustering, an automated transfer of data is performed from one *VOSviewer* network environment to another using the *Pajek* network calculator [21].

Working in *Pajek* starts with three file extensions characterizing certain types of data: networks, partition, vectors. When data are loaded into the program, the parameters characterizing the dynamic state of network links are investigated. We note that the *Pajek* network calculator function ideally suits it for performing such tasks.

The data processed in *Pajek* are shown in the summary table. Only parameters characterizing the dynamic state of network links are presented here for the term integrator.

The results of exploratory data analysis implemented in the universal integrated package *STATISTICA* with a brief description of the parameters are shown below.

The Total Link Strength parameter characterizes the number of links in a simple network. Another important parameter for the study is the average number of links per node known as the Average Degree. The Average Degree of all nodes in an individual network is a measure of the structural cohesion of the network. Since this index does not depend on the size of the network, it can be compared between networks of different sizes.

In Fig. 3a, the dynamics of Average Degree behavior leads to average values of 20–30 link units per node. This can be explained by the fact that the interest of the scientific community in this area does not decrease steadily. In our case, the presence of maxima in 2007 and 2009 may be a problem area.

The proposed hypothesis assumes the influence of the single keyword *quantum memory* on the other words by the effect of the aftereffect. In Fig. 3b, an increasing trend in the total number of links for *quantum memory* can be clearly seen. Since this indicates that the direction in this period was relevant, the total number of links for the remaining words determines the dynamic behavior of the overall network. The introduction of the parameter *MADSTA* shows a smooth increase in the total number of links in the network, which leads to the analysis of the next dynamic parameter—Density.

Density is responsible for the number of lines in the simple network, expressed as a fraction of the maximum possible number of lines. The parameters for determining the correlation dependence (Density) cover the maximum time period because the keywords were entered in the studied network alternately and at different time intervals.

Table. Dynamics of parameters characterizing the state of terminology network links for the keyword integrator MADSTA

Year	Total Link Strength	Average Degree	Density	Degree Centralization	Betweenness Centralization
2004	6140	19.039	0.029	0.139	0.073
2005	15292	29.896	0.029	0.146	0.192
2006	15167	29.827	0.029	0.184	0.092
2007	34415	44.899	0.029	0.211	0.054
2008	22696	27.831	0.017	0.194	0.120
2009	41099	40.833	0.020	0.117	0.034
2010	27976	30.017	0.016	0.236	0.201
2011	30205	22.366	0.008	0.151	0.118
2012	27010	22.813	0.009	0.210	0.240
2013	35111	29.419	0.012	0.172	0.101
2014	32007	29.230	0.013	0.294	0.236
2015	32552	29.232	0.012	0.101	0.075
2016	31683	27.780	0.012	0.110	0.065
2017	35182	27.358	0.011	0.084	0.052
2018	34183	26.726	0.010	0.117	0.070
2019	38765	25.878	0.009	0.148	0.140
2020	43288	27.285	0.009	0.126	0.065
2021	44552	26.488	0.008	0.082	0.072

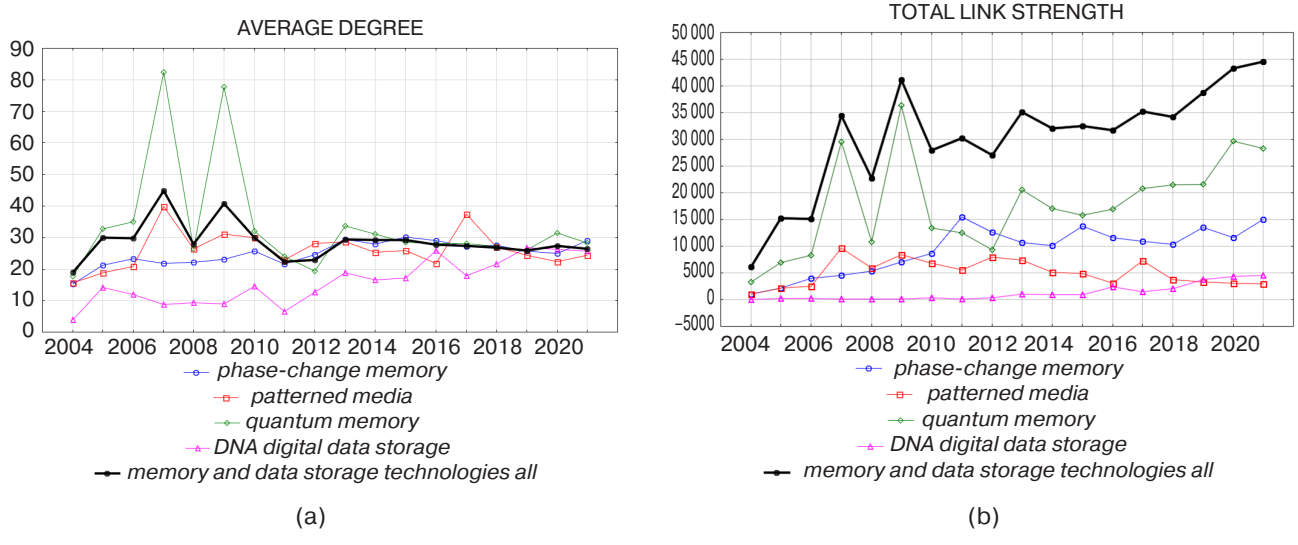


**Fig. 3.** Dependence of the average degree and the total link strength on time:

(a) dependence of the average degree of all vertices, taking into account the introduced parameter, on time;

(b) dependence of the total number of links in the network on time

Figure 4 shows that the integrative increase in the number of links in the network complicates the interaction structure due to the growth of the maximum possible number of lines. Consequently, the dependencies will tend to return minimum values. In this case, the behavior of the *MADSTA* parameter in the graph reveals that the integration of 4 keywords does not lead to changes in the dynamics of the behavior of the index of network density. The *MADSTA* parameter, which correlates with the curves, confirms the correctness of the choice of methodology for detailing the study by year.

The first parameter Degree Centralization (DC) represents the variation of the degree centrality of the network vertices divided by the maximum degree value that is possible in a network of the same size.

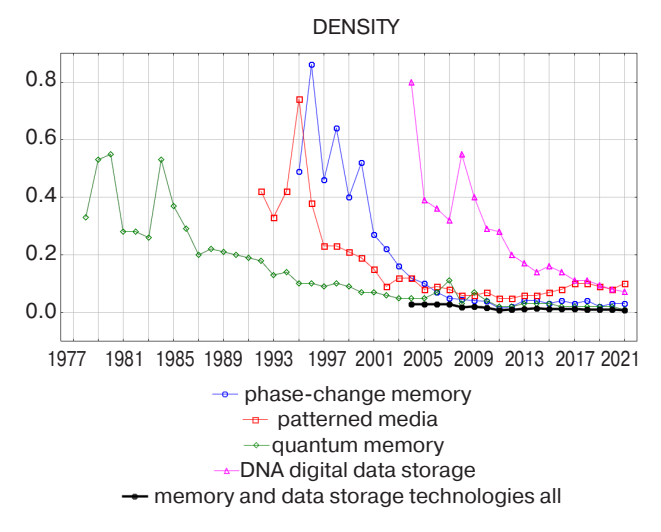


**Fig. 4.** Dependence of the network density index on time

As can be seen in Fig. 5a, oscillations of the DC indicator for the four keywords result in a mutual relationship over the interval from 2004 to 2021. The values of the integrating parameter in this relationship show a weak correlation.

Betweenness Centralization (BC) represents the variation of betweenness scores between network nodes divided by the maximum value of betweenness score possible in a network of the same size. For a single node, betweenness shows the level of its inclusion in combinations of links between other nodes.

In Fig. 5b shows that the oscillation of the BC indicator of keywords in this dependence on the interval from 2004 to 2021 is synchronous, which refers to the same phase of the curve behavior. Graphically, there is a strong correlation between the extremums of keywords and *MADSTA* on a given interval. This can be explained in terms of the emergence of the trend associated with the oscillations of the *phase-change memory* indicator comprising an impulse for other terms, in which the semantic links on the shortest paths between the nodes are more clearly manifested.

Thus, empirical research provides an opportunity to find latent dependencies of dynamic parameters of network interactions on time during the exploratory analysis stage, creating a basis for quantitative assessment of clustering and percolation transitions.

The analysis of the graphs shows that the introduction of the integrating parameter *MADSTA* displays the interaction of the keywords under study. This is confirmed by the close correlation on the graphs of the dependencies of the dynamic parameters of the network (average degree, betweenness score and density) on a given interval. The formation of new clusters (C4, C5) is explained by the increased total number of links.

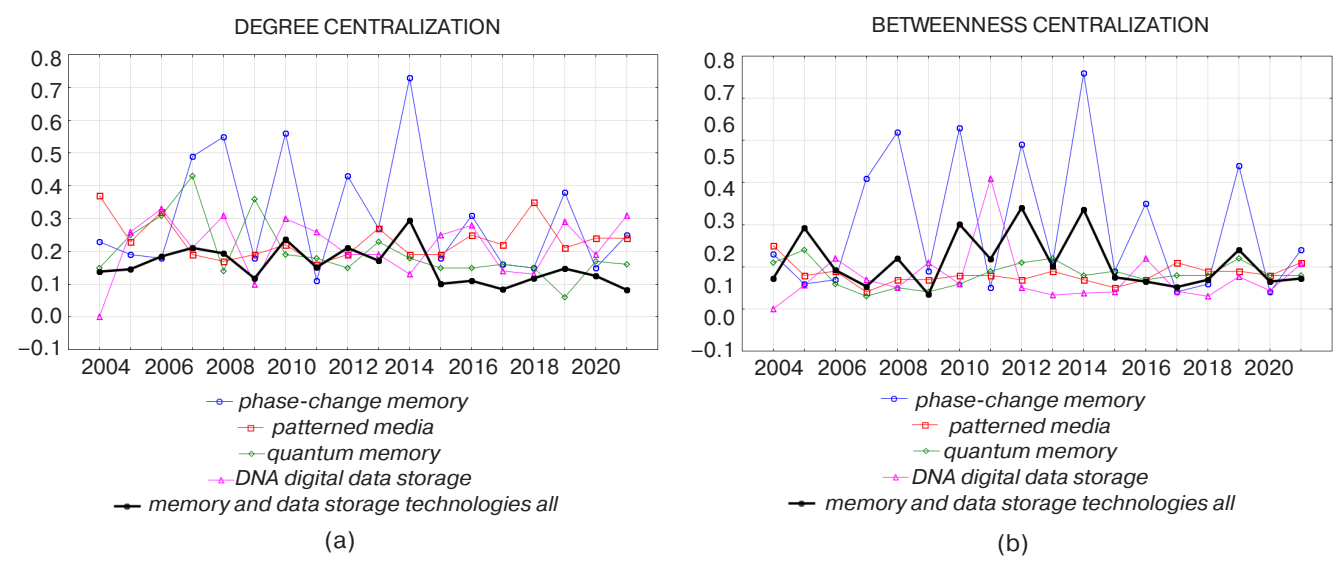


Fig. 5. Dependence of DC and BC of the network on time:

(a) dependence of the degree of centrality of the network vertices on time; (b) dependence of betweenness centralization index of the network vertices on time

### **CONCLUSIONS**

The algorithmic approach implemented in the work allows for the maximum objectivity of the search and the speed with which it allows a given subject area of research to be analyzed. The level of reliability of the obtained information is increased due to the formation of a combined algorithm for term extraction based on an expanded expert environment and scientifically reliable qualitative research databases.

By implementing algorithmic queries using the Scopus bibliographic database, an extended terminological base is created, which in terms of 2004–2021 dynamics contains the range of 645–3364 terms of the memory and data storage technologies category, providing data output in the .csv format for further processing and analysis in specialized software tools.

A comparative analysis of the data visualization map of the terms performed in the software environment *VOSviewer*, which are integrated into a total of 23 clusters, reveals active clustering associated with the term C5 *post-quantum cryptography* in the area of cluster C1 (*quantum memory*), allowing qualitative

conclusions to be drawn about the local dynamics of the scientific landscape.

The result of empirical study of the dynamics of the formation of interactions of terms in the *Pajek* network calculator and subsequent processing of the obtained parameters in the package *STATISTICA* is the construction of time series on the change in the average degree and the total number of links, network density, the degree centralization and the betweenness score of the bibliographic network.

To continue the analysis, it is necessary to supplement the obtained empirical material with data on general network parameters characterizing the number and size of components in the network, the distribution of distances in the network, and the degree of distribution of network fragments, including the presence of a giant component.

The formation of a complete set of basic parameters is necessary in the subsequent mathematical and computational modeling of information networks, during which the dynamics of network clustering and achieving the threshold of percolation over time will be evaluated.

**Authors' contribution.** All authors equally contributed to the research work.

### **REFERENCES**

- 1. Maltseva D., Batagelj V. Journals publishing social network analysis. *Scientometrics*. 2021;126(4): 3593–3620. https://doi.org/10.1007/s11192-021-03889-z
- 2. Zhukov D.O., Khvatova T.Yu., Zal'tsman A.D. Modeling of the stochastic dynamics of changes in node states and percolation transitions in social networks with self-organization and memory. *Informatika i ee Primeneniya* = *Informatics and Applications*. 2021;15(1):102–110 (in Russ.). https://doi.org/10.14357/19922264210114

### СПИСОК ЛИТЕРАТУРЫ

- Maltseva D., Batagelj V. Journals publishing social network analysis. *Scientometrics*. 2021;126(4): 3593–3620. https://doi.org/10.1007/s11192-021-03889-z
- 2. Жуков Д.О., Хватова Т.Ю., Зальцман А.Д. Моделирование стохастической динамики изменения состояний узлов и перколяционных переходов в социальных сетях с учетом самоорганизации и наличия памяти. *Информатика и ее применения*. 2021;15(1):102–110. https://doi.org/10.14357/19922264210114

- 3. Chkhartishvili A.G., Gubanov D.A., Novikov D.A. Models of influence in social networks. In: *Social Networks: Models of Information Influence, Control and Confrontation. Studies in Systems, Decision and Control.* 2019;189:1–40. https://doi.org/10.1007/978-3-030-05429-8 1
- 4. Newman M.E.J. The structure and function of complex networks. *SIAM Rev.* 2003;45(2):167–256. https://doi.org/10.1137/S003614450342480
- 5. Dashko Yu.V., Kramarov S.O., Zhdanov A.V. Sintering of polycristalline ferroelectrics and the percolation problem in stochastically packed networks. *Ferroelectrics*. 1996;186(1):85–88. https://doi.org/10.1080/00150199608218039
- Broadbent S.R., Hammersley J.M. Percolation processes:
   I. Crystals and mazes. *Math. Proc. Cambridge Philos. Soc.* 1957;53(3):629–641. https://doi.org/10.1017/S0305004100032680
- Li M., Liu R.-R., Lu L., Hu M.-B., Xu S., Zhang Y.-C. Percolation on complex networks: Theory and application. *Phys. Rep.* 2021;907:1–68. https://doi.org/10.1016/j. physrep.2020.12.003
- 8. Brunk N.E., Twarock R. Percolation theory reveals biophysical properties of virus-like particles. *ACS Nano*. 2021;15(8):12988–12995. https://doi.org/10.1021/acsnano.1c01882
- 9. Shao J., Havlin S., Stanley H.E. Dynamic opinion model and invasion percolation. *Phys. Rev. Lett.* 2009;103(1):018701. https://doi.org/10.1103/PhysRevLett.103.018701
- Bodrunov S.D. *Noonomika (Noonomics)*. Moscow: Kul'turnaya revolyutsiya; 2018. 432 p. (in Russ.). ISBN 978-5-6040343-1-6
- 11. Wickham H., Grolemund G. *R for data science: import, tidy, transform, visualize, and model data.* O'Reilly Media, Inc.; 2016. 492 p.
- 12. Popov O.R., Kramarov S.O. The study of information dissemination in networks arranged from a set of forecasting terms. *Vestnik kibernetiki = Proceedings in Cybernetics*. 2022;1(45):38–45 (in Russ.). https://doi.org/10.34822/1999-7604-2022-1-38-45
- 13. Popov O.R. Adaptation of world practices to the problem of long-term technological forecasting of the state of self-organizing intelligent systems. *Intellektual'nye resursy regional'nomu razvitiyu = Intellectual Resources Regional Development.* 2021;2:91–98 (in Russ.).
- 14. Kogai V.N., Pak V.S. Algorithmic model of computer system of keywords extracting from text based on ontology. *Problemy sovremennoi nauki i obrazovaniya = Problems of Modern Science and Education.* 2016;16(58):33–40 (in Russ.).
- 15. Panin S.B. Modern scientometric systems "WoS" and "Scopus": publishing problems and new guidelines for Russian university science. *Gumanitarnye issledovaniya Tsentral'noi Rossii = Humanities Researches of the Central Russia*. 2019;3:51–65 (in Russ.). https://doi.org/10.24411/2541-9056-2019-11030
- Thilakaratne M., Falkner K., Atapattu T. A systematic review on literature-based discovery: general overview, methodology, & statistical analysis. ACM Computing Surveys. 2019;52(6):Article 129. https://doi. org/10.1145/3365756

- 3. Chkhartishvili A.G., Gubanov D.A., Novikov D.A. Models of influence in social networks. In: Social Networks: Models of Information Influence, Control and Confrontation. Studies in Systems, Decision and Control. 2019;189:1–40. https://doi.org/10.1007/978-3-030-05429-8 1
- Newman M.E.J. The structure and function of complex networks. SIAM Rev. 2003;45(2):167–256. https://doi. org/10.1137/S003614450342480
- 5. Dashko Yu.V., Kramarov S.O., Zhdanov A.V. Sintering of polycristalline ferroelectrics and the percolation problem in stochastically packed networks. Ferroelectrics. 1996;186(1): 85-88. https://doi.org/10.1080/00150199608218039
- Broadbent S.R., Hammersley J.M. Percolation processes:
   I. Crystals and mazes. *Math. Proc. Cambridge Philos. Soc.* 1957;53(3):629–641. https://doi.org/10.1017/S0305004100032680
- Li M., Liu R.-R., Lu L., Hu M.-B., Xu S., Zhang Y.-C. Percolation on complex networks: Theory and application. *Phys. Rep.* 2021;907:1–68. https://doi.org/10.1016/j. physrep.2020.12.003
- 8. Brunk N.E., Twarock R. Percolation theory reveals biophysical properties of virus-like particles. *ACS Nano*. 2021;15(8): 12988–12995. https://doi.org/10.1021/acsnano.1c01882
- Shao J., Havlin S., Stanley H.E. Dynamic opinion model and invasion percolation. *Phys. Rev. Lett.* 2009;103(1):018701. https://doi.org/10.1103/PhysRevLett. 103.018701
- 10. Бодрунов С.Д. *Ноономика*. М.: Культурная революция; 2018. 432 с. ISBN 978-5-6040343-1-6
- 11. Wickham H., Grolemund G. *R for data science: import, tidy, transform, visualize, and model data.* O'Reilly Media, Inc.; 2016. 492 p.
- 12. Попов О.Р., Крамаров С.О. Исследование распространения информации в сетях, структурированных из набора прогностических терминов. *Вестинк кибернетики*. 2022;1(45):38–45. https://doi.org/10.34822/1999-7604-2022-1-38-45
- Попов О.Р. Адаптация мировых практик к проблеме долгосрочного технологического прогнозирования состояния самоорганизующихся интеллектуальных систем. Интеллектуальные ресурсы – региональному развитию. 2021;2:91–98.
- 14. Когай В.Н., Пак В.С. Алгоритмическая модель компьютерной системы выделения ключевых слов из текста на базе онтологий. *Проблемы современной науки и образования*. 2016;16(58):33–40.
- Панин С.Б. Современные наукометрические системы «WoS» и «Scopus»: издательские проблемы и новые ориентиры для российской вузовской науки. Гуманитарные исследования Центральной России. 2019;3:51–65. https://doi.org/10.24411/2541-9056-2019-11030
- Thilakaratne M., Falkner K., Atapattu T. A systematic review on literature-based discovery: general overview, methodology, & statistical analysis. ACM Computing Surveys. 2019;52(6):Article 129. https://doi. org/10.1145/3365756

- 17. Gerlach M., Peixoto T.P., Altmann E.G. A network approach to topic models. *Sci. Adv.* 2018;4(7):eaaq1360. https://doi.org/10.1126/sciadv.aaq1360
- Zelenkov Yu. The topic dynamics in knowledge management research. In: Uden L., Ting I.H., Corchado J. (Eds.). Knowledge Management in Organizations (KMO 2019): Proceedings of the 14th International Conference. 2019. P. 324–335. https://doi.org/10.1007/978-3-030-21451-7 28
- Van Eck N.J., Waltman L. Visualizing bibliometric networks. In: Ding Y., Rousseau R., Wolfram D. (Eds.). *Measuring Scholarly Impact: Methods and Practice*. Springer; 2014. P. 284–321. https://doi.org/10.1007/978-3-319-10377-8 13
- Van Eck N.J., Waltman L. Accuracy of citation data in Web of Science and Scopus. arXiv preprint arXiv:1906.07011. 2019. https://doi.org/10.48550/arXiv.1906.07011
- 21. Erdös P., Rényi A. On random graphs I. *Publ. Math. Debrecen.* 1959;6:290–297. Available from URL: https://studylib.net/doc/25387956/on-random-graphs--1959-by-p.-erdos-and-a.-renyi
- 22. De Nooy W., Mrvar A., Batagelj V. *Exploratory social network analysis with Pajek: Revised and epanded edition for updated software*. 3rd ed. Series: Structural Analysis in the Social Sciences. Cambridge: Cambridge University Press; 2018. 484 p. https://doi.org/10.1017/9781108565691
- 23. Doreian P., Batagelj V., Ferligoj A. (Eds.). *Advances in network clustering and blockmodeling*. John Wiley & Sons; 2020. 414 p.
- 24. Zuanazzi N.R., de Castilhos Ghisi N., Oliveira E.C. Analysis of global trends and gaps for studies about 2, 4-D herbicide toxicity: A scientometric review. *Chemosphere*. 2020;241:125016. https://doi.org/10.1016/j.chemosphere. 2019.125016
- 25. Sigov A.S., Andrianova E.G., Zhukov D.O., Zykov S.V., Tarasov I.E. Quantum informatics: Overview of the main achievements. *Russ. Technol. J.* 2019;7(1):5–37 (in Russ.). https://doi.org/10.32362/2500-316X-2019-7-1-5-37

- 17. Gerlach M., Peixoto T.P., Altmann E.G. A network approach to topic models. *Sci. Adv.* 2018;4(7):eaaq1360. https://doi.org/10.1126/sciadv.aaq1360
- Zelenkov Yu. The topic dynamics in knowledge management research. In: Uden L., Ting I.H., Corchado J. (Eds.). Knowledge Management in Organizations (KMO 2019): Proceedings of the 14th International Conference. 2019. P. 324–335. https://doi.org/10.1007/978-3-030-21451-7 28
- Van Eck N.J., Waltman L. Visualizing bibliometric networks. In: Ding Y., Rousseau R., Wolfram D. (Eds.). *Measuring Scholarly Impact: Methods and Practice*. Springer; 2014. P. 284–321. https://doi.org/10.1007/978-3-319-10377-8 13
- Van Eck N.J., Waltman L. Accuracy of citation data in Web of Science and Scopus. arXiv preprint arXiv:1906.07011. 2019. https://doi.org/10.48550/arXiv.1906.07011
- Erdös P., Rényi A. On random graphs I. *Publ. Math. Debrecen.* 1959;6:290–297. URL: https://studylib.net/doc/25387956/on-random-graphs--1959--by-p.-erdos-and-a.-renyi
- De Nooy W., Mrvar A., Batagelj V. Exploratory social network analysis with Pajek: Revised and epanded edition for updated software.
   Structural Analysis in the Social Sciences. Cambridge: Cambridge University Press; 2018. 484 p. https://doi.org/10.1017/9781108565691
- 23. Doreian P., Batagelj V., Ferligoj A. (Eds.). *Advances in network clustering and blockmodeling*. John Wiley & Sons; 2020. 414 p.
- Zuanazzi N.R., de Castilhos Ghisi N., Oliveira E.C. Analysis of global trends and gaps for studies about 2, 4-D herbicide toxicity: A scientometric review. *Chemosphere*. 2020;241:125016. https://doi.org/10.1016/j.chemosphere. 2019.125016
- 25. Сигов А.С., Андрианова Е.Г., Жуков Д.О., Зыков С.В., Тарасов И.Е. Квантовая информатика: обзор основных достижений. *Russ. Technol. J.* 2019;7(1):5–37. https://doi.org/10.32362/2500-316X-2019-7-1-5-37

### **About the authors**

**Sergey O. Kramarov,** Dr. Sci. (Phys.-Math.), Professor, Advisor to the President of the University, MIREA – Russian Technological University (78, Vernadskogo pr., Moscow, 119454 Russia); Chief Researcher, Surgut State University (22, Energetikov ul., Surgut, 628408 Russia). E-mail: maoovo@yandex.ru. Scopus Author ID 56638328000, ResearcherID E-9333-2016, https://orcid.org/0000-0003-3743-6513

**Oleg R. Popov**, Cand. Sci. (Eng.), Associate Professor, Expert-Analyst of the Temporary Scientific Team of the Department of Technology and Professional and Pedagogical Education, Southern Federal University (105/42, Bolshaya Sadovaya ul., Rostov-on-Don, 344006 Russia). E-mail: cs41825@aaanet.ru. ResearcherID AAT-8018-2021, http://orcid.org/0000-0001-6209-3554

**Ismail E. Dzhariev,** Junior Researcher, Postgraduate Student, Department of Automated Information Processing and Management Systems of the Polytechnic Institute, Surgut State University (22, Energetikov ul., Surgut, 628408 Russia). E-mail: dzhariev2 ie@edu.surgu.ru. https://orcid.org/0000-0003-4068-1050

**Egor A. Petrov,** Junior Researcher, Postgraduate Student, Department of Automated Information Processing and Management Systems of the Polytechnic Institute, Surgut State University (22, Energetikov ul., Surgut, 628408 Russia). E-mail: petrov2 ea@edu.surgu.ru. https://orcid.org/0000-0002-4151-197X

### Об авторах

**Крамаров Сергей Олегович,** д.ф.-м.н., профессор, советник президента университета, ФГБОУ ВО «МИРЭА – Российский технологический университет» (119454, Россия, Москва, пр-т Вернадского, д. 78); главный научный сотрудник, БУ ВО «Сургутский государственный университет» (628408, Россия, Сургут, ул. Энергетиков, д. 22). E-mail: maoovo@yandex.ru. Scopus Author ID 56638328000, ResearcherID E-9333-2016, https://orcid.org/0000-0003-3743-6513

**Попов Олег Русланович,** к.т.н., доцент, эксперт-аналитик временной научной группы кафедры технологии и профессионально-педагогического образования, ФГАОУ ВО «Южный федеральный университет» (344006, Россия, Ростов-на-Дону, ул. Б. Садовая, д. 105/42). E-mail: cs41825@aaanet.ru. ResearcherlD AAT-8018-2021, http://orcid.org/0000-0001-6209-3554

**Джариев Исмаил Эльшан оглы**, младший научный сотрудник, аспирант кафедры автоматизированных систем обработки информации и управления Политехнического института БУ ВО «Сургутский государственный университет» (628408, Россия, Сургут, ул. Энергетиков, д. 22). E-mail: dzhariev2\_ie@edu.surgu.ru. https://orcid.org/0000-0003-4068-1050

**Петров Егор Аркадьевич,** младший научный сотрудник, аспирант кафедры автоматизированных систем обработки информации и управления Политехнического института БУ ВО «Сургутский государственный университет» (628408, Россия, Сургут, ул. Энергетиков, д. 22). E-mail: petrov2\_ea@edu.surgu.ru. https://orcid.org/0000-0002-4151-197X

Translated from Russian into English by Lyudmila O. Bychkova Edited for English language and spelling by Thomas A. Beavitt

### Modern radio engineering and telecommunication systems Современные радиотехнические и телекоммуникационные системы

UDC 621.391.072 https://doi.org/10.32362/2500-316X-2023-11-3-30-37



### RESEARCH ARTICLE

# Effect of synchronization system errors on the reception noise immunity of amplitude-phase shift keyed signals

Gennady V. Kulikov <sup>1, @</sup>, Xuan Khang Dang <sup>1</sup>, Alexey G. Kulikov <sup>2</sup>

### Abstract

**Objectives.** An urgent task in the context of modern radio and television systems is to improve the quality and quantity of transmitted information. For example, the use of multiple amplitude-phase shift keyed (APSK) signals—16-APSK and 32-APSK—in digital satellite television systems of the Digital Video Broadcasting—Satellite2 (DVB-S2) standard made it possible to transmit 30% more data in the same frequency bands in comparison with the previous DVB-S standard. Such increases in information transmission rates impose more stringent requirements on hardware. An important role in the reception of APSK signals, as well as the signals of other coherent signal processing systems, is played by the stability of synchronization systems. The presence of operational errors can significantly reduce the quality of information reception. The aim of the present work was to analyze the effect of phase and clock synchronization errors on the reception noise immunity of APSK signals with a ring signal constellation structure.

**Methods.** The study used statistical radio engineering methods informed by optimal signal reception theory. **Results.** The effect of phase and clock synchronization errors on the reception noise immunity of APSK signals having a signal constellation ring structure is analyzed. The dependencies of the bit error probability on the magnitude of the phase shift and the clock offset were characterized. The effect of synchronization errors on reception quality were compared with the known results for quadrature amplitude modulation (QAM) signals.

**Conclusions.** At an acceptable energy loss of no more than 1 dB, the critical phase error can be considered as  $2^{\circ}-3^{\circ}$ , while the critical clock error is 3-4%. A coherent receiver of APSK signals is more sensitive to the phase error of reference oscillations than a similar receiver of QAM signals, whereas clock errors have the same effect on the reception quality of these signals.

Keywords: amplitude-phase shift keying, synchronization, phase error, clock error, noise immunity

• Submitted: 23.11.2022 • Revised: 14.12.2022 • Accepted: 03.03.2023

**For citation:** Kulikov G.V., Dang X.Kh., Kulikov A.G. Effect of synchronization system errors on the reception noise immunity of amplitude-phase shift keyed signals. *Russ. Technol. J.* 2023;11(3):30–37. https://doi.org/10.32362/2500-316X-2023-11-3-30-37

Financial disclosure: The authors have no a financial or property interest in any material or method mentioned.

The authors declare no conflicts of interest.

<sup>&</sup>lt;sup>1</sup> MIREA – Russian Technological University, Moscow, 119454 Russia

<sup>&</sup>lt;sup>2</sup> CGF, Moscow, 105082 Russia

<sup>&</sup>lt;sup>®</sup> Corresponding author, e-mail: kulikov@mirea.ru

### НАУЧНАЯ СТАТЬЯ

# Влияние погрешностей системы синхронизации на помехоустойчивость приема сигналов с амплитудно-фазовой манипуляцией

Г.В. Куликов <sup>1, @</sup>, С.Х. Данг <sup>1</sup>, А.Г. Куликов <sup>2</sup>

#### Резюме

**Цели.** Актуальной задачей современных систем радиосвязи и телевидения является повышение качества и количества передаваемой информации. Применение многопозиционных сигналов с амплитудно-фазовой манипуляцией (АФМ) 16-АФМ и 32-АФМ в системах цифрового спутникового телевидения стандарта DVB-S2 обеспечило возможность передачи на 30% больше данных в тех же полосах частот по сравнению с предыдущим стандартом DVB-S. Такое увеличение скорости передачи информации определило более жесткие требования к аппаратному обеспечению этих систем. Для приема сигналов АФМ, как и для многих других систем, использующих когерентную обработку сигналов, важную роль играет стабильность работы систем синхронизации. Наличие погрешностей в их работе может значительно снизить качество приема информации. Цель работы – анализ влияния погрешностей фазовой и тактовой синхронизации на помехоустойчивость приема сигналов с амплитудно-фазовой манипуляцией с кольцевой структурой сигнального созвездия.

**Методы.** Использованы методы статистической радиотехники и теории оптимального приема сигналов. **Результаты.** Проведен анализ влияния погрешностей фазовой и тактовой синхронизации на помехоустойчивость приема сигналов с амплитудно-фазовой манипуляцией с кольцевой структурой сигнального созвездия. Получены зависимости вероятности битовой ошибки от величины фазового сдвига и смещения тактовых моментов. Проведено сравнение влияния погрешностей синхронизации на качество приема с известными результатами для сигналов с квадратурной амплитудной модуляцией (КАМ).

**Выводы.** Установлено, что при допустимых энергетических потерях не более 1 дБ критической фазовой погрешностью можно считать величину 2–3 градуса, а критическая тактовая погрешность составляет 3–4%. Когерентный приемник сигналов АФМ более чувствителен к фазовой погрешности опорных колебаний, чем аналогичный приемник сигналов КАМ, а тактовые погрешности одинаково сказываются на качестве приема этих сигналов.

**Ключевые слова:** амплитудно-фазовая манипуляция, синхронизация, фазовая погрешность, тактовая погрешность, помехоустойчивость

• Поступила: 23.11.2022 • Доработана: 14.12.2022 • Принята к опубликованию: 03.03.2023

**Для цитирования:** Куликов Г.В., Данг С.Х., Куликов А.Г. Влияние погрешностей системы синхронизации на помехоустойчивость приема сигналов с амплитудно-фазовой манипуляцией. *Russ. Technol. J.* 2023;11(3):30-37. https://doi.org/10.32362/2500-316X-2023-11-3-30-37

**Прозрачность финансовой деятельности:** Авторы не имеют финансовой заинтересованности в представленных материалах или методах.

Авторы заявляют об отсутствии конфликта интересов.

<sup>1</sup> МИРЭА – Российский технологический университет, Москва, 119454 Россия

<sup>&</sup>lt;sup>2</sup> CGF, Москва, 105082 Россия

<sup>&</sup>lt;sup>®</sup> Автор для переписки, e-mail: kulikov@mirea.ru

### **INTRODUCTION**

A remaining challenge in contemporary radio and television systems consists in improving the quality and quantity of transmitted information. For example, multiple amplitude-phase shift keyed (APSK) 16-APSK and 32-APSK signals in the new-generation DVB-S2 digital satellite television systems can be used to transmit 30% more data than the previous DVB-S standard within the same frequency bands<sup>1</sup> [1]. Such increases in the information transmission rate have imposed additional requirements on the hardware used in these systems. As with other coherent signal processing systems, the stability of synchronization systems plays an important role is played in the reception of APSK signals. The presence of errors in their operation can significantly reduce the quality of information reception. The effect of synchronization errors on the reception noise immunity of multiple quadrature amplitude modulation (QAM) signals has been analyzed in previously published works [2-12]. In the present work, a study was made of the effect of phase and clock synchronization errors on the reception noise immunity of APSK signals having a ring signal constellation structure.

### **CALCULATION PROCEDURE**

Let us write a model of an APSK signal in clock cycle time  $T_s$  in the form

$$s_i(t) = A_{av} r_i \cos(\omega_0 t + \varphi_i), t \in (0, T_s], i = \overline{0, M - 1},$$
 (1)

where  $A_{\rm av}$  is the average signal amplitude;  $\omega_0$  is the carrier frequency;  $r_i$  and  $\varphi_i$  are quantities determining the amplitude and phase of the signal, respectively; and M is the number of the constellation points.

Let us consider the operation of a multichannel coherent receiver of APSK signals (Fig. 1) [13, 14] in the presence of white Gaussian noise n(t) with parameters

$$< n(t) > = 0; < n(t_1)n(t_2) > = \frac{N_0}{2}\delta(t_2 - t_1),$$

where  $N_0$  is the one-sided noise power spectral density,  $\delta$  is the delta function, and  $t_1$  and  $t_2$  are moments of time.

The receiver correlators calculate the convolution integrals

$$J_{i} = \frac{2}{N_{0}} \int_{0}^{T_{s}} x(t) s_{\text{ref}i}(t) dt, \ i = \overline{0, M - 1}$$
 (2)

of the received process  $x(t) = s_i(t) + n(t)$  with reference signals  $s_{\text{ref}i}(t)$ . Comparison of the received  $J_i$  values and their combinations with the thresholds set in the solver (maximum selection unit) allows one to determine the transmitted channel symbol.

The probability of erroneous reception of any (*m*th) channel symbol is found under the condition  $J_m > \{J_i + \delta_{mi}\}; i \neq m; i, m = \overline{0, M - 1}, \text{ namely,}$ 

$$P_{\text{es}\,m} = 1 - \prod_{\substack{i=0\\ m \neq i}}^{M-1} p(J_m - J_i > \delta_{mi}) \Big|_m, \tag{3}$$

where  $p(J_m - J_i > \delta_{mi})|_m$  is the probability that the output value of the *m*th correlator is higher than the output value of any other (*i*th) correlator, provided that the *m*th symbol

was transmitted; 
$$\delta_{mi} = \frac{E_{s_m} - E_{s_i}}{N_0} = \frac{E_{s \text{ av}}}{N_0} (r_m^2 - r_i^2) =$$

$$= \frac{E_b \log_2 M}{N_0} (r_m^2 - r_i^2)$$
 is the decision threshold;  $E_b$  is the average signal energy per 1 bit of information; and  $E_{s_m}$  and  $E_s$  are the energies of the *m*th and *i*th signal

and  $E_{s_i}$  are the energies of the *m*th and *i*th signal transmissions, respectively;  $E_{\rm s}$  av is the average energy of signal transmissions.

The probabilities  $p(J_m - J_i > \delta_{mi})|_m$  can be calculated by determining the statistical characteristics  $J_i$  of the distributions of random processes and their linear combinations—means  $m_{mi}$  and variances  $D_{mi}$  [15]:

$$p(I_m - I_i > \delta_i)\Big|_m = 1 - Q\left(\frac{m_{mi}}{\sqrt{D_{mi}}}\right),$$

$$Q(x) = \frac{1}{\sqrt{2\pi}} \int_{-\infty}^{\infty} e^{-t^2/2} dt,$$
 (4)

where Q(x) is the Q-function.

The bit error probability using the Gray code can be found from the relation [13]

$$P_{\rm eb} = \frac{P_{\rm es}}{\log_2 M}.$$
 (5)

The presence of errors in the generation of reference signals  $s_{\text{refi}}(t)$  causes errors in the calculation of correlation integrals (2) and, as a result, an increase in error probabilities (3) and (5).

### EFFECT OF THE PHASE ERROR IN THE REFERENCE OSCILLATION GENERATION UNIT

The phase error  $s_{\text{refi}}(t)$  of the reference oscillation generation unit is caused by additional phase shift  $\phi$ ,

<sup>&</sup>lt;sup>1</sup> DVB. https://www.dvb.org/standards/dvb-s2x. Accessed December 20, 2022.

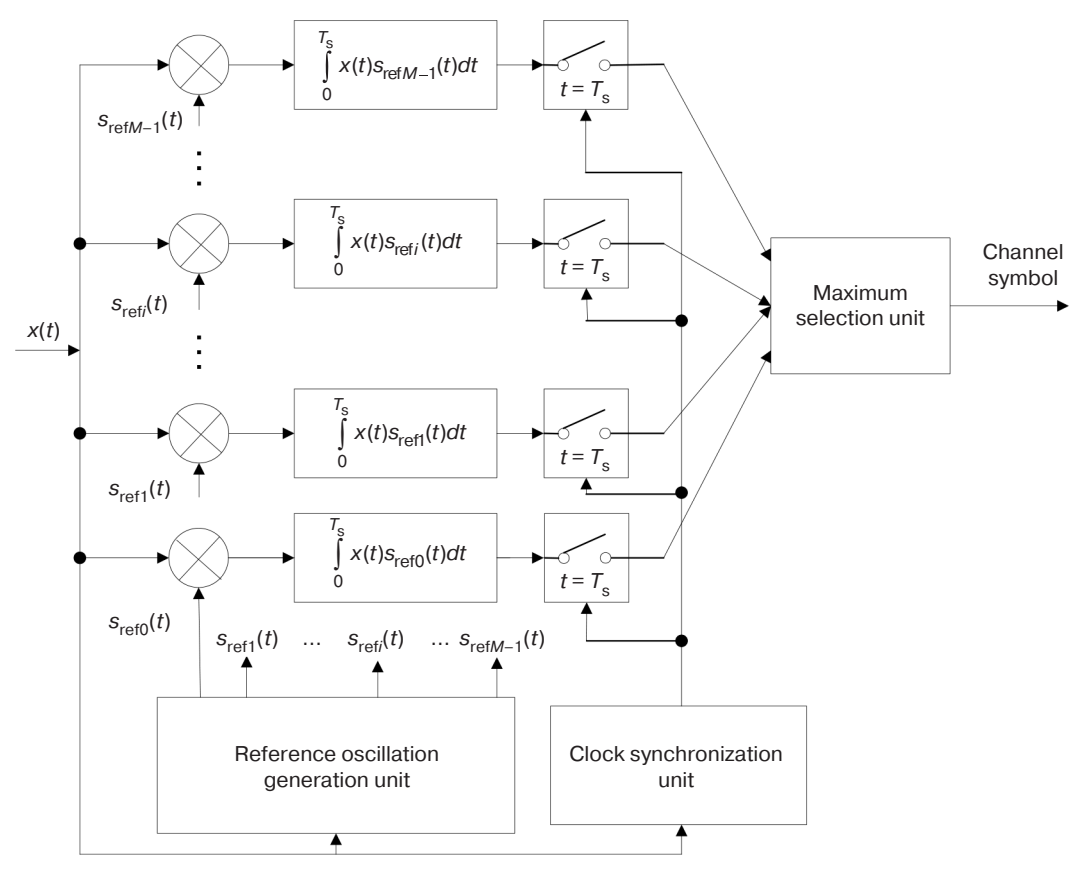


Fig. 1. Flowchart of a multichannel coherent receiver of APSK signals

e.g., due to the nonideality of the characteristics of the phase-locked loop system:

$$s_{\text{ref}i}(t) = A_{\text{av}}r_i\cos(\omega_0 t + \varphi_i + \phi), \ i = \overline{0, M - 1}.$$

Figure 2 presents an example of the effect of such a shift on the shape of the signal constellation of a 16-APSK signal.

In this case, the means  $m_{mi}$  and variances  $D_{mi}$  in expression (4) have the form

$$m_{mi} = \frac{E_{\text{s av}}}{N_0} (2r_m^2 \cos \phi - 2r_m r_i \cos(\phi_m - \phi_i - \phi) - r_m^2 + r_i^2),$$

$$D_{mi} = \frac{2E_{\text{s av}}}{N_0} (r_m^2 + r_i^2 - 2r_m r_i \cos(\varphi_m - \varphi_i)).$$

Calculation of the bit error probability from formulas (3)–(5) for signals 16-APSK and 32-APSK gives the following results (Figs. 3 and 4).

It can be seen that, at a small phase shift of  $\phi < \pi/90$  (2°), the bit error probability decreases insignificantly, but with an increase in the phase shift, the noise immunity noticeably deteriorates, and at  $\phi > \pi/45 = 4^\circ$ , the  $P_{\rm eb}$  value can increase by an order of magnitude. Calculations show that, for  $P_{\rm eb} = 10^{-4}$  at  $\phi = \pi/36 = 5^\circ$ , this is equivalent

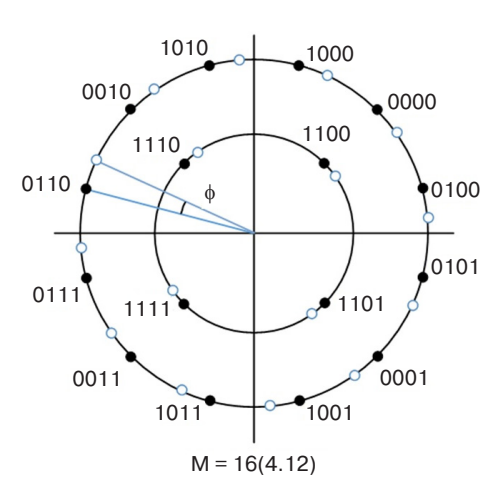
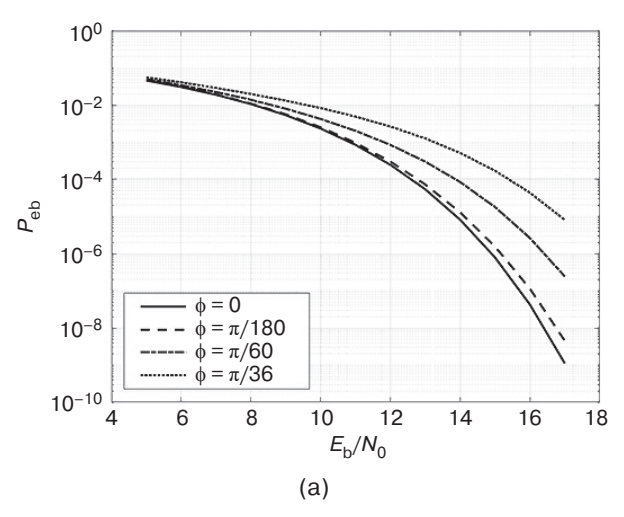


Fig. 2. Change in the signal constellation of a 16-APSK signal in the presence of phase shift φ

to energy losses of about 2.5 and 3.0 dB at M = 16 and 32, respectively.

A comparison of the results of this work with the published results [5, 9] for QAM signals shows that, at the same M, the coherent reception of signals with the square shape of the signal constellation is somewhat more resistant to phase errors in reference oscillations than that of signals with the ring shape of the signal constellation. For example, at  $\phi = \pi/60 = 3^{\circ}$  and  $P_{\rm eb} = 10^{-4}$ , the energy losses are 1.0 dB and 1.2 dB, respectively.



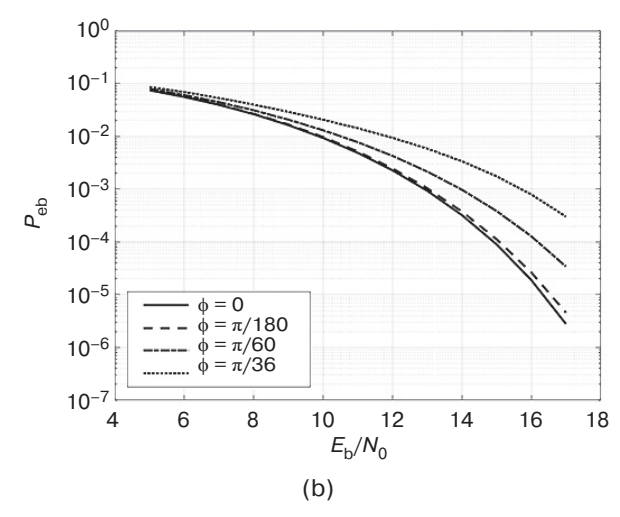
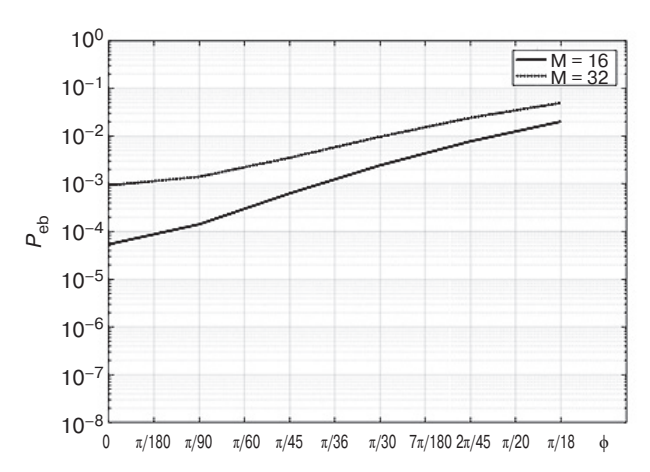


Fig. 3. Dependence of the bit error probability on the signal-to-noise ratio at phase shift φ of reference oscillations for (a) 16-APSK and (b) 32-APSK signals



**Fig. 4.** Dependence of the bit error probability on the phase shift  $\phi$  of reference oscillations at  $E_{\rm h}/N_0=13$  dB

### EFFECT OF THE CLOCK OFFSET IN THE CLOCK SYNCHRONIZATION UNIT

Errors in the clock synchronization unit can lead to certain clock offset  $\xi$  in the clock cycle time  $T_s$ , which determines the limits of integration in expression (2).

In this case, the convolution integrals

$$J_i = \frac{2A_{\text{av}}}{N_0} \int_{\xi}^{T_{\text{s}} + \xi} x(t)r_i \cos(\omega_0 t + \varphi_i) dt$$

are calculated at the following parameters of the received and reference signals:

$$s(t) = \begin{cases} A_{\text{av}} r_i \cos(\omega_0 t + \varphi_i), & t \in (\xi, T_{\text{s}}), \\ A_{\text{av}} r_i \cos(\omega_0 t + \varphi_i), & t \in [T_{\text{s}}, T_{\text{s}} + \xi), \end{cases}$$

$$s_{\text{ref}i}(t) = A_{\text{av}}r_i\cos(\omega_0 t + \varphi_i), t \in (\xi, T_s + \xi),$$

where the subscript *j* refers to the next channel symbol.

In this case, the means  $m_{mi}$  and variances  $D_{mi}$  in expression (4) take the form

$$\begin{split} m_{mi} &= \frac{2E_{\text{s av}}}{N_0} r_m \left( 1 - \frac{\xi}{T_{\text{s}}} \right) (r_m - r_i \cos(\varphi_m - \varphi_i)) + \\ &+ \frac{2E_{\text{s av}}}{N_0} r_j \frac{\xi}{T_{\text{s}}} (r_m \cos(\varphi_j - \varphi_m) - \\ &- r_i \cos(\varphi_j - \varphi_i)) - \frac{E_{\text{s av}}}{N_0} (r_m^2 - r_i^2), \end{split}$$

$$D_{mi} = \frac{2E_{\text{s av}}}{N_0} (r_m^2 + r_i^2 - 2r_m r_i \cos(\varphi_m - \varphi_i)).$$

Figures 5 and 6 illustrate the dependences of the bit error probability at various clock offsets.

One can see that a large error in the clock synchronization system significantly reduces the noise immunity of reception of APSK signals. For example, for

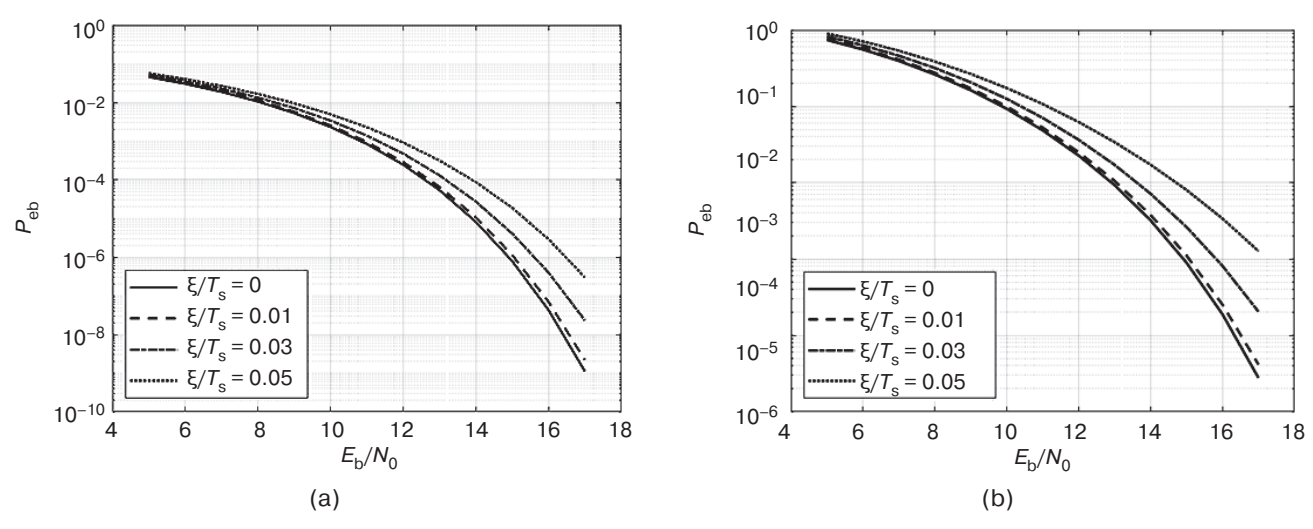


**Fig. 5.** Dependence of the bit error probability on the signal-to-noise ratio at various clock offsets  $\xi/T_s$  for (a) 16-APSK and (b) 32-APSK signals

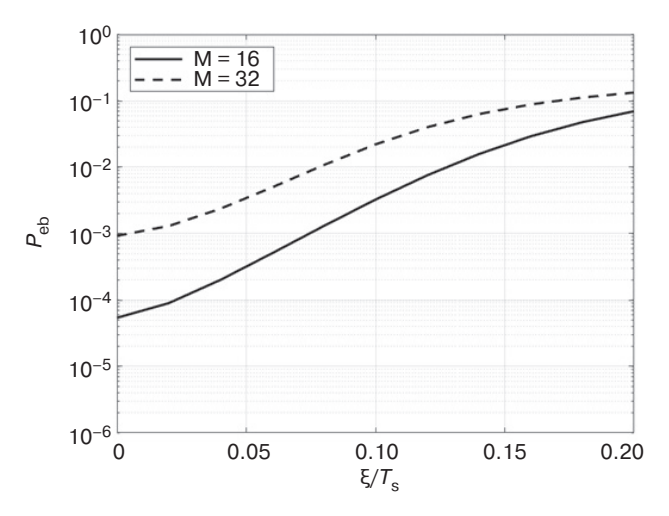


**Fig. 6.** Dependence of the bit error probability on the clock offset  $\xi/T_s$  at  $E_b/N_0 = 13$  dB

 $P_{\rm eb}$  = 10<sup>-4</sup> already at  $\xi/T_{\rm s}$  = 0.05 (or 5%), the equivalent energy loss is about 1.5 and 2.0 dB at M = 16 and 32, respectively.

A previous similar analysis of QAM signals [5, 9] showed that clock errors have the same effect on the reception quality of QAM and APSK signals.

### **CONCLUSIONS**

From the obtained results, the following conclusions can be drawn.

1) The presence of a phase shift of reference oscillations during the coherent reception of APSK signals can noticeably deteriorate the noise immunity. At an acceptable energy loss of no more than 1 dB, the

critical phase error can be considered as around  $2^{\circ}-3^{\circ}$ .

- 2) The presence of an error in the clock synchronization unit during the coherent reception of APSK signals can also significantly reduce the noise immunity. At an acceptable energy loss of no more than 1 dB, the critical clock error can be considered to be 3–4%.
- 3) Although a coherent receiver of APSK signals is more sensitive to phase errors of reference oscillations than a similar receiver of QAM signals, clock errors affect the reception quality of these signals in the same way.

**Authors' contribution.** All authors equally contributed to the research work.

## **REFERENCES**

- 1. Minoli D. *Innovations in satellite communications and satellite technology: The industry implications of DVB-S2X, High Throughput Satellites, Ultra HD, M2M, and IP.* New York: John Wiley & Sons; 2015. 448 p. ISBN 978-1-118-98408-6
- 2. Savishchenko N.V. Noise immunity of coherent reception of multi-position QAM and PSK signals in the case of non-ideal synchronization. *Informatsionno-upravlyayushchie sistemy = Information and Control Systems*. 2010;1(44):53–63 (in Russ.).
- 3. Artemenko A.A., Maltsev A.A., Rubtsov A.E. Effect of the carrier-phase estimation error on the bit-error rate in M-QAM data transmission systems. *Vestnik Nizhegorodskogo universiteta im. N.I. Lobachevskogo = Vestnik of Lobachevsky University of Nizhny Novgorod.* 2007;2:81–87 (in Russ.).
- 4. Kulikov G.V., Van Dung N. Influence of synchronization errorsonthenoise immunity of coherent reception of M-PSK signals. *Russ. Technol. J.* 2019;7(5):47–61 (in Russ.). https://doi.org/10.32362/2500-316X-2019-7-5-47-61
- Kulikov G.V., Lelyukh A.A., Batalov E.V. Influence of phase and clock synchronization errors on the noise immunity of coherent reception of signals with quadrature amplitude modulation. *Russ. Technol. J.* 2021;9(2): 35–43 (in Russ.). https://doi.org/10.32362/2500-316X-2021-9-2-35-43
- 6. Dovbnya V.G., Sevryukov A.E. Influence of performance quality of clock synchronization system on noise immunity of QAM signal reception. *Telekommunikatsii* = *Telecommunications*. 2016;4:43–47 (in Russ.).
- 7. Saeedi-Sourck H., Sadri S., Wu Y., Bergmans J.W.M., Farhang-Boroujeny B. Sensitivity analysis of offset QAM multicarrier systems to residual carrier frequency and timing offsets. *Signal Process*. 2011;91(7):1604–1612. https://doi.org/10.1016/j.sigpro.2010.12.019
- Chung W., Kim B., Choi M., Nam H., Yu H., Choi S., Hong D. Synchronization error in QAM-based FBMC system. In: 2014 IEEE Military Communications Conference. 2014. P. 699–705. https://doi.org/10.1109/ MILCOM.2014.122
- Kulikov G.V., Van Dung N., Kulagin V.P., Lelyukh A.A. Influence of synchronization errors on the noise immunity of receiving multi-position M-PSK and M-QAM signals. In: 2020 Systems of Signal Synchronization, Generating and Processing in Telecommunications (SYNCHROINFO). 2020:9166034. https://doi.org/10.1109/ SYNCHROINFO49631.2020.9166034
- Teng K., Zhang Y., Yuan X., Liu Q. Implementation of a novel M-QAM OFDM timing synchronization method with FSO RoF system. In: 2019 7th International Conference on Information, Communication and Networks (ICICN). 2019. P. 48–52. https://doi.org/10.1109/ ICICN.2019.8834953
- 11. Huang Y., Song Q., Wang S., Jamalipour A. Symbol error rate analysis for M-QAM modulated physical-layer network coding with phase errors. In: 2012 IEEE 23rd International Symposium on Personal, Indoor and Mobile Radio Communications (PIMRC). 2012. P. 2003—2008. https://doi.org/10.1109/PIMRC.2012.6362683

## СПИСОК ЛИТЕРАТУРЫ

- 1. Minoli D. Innovations in satellite communications and satellite technology: The industry implications of DVB-S2X, High Throughput Satellites, Ultra HD, M2M, and IP. New York: John Wiley & Sons; 2015. 448 p. ISBN 978-1-118-98408-6
- 2. Савищенко Н.В. Помехоустойчивость когерентного приема многопозиционных сигналов КАМ и ФМ при неидеальной синхронизации. *Информационно-управляющие системы*. 2010;1(44):53–63.
- 3. Артеменко А.А., Мальцев А.А., Рубцов А.Е. Влияние неточности оценивания фазы несущей на вероятность битовых ошибок в М-КАМ системах передачи данных. Вестник Нижегородского университета им. Н.И. Лобачевского. 2007;2:81–87.
- 4. Куликов Г.В., Ван Зунг Н. Влияние погрешностей синхронизации на помехоустойчивость когерентного приема сигналов М-ФМ. *Russ. Technol. J.* 2019;7(5):47–61. https://doi.org/10.32362/2500-316X-2019-7-5-47-61
- 5. Куликов Г.В., Лелюх А.А., Баталов Е.В. Влияние погрешностей фазовой и тактовой синхронизации на помехоустойчивость когерентного приема сигналов с квадратурной амплитудной модуляцией. *Russ. Technol. J.* 2021;9(2):35–43. https://doi.org/10.32362/2500-316X-2021-9-2-35-43
- 6. Довбня В.Г., Севрюков А.Е. Влияние качества функционирования системы тактовой синхронизации на помехоустойчивость приема КАМ-сигналов. *Телеком-муникации*. 2016:4:43–47.
- Saeedi-Sourck H., Sadri S., Wu Y., Bergmans J.W.M., Farhang-Boroujeny B. Sensitivity analysis of offset QAM multicarrier systems to residual carrier frequency and timing offsets. *Signal Process*. 2011;91(7):1604–1612. https://doi.org/10.1016/j.sigpro.2010.12.019
- Chung W., Kim B., Choi M., Nam H., Yu H., Choi S., Hong D. Synchronization error in QAM-based FBMC system. In: 2014 IEEE Military Communications Conference. 2014. P. 699–705. https://doi.org/10.1109/ MILCOM.2014.122
- Kulikov G.V., Van Dung N., Kulagin V.P., Lelyukh A.A. Influence of synchronization errors on the noise immunity of receiving multi-position M-PSK and M-QAM signals. In: 2020 Systems of Signal Synchronization, Generating and Processing in Telecommunications (SYNCHROINFO). 2020:9166034. https://doi. org/10.1109/SYNCHROINFO49631.2020.9166034
- Teng K., Zhang Y., Yuan X., Liu Q. Implementation of a novel M-QAM OFDM timing synchronization method with FSO RoF system. In: 2019 7th International Conference on Information, Communication and Networks (ICICN). 2019. P. 48–52. https://doi. org/10.1109/ICICN.2019.8834953
- 11. Huang Y., Song Q., Wang S., Jamalipour A. Symbol error rate analysis for M-QAM modulated physical-layer network coding with phase errors. In: 2012 IEEE 23rd International Symposium on Personal, Indoor and Mobile Radio Communications (PIMRC). 2012. P. 2003–2008. https://doi.org/10.1109/PIMRC.2012.6362683

- Matta M., Cardarilli G.C., Di Nunzio L., Fazzolari R. A reinforcement learning-based QAM/PSK symbol synchronizer. In: *IEEE Access*. 2019;7:124147–124157. https://doi.org/10.1109/ACCESS.2019.2938390
- Proakis J.G. Digital communications. 4th ed. McGraw-Hill; 2001. 1002 p.
- 14. Fuqin Xiong. *Digital modulation techniques*. 2nd ed. Boston, London: Artech House; 2006. 1039 p.
- 15. Tikhonov V.I. *Statisticheskaya radiotekhnika (Statistical radio engineering*). 2nd ed. Moscow: Radio i svyaz'; 1982. 624 p. (in Russ.).
- Matta M., Cardarilli G.C., Di Nunzio L., Fazzolari R. A reinforcement learning-based QAM/PSK symbol synchronizer. In: *IEEE Access*. 2019;7:124147–124157. https://doi.org/10.1109/ACCESS.2019.2938390
- Proakis J.G. Digital communications. 4th ed. McGraw-Hill; 2001. 1002 p.
- 14. Fuqin Xiong. *Digital modulation techniques*. 2nd ed. Boston, London: Artech House; 2006. 1039 p.
- 15. Тихонов В.И. Статистическая радиотехника. 2-е изд., перераб. и доп. М.: Радио и связь; 1982. 624 с.

## About the authors

**Gennady V. Kulikov,** Dr. Sci. (Eng.), Professor, Department of Radio Electronic Systems and Complexes, Institute of Radio Electronics and Informatics, MIREA – Russian Technological University (78, Vernadskogo pr., Moscow, 119454 Russia). E-mail: kulikov@mirea.ru. Scopus Author ID 36930533000, RSCI SPIN-code 2844-8073, http://orcid.org/0000-0001-7964-6653

**Xuan Khang Dang,** Postgraduate Student, Department of Radio Electronic Systems and Complexes, Institute of Radio Electronics and Informatics, MIREA – Russian Technological University (78, Vernadskogo pr., Moscow, 119454 Russia). E-mail: dangxuankhang147@gmail.com. https://orcid.org/0000-0002-3372-7172

**Alexey G. Kulikov,** CGF employee (73/1, Bakuninskaya ul., Moscow, 105082 Russia). E-mail: onemoreuser@yandex.ru. https://orcid.org/0000-0002-8241-9619

## Об авторах

**Куликов Геннадий Валентинович,** д.т.н., профессор, кафедра радиоэлектронных систем и комплексов Института радиоэлектроники и информатики ФГБОУ ВО «МИРЭА – Российский технологический университет» (119454, Россия, Москва, пр-т Вернадского, д. 78). E-mail: kulikov@mirea.ru. Scopus Author ID 36930533000, SPIN-код РИНЦ 2844-8073, http://orcid.org/0000-0001-7964-6653

**Данг Суан Ханг,** аспирант, кафедра радиоэлектронных систем и комплексов Института радиоэлектроники и информатики ФГБОУ ВО «МИРЭА – Российский технологический университет» (119454, Россия, Москва, пр-т Вернадского, д. 78). E-mail: dangxuankhang147@gmail.com. https://orcid.org/0000-0002-3372-7172

**Куликов Алексей Геннадьевич,** сотрудник компании CGF (105082, Россия, Москва, Бакунинская улица, д. 73, стр. 1). E-mail: onemoreuser@yandex.ru. https://orcid.org/0000-0002-8241-9619

Translated from Russian into English by Vladislav V. Glyanchenko Edited for English language and spelling by Thomas A. Beavitt

## Micro- and nanoelectronics. Condensed matter physics Микро- и наноэлектроника. Физика конденсированного состояния

UDC 538.913 https://doi.org/10.32362/2500-316X-2023-11-3-38-45



RESEARCH ARTICLE

## Dispersion of optical constants of Si:PbGeO crystal in the terahertz range

Vladislav R. Bilyk <sup>1</sup>, Kirill A. Brekhov <sup>1, @</sup>, Mikhail B. Agranat <sup>2</sup>, Elena D. Mishina <sup>1</sup>

## Abstract

**Objectives.** Advances in laser physics over the last decade have led to the creation of sources of single-period electromagnetic pulses having a duration of about 1 ps, corresponding to the terahertz (THz) frequency range and a field amplitude of several tens of MV/cm. This allows the electrode-free application of an electric field to a ferroelectric for observing not only the excitation of coherent phonons, but also ultrafast (at the sub-picosecond timescale) dynamic polarization switching. To detect polarization switching, a pump-probe technique is used in which a THz pulse is used with an optical probe. Since its intensity is proportional to the square of the polarization, the signal of the optical second harmonic is used to measure polarization switching under the action of a THz pulse. To evaluate switching efficiency, both linear (refractive index and absorption coefficient) and non-linear optical characteristics (quadratic and cubic susceptibilities) are required. For any application of ferroelectric crystals in the THz range, knowledge of the relevant linear optical characteristics is also necessary.

**Methods.** The technique of THz spectroscopy in the time domain was used; here, a picosecond THz pulse transmitted through the crystal is recorded by strobing the detector with a femtosecond optical pulse. The THz -induced dynamics of the order parameter in a ferroelectric was studied by detecting the intensity of a nonlinear optical signal at the frequency of the optical second harmonic.

**Results.** The transmission of a THz wave and the intensity of second harmonic generation on a lead germanate crystal doped with silicon in the time and spectral domains were measured. On this basis, the absorption coefficient dispersion and cubic nonlinear susceptibility were calculated in the range of 0.5–2.0 THz. The presence of a region of fundamental absorption near the phonon modes was confirmed along with a resonant enhancement of the cubic nonlinear susceptibility for two phonon modes  $\Omega_1$  = 1.3 THz and  $\Omega_2$  = 2.0 THz.

**Conclusions.** The proposed technique is effective for analyzing the dispersion of the optical characteristics of ferroelectric crystals. The significantly improved spectral resolution (0.1 THz) increases the accuracy of determining nonlinear susceptibility due to the detailed analysis of the linear and nonlinear contributions to the second harmonic intensity.

Keywords: terahertz radiation, ferroelectrics, spectroscopy, optical second harmonic generation

<sup>&</sup>lt;sup>1</sup> MIREA – Russian Technological University, Moscow, 119454 Russia

<sup>&</sup>lt;sup>2</sup> Joint Institute for High Temperatures, Russian Academy of Sciences, Moscow, 125412 Russia

<sup>@</sup> Corresponding author, e-mail: brekhov ka@mail.ru

• Submitted: 12.12.2022 • Revised: 14.01.2023 • Accepted: 24.02.2023

For citation: Bilyk V.R., Brekhov K.A., Agranat M.B., Mishina E.D. Dispersion of optical constants of Si:PbGeO crystal in the terahertz range. *Russ. Technol. J.* 2023;11(3):38–45. https://doi.org/10.32362/2500-316X-2023-11-3-38-45

Financial disclosure: The authors have no a financial or property interest in any material or method mentioned.

The authors declare no conflicts of interest.

## НАУЧНАЯ СТАТЬЯ

## Дисперсия оптических характеристик кристалла Si:PbGeO в терагерцовом диапазоне

В.Р. Билык <sup>1</sup>, К.А. Брехов <sup>1, @</sup>, М.Б. Агранат <sup>2</sup>, Е.Д. Мишина <sup>1</sup>

## Резюме

**Цели.** Успехи лазерной физики последнего десятилетия привели к созданию источников однопериодных электромагнитных импульсов длительностью порядка 1 пс, что соответствует терагерцовому (ТГц) диапазону частот, с амплитудой поля в несколько десятков МВ/см. Это позволило приложить электрическое поле к сегнетоэлектрику без электродов и наблюдать не только возбуждение когерентных фононов, но и сверхбыстрое, в субпикосекундном масштабе времени, динамическое переключение поляризации. Для обнаружения переключения поляризации используется метод накачки-зондирования, где в качестве накачки используется ТГц-импульс, а зонд является оптическим. Мерой переключения поляризации под действием ТГц-импульса служит сигнал оптической второй гармоники, поскольку ее интенсивность пропорциональна квадрату поляризации. Для оценки эффективности переключения требуются как линейные (показатель преломления и коэффициент поглощения), так и нелинейные оптические характеристики (квадратичная и кубичная восприимчивости). Знание линейных оптических характеристик необходимо также для любых применений рассматриваемых кристаллов в ТГц-диапазоне.

**Методы.** Использована методика терагерцовой спектроскопии во временной области, в которой на вещество направляется пикосекундный ТГц-импульс, а регистрируется ТГц-импульс, прошедший через вещество, путем стробирования детектора фемтосекундным оптическим импульсом. Исследование ТГц-индуцированной динамики параметра порядка в сегнетоэлектрике проводилось путем детектирования интенсивности нелинейно-оптического сигнала на частоте второй оптической гармоники.

**Результаты.** На кристалле германата свинца, легированного кремнием, измерены пропускание ТГц-волны и интенсивность генерации второй гармоники во временной и спектральной областях, на основании чего рассчитаны дисперсия коэффициента поглощения и кубичной нелинейной восприимчивости в диапазоне 0.5–2.0 ТГц. Обнаружено наличие области фундаментального поглощения вблизи фононных мод, а также резонансное усиление кубичной нелинейной восприимчивости для двух фононных мод  $\Omega_1 = 1.3$  ТГц и  $\Omega_2 = 2.0$  ТГц.

**Выводы.** Предложенная методика эффективна для анализа дисперсии оптических характеристик сегнетоэлектрических кристаллов. Существенно улучшено спектральное разрешение, составляющее в данной работе 0.1 ТГц, а также точность определения нелинейной восприимчивости за счет детального анализа линейного и нелинейного вкладов в интенсивность второй гармоники.

**Ключевые слова:** терагерцовое излучение, сегнетоэлектрики, спектроскопия, генерация второй оптической гармоники

<sup>1</sup> МИРЭА – Российский технологический университет, Москва, 119454 Россия

<sup>&</sup>lt;sup>2</sup> Объединенный институт высоких температур Российской академии наук, Москва, 125412 Россия

<sup>&</sup>lt;sup>®</sup> Автор для переписки, e-mail: brekhov ka@mail.ru

• Поступила: 12.12.2022 • Доработана: 14.01.2023 • Принята к опубликованию: 24.02.2023

**Для цитирования:** Билык В.Р., Брехов К.А., Агранат М.Б., Мишина Е.Д. Дисперсия оптических характеристик кристалла Si:PbGeO в терагерцовом диапазоне. *Russ. Technol. J.* 2023;11(3):38-45. https://doi.org/10.32362/2500-316X-2023-11-3-38-45

**Прозрачность финансовой деятельности:** Авторы не имеют финансовой заинтересованности в представленных материалах или методах.

Авторы заявляют об отсутствии конфликта интересов.

## INTRODUCTION

Lead germanate crystals (Pb<sub>5</sub>Ge<sub>3</sub>O<sub>11</sub>, PGO) are uniaxial ferroelectrics having a Curie temperature  $T_{\rm C}$  = 450 K [1]. Along with silicon-containing solid solutions based on them, these crystals exhibit features of spontaneous polarization switching as well as pyroelectric and photorefractive effects that have a number of potential applications. By changing the silicon concentration in the solid solution, the Curie point can be controlled in order to transfer the main features into the temperature range from room temperature to  $T_C$ , thus significantly expanding the potential areas of application of these crystals, including as elements of pyroelectric receivers and ferroelectric memory devices. While a number of works deal with the structure of these materials, as well as their dielectric, piezo- and pyroelectric, mechanical, and other properties, these have mainly been focused on the low-frequency region [2].

The frequency domain of 1–10 THz is of great interest for studying ferroelectrics, since it is in this domain that phonon modes, including soft phonon mode, occur. Until recently, the Raman spectroscopy technique has mainly been used to study incoherent processes in this domain [3, 4].

Advances in laser physics taking place over the last decade have led to the creation of sources of single-period electromagnetic pulses with a duration of about 1 ps, which corresponds to the terahertz (THz) frequency range and a field amplitude of several tens of MV/cm. By this means, an electric field can be applied to a ferroelectric without electrodes to observe not only the excitation of coherent phonons, but also ultrafast (at the sub-picosecond timescale) dynamic polarization switching. To detect polarization switching, a pump-probe method is used, in which a THz pulse is used as pump while the probe is either optical or X-ray. The theory of coherent oscillation generation in THz pump-probe spectroscopy is described in [5].

As well as being used to distinguish between linear and nonlinear modes of mode oscillations [6, 7], the optical probe is capable of detecting dynamic and permanent polarization switching if the latter occurs [8]. The measure of polarization switching under the action

of a THz pulse serves as the optical second harmonic SHsignal, its intensity being proportional to the square of polarization. Both linear (refractive index and absorption coefficient) and nonlinear optical characteristics (quadratic and cubic susceptibilities) are required for evaluating switching efficiency. For any applications of the crystals under consideration in the THz range, it is necessary to obtain information concerning their linear optical characteristics.

THz time domain spectroscopy (THz-TDS), in which the passage of a picosecond THz pulse through the substance is registered by gating the detector with a femtosecond optical pulse, is applicable for determining both linear and nonlinear optical constants. Since the generation and detection schemes are sensitive to the effect of the sample on both the amplitude and the phase of the registered THz radiation, it can be used to obtain both real and imaginary parts of optical constants.

The THz-TDS technique is widely used to determine the dispersion of optical constants, especially in organic materials (see review [9]). While certain successes have also been achieved in the study of phonon modes of ferroelectric crystals [10, 11], the results obtained by the majority of studies are based on low-power THz sources with standard parameters providing so-called broadband spectroscopy, where the generated spectrum region when pumped by a picosecond pulse is 0.5–2 THz with a center in the 1 THz region. However, in many ferroelectric materials, the phonon spectrum—including the most interesting soft mode—lies in the region above 1.5 THz.

In this connection, PGO represents a truly unique material, its pronounced ferroelectric properties occurring at a relatively high phase transition temperature (about 450 K) with a soft-mode frequency close to 1 THz; thus, there is a fairly wide range of phonon modes falling within the operating range of desktop installations. Results of a previous study [12] into PGO crystal using broadband spectroscopy with spectral resolution of 0.25 THz include a determination of the spectral dependencies of the electrically-induced optical SH.

In the present paper, narrow-band THz spectroscopy is used for the first time to determine the absorption

coefficient and nonlinear (cubic) susceptibility of a silicon-doped PGO crystal. The accuracy of nonlinear susceptibility determination is substantially improved by carrying out a detailed analysis of linear and nonlinear contributions to the SH intensity obtained at a spectral resolution of 0.1 THz.

## **EXPERIMENT**

The silicon-doped PGO crystal Pb<sub>5</sub>(Ge $_{0.74}$ Si $_{0.26}$ ) $_3$ O $_{11}$  (made and provided by A.A. Bush, MIREA – Russian Technological University, Russia) is used for experimental studies. At this stoichiometric composition, the Curie temperature decreases to 346 K, as compared to the undoped crystal [2]. The thickness of the crystal under study is ~1.1 mm. The crystallographic orientation of the surface is (100); at this orientation, the polarization vector is aligned in the surface plane. The phonon spectrum of the crystal under study allows exciting effectively several frequencies of crystal lattice vibrations lying in the range of exciting THz radiation including the soft phonon mode frequency [13].

The narrow-band THz pulses generated using the Cr:forsterite laser system described in [12] have a wavelength of 1240 nm, pulse repetition rate of 10 Hz, and duration of 100 fs. The organic crystal OH1 serves as the generator of THz pulses [14].

For generating narrow-band THz pulses, the amplified laser pulse is divided into two, each passing through one of the arms of the Mach–Zehnder type interferometer. By varying the delay between these pulses before their subsequent compression in the compressor, beating

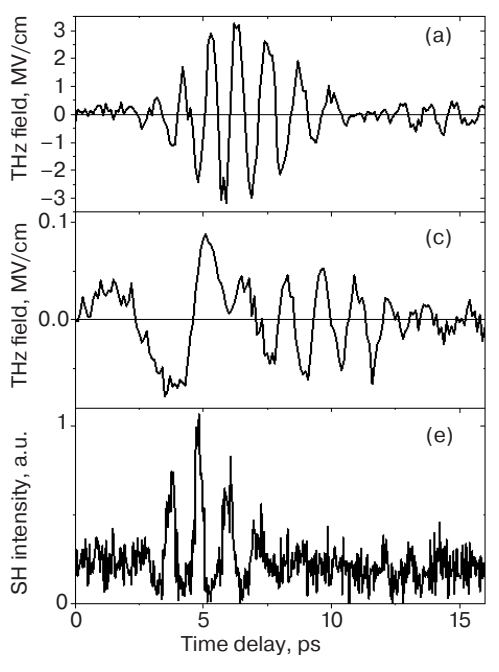
optical pulses can be generated at a given frequency. The resulting frequency-modulated optical chirp irradiates the OH1 crystal to generate narrowband THz radiation [15]. The broadband pulse energy of 90  $\mu$ J is sufficient to generate narrowband radiation having a spectral width of ~200 GHz. According to measurements of the electric field strength profile using the THz-TDS method, such pulses, which comprise ~5 periods, have a duration of about 5 ps. The energy of the THz wave as measured by the Golay cell averages 4  $\mu$ J.

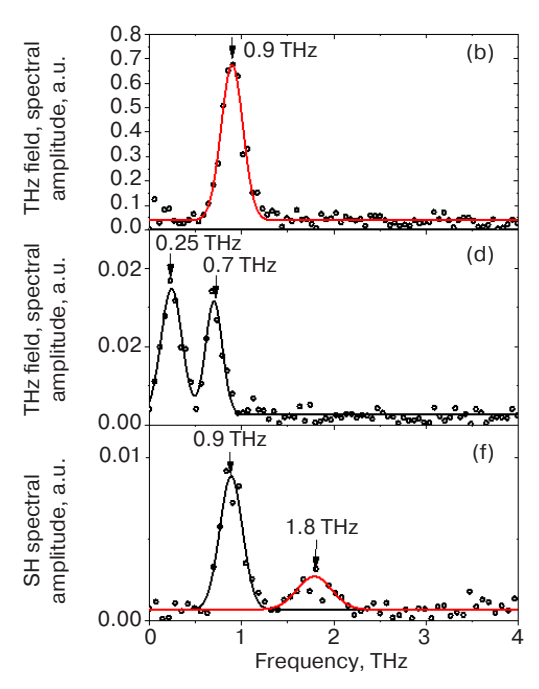
The THz-induced dynamics of the order parameter in the ferroelectric is studied by detecting the nonlinear optical signal intensity at the optical SH frequency [12].

Figure 1 depicts the typical time and spectral shapes of the incident THz wave, the THz wave passed through the sample, and the optical SH wave induced by the electric field of the THz pulse.

The energy of the incident wave changes (to a maximum at the frequency of 1.2 THz) when its frequency is changed. In the time shape (Fig. 1a), only the period changes, while the character of the dependence remains approximately the same for all frequencies in the range of 0.5–2.2 THz. For 0.9 THz, the pulse duration is ~8 ps. When trying to further increase the frequency, the signal becomes indistinguishable from noise. In the frequency domain (Fig. 1b), the pulse frequency shifts, its half-width changing weakly in the range of 0.25–0.3 THz (which corresponds to the observed pulse duration).

The crystal transforms the incident pulse significantly. The amplitude of the passed wave decreases sharply (at the incident wave frequency of 0.9 THz,





**Fig. 1.** For the 0.9 THz frequency, time (left) and spectral (right) dependencies of the incident THz wave (a), (b); of the THz wave passed through the sample (c), (d); of the optical SH wave induced by the electric field of THz pulse (e), (f)

the field amplitude is reduced by 30 times). Within the time dependence, the periodic function resembling the incident pulse is shifted by half of the pulse at its beginning while the aperiodic signal dominates. Accordingly, the frequency of 0.7 THz, i.e., decreased in comparison with the incident field frequency, appears in the spectrum of the passed THz pulse. In addition, the low-frequency component of 0.25 THz appears. It should be noted that 0.9 THz is the frequency of a sharp change in the transmittance character of THz radiation. At lower frequencies, a higher-frequency maximum dominates, its frequency approaching that of the incident wave. At higher frequencies, the pulse amplitude drops sharply, and only a low-frequency peak remains in the transmitted radiation. This corresponds to the absorption boundary found in broadband THz radiation in [12].

While the intensity of the SH looks like the incident pulse in the time domain, the two frequencies appearing in the frequency domain are those of the incident wave and its upper octave. This corresponds to quadratic dependence of the SH intensity on external field (on polarization in ferroelectrics) in the presence of the significant inactive by field contribution (non-switching polarization in ferroelectrics).

The SH intensity in the THz field can be represented as the decomposition either by the THz field  $E_{\Omega}$  in the case of a non-ferroelectric crystal, as follows:

$$I^{2\omega}(E_{\Omega}) \propto (\chi^{(2)} + \chi_{\rm E}^{(3)} E_{\Omega})^2 (I^{\omega})^2, \tag{1}$$

or by polarization  $P(E_{\Omega})$  in the case of ferroelectric crystal, as follows:

$$I^{2\omega}(P(E_\Omega)) \propto (P_0 + \chi_{\rm P}^{(3)} P(E_\Omega))^2 (I^\omega)^2, \qquad (2)$$

where  $\chi^{(2)}(2\omega, \omega, \omega)$  is crystallographic quadratic susceptibility;  $\chi_E^{(3)}(2\omega, \Omega, \omega, \omega)$  is cubic susceptibility.

Obviously, relations (1) and (2) are identical in the case of linear dependence of  $P(E_{\Omega})$ , for example, in weak fields. In general, the dependencies of the SH intensity on the THz field should be studied for distinguishing (1) and (2).

When decomposing the square of sum, two field-dependent terms that are linear  $I_2$  and quadratic  $I_3$  appear, as follows:

$$I_2 \propto \chi^{(2)} \chi_{\rm E}^{(3)} E_{\Omega}, \tag{3a}$$

$$I_3 \propto (\chi_E^{(3)})^2 (E_{\Omega})^2.$$
 (3b)

It is these in the Fourier decomposition that give, respectively, the signals at the fundamental  $\Omega$  and doubled  $2\Omega$  frequencies of the incident wave.

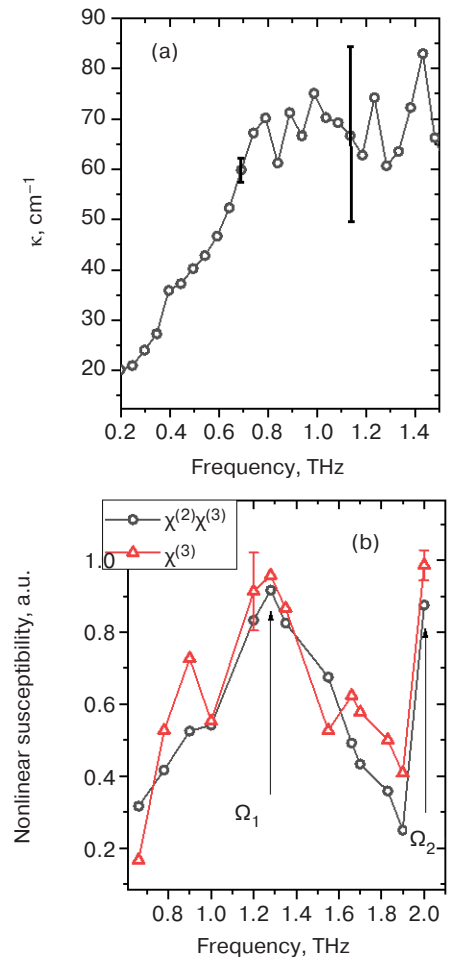


Fig. 2. Dispersion of the absorption coefficient and nonlinear susceptibility of PGO crystal

The dispersion dependencies of the absorption coefficient and nonlinear susceptibility of PGO crystal are shown in Fig. 2. The absorption coefficient (Fig. 2a) grows significantly up to the frequency of 0.7 THz where the accuracy of its determination does not exceed 5%. This is close to the value obtained earlier using the broadband THz spectroscopy technique. At higher frequencies, the error increases significantly. This is due to the fact that in narrow-band sensing the spectral lines of radiation are significantly deformed as they pass through the crystal (Fig. 1d). Finding the ratio of spectral amplitudes of the transmitted and incident radiation beyond the FWHM (full width at half maximum is pulse duration at half amplitude level) of the incident wave results in "division by 0", or rather, by the noise signal. Similarly, beyond the FWHM of the passed wave, the division of the noise signal by a non-zero spectral amplitude occurs in the region of the incident wave spectral amplitude maximum. It is also possible to find spectral regions where both signals are noisy. At frequencies above 1.4 THz, the signal does not stand out against the noise.

The nonlinear susceptibility is calculated on the basis of spectral dependencies of the SH intensity (Fig. 1g) for

maxima at fundamental frequency by formula (3a) and at the doubled frequency by formula (3b). The result is shown in Fig. 2b. The dependencies are normalized to the maximum nonlinear susceptibility. It should be noted that the dependencies  $\chi^{(2)}\chi_E^{(3)}$  and  $\chi_E^{(3)}$  practically coincide. This implies the absence of spectral features in the THz range in the crystallographic susceptibility  $\chi^{(2)}$ , which corresponds to the nature of this susceptibility being the electronic type susceptibility. Thus,  $\chi^{(2)}$  is simply a constant in the problem.

Cubic susceptibility  $\chi_E^{(3)}$  clearly shows two maxima at  $\Omega_1=1.3$  THz and  $\Omega_2=2$  THz. While it has not yet been possible to measure the second maximum in more detail, attention is drawn to the measurement error at this point. The observed maxima correspond to the phonon modes of PGO crystal.

The studies show that in the case of THz spectroscopy in the area of phonon resonances, the generation technique of the SH induced by the narrow-band THz field is more informative compared to the commonly used TDS technique due to its significantly higher spectral resolution. This is due to the presence of the resonance denominator at the frequencies of the phonon modes  $\chi_{\rm E}^{(3)} \propto (\Omega - \Omega_0 - i\gamma\Omega)^{-1}$  in the expression for the cubic nonlinear susceptibility [16]. In addition, the distortion of the spectrum in propagation of the THz wave does not play a significant role, since the resonance itself "selects" the frequencies at which the resonance amplification occurs.

## **CONCLUSIONS**

The presented investigation of the spectral characteristics of the absorption coefficient and

nonlinear susceptibility based on the techniques of TDS and THz induced electric field generation of the optical SH demonstrates the presence of the region of fundamental absorption near phonon modes, as well as the resonance amplification of the cubic nonlinear susceptibility for two phonon modes  $\Omega_1 = 1.3$  THz and  $\Omega_2 = 2$  THz. The results are consistent with both earlier results from broadband TDS spectroscopy (absorption coefficient) and the results of Raman spectroscopy to determine the phonon mode frequencies. The spectral dependence of the cubic nonlinear susceptibility in the THz range is obtained for the first time. The results are important for understanding the physics of interaction processes of THz radiation with ferroelectric crystals. The obtained values of the absorption coefficient can be used for developing THz devices on PGO crystals.

## **ACKNOWLEDGMENTS**

This work was supported by the Russian Science Foundation (grant No. 22-12-00334) and the Russian Foundation for Basic Research (grant No. 20-21-00043). The authors also thank A.A. Bush for the PGO crystal.

## **Authors' contributions**

- **V.R. Bilyk**—experimental studies of the THz-TDS of the PGO crystal; analysis of experimental data.
- **K.A. Brekhov**—experimental studies of the PGO crystal nonlinear response dynamics.
- **M.B.** Agranat—definition of the research concept; writing the initial text of the manuscript.
- **E.D. Mishina**—definition of the research concept; writing the initial text of the manuscript; analysis of experimental data, calculation of the PGO crystal optical constants.

## **REFERENCES**

- Iwasaki H., Sugii K., Yamada T., Niizeki N. 5PbO·3GeO<sub>2</sub> Crystal; a new ferroelectric. *Appl. Phys. Lett.* 1971;18(10): 444–445. http://aip.scitation.org/doi/10.1063/1.1653487
- Bush A.A., Kamentsev K.E., Mamin R.F. Transformation of dielectric properties and appearance of relaxation behavior in Pb<sub>5</sub>(Ge<sub>1-x</sub>Si<sub>x</sub>)<sub>3</sub>O<sub>11</sub> crystals. *J. Exp. Theor Phys.* 2005;100(1):139–151. http://link.springer.com/10.1134/1.1866206
- 3. Hosea T.J.C. Raman scattering from soft modes in barium-doped lead germanate. *J. Raman Spectrosc.* 1990;21(11): 717–724. https://doi.org/10.1002/jrs.1250211104
- 4. Gorelik V.S., Pyatyshev A.Y. Raman scattering from the effective soft mode in lead germanate crystal. *J. Raman Spectrosc.* 2020;51(6):969–977. https://doi.org/10.1002/jrs.5854
- 5. Udina M., Cea T., Benfatto L. Theory of coherent-oscillations generation in terahertz pump-probe spectroscopy: From phonons to electronic collective modes. *Phys. Rev. B.* 2019;100(16):165131. https://doi.org/10.1103/PhysRevB.97.214304

- Melnikov A.A., Boldyrev K.N., Selivanov Y.G., Martovitskii V.P., Chekalin S.V., Ryabov E.A. Coherent phonons in a Bi<sub>2</sub>Se<sub>3</sub> film generated by an intense singlecycle THz pulse. *Phys. Rev. B.* 2018;97(21):214304. https://doi.org/10.1103/PhysRevB.97.214304
- Kozina M., Fechner M., Marsik P., van Driel T., Glownia J.M., Bernhard C., Radovic M., Zhu D., Bonetti S., Staub U., Hoffmann M.C. Terahertz-driven phonon upconversion in SrTiO<sub>3</sub>. *Nat. Phys.* 2019;15(4):387–392. https://doi.org/10.1038/s41567-018-0408-1
- Salén P., Basini M., Bonetti S., Hebling J., Krasilnikov M., Nikitin A.Y., Shamuilov G., Tibaid Z., Zhaunerchyk V., Goryashko V. Matter manipulation with extreme terahertz light: Progress in the enabling THz technology. *Phys. Rep.* 2019;836–837:1–74. https://doi.org/10.1016/j. physrep.2019.09.002
- Bawuah P., Zeitler J.A. Advances in terahertz timedomain spectroscopy of pharmaceutical solids: A review. TrAC Trends Anal. Chem. 2021;139(40):116272. https://doi.org/10.1016/j.trac.2021.116272

- Ryu H.-C., Kwak M.-H., Kang S.-B., Jeong S.-Y., Paek M.-C., Kang K.-Y., Lee S.-J., Moon S.E., Park S.-O. A dielectric property analysis of ferroelectric thin film using terahertz time-domain spectroscopy. *Integr. Ferroelectr.* 2007;95(1):83–91. https://doi. org/10.1080/10584580701756573
- 11. Bilyk V.R., Grishunin K.A. Complex refractive index of strontium titanate in the terahertz frequency range. *Russ. Technol. J.* 2019;7(4):71–80 (in Russ.). https://doi.org/10.32362/2500-316X-2019-7-4-71-80
- Bilyk V., Mishina E., Sherstyuk N., Bush A., Ovchinnikov A., Agranat M. Transient polarization reversal using an intense THz pulse in silicon-doped lead germanate. *Phys. Status Solidi (RRL) – Rapid Res. Lett.* 2021;15(1):2000460. https://doi.org/10.1002/ pssr.202000460, https://onlinelibrary.wiley.com/ doi/10.1002/pssr.202000460
- 13. Lockwood D.J., Hosea T.J., Taylor W. The complete Raman spectrum of paraelectric and ferroelectric lead germanate. *J. Phys. C: Solid State Phys.* 1980;13(8):1539. https://doi.org/10.1088/0022-3719/13/8/023

- Vicario C., Jazbinsek M., Ovchinnikov A.V., Chefonov O.V., Ashitkov S.I., Agranat M.B., Hauri C.P. High efficiency THz generation in DSTMS, DAST and OH1 pumped by Cr:forsterite laser. *Opt. Express*. 2015;23(4):4573–4580. https://doi.org/10.1364/OE.23. 004573
- Ovchinnikov A.V., Chefonov O.V., Agranat M.B., Fortov V.E., Jazbinsek M., Hauri C.P. Generation of strong-field spectrally tunable terahertz pulses. *Opt. Express.* 2020;28(23):33921–33936. https://doi. org/10.1364/OE.405545, https://opg.optica.org/abstract. cfm?URI=oe-28-23-33921
- Blombergen N. Nelineinaya optika (Nonlinear Optics);
   transl. from Engl. Akhmanov S.A., Khokhlov R.V. (Eds.).
   Moscow: Mir; 1966. 424 p. (in Russ.).
   [Bloembergen N. Nonlinear Optics. Harvard University.
   New-York, Amsterdam: Benjamin W.A.; 1965. 220 p.]

## About the authors

**Vladislav R. Bilyk,** Cand. Sci. (Phys.-Math.), Junior Researcher, Department of Nanoelectronics, Institute for Advanced Technologies and Industrial Programming, MIREA – Russian Technological University (78, Vernadskogo pr., Moscow, 119454 Russia). E-mail: vrbilyk@mail.ru. ResearcherID AAH-4586-2019, Scopus Author ID 57194048515, https://orcid.org/0000-0002-3013-8655

**Kirill A. Brekhov,** Cand. Sci. (Phys.-Math.), Research Engineer, Department of Nanoelectronics, Institute for Advanced Technologies and Industrial Programming, MIREA – Russian Technological University (78, Vernadskogo pr., Moscow, 119454 Russia). E-mail: brekhov\_ka@mail.ru. ResearcherID Q-1014-2017, Scopus Author ID 55452447100, https://orcid.org/0000-0001-9091-2609

**Mikhail B. Agranat,** Dr. Sci. (Phys.–Math.), Chief Researcher, Joint Institute for High Temperatures, Russian Academy of Sciences (13/2, Izhorskaya ul., Moscow, 125412 Russia). E-mail: agranat2004@mail.ru. Scopus Author ID 6602697816, https://orcid.org/0000-0001-7819-822X

**Elena D. Mishina,** Dr. Sci. (Phys.–Math.), Professor, Head of the Laboratory, Department of Nanoelectronics, Institute for Advanced Technologies and Industrial Programming, MIREA – Russian Technological University (78, Vernadskogo pr., Moscow, 119454 Russia). E-mail: mishina\_elena57@mail.ru. ResearcherID D-6402-2014, Scopus Author ID 7005350309, https://orcid.org/0000-0003-0387-5016

## Об авторах

**Билык Владислав Романович,** к.ф.-м.н., младший научный сотрудник, кафедра наноэлектроники Института перспективных технологий и индустриального программирования ФГБОУ ВО «МИРЭА – Российский технологический университет» (119454, Россия, Москва, пр-т Вернадского, д. 78). E-mail: vrbilyk@mail.ru. ResearcherID AAH-4586-2019, Scopus Author ID 57194048515, https://orcid.org/0000-0002-3013-8655

**Брехов Кирилл Алексеевич,** к.ф.-м.н., инженер-исследователь, кафедра наноэлектроники Института перспективных технологий и индустриального программирования ФГБОУ ВО «МИРЭА – Российский технологический университет» (119454, Россия, Москва, пр-т Вернадского, д. 78). E-mail: brekhov\_ka@mail.ru. ResearcherID Q-1014-2017, Scopus Author ID 55452447100, https://orcid.org/0000-0001-9091-2609

**Агранат Михаил Борисович,** д.ф.-м.н., главный научный сотрудник, ФГБУН Объединенный институт высоких температур Российской академии наук (125412, Россия, Москва, ул. Ижорская, д. 13, стр. 2). E-mail: agranat2004@mail.ru. Scopus Author ID 6602697816, https://orcid.org/0000-0001-7819-822X

**Мишина Елена Дмитриевна,** д.ф.-м.н., профессор, заведующий лабораторией, кафедра наноэлектроники Института перспективных технологий и индустриального программирования ФГБОУ ВО «МИРЭА – Российский технологический университет» (119454, Россия, Москва, пр-т Вернадского, д. 78). E-mail: mishina\_elena57@mail.ru. ResearcherID D-6402-2014, Scopus Author ID 7005350309, https://orcid.org/0000-0003-0387-5016

Translated from Russian into English by Kirill V. Nazarov Edited for English language and spelling by Thomas A. Beavitt

## Micro- and nanoelectronics. Condensed matter physics Микро- и наноэлектроника. Физика конденсированного состояния

UDC 004.312.44 https://doi.org/10.32362/2500-316X-2023-11-3-46-55



RESEARCH ARTICLE

## Method for synthesizing a logic element that implements several functions simultaneously

Stanislav I. Sovetov <sup>1, @</sup>, Sergey F. Tyurin <sup>1, 2</sup>

## **Abstract**

**Objectives.** The basic element of a field-programmable gate array is a lookup table (LUT). While in canonical normal form LUTs generally implement only one logical function for a given configuration, in this case, there is always an inactive pass transistor element. Moreover, using a single LUT for a single function reduces system-on-a-chip (SoC) scalability. Therefore, the purpose of the present work is to develop a LUT structure for implementing several logic functions simultaneously on inactive transmitting transistors.

**Methods.** The evolution of LUT structure is presented for three variables, in which the number of simultaneously implemented functions increases. To implement additional functions, the logical device was decomposed with a different number of variables. The structures were modeled in the *Multisim* electrical simulation system.

**Results.** The presented simulation of more than two logic functions on inactive parts of the LUT shows the simultaneous operation of two and four logic functions. The complexity for a different number of variables and number of implemented functions is compared.

**Conclusions.** The simulation results demonstrate the operability of LUT structures in which several logical functions are performed. Thus, when implementing additional functions in the new structure, a smaller number of transmitting transistors is required as compared to a conventional LUT, thus increasing device functionality. The presented solution can be used to increase the number of simultaneously implemented functions of the same variables, which can be important e.g., when implementing code transformations.

Keywords: field-programmable gate array, LUT, transmitting transistors, truth table, logic function

• Submitted: 06.12.2022 • Revised: 13.01.2023 • Accepted: 22.02.2023

For citation: Sovetov S.I., Tyurin S.F. Method for synthesizing a logic element that implements several functions simultaneously. *Russ. Technol. J.* 2023;11(3):46–55. https://doi.org/10.32362/2500-316X-2023-11-3-46-55

Financial disclosure: The authors have no a financial or property interest in any material or method mentioned.

The authors declare no conflicts of interest.

<sup>&</sup>lt;sup>1</sup> Perm National Research Polytechnic University, Perm, 614990 Russia

<sup>&</sup>lt;sup>2</sup> Perm State University, Perm, 614068 Russia

<sup>@</sup> Corresponding author, e-mail: fizikoz@gmail.com

## НАУЧНАЯ СТАТЬЯ

## Метод синтеза логического элемента, реализующего несколько функций одновременно

С.И. Советов <sup>1, @</sup>, С.Ф. Тюрин <sup>1, 2</sup>

### Резюме

**Цель.** Базовый элемент программируемой логической интегральной схемы (ПЛИС) реализует логические функции с помощью таблиц истинности (LUT). Строение обычных LUT позволяет реализовывать только одну логическую функцию нескольких переменных в совершенной дизъюнктивной нормальной форме (СДНФ). При этом всегда остается часть неактивных передающих транзисторов. Использование одной LUT для одной функции усложняет масштабирование архитектуры на кристалле (SoC). Целью данной работы является разработка структуры LUT для реализации нескольких логических функций одновременно на неактивных передающих транзисторах.

**Методы.** Приведена эволюция структуры LUT для трех переменных, в которой увеличивается количество одновременно реализуемых функций. Для реализации дополнительных функций выполнена декомпозиция логического устройства с различным количеством переменных. Проведено моделирование структур в системе электротехнического моделирования *Multisim*.

**Результаты.** Продемонстрировано моделирование более двух логических функций на неактивных частях LUT, при котором отображена одновременная работа двух и четырех логических функций. Приведено сравнение сложности для разного количества переменных и количества реализованных функций.

**Выводы.** Результаты моделирования демонстрируют работоспособность структур LUT, в которых выполняется несколько логических функций. Таким образом, при реализации дополнительных функций в новой структуре требуется меньшее количество передающих транзисторов по сравнению с обычным LUT, что увеличивает функциональность устройства. Новое решение позволяет увеличить число одновременно реализуемых функций одних и тех же переменных, что важно при реализации, например, кодовых преобразований.

Ключевые слова: ПЛИС, LUT, передающие транзисторы, таблица истинности, логическая функция

• Поступила: 06.12.2022 • Доработана: 13.01.2023 • Принята к опубликованию: 22.02.2023

**Для цитирования:** Советов С.И., Тюрин С.Ф. Метод синтеза логического элемента, реализующего несколько функций одновременно. *Russ. Technol. J.* 2023;11(3):46-55. https://doi.org/10.32362/2500-316X-2023-11-3-46-55

**Прозрачность финансовой деятельности:** Авторы не имеют финансовой заинтересованности в представленных материалах или методах.

Авторы заявляют об отсутствии конфликта интересов.

## **INTRODUCTION**

Field-programmable gate arrays (FPGAs), where a configurable logic unit is used as a basic element, are currently common in electronic devices. The basic element of this block comprises a lookup table (LUT), which implements some logical function. Modern LUTs are configurable multiplexers for realization of logic functions with  $2^n$  inputs and one output for n variables [1, 2]. The use of existing LUTs for n variables requires memory cells and  $2^{n+1} - 2$  transistors; in this case, only one logic function is realized. Although,

<sup>1</sup> Пермский национальный исследовательский политехнический университет, Пермь, 614990 Россия

<sup>&</sup>lt;sup>2</sup> Пермский государственный национальный исследовательский университет, Пермь, 614068 Россия

<sup>&</sup>lt;sup>®</sup> Автор для переписки, e-mail: fizikoz@gmail.com

the same number of LUTs must be used when implementing n logic functions simultaneously, when using a single function in an LUT, the second half of the tree of transistors in the number of  $2^{n-1}$  remains inactive [3, 4]. In previous works, the simultaneous implementation of two logic functions on one tree of transmitting transistors was proposed [5–7].

The 3-LUT tree shown in Fig. 1 consists of three NMOS (N-type metal-oxide-semiconductor) cascades of pass transistors<sup>1</sup> [8, 9]. For any of the eight values on the static random-access memory (SRAM) inputs, only one chain of passing transistors is enabled, while, on the remaining passing transistors, at least one chain is completely inactive.

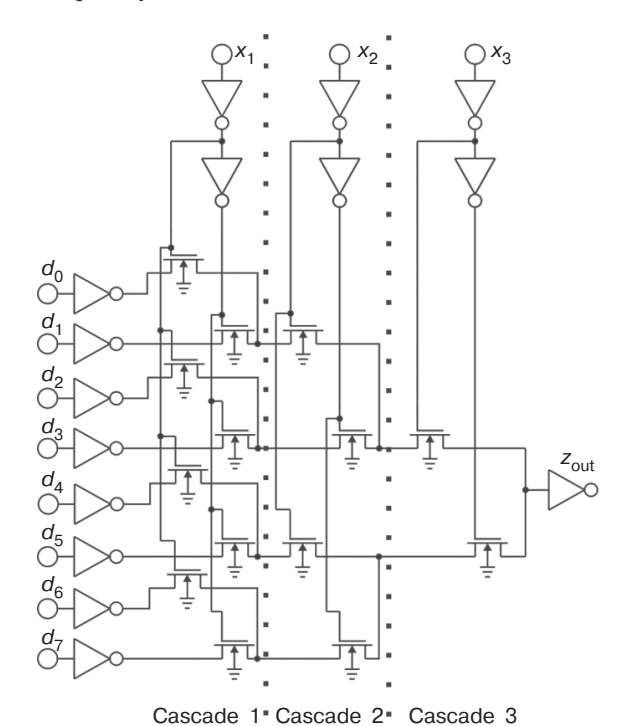


Fig. 1. Tree of LUT of the table of three variables

The 3-LUT logic function can be represented linearly as follows:

$$z(x_3x_2x_1d) = d_0 \cdot \overline{x}_3\overline{x}_2\overline{x}_1 \lor d_1 \cdot \overline{x}_3\overline{x}_2x_1 \lor \lor d_2 \cdot \overline{x}_3x_2\overline{x}_1 \lor d_3 \cdot \overline{x}_3x_2x_1 \lor d_4 \cdot x_3\overline{x}_2\overline{x}_1 \lor \lor d_5 \cdot x_3\overline{x}_2x_1 \lor d_6 \cdot x_3x_2\overline{x}_1 \lor d_7 \cdot x_3x_2x_1,$$
 (1)

where  $d_0$ ,  $d_1$ ,  $d_2$ ,  $d_3$ ,  $d_4$ ,  $d_5$ ,  $d_6$ ,  $d_7$  are configuration data of the three variables function  $z(x_3x_2x_1)$ . By combining  $d_0$ ,  $d_1$ ,  $d_2$ ,  $d_3$ ,  $d_4$ ,  $d_5$ ,  $d_6$ ,  $d_7$ , we can get  $2^8$  functions.

In minterm canonical form (MCF) or canonical disjunctive normal form (CDNF), all LUTs of n variables perform a single logical function of n arguments [10, 11].

At the same time, another logical function of the same arguments can be activated on each inactive chain, e.g., summation or carry functions. By combining these chains in OR, we can get a logic element with several outputs.

In the present work, an improved array is proposed that uses the inactive branches of the transmitting transistor tree. By introducing additional LUTs of two variables at stage 2, it is possible to use additional functions on inactive tree circuits.

This novel solution allows the number of simultaneously realized functions of the same variables to be increased; this can important when implementing code conversions.

## SYNTHESIS OF A MULTIFUNCTIONAL LOGIC ELEMENT

In order to implement both functions, a single variable LUT was added to the array. This consists of an output inverter and two transmitting transistors, whose outputs are combined and connected to the inverter. LUT inputs of the single variable transistors are connected to the outputs of the second cascade of transmitting transistors. Two transmitting transistors each are added to the input setting inverters; these are controlled by the senior variable, whose outputs are combined and connected to the inverter. This results in a three-variable LUT circuit with two simultaneous functions (Fig. 2).

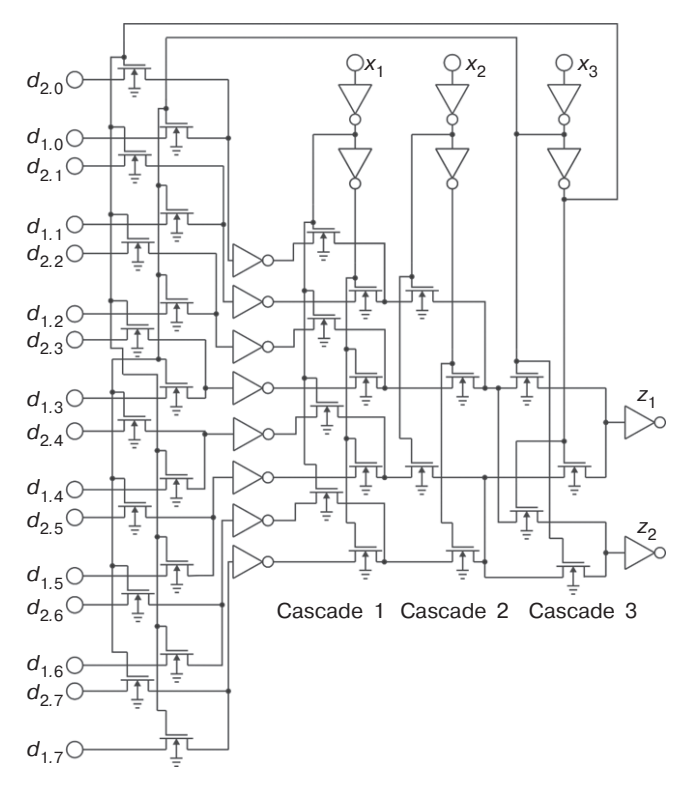


Fig. 2. Tree of three-variable LUT performing two functions simultaneously

<sup>&</sup>lt;sup>1</sup> Intel<sup>®</sup> FPGAs and SoC FPGAs. https://www.intel.in/content/www/in/en/products/details/fpga/cyclone.html. Accessed November 17, 2022.

To implement two functions, we decompose a logical device by a higher variable  $(x_3)$ :

First function:

$$z_{1}(x_{3}x_{2}x_{1}d) =$$

$$= \overline{x}_{3} \Big[ d_{1.0} \cdot \overline{x}_{2}\overline{x}_{1} \vee d_{1.1} \cdot \overline{x}_{2}x_{1} \vee$$

$$\vee d_{1.2} \cdot x_{2}\overline{x}_{1} \vee d_{1.3} \cdot x_{2}x_{1} \Big] \vee$$

$$\vee x_{3} \Big[ d_{1.4} \cdot \overline{x}_{2}\overline{x}_{1} \vee d_{1.5} \cdot \overline{x}_{2}x_{1} \vee$$

$$\vee d_{1.6} \cdot x_{2}\overline{x}_{1} \vee d_{1.7} \cdot x_{2}x_{1} \Big].$$
(2)

Second function:

$$z_{2}(x_{3}x_{2}x_{1}d) =$$

$$= x_{3} \Big[ d_{2.4(0)} \cdot \overline{x}_{2}\overline{x}_{1} \vee d_{2.5(1)} \cdot \overline{x}_{2}x_{1} \vee$$

$$\vee d_{2.6(2)} \cdot x_{2}\overline{x}_{1} \vee d_{2.7(3)} \cdot x_{2}x_{1} \Big] \vee$$

$$\vee \overline{x}_{3} \Big[ d_{2.0(4)} \cdot \overline{x}_{2}\overline{x}_{1} \vee d_{2.1(5)} \cdot \overline{x}_{2}x_{1} \vee$$

$$\vee d_{2.2(6)} \cdot x_{2}\overline{x}_{1} \vee d_{2.3(7)} \cdot x_{2}x_{1} \Big],$$
(3)

where  $d_{i,j}$ ;  $i = 1, 2(2^{v})$ ;  $j = 1, 2, 3, 4, ..., 2^{3}(2^{n})$ , v is the number of implemented functions.

The setting constant is specified in the format  $d_{i,j(k)}$ , where k defines the number of the function set and j is the number of the input used to connect it. In our case

*k* is obtained from *j* by inverting the older variable. Thus, the top half of the SRAM is swapped with the bottom half to use the inactive part of the pass transistors. As a result, two chains from SRAM to output inverters in this LUT configuration of three variables are active, i.e., two functions are implemented simultaneously.

To further increase the number of simultaneously executed functions on the LUT of three variables an additional LUT tree of two variables for each function is introduced, whose inputs are connected to the outputs of the transmitting transistors of the first stage. Additionally, a cascade of transmitting tuning transistors controlled by the second variable  $(x_2)$  is introduced. The outputs of the transistors are combined and connected to the inputs of the first transmitting tuning transistor stage. The general schematic of a four-function LUT of three variables is shown in Fig. 3.

To implement four functions, we decompose the logical unit into a higher variable  $(x_3)$  and a second variable  $(x_2)$ :

First function:

$$z_{1}(x_{3}x_{2}x_{1}d) = \overline{x}_{3}\overline{x}_{2} \left[ d_{1.0} \cdot \overline{x}_{1} \vee d_{1.1} \cdot x_{1} \right] \vee$$

$$\vee \overline{x}_{3}x_{2} \left[ d_{1.2} \cdot \overline{x}_{1} \vee d_{1.3} \cdot x_{1} \right] \vee$$

$$\vee x_{3}\overline{x}_{2} \left[ d_{1.4} \cdot \overline{x}_{1} \vee d_{1.5} \cdot x_{1} \right] \vee$$

$$\vee x_{3}x_{2} \left[ d_{1.6} \cdot \overline{x}_{1} \vee d_{1.7} \cdot x_{1} \right].$$

$$(4)$$

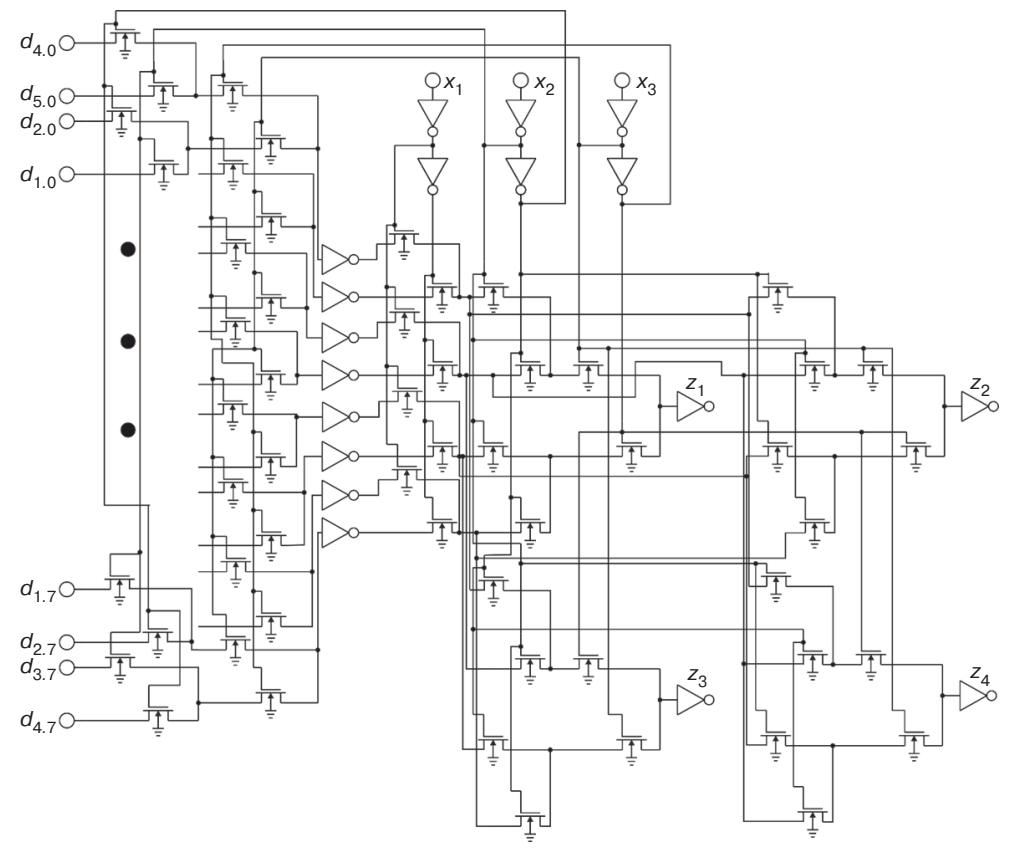


Fig. 3. Tree of three-variable LUT performing four functions simultaneously

Table. Setting the logical levels of SRAM cells for a LUT of three variables performing four functions

No. of input	Configuration for $z_1$	Configuration for $z_2$	Configuration for $z_3$	Configuration for $z_4$
1	0	0	1	0
2	1	1	1	1
3	1	0	1	0
4	0	0	1	0
5	1	1	0	0
6	0	1	1	0
7	0	0	1	0
8	1	1	1	0

(5)

Second function:

$$z_{2}(x_{3}x_{2}x_{1}d) =$$

$$= \overline{x}_{3}x_{2} \left[ d_{2.2(0)} \cdot \overline{x}_{1} \vee d_{2.3(1)} \cdot x_{1} \right] \vee$$

$$\vee x_{3}\overline{x}_{2} \left[ d_{2.4(2)} \cdot \overline{x}_{1} \vee d_{2.5(3)} \cdot x_{1} \right] \vee$$

$$\vee x_{3}x_{2} \left[ d_{2.6(4)} \cdot \overline{x}_{1} \vee d_{2.7(5)} \cdot x_{1} \right] \vee$$

$$\vee \overline{x}_{3}\overline{x}_{2} \left[ d_{2.0(6)} \cdot \overline{x}_{1} \vee d_{2.1(7)} \cdot x_{1} \right].$$

Third function:

$$z_{3}(x_{3}x_{2}x_{1}d) =$$

$$= x_{3}\overline{x}_{2} \left[ d_{3.4(0)} \cdot \overline{x}_{1} \vee d_{3.5(1)} \cdot x_{1} \right] \vee$$

$$\vee x_{3}x_{2} \left[ d_{3.6(2)} \cdot \overline{x}_{1} \vee d_{3.7(3)} \cdot x_{1} \right] \vee$$

$$\vee \overline{x}_{3}\overline{x}_{2} \left[ d_{3.0(4)} \cdot \overline{x}_{1} \vee d_{3.1(5)} \cdot x_{1} \right] \vee$$

$$\vee \overline{x}_{3}x_{2} \left[ d_{3.2(6)} \cdot \overline{x}_{1} \vee d_{3.3(7)} \cdot x_{1} \right].$$
(6)

Fourth function:

$$z_{4}(x_{3}x_{2}x_{1}d) =$$

$$= x_{3}x_{2} \left[ d_{4.6(0)} \cdot \overline{x}_{1} \vee d_{4.7(1)} \cdot x_{1} \right] \vee$$

$$\vee \overline{x}_{3}\overline{x}_{2} \left[ d_{4.0(2)} \cdot \overline{x}_{1} \vee d_{4.1(3)} \cdot x_{1} \right] \vee$$

$$\vee \overline{x}_{3}x_{2} \left[ d_{4.2(4)} \cdot \overline{x}_{1} \vee d_{4.3(5)} \cdot x_{1} \right] \vee$$

$$\vee x_{3}\overline{x}_{2} \left[ d_{4.4(6)} \cdot \overline{x}_{1} \vee d_{4.5(7)} \cdot x_{1} \right].$$
(7)

The configuration levels derived from the decomposition of the four functions: exclusive OR  $(z_1)$ , majority  $(z_2)$ , disjunction  $(z_3)$ , and conjunction  $(z_4)$  are shown in Table.

## **LUT SIMLATION**

Simulation of a three-variable multifunction LUT was performed in the National Instruments *Multisim*<sup>2</sup> dynamic simulation system. For the NMOS transistors, the BSIM 4.8.0<sup>3,4</sup> transistor model was used. The schematic of the inverter implemented on two field-effect transistors is shown in Fig. 4.

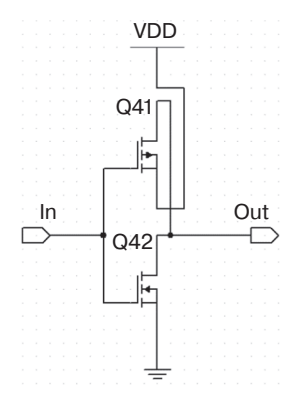


**Fig. 4.** Field-effect transistor inverter diagram (In the diagrams that follow, the designations adopted in the GOST 2.710-81<sup>5</sup> standard are used.)

First of all, we consider the general diagram of implementation of LUT for two functions (exclusive OR, majority) as shown in Fig. 5.

<sup>&</sup>lt;sup>2</sup> https://www.multisim.com/. Accessed November 17, 2022.

<sup>&</sup>lt;sup>3</sup> Microwind & Dsch Version 3.5. https://www.yumpu.com/en/document/view/40386405/microwind-manual-lite-v35pdf-moodle. Accessed November 17, 2022.

<sup>&</sup>lt;sup>4</sup> Mead C.A., Conway L. *Introduction to VLSI Systems*. Reading, MA, Addison-Wesley Publishing Co.;1980. 426 p. https://www.researchgate.net/publication/234388249\_Introduction\_to\_VLSI systems. Accessed November 17, 2022.

<sup>&</sup>lt;sup>5</sup> GOST 2.710-81. *Unified system for design documentation. Alpha-numerical designations in electrical diagrams.* Moscow: Standartinform; 2008 (in Russ.).

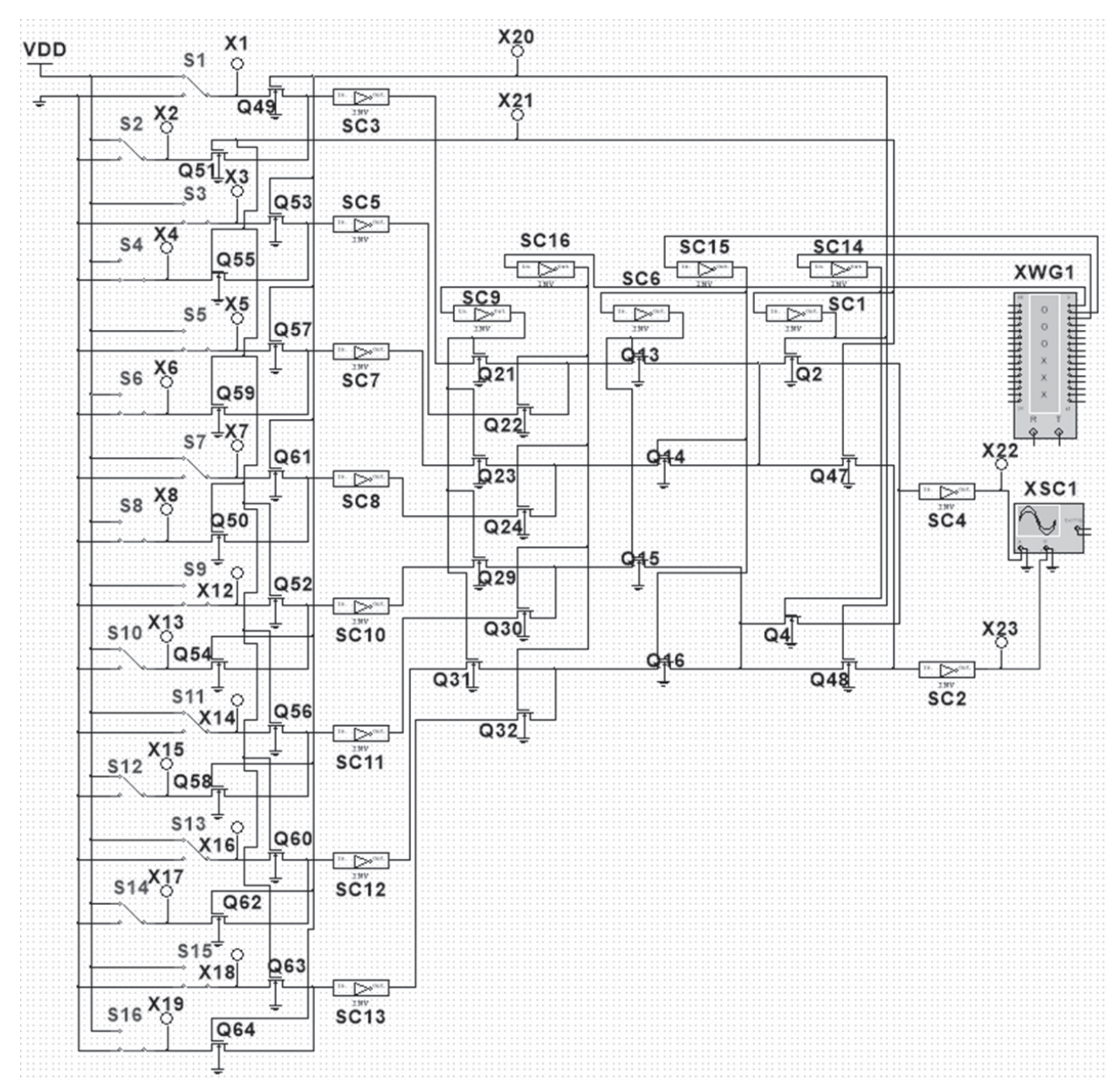


Fig. 5. Diagram of the three-variable LUT performing two functions simultaneously

A modified three-variable LUT scheme for performing four functions simultaneously (exclusive OR, majority, disjunction, and conjunction) is shown in Fig. 6 (see p. 52).

The input setting signal of the SRAM cells was set with the dynamic switches according to Table. The high voltage level (VDD 5V) corresponds to the logical variant, while the low voltage level (GND 0V) corresponds to logical zero.

The variable signals were set using the *Word Generator*, in which a three-bit Gray code is set (Fig. 7). Since the *Word Generator* has a frequency of 1 kHz, it requires 8 ms to completely pass the given Gray code

Function outputs are connected to the oscilloscope.

The results of the simulation of two and four functions are shown in Figs. 8 and 9 respectively.

The upper oscillogram corresponds to the "exclusive OR" function  $(z_1)$ . The lower oscillogram corresponds to the majority function  $(z_2)$ . Each time division of the oscilloscope corresponds to one combination of the Gray code.

In contrast to the basic three-variable LUT diagram, which uses only one half of the transmitting transistors, the proposed new circuit additionally uses the inactive part at  $2^{n-1}$  high order variables.

Complexity in terms of the number of LUT transistors depending on the number of variables  $n, n \in \mathbb{N}$  is calculated as follows:

$$\begin{split} L_1(n) &= \\ &= (2+2) \cdot 2^n + (2^{n+1}-2) + 2n + 2 + 2 = \\ &= 2^{n+2} + 2^{n+1} + 2n + 2 = 3 \cdot 2^{n+1} + 2n + 2. \end{split}$$

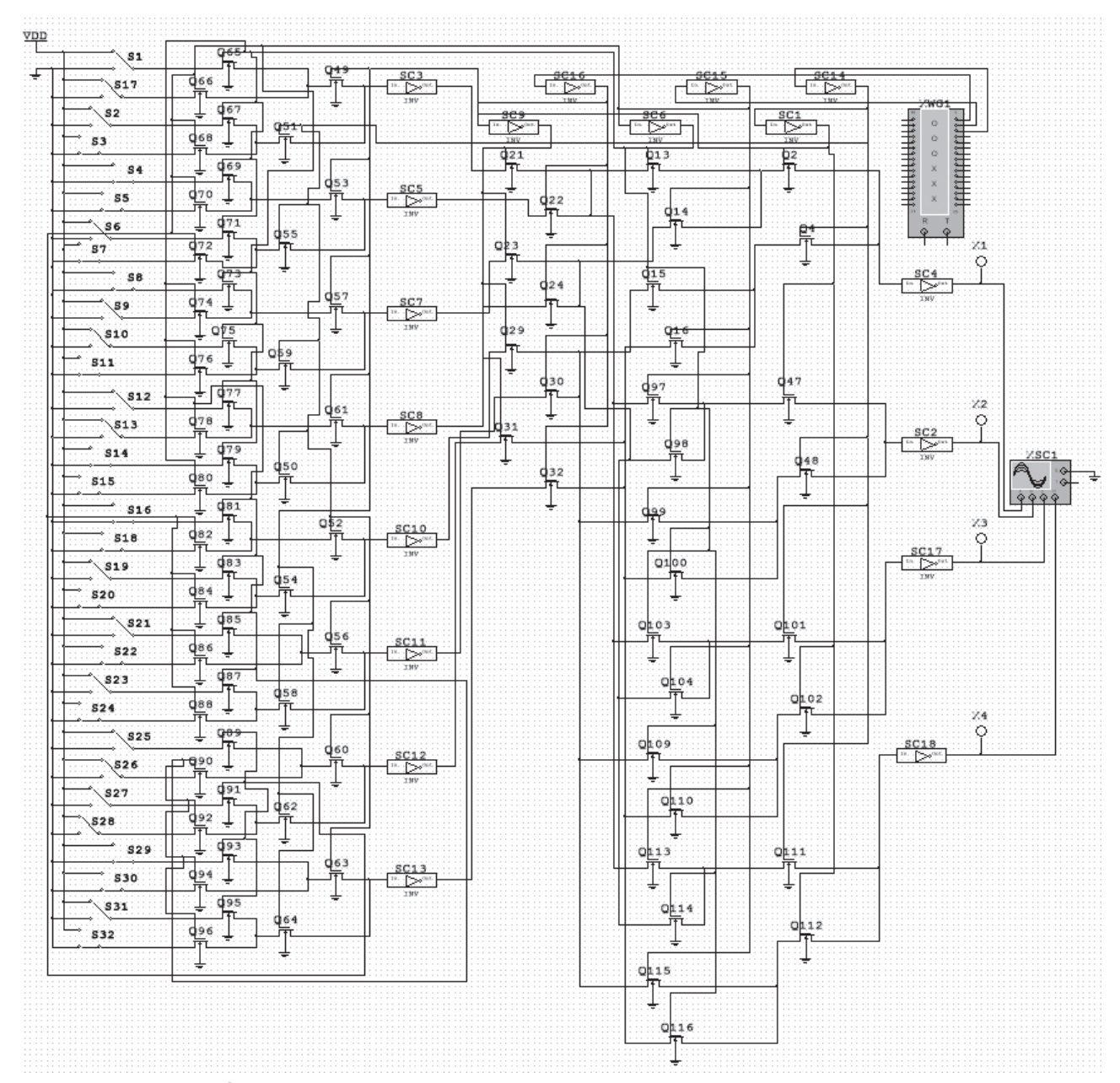


Fig. 6. Diagram of the three-variable LUT performing four functions simultaneously

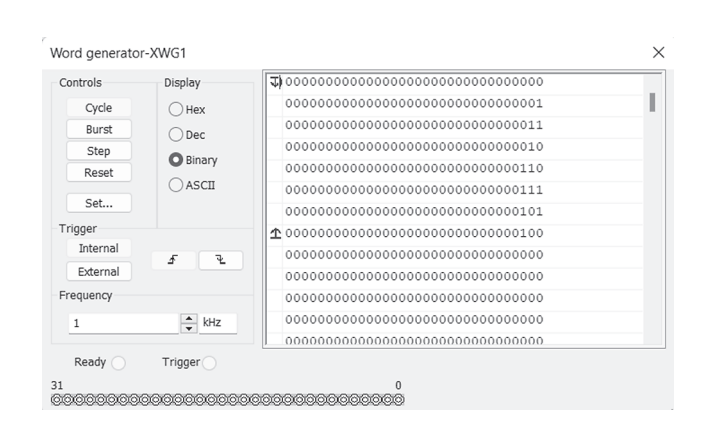


Fig. 7. Gray code in Word Generator

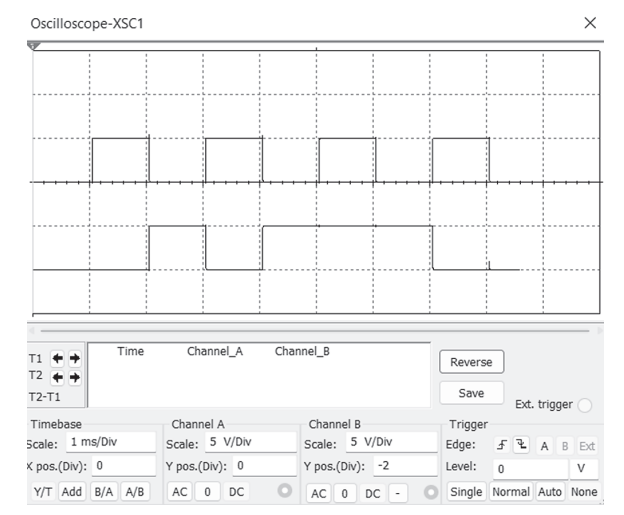
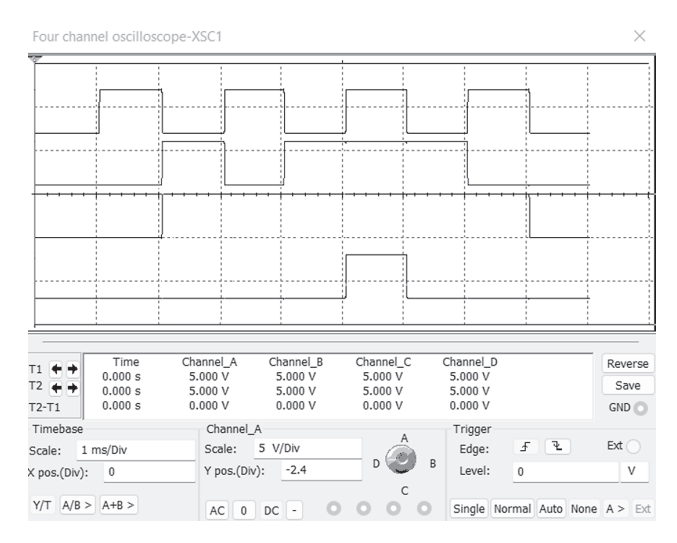


Fig. 8. Oscillogram of two functions of three-variable LUT



**Fig. 9.** Oscillogram of four functions of three-variable LUT

To calculate  $2^{\nu}$  functions in the proposed scheme we obtain the complexity:

$$\begin{split} L_{\nu}(\nu,n) &= \\ &= (2^{\nu+1}-2+2)\cdot 2^n + 2^{n+1} + 2n + \\ &+ (2^{\nu+1}-2)(2^{\nu}-1) + 2(2^{\nu}-1) = \\ &= 2^{\nu+1}\cdot 2^n + 2^{n+1} + 2n + 2^{\nu+1}\cdot (2^{\nu}-1). \end{split}$$

Thus, for example, implementing four logic functions (v = 2) of the same variables (n = 4) requires two LUTs for a total use of 212 transistors, while, in the proposed LUT design, which implements all four functions, the number of required transistors is 192.

The complexity diagrams representing the usual LUT  $L_{v1}(v)$  and the multifunctional LUT  $L_{v}(v)$  implementing v logic functions with the number of variables n=8 are shown in Fig. 10.

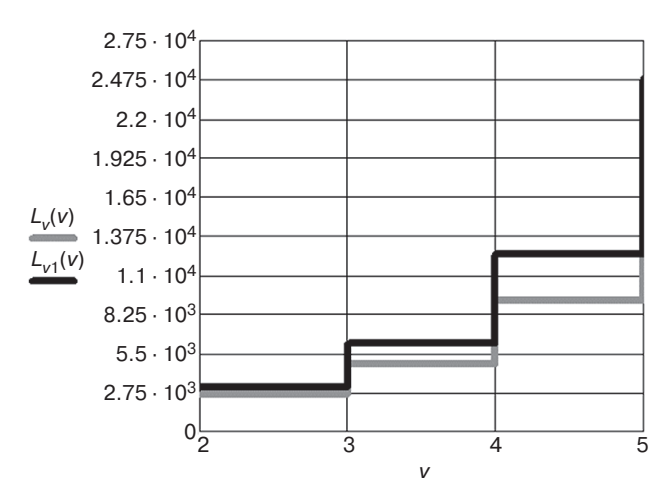


Fig. 10. Comparison of the complexity of a conventional LUT and a multifunctional LUT

As can be seen from the diagram, there is a complexity benefit in terms of the number of transistors for a multifunctional LUT in relation to the corresponding number for conventional LUTs.

## **CONCLUSIONS**

Thus, the possibility of simultaneous implementation of  $2^{n-1}$  logic functions on inactive parts of the circuits of the transmitting transistors in the FPGA, which increases the functionality of the device, is demonstrated. In order to implement the same number of logic functions,  $2^{n-2}$  LUTs are required. Despite the additional cost, there is a benefit in terms of complexity as compared to the number of required transistors.

## **Authors' contributions**

- **S.I. Sovetov**—preparation of research, literature analysis, modeling, writing the text of the article, formulation of conclusions.
- **S.F. Tyurin**—the idea of research, setting goals and objectives, consultations on research issues, editing the article.

## **REFERENCES**

- Drozd O., Perebeinos I., Martynyuk O., Zashcholkin K., Ivanova O., Drozd M. Hidden faultanalysis of FPG Aprojects for critical applications. In: 2020 IEEE 15th International Conference on Advanced Trends in Radioelectronics, Telecommunications and Computer Engineering (TCSET). Lviv-Slavske, Ukraine, 2020. P. 467–471. https://doi. org/10.1109/TCSET49122.2020.235591
- Drozd O., Nikul V., Antoniuk V., Drozd M. Hidden faults in FPGA-built digital components of safety-related systems. In: 2018 14th International Conference on Advanced Trends in Radioelectronics, Telecommunications and Computer Engineering (TCSET). Lviv-Slavske, Ukraine, 2018. P. 805–809. https://doi.org/10.1109/ TCSET.2018.8336320

## СПИСОК ЛИТЕРАТУРЫ

- Drozd O., Perebeinos I., Martynyuk O., Zashcholkin K., Ivanova O., Drozd M. Hidden fault analysis of FPGA projects for critical applications. In: 2020 IEEE 15th International Conference on Advanced Trends in Radioelectronics, Telecommunications and Computer Engineering (TCSET). Lviv-Slavske, Ukraine, 2020. P. 467–471. https://doi. org/10.1109/TCSET49122.2020.235591
- Drozd O., Nikul V., Antoniuk V., Drozd M. Hidden faults in FPGA-built digital components of safety-related systems. In: 2018 14th International Conference on Advanced Trends in Radioelectronics, Telecommunications and Computer Engineering (TCSET). Lviv-Slavske, Ukraine, 2018. P. 805–809. https://doi.org/10.1109/ TCSET.2018.8336320

- 3. Vikhorev R. Universal logic cells to implement systems functions. In: 2016 IEEE NW Russia Young Researchers in Electrical and Electronic Engineering Conference (ELConRusNW). St. Petersburg, Russia, 2016. P. 373–375. https://doi.org/10.1109/EIConRusNW.2016.7448197
- Vikhorev R. Improved FPGA logic elements and their simulation. In: 2018 IEEE Conference of Russian Young Researchers in Electrical and Electronic Engineering (EIConRus). Moscow and St. Petersburg, Russia, 2018. P. 259–264. https://doi.org/10.1109/EIConRus.2018.8317080
- Skornyakova A.Yu., Vikhorev R.V. Self-timed LUT layout simulation. In: 2020 IEEE Conference of Russian Young Researchers in Electrical and Electronic Engineering (EIConRus).
   St. Petersburg and Moscow, Russia, 2020. P. 176–179. https://doi.org/10.1109/EIConRus49466.2020.9039374
- Tyurin S.F. Green logic: Green LUT FPGA concepts, models and evaluations. In: Kharchenko V., Kondratenko Y., Kacprzyk J. (Eds.). Green IT Engineering: Components, Networks and Systems Implementation. Studies in Systems, Decision and Control. 2017;105: 241–261. https://doi.org/10.1007/978-3-319-55595-9 12
- 7. Tyurin S.F., Prokhorov A.S. *Programmable logic device*: RF Pat. 2637462. Publ. 04.12.2017 (in Russ.).
- 8. Tyurin S.F. LUT's sliding backup. *IEEE Transactions on Device and Materials Reliability*. 2019;19(1):221–225. https://doi.org/10.1109/TDMR.2019.2898724
- 9. Strogonov A., Tsybin S. Programmable switching FPGA Insights. *Komponenty i tekhnologii = Components & Technologies*. 2010;11(112):56–62 (in Russ.). Available from URL: https://kit-e.ru/wp-content/uploads/2010 11 56.pdf (accessed November 17, 2022).
- Strogonov A., Gorodkov P. Current trends in FPGA development: from system integration to artificial intelligence. *Elektronika: Nauka, tekhnologiya, biznes = Electronics: Science, Technology, Business.* 2020;4(195): 46–56 (in Russ.). https://doi.org/10.22184/1992-4178.2020. 195.4.46.56
- Danilova E.Y. FPGAs logic checking method by genetic algorithms. In: 2020 IEEE Conference of Russian Young Researchers in Electrical and Electronic Engineering (EIConRus). St. Petersburg and Moscow, Russia, 2020. P. 1787–1790. https://doi.org/10.1109/ EIConRus49466.2020.9039052

- 3. Vikhorev R. Universal logic cells to implement systems functions. In: 2016 IEEE NW Russia Young Researchers in Electrical and Electronic Engineering Conference (ELConRusNW). St. Petersburg, Russia, 2016. P. 373–375. https://doi.org/10.1109/EIConRusNW.2016.7448197
- Vikhorev R. Improved FPGA logic elements and their simulation. In: 2018 IEEE Conference of Russian Young Researchers in Electrical and Electronic Engineering (EIConRus). Moscow and St. Petersburg, Russia, 2018. P.259–264. https://doi.org/10.1109/EIConRus.2018.8317080
- Skornyakova A.Yu., Vikhorev R.V. Self-timed LUT layout simulation. In: 2020 IEEE Conference of Russian Young Researchers in Electrical and Electronic Engineering (EIConRus).
   St. Petersburg and Moscow, Russia, 2020. P. 176–179. https://doi.org/10.1109/EIConRus49466.2020.9039374
- Tyurin S.F. Green logic: Green LUT FPGA concepts, models and evaluations. In: Kharchenko V., Kondratenko Y., Kacprzyk J. (Eds.). Green IT Engineering: Components, Networks and Systems Implementation. Studies in Systems, Decision and Control. 2017;105: 241–261. https://doi.org/10.1007/978-3-319-55595-9 12
- 7. Тюрин С.Ф., Прохоров А.С. *Программируемое ло-гическое устройство*: Пат. 2637462 РФ. Заявка № 2016131738; заявл. 01.08.2016; опубл. 04.12.2017.
- 8. Tyurin S.F. LUT's sliding backup. *IEEE Transactions on Device and Materials Reliability*. 2019;19(1):221–225. https://doi.org/10.1109/TDMR.2019.2898724
- 9. Строгонов А., Цыбин С. Программируемая коммутация ПЛИС: взгляд изнутри. *Компоненты и технологии*. 2010;11(112):56–62. URL: https://kit-e.ru/wp-content/uploads/2010\_11\_56.pdf (дата обращения 17.11.2022).
- 10. Строгонов А., Городков П. Современные тенденции развития ПЛИС: от системной интеграции к искусственному интеллекту. Электроника: Наука, технология, бизнес. 2020;4(195):46–56. https://doi.org/10.22184/1992-4178.2020.195.4.46.56
- Danilova E.Y. FPGAs logic checking method by genetic algorithms. In: 2020 IEEE Conference of Russian Young Researchers in Electrical and Electronic Engineering (EIConRus). St. Petersburg and Moscow, Russia, 2020. P. 1787–1790. https://doi.org/10.1109/ EIConRus49466.2020.9039052

## About the authors

**Stanislav I. Sovetov,** Postgraduate Student, Department of Automation and Telemechanics, Perm National Research Polytechnic University (29, Komsomolskii pr., Perm, 614990 Russia). E-mail: fizikoz@gmail.com. https://orcid.org/0000-0003-4311-1045

**Sergey F. Tyurin,** Dr. Sci. (Eng.), Professor, Department of Automation and Telemechanics, Perm National Research Polytechnic University (29, Komsomolskii pr., Perm, 614990 Russia); Professor, Department of Software Computing Systems, Perm State University (15, Bukireva ul., Perm, 614068 Russia). E-mail: tyurinsergfeo@yandex.ru. Scopus Author ID 6603805561, https://orcid.org/0000-0002-5707-5404

## Об авторах

**Советов Станислав Игоревич,** аспирант, кафедра автоматики и телемеханики ФГАОУ ВО «Пермский национальный исследовательский политехнический университет» (614990, Россия, Пермь, Комсомольский пр-т, д. 29). E-mail: fizikoz@gmail.com. https://orcid.org/0000-0003-4311-1045

**Тюрин Сергей Феофентович,** д.т.н., профессор, кафедра автоматики и телемеханики ФГАОУ ВО «Пермский национальный исследовательский политехнический университет» (614990, Россия, Пермь, Комсомольский пр-т, д. 29); профессор, кафедра «Математическое обеспечение вычислительных систем», ФГАОУ ВО «Пермский государственный национальный исследовательский университет» (614068, Россия, Пермь, ул. Букирева, д. 15). E-mail: tyurinsergfeo@yandex.ru. Scopus Author ID 6603805561, https://orcid.org/0000-0002-5707-5404

Translated from Russian into English by Lyudmila O. Bychkova Edited for English language and spelling by Thomas A. Beavitt

## Mathematical modeling

## Математическое моделирование

UDC 004.942 https://doi.org/10.32362/2500-316X-2023-11-3-56-69



RESEARCH ARTICLE

## Statistical model for assessing the reliability of non-destructive testing systems by solving inverse problems

Alexander E. Alexandrov, Sergey P. Borisov, Ludmila V. Bunina, Sergey S. Bikovsky <sup>®</sup>, Irina V. Stepanova, Andrey P. Titov

MIREA – Russian Technological University, Moscow, 119454 Russia <sup>®</sup> Corresponding author, e-mail: bykovskij@mirea.ru

## **Abstract**

**Objectives.** The wear monitoring of metal structural elements of power plants—in particular, pipelines of nuclear power plants—is an essential means of ensuring safety during their operation. Monitoring the state of the pipeline by direct inspection requires a considerable amount of labor, as well as, in some cases, the suspension of power plant operation. In order to reduce costs during monitoring measures, it is proposed to use mathematical modeling. This work aimes to develop a mathematical model of a diagnostic system for assessing the probability of detection of defects by solving inverse problems.

**Methods.** A binomial model for assessing the reliability of monitoring, comprising the Berens–Hovey parametric model of the probability of detection of defects and a parametric model based on studying test samples, was analyzed. As an alternative to this binomial model, a computational method for assessing the reliability of non-destructive testing systems by solving an inverse problem was proposed. To determine the parameters of the defect detection probability curve, the model uses data obtained by various monitoring teams over a long period of power plant operation. To serve as initial data, the defect distribution density over one or more of the following characteristics can be used: depth, length, and/or cross-sectional area of the defect. Using the proposed mathematical model, a series of test calculations was performed based on nine combinations of initial data. The combinations differed in the confidence coefficient of the initial monitoring system, the parameters of the distribution of defects, and the sensitivity of the monitoring system.

**Results.** The calculation data were used to construct curves of the probability density of detected defects as a function of the defect size, recover the values of the defect distribution parameters under various test conditions, and estimate the error of recovering the parameters. The degree of imperfection of the system was estimated using the curve of the detection probability of a defect by a certain monitoring system.

**Conclusions.** Under constraints on the data sample size, the proposed methodology allows the metal monitoring results to be applied with greater confidence than currently used methods at the same time as evaluating the efficiency of monitoring carried out by individual test teams or laboratories. In future, this can be used to form the basis of a recommendation of the involvement of a particular team to perform diagnostic work.

**Keywords:** non-destructive testing, reliability of power plants, mathematical modeling, statistical analysis, inverse problems

• Submitted: 14.10.2022 • Revised: 28.01.2023 • Accepted: 10.03.2023

**For citation:** Alexandrov A.E., Borisov S.P., Bunina L.V., Bikovsky S.S., Stepanova I.V., Titov A.P. Statistical model for assessing the reliability of non-destructive testing systems by solving inverse problems. *Russ. Technol. J.* 2023;11(3):56–69. https://doi.org/10.32362/2500-316X-2023-11-3-56-69

Financial disclosure: The authors have no a financial or property interest in any material or method mentioned.

The authors declare no conflicts of interest.

НАУЧНАЯ СТАТЬЯ

## Статистическая модель оценки надежности систем неразрушающего контроля на основе решения обратных задач

А.Е. Александров, С.П. Борисов, Л.В. Бунина, С.С. Быковский <sup>®</sup>, И.В. Степанова, А.П. Титов

МИРЭА – Российский технологический университет, Москва, 119454 Россия <sup>®</sup> Автор для переписки, e-mail: bykovskij@mirea.ru

## Резюме

**Цели.** Контроль износа конструктивных элементов энергоустановок, в частности трубопроводов атомных электростанций, является неотъемлемым компонентом обеспечения безопасности при их эксплуатации. Контроль путем непосредственного обследования состояния трубопровода требует, во-первых, достаточно больших трудозатрат, во-вторых, в некоторых случаях, временной остановки работы. Поэтому при проведении контрольных мероприятий предлагается использовать математическое моделирование. Цель статьи – разработка математической модели системы диагностики для оценки вероятности обнаружения дефектов на основе решения обратных задач.

Методы. Анализируются биномиальная модель оценки надежности контроля, параметрическая модель Беренса и Хови вероятности обнаружения дефектов, параметрическая модель на основе исследования тест-образцов. В качестве альтернативы данным моделям предлагается расчетный метод оценки надежности систем неразрушающего контроля на основе решения обратной задачи. Для определения параметров кривой вероятности обнаружения дефектов модель использует данные, полученные различными контролирующими бригадами за длительный период эксплуатации энергоустановки. В качестве исходных данных можно использовать плотности распределения дефектов по одной или нескольким из следующих характеристик: глубине, длине, площади сечения дефекта. С помощью предлагаемой математической модели выполнен набор тестовых расчетов на основе девяти комбинаций исходных данных. Комбинации отличаются между собой коэффициентом достоверности исходной системы контроля, параметром распределения дефектов, чувствительностью системы контроля.

**Результаты.** По итогам проведенных расчетов построены кривые плотности вероятности обнаруженных дефектов в зависимости от размера дефекта, определены восстановленные значения параметров распределения дефектов при различных условиях испытаний, сделана оценка погрешности восстановления параметров. Для оценки степени несовершенства системы используется кривая вероятности обнаружения дефекта конкретной системой контроля.

**Выводы.** С учетом ограничений, связанных с размером выборки, предлагаемая методика, во-первых, позволяет применять результаты, полученные по контролю металла, с большей уверенностью, чем методики, используемые в настоящее время, во-вторых, оценивать эффективность контроля, проводимого отдельными бригадами испытателей либо лабораториями. В перспективе это позволит рекомендовать или не рекомендовать привлечение той или иной бригады к выполнению диагностических работ.

**Ключевые слова:** неразрушающий контроль, надежность энергетических установок, математическое моделирование, статистический анализ, обратные задачи

• Поступила: 14.10.2022 • Доработана: 28.01.2023 • Принята к опубликованию: 10.03.2023

**Для цитирования:** Александров А.Е., Борисов С.П., Бунина Л.В., Быковский С.С., Степанова И.В., Титов А.П. Статистическая модель оценки надежности систем неразрушающего контроля на основе решения обратных задач. *Russ. Technol. J.* 2023;11(3):56–69. https://doi.org/10.32362/2500-316X-2023-11-3-56-69

**Прозрачность финансовой деятельности:** Авторы не имеют финансовой заинтересованности в представленных материалах или методах.

Авторы заявляют об отсутствии конфликта интересов.

## **INTRODUCTION**

One of the most important issues in the operation of large power plants is ensuring the safety of their use. In order to solve this problem, it is necessary to ensure the integrity of the structures of nuclear power plants, including equipment and piping, over the entire working life of the power plant¹. Regardless of the types of nuclear power plants and operating conditions, damage to the structural elements of nuclear power plants (including cracks) is detected almost every year. The problem can be described in terms of insufficient knowledge of damage models and mechanisms, which corresponds to the impossibility of solving this problem at the design stage.

One approach to solving this problem is to create a system for maintaining a given level of reliability by carrying out periodic diagnostics of the technical state of the most critical objects of the operated power plant, i.e., the organization and performance of works for non-destructive testing of metal of equipment and piping. Based on the current state of the tested objects, the future situation can be predicted and a decision taken to terminate or continue the further operation of the objects.

## 1. STATISTICAL MODELS FOR ASSESSING THE RELIABILITY OF NON-DESTRUCTIVE TESTING SYSTEMS

In order to assess the current state of the objects being tested, it is necessary to measure the reliability of non-destructive testing. In order to obtain such a metric, the probability-of-detection (*PoD*) curve is used [1, 2] to describe the defect size distribution of the defect detection probability. In practice, this curve can depend on many factors, including the capabilities of the method and monitoring equipment at a selected sensitivity, the location and geometry of the defect, and the properties of the material.

Human factors are also taken into account, among which are staff fatigue, stressful situations, and difficult inspection conditions.

For constructing the *PoD* curve, the monitoring results are used as experimental data. These can be obtained using systems similar to those described in the literature [3–5] and materials of the American Society for Nondestructive Testing<sup>2</sup>. The monitoring system used in this case can be used to detect both real defects formed during the operation of equipment and piping of a power plant, and artificially created defects with specified dimensions. Artificially created defects 3 should have the same features as real defects. The most suitable are samples of real objects with real cracks formed during operation. The types of fracture—ductile and brittle—are also taken into account [6].

In general, the assessment test methodology only provides qualitative conclusions about the ability of the non-destructive testing system to detect defects. Most works give results only for the averaged *PoD* curves obtained by testing the same object by different laboratories. An example is the results of interlaboratory comparative non-destructive tests that were conducted in 2018–2019 by nuclear industry organizations<sup>4</sup>. Data obtained by nine laboratories was not suitable for use in the construction of *PoD* curves for individual laboratories due to the small number of measurements for a single defect size. In this case, an averaged *PoD* curve was drawn based on the results

<sup>&</sup>lt;sup>1</sup> Requirements for equipment and piping time management in nuclear power plants. Basic provisions (NP-096-15). http://www.cntr-nrs.gosnadzor.ru/about/AKTS/HΠ-096-15.pdf. Accessed December 15, 2022 (in Russ.).

<sup>&</sup>lt;sup>2</sup> Bouis J. NDT to evaluate crevice corrosion initiation sites in alloy pipe and tubing. *The NDT Technician*. 2022;21(1). https://blog.asnt.org/ndt-to-evaluate-crevice-corrosion-initiation-sites-in-alloy-pipe-and-tubing/. Accessed December 15, 2022.

<sup>&</sup>lt;sup>3</sup> Kanzler D., Müller C., Pitkänen J., Ewert U. Bayesian approach for the evaluation of the reliability of non-destructive testing methods: combination of data from artificial and real defects. *Proceedings: 18th World Conference on Nondestructive Testing WCNDT. Special Issue. e-Journal of Nondestructive Testing (eJNDT)*. 2012;17(7). http://www.ndt.net/?id=12748. Accessed December 15, 2022.

<sup>&</sup>lt;sup>4</sup> Analytical report No. 532/789-2019 "On conducting interlaboratory comparative non-destructive tests in organizations of the nuclear industry under the program P.MSI.NKSS-533/009-2018," Part 2. Moscow: ROSATOM, VNIINM; 2019 (in Russ.).

of all nine laboratories. This situation is typical for constructing *PoD* curves.

The output characteristic of the monitoring system used is a signal (peak voltage or amplitude), which is compared with a threshold value and can be interpreted as a function of the size of the defect. Comparative analysis between the output signal of the monitoring system and defects of known size a gives estimate PoD(a) of the probability-of-detection curve. The PoD(a) estimate can be found from the number of monitoring events performed by the initial system for a given size  $a_i$  as

$$PoD(a_i) = \frac{n_i}{n},\tag{1}$$

where  $PoD(a_i)$  is the probability of detection of a defect of size  $a_i$ ,  $n_i$  is the number of defects of size  $a_i$  detected during the monitoring, and n is the total number of defects of size  $a_i$  in the test sample.

Repeated use of formula (1) at different sizes of defects  $a_i$  gives the defect size distribution of the frequency of detection of defects.

## 1.1. Binomial model for assessing the reliability of the monitoring system

Let us assume that a given general population contains a fraction of defects of a given size. Then, taking N objects from this population and studying them using the initial monitoring system, it can be hoped that, with an increase in the number N, all defects of a given size will be detected. In this case, each experiment can be considered as an independent trial, while the frequency of occurrence of an event,  $\omega = n_i/N$ , can be calculated by Bernoulli's formula [7, 8]

$$P\left\{\omega = \frac{n_i}{N}\right\} = \frac{N!}{n_i!(N - n_i)!} p^{n_i} (1 - p)^{N - n_i}, \qquad (2)$$

where *p* is the probability of detection of a single defect.

The lower confidence bound on the probability of detection at a given confidence level and a given sample size can be obtained by solving the equation

$$p_{MS} = \sup \left\{ p : \sum_{n_i=0}^{N-1} \frac{N!}{n_i! (N-n_i)!} p^{n_i} (1-p)^{N-n_i} \ge 1-\alpha \right\},$$
 (3)

where  $(1 - \alpha)$  is the lower confidence bound on a given probability, and MS refers to the monitoring system used.

Having obtained a solution to equation (3), the probability detecting a defect of a given size above 0.9 can be ensured with a given confidence interval of 95% if all 29 defects of 29 given defects are found in 29 trials. Such tests can additionally be used to assess the monitoring system: by setting the number of checks and assuming that all defects will be found by the monitoring system being tested, the detection probability can be determined at a given confidence interval. If the lower confidence interval for a fraction of detected cracks exceeds the specified detection probability value, then the monitoring system is considered to provide the required level of reliability.

However, as already noted [9, 10], the use of a binomial model to assess the reliability of the monitoring system can lead to serious problems. These arise when constructing a *PoD* curve with changing defect sizes. In this case, the confidence bounds on the *PoD* curve have a very unstable behavior, which depends on the chosen analysis method. Moreover, the *PoD* curve throughout the range of defect sizes can be constructed only if the number of defects is sufficiently large due to the need to multiply the defect sample size for one defect size by the number of points required to construct the *PoD* curve.

## 1.2. Berens-Hovey parametric model for the *PoD* curve

As an alternative to the binomial model, a parametric model was proposed for constructing the *PoD* curve. Berens and Hovey [11, 12] used a different statistical framework to represent the PoD curve as a mathematical function. The statistical model proposed by Berens and Hovey [12] is based on a representation of the output signal of the monitoring system as the main component (characterizing the changes in the average signal from one defect to another), together with a random component (describing the changes in the signal when testing the same defect). The properties of the material, the location of the defect, and its orientation, which are represented by the main component, do not change from one test to another. The random component is due to the human factor and the instrumentation used. In turn, the instrumentation depends on the method, methodology, and equipment for monitoring at a selected sensitivity. A possible way to improve the confidence of, e.g., ultrasonic testing was described previously [12]. It is important to note that the human factor is subjective and can change for many reasons, whereas instrumentation factors have objective characteristics, which can be assessed in terms of the error of the method used.

In accordance with the above ideas, Berens and Hovey [13] proposed a statistical model, in which the response signal of the monitoring system is divided into separate components. These components can be written as the following functional relationship

$$\hat{a} = h(a) + \delta + \varepsilon, \tag{4}$$

where  $\hat{a}$  is the output signal of the monitoring system; h(a) is the main component, which characterizes the average change in the signal as a function of the defect size;  $\delta$  is an additional component, which is due to the instrumentation used and is defined as the error of the method used; and  $\varepsilon$  is an additional component, which is due to the human factor.

According to Berens and Hovey, h(a) is a random variable with its mean value, while  $\delta$  and  $\epsilon$  are random variables with zero means.

## 1.3. Parametric model of the *PoD* curve based on the results of statistical processing of test samples

The proposed model can only be used in equation (4) for constructing the PoD(a) curve if the sizes of defects and their distribution are known in advance, i.e., if the defects are artificially created as test samples. These data can be obtained from the results of non-destructive tests in organizations of the nuclear industry [14].

This method of constructing the *PoD* curve can be referred to as a direct method. However, organizing and conducting such tests involve significant costs. Since the data obtained from the results of such tests are limited, only data on the average *PoD* are typically presented. In this case, the averaging of the data complicates their further use for solving practical problems and makes it impossible to make an individual assessment of the confidence by different laboratories.

As was noted [9], this is a big drawback because individual assessments by different laboratories allow one to identify more reliable laboratories and use their experience in further work. Additional difficulties arising in the construction of *PoD* curves were described in the literature [15]. The noted shortcomings require the search for alternative methods for estimating the *PoD* curve.

## 2. STATISTICAL MODEL FOR ASSESSING THE RELIABILITY OF NON-DESTRUCTIVE TESTING SYSTEMS BY SOLVING INVERSE PROBLEMS

As an alternative to direct methods, computational methods based on solving inverse problems [16], as well as computer simulation tools<sup>5</sup>, can be used.

The *PoD* curve is constructed using data on real defects found by testing metal structures. An essential component is the selection of a sample of initial data [18, 19].

Let defects of different sizes  $a_i$  be found in a structure operating for time t. After constructing the defect size distribution of the frequency of detection of defects for the obtained sample (Fig. 1), the density distribution of detected defects,  $p_j(a)$ , can be obtained. A dimensional scale should be chosen as the defect size  $a_i$ , e.g., depth, length, or cross-sectional area of the defect. Because of the imperfection of the monitoring system used, some of the defects remain undetected. As mentioned above, the degree of imperfection of the monitoring system is characterized by the probability-of-detection curve  $PoD_{MS}(a)$ , where the subscript MS refers to a certain monitoring system.

The set of detected and undetected defects is described by the initial random defect size distribution. Let us call this distribution the real defect density distribution and denote it  $p_a(a)$ .

In accordance with the introduced definitions, the expression for the density of detected defects has the form

$$p_f(a) = \frac{p_a(a)PoD_{MS}(a)}{\int\limits_{a_0}^{S} p_a(a)PoD_{MS}(a)da},$$
 (5)

where  $p_i(a)$  is the density distribution of detected defects by the initial monitoring system,  $p_a(a)$  is the real defect density distribution in the test object,  $PoD_{MS}(a)$  is the probability-of-detection curve for the initial monitoring system MS, S is the maximum size of a defect that can occur in the test object,  $a_0$  is the sensitivity of the initial monitoring system (minimum size of a defect that can be detected by the initial system), and a is the dimensional defect scale.

Considering expression (5), the problem of finding the functions  $p_a(a)$  and  $PoD_{MS}(a)$  from the known distribution function  $p_f(a)$  can be posed. Such a problem is an inverse problem [19–21]. To solve this problem, it is necessary to know the specific form of the functions  $p_a(a)$  and  $PoD_{MS}(a)$ .

The distribution function of the real sizes of defects should theoretically be exponential because the number of defects increases with a decrease in the size scale. Under this assumption, let us write the real defect distribution density as

$$p_{a}(a) = \frac{\exp(-\lambda a)}{\sum_{a_{0}}^{S} \exp(-\lambda a) da},$$
 (6)

where  $\lambda$  is the parameter of the real defect distribution.

<sup>&</sup>lt;sup>5</sup> Genc K. Simulating reality: Going beyond counting pores and cracks in additive-manufactured parts. *FOCUS The NDT Technician*. 2020;19(2). 3 p. https://www.asnt.org/-/media/Files/Publications/TNT/TNT\_19-2.pdf?la=en. Accessed December 15, 2022.

The form of the function  $PoD_{MS}(a)$  was chosen so that it has few parameters, but takes into account the features of statistical model (4) proposed by Berens and Hovey. With these requirements in mind, the following form was used:

$$PoD_{MS}(a) = 1 - \exp(-r(a - a_0)),$$
 (7)

where r is the confidence coefficient of the initial monitoring system.

The confidence coefficient r in formula (7) includes both the main component of the function  $PoD_{MS}(a)$  of the defect size and the additional component due to the human factor [22], which is found from the results of statistical processing of the initial sample. The same is valid for the parameter  $a_0$ .

Substitution of formulas (6) and (7) into relation (5) gives

$$p_{f}(a) = \frac{\exp(-a/\lambda) \left[1 - \exp(-r(a - a_{0}))\right]}{\int_{a_{0}}^{S} \exp(-a/\lambda) \left[1 - \exp(-r(a - a_{0}))\right] da}.$$
 (8)

It follows from relation (8) that, knowing the distribution  $p_j(a)$ , the following three parameters should be obtained: the distribution parameter  $\lambda$ , the confidence coefficient r, and the sensitivity  $a_0$  of the initial monitoring system. The construction of the PoD curve of several independent variables was described in the literature [23].

## 2.1. Calculation procedure

An important feature of the function  $p_f(a)$  should be noted. Since this function is defined as the product of the monotonically decreasing function  $p_a(a)$  and the monotonically increasing function  $PoD_{MS}(a)$ , the function  $p_f(a)$  can be assumed to have a maximum. The coordinate of the maximum value should be related to the parameters of the functions  $p_a(a)$  and  $PoD_{MS}(a)$ . Simple calculations give the abscissa of the point of maximum:

$$a_{\text{max}} = a_0 - \frac{\ln\left(1 + \frac{r}{\lambda}\right)}{r}.$$
 (9)

Substitution of  $a_{\text{max}}$  into relation (8) gives the ordinate of the point of maximum:

$$p_{\mathbf{f}}(a_{\text{max}}) = y_{\text{max}}. (10)$$

These coordinates  $(a_{\text{max}}, y_{\text{max}})$  can be determined from the experimentally obtained density distribution of detected defects (Fig. 1).

An additional feature of the selected functions should also be noted. Substitution of  $a_{\text{max}}$  into formula (6) gives almost the same ordinate of the point of maximum as that in formula (10), i.e.,

$$p_a(a_{\text{max}}) = y_{\text{max}}. (11)$$

The ordinates in formulas (10) and (11) exactly coincide if the used limits of integration in the expressions are 0 and  $\infty$ . The difference between the  $y_{\text{max}}$  values calculated by formulas (10) and (11) depends on the  $a_0$  value and the chosen value of the maximum defect size S in the region under study. At S > 20 mm, the relative error of the difference between these values does not exceed  $10^{-4}$ .

In essence, this means that the probability density distribution function  $p_a(a)$  passes through the point of maximum of the density distribution of detected defects  $p_f(a)$ . Using this property, the nonlinear equation for the unknown parameters  $a_0$  and  $\lambda$  can be written:

$$F(a_0, \lambda) = y_{\text{max}} - \frac{\exp(-\lambda a_{\text{max}})}{\int\limits_{a_0}^{S} \exp(-\lambda a) da} = 0.$$
 (12)

The unknown parameter  $a_0$  can be found from the experimentally obtained density distribution of detected defects as the intersection of the curve of the distribution of detected defects with the abscissa axis. Knowing the obtained value  $a_0$  and using equation (12), the second unknown parameter,  $\lambda$ , can also be found by considering nonlinear equation (12) in only one parameter  $\lambda$ .

The parameter r was found by the method of successive approximations. Given a set of parameter r values, let us calculate the parameter  $\lambda$  value at each r. Let us divide the initial region of size  $(a_0, S)$  into n intervals. The choice of the number of intervals and their sizes is determined by a preliminary analysis of the initial sample. According to formula (6), the probability that real defects of sizes from a to b are in the interval (a, b) has the form

$$p_{a}(a,b) = \frac{\int_{a}^{b} \exp(-a/\lambda)da}{\int_{a_{0}}^{c} \exp(-a/\lambda)da}.$$
 (13)

If the total number  $N_{a\Sigma}$  of real defects throughout the region is known, then the number of real defects in the ith interval is

$$N_a^i = p_a(a_i, a_{i+1}) N_{a\Sigma}. \tag{14}$$

If the number  $N_f^i$  of detected defects in each interval is known, then the total number of real defects can be found from the expression

$$N_{a\Sigma} = \sum_{i=1}^{n} N_f^i \frac{1}{1 - \exp\left(-r\left(\frac{a_i + a_{i+1}}{2} - a_0\right)\right)}.$$
 (15)

Thus, by giving the r value and using expression (15),  $N_{a\Sigma}$  is found. Then, using formula (14), the number  $N_a^i$  of real defects in each (ith) interval is determined. Further, the parameter  $\lambda(r)$  is obtained from the known  $N_a^i$  values by linear regression.

The  $\lambda(r)$  value that is closest to the parameter  $\lambda$  value found from equation (12) is the initial parameter r value.

### 2.2. Test calculations

The accuracy of the above calculation procedure was checked by test calculations on models. In this case, data modeling offers an important advantage: the results of the calculations can be compared with the known behavior of the general population, which cannot be done by comparing only laboratory data. Some issues of the quality of the recovery procedure were described previously [24, 25].

Let the initial data be a given structure containing a total of  $N_{a\Sigma}$  real defects with an exponential defect size distribution with known parameter  $\lambda$ . The current state of the structure is assessed by a non-destructive testing system with known PoD(a) of given form (7) with known characteristics r (confidence coefficient) and  $a_0$  (sensitivity of the initial monitoring system). The monitoring detected  $N_{a\Sigma}$  defects of different sizes, which can be sorted by size. The thus-obtained

Table 1. Initial data for modeling

No. of series of calculations	Parameter $a_0$ , mm	Parameter λ, mm <sup>-1</sup>	Parameter <i>r</i> , mm <sup>-1</sup>
1	0.5	0.2	0.1
2	0.5	0.2	0.5
3	0.5	0.2	1.0
4	0.5	0.5	0.1
5	0.5	0.5	0.5
6	0.5	0.5	1.0
7	0.5	1.0	0.1
8	0.5	1.0	0.5
9	0.5	1.0	1.0

population of  $N_{a\Sigma}$  detected defects is the initial sample, which was processed according to the proposed procedure. The obtained values were compared with the initial data. To study the effect of a combination of values of the initial parameters on the recovered characteristics, the initial data were grouped for nine series of calculations (Table 1). For all the selected series, the total number of real defects was assumed to be  $N_{a\Sigma}=1000$ . The pipe wall thickness was chosen to be S=20 mm.

## 2.2.1. Determination of parameter a<sub>0</sub>

The parameter  $a_0$  was determined by finding the point of intersection of the curve of the density of detected defects with the abscissa axis. The density curve was approximated by a parabola constructed through two points, including the point of maximum of the initial density of detected defects. The following initial parameters of the fourth series were chosen as an example of calculation:  $\lambda = 0.5 \text{ mm}^{-1}$ ,  $r = 0.1 \text{ mm}^{-1}$ , and  $a_0 = 0.5 \text{ mm}$ .

The initial parameters were used to plot the real defect density curve by formula (6). After specifying the number of intervals of division of the initial region (at n = 27), the number of real defects within the obtained intervals is found from formula (14). Knowing the number of real defects within the obtained intervals, the number of detected defects in each interval can be calculated using the dependence

$$N_f^i = N_d^i \int_{a_i}^{a_{i+1}} (1 - \exp(-r(a - a_0))) da.$$
 (16)

Rounding of the number  $N_f^i$  to an integer gives the initial sample of detected defects grouped by their size. The obtained values of detected defects can be rounded down (truncation of the fractional part if it is less than 0.5) and up (increase to the next integer if the fractional part is greater than or equal to 0.5), which leads to two different frequency distributions (Fig. 1, red and blue columns).

For the obtained distribution, let us choose two points (first and third), including the point of maximum of the density, and draw a parabola through them. The point of intersection of the parabola with the abscissa axis gives the parameter  $a_0$  value (Fig. 2). The parameter  $a_0$  can be calculated with the frequency characteristics rounded either down ( $a_0^- = 0.365$ ) or up ( $a_0^+ = 0.309$ ). The average value of the parameter  $a_0$  is  $a_0^{\rm s} = 0.337$ . The initial  $a_0$  value is 0.5 mm. The error in calculating the parameter  $a_0$  is  $\delta a_0 = 0.326$  or 32.6%.

The parameter  $a_0$  values can similarly be calculated at other initial values of the parameters  $\lambda$  and r. Table 2 presents the results of such calculations.

**Table 2.** Results of the recovery of the parameter  $a_0^{\rm S}$ 

Initial value of λ	Confidence coefficient	Recovered value $a_0^{\rm s}$	Error $\delta a_0$ , %
	r = 0.1	0.189	62.2
$\lambda = 0.2$	r = 0.5	0.303	39.4
	r = 1.0	0.321	35.8
	r = 0.1	0.337	32.6
$\lambda = 0.5$	r = 0.5	0.402	19.6
	r = 1.0	0.424	15.2
	r = 0.1	0.468	6.4
$\lambda = 1.0$	r = 0.5	0.460	8.0
	r = 1.0	0.446	10.0

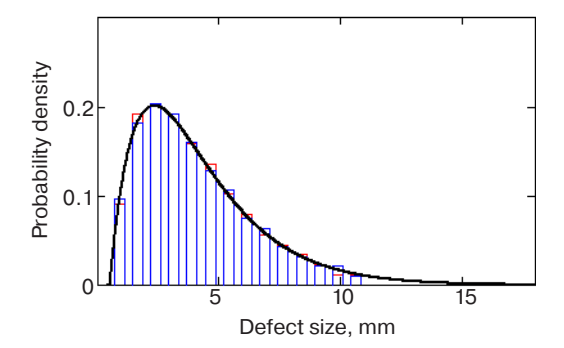


**Fig. 1.** Defect size distribution of detected defects (all series)

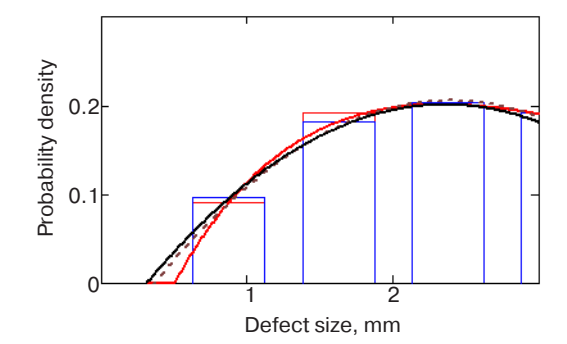


**Fig. 2.** Two variants of the determination of the parameter  $a_0$  with the frequency characteristics rounded down and up

## 2.2.2. Determination of the calculated (recovered) value $\tilde{\lambda}$ of the parameter $\lambda$

The parameter  $\lambda$  was determined from equation (12). The coordinates of the maximum point of the sample are found using the initial sample of defects (Fig. 1). Knowing these coordinates and using the parameter  $a_0^s$  value from Table 2, one can solve nonlinear equation (12) for  $\lambda$ . As a result, the sought-for parameter

 $\tilde{\lambda}$  is obtained. Table 3 presents the results of these calculations.

## 2.2.3. Determination of the parameter r

Let us consider an example of calculating the soughtfor parameter r at the above initial parameter values of the fifth series:  $\lambda = 0.5 \text{ mm}^{-1}$ ,  $r = 0.5 \text{ mm}^{-1}$ , and  $a_0 = 0.5 \text{ mm}^{-1}$ . The number of intervals of division of the

**Table 3.** Results of the recovery of the parameter  $\tilde{\lambda}$ 

Initial value of λ	Confidence coefficient	Recovered value $\tilde{\lambda}$	Error δã, %
	r = 0.1	0.199	0.5
$\lambda = 0.2$	r = 0.5	0.232	16.0
	r = 1.0	0.235	12.5
	r = 0.1	0.529	5.8
$\lambda = 0.5$	r = 0.5	0.594	18.8
	r = 1.0	0.574	14.8
	r = 0.1	0.969	6.4
$\lambda = 1.0$	r = 0.5	1.084	8.4
	r = 1.0	1.075	7.5

Note.  $\delta \tilde{\lambda}$  is the relative error of calculating the parameter  $\tilde{\lambda}$ 

initial region was specified as n = 36. Figure 3 presents the constructed frequency characteristic of detected defects for this series. By setting different values of the parameter r for the initial frequency distribution of detected defects, the corresponding distributions of real defects were obtained. Figure 4 shows one of the obtained distributions of real defects. The real distribution was processed by linear regression, while the parameter  $\lambda$  values were calculated at a given value of r. Table 4 presents the results of such calculations for the fifth series. Comparison of the obtained results with the parameter value (0.954) recovered earlier for this series gave a close value of 0.579; the parameter r values was taken to be 0.27. Note that the initial value of the parameter r was 0.5; i.e., the recovery error of this parameter is 46%.

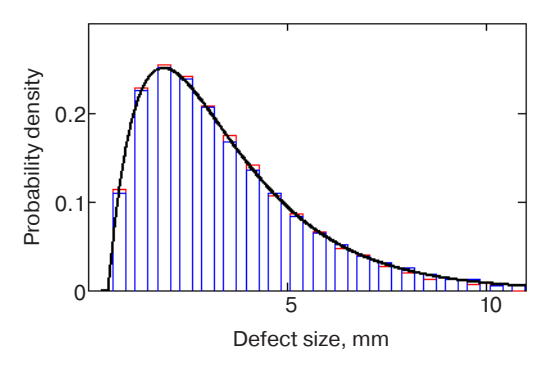


**Fig. 3.** Defect size distributions of the frequency and density of detected defects for the fifth series

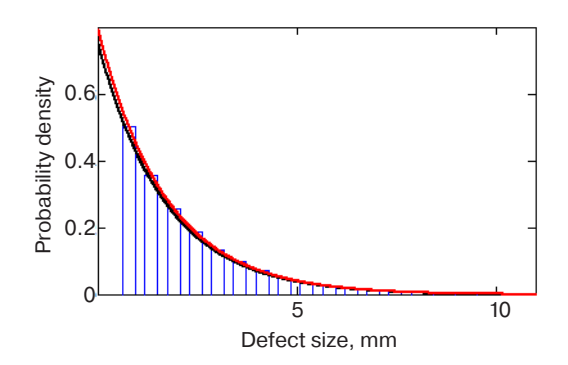


**Fig. 4.** Defect size distributions of the frequency and density of real defects for the fifth series

The black line in Fig. 4 was constructed by formula (6) at the calculated parameters of the fifth series ( $a_0 = 0.402$  from Table 2,  $\lambda = 0.594$  from Table 3). The red line was constructed by approximation using formula (17) obtained from the linear regression of the real distribution at r = 0.27:

$$p_a^{\exp}(a) = \exp(-0.226 - 0.593a).$$
 (17)

Similarly, the parameter r values were recovered and the errors for the remaining calculation series were calculated. Table 5 presents he results of the calculations.

The features of the implementation of the developed procedure were described in more detail in the literature [26].

**Table 4.** Results of the recovery of the parameter  $\tilde{\lambda}$  at various confidence coefficients

No. of series	Recovered parameter $r$ , $$ $$ $$ $$ $$ $$ $$ $$ $$ $$	Recovered parameter $\tilde{\lambda}$ , mm <sup>-1</sup>	Degree of approximation of recovered parameter $\tilde{\lambda}$ to reference value $\lambda_0$ =0.594, $\Delta \lambda = \left  \frac{\lambda_0 - \overline{\lambda}}{\lambda_0} \right $
1	0.25	0.601	0.012
2	0.26	0.595	$1.7 \cdot 10^{-3}$
3	0.27	0.593	$1.684 \cdot 10^{-3}$
4	0.28	0.588	0.010
5	0.29	0.585	0.015
6	0.30	0.579	0.025
7	0.33	0.568	0.044
8	0.35	0.560	0.057
9	0.4	0.541	0.089
10	0.5	0.502	0.155

Table 5. Results of the recovery of the confidence coefficient

Initial value of parameter $\lambda$	Confidence coefficient	Parameter $\tilde{r}$	Error $\delta \tilde{r}$ , %
	r = 0.1	0.095	5.0
$\lambda = 0.2$	r = 0.5	0.4	20.0
	r = 1.0	0.9	10.0
	r = 0.1	0.05	50.0
$\lambda = 0.5$	r = 0.5	0.3	40.0
	r = 1.0	0.7	30.0
	r = 0.1	0.08	20.0
$\lambda = 1.0$	r = 0.5	0.55	10.0
	r = 1.0	0.80	20.0

## 3. ANALYSIS OF THE OBTAINED RESULTS

Comparison of the obtained modeling results and the given initial values of the parameters suggests the following conclusions.

When recovering the parameter  $a_0$ , the error was maximum in the series of calculations with the initial value  $\lambda=0.2$  (the maximum error  $\delta a_0$  was 62.2% at r=0.1). With increasing parameter r from 0.5 to 1.0, the error decreased from 39.4 to 35.8%. With increasing parameter  $\lambda$  from 0.5 to 1.0, the error  $\delta a_0$  also decreased: the minimum value at  $\lambda=0.5$  was 15.2% at r=1.0; the minimum value at  $\lambda=1.0$  was 6.4% at r=0.1. The error range was 6.4–62.2%.

When recovering the parameter  $\lambda$ , the error in all the series of calculations, which did not exceed 18.8%, ranged from 0.5 to 18.8%.

When recovering the parameter r, the maximum error was 50% at the initial parameter values  $\lambda = 0.5$  and r = 0.1, while the minimum error was 5% at the initial parameter values  $\lambda = 0.2$  and r = 0.1. The error range was 5–50%.

The obtained results of numerical modeling showed the fundamental possibility of using the developed procedure to determine both the probability-of-detection curve and the probability distribution of actual defects from the monitoring results.

## 4. CONCLUSIONS

In this work, the following features of the proposed procedure were identified:

1) The recovery of the probability distribution of real defects is based on statistical processing of only the fraction of the experimental values of the initial sample that determine its extreme value.

- 2) The obtained extreme value of the initial sample can be used to directly determine the parameter  $\lambda$  of the real defect distribution by solving a nonlinear equation.
- 3) The recovery of the confidence curve (determination of the parameter *r*) uses the entire initial sample to solve the inverse problem, which belongs to the class of problems of interpretation of observational or diagnostic data [16–18].

The developed procedure makes it possible to use metal monitoring data both for analyzing the current state of equipment and piping, as well as for predicting their future behavior with greater confidence than currently used methods. This is primarily due to the possibility of using the procedure to assess the reliability (determine the probability-of-detection (*PoD*) curve) for individual test teams directly from the results of experimental tests. An individual assessment of the efficiency of the monitoring carried out by the laboratory also allows the identification of bad and good test teams, whereas the averaging of the results when constructing the *PoD* curve excludes this possibility.

However, it should be noted that the developed methodology only supplements currently existing methods of assessment tests, but does not replace them.

An important application of the developed procedure is to analyze large data arrays obtained by metal monitoring in power plants. In this case, groups of defects can be formed depending on various factors, including types of structural elements, operating conditions, materials used (stainless steel, black steel, composite welded joints), monitoring systems, as well as the quality of work performed by different test teams.

## **Authors' contributions**

- **A.E. Alexandrov**—collecting the results of field measurements, developing a mathematical model, general coordination of the work.
  - **A.P. Titov**—developing a mathematical model.
- **S.P. Borisov** and **S.S. Bikovsky**—design of independent software implementations of a mathematical model.
- **I.V. Stepanova** and **L.V. Bunina**—testing and verification of the software model, direct modeling.

## **REFERENCES**

- 1. Berens A.P. Probability of Detection (PoD) Analysis for the Advanced Retirement for Cause (RFC). Engine Structural Integrity Program (ENSIP) Nondestructive Evaluation (NDE) System Development. V. 1. PoD Analysis. Technical Report. Dayton: University of Dayton, Research Institute; 2000. 88 p.
- Berens A.P. NDE reliability data analysis. In: ASM Metals Handbook. V. 17. Non-Destructive Evaluation and Quality Control: Qualitative Non-Destructive Evaluation. 1989:17:689–701.
- 3. Subair S.M., Balasubramaniama K., Rajagopala P., Kumar A., Rao B.P., Jayakumar T. Finite element simulations to predict probability of detection (PoD) curves for ultrasonic inspection of nuclear components. *Procedia Engineering: 1st International Conference on Structural Integrity.* 2014;86:461–468. https://doi.org/10.1016/j.proeng.2014.11.059
- Filinov V.V., Mikaeva S.A., Rodyukov M.S., Filinova A.V. Modern architecture board information and control systems of heavy vehicles. *Russ. Technol. J.* 2017;5(3):114–123 (in Russ.). https://doi.org/10.32362/2500-316X-2017-5-3-114-123
- Link R., Riess N. Non-Destructive Material Testing: Surface Crack Detection. V. 1. Hamburg: Helling GmbH; 2014.
- Aleksandrov A.E., Azhder T.B., Stepanova I.V. A probabilistic model for calculating pipelines by the mechanism of ductile and brittle fracture. *Informatsionnye Tekhnologii = Information Technologies*. 2020;26(8): 443–450 (in Russ.). https://doi.org/10.17587/it.26.443-450
- 7. Casella G., Berger R. *Statistical inference*. 2nd ed. Duxbury Press; 2007. 650 p.
- 8. Kutner M.H., Nachtsheim C.I., Neter J., Li W. *Applied Linear Statistical Models*. 5th ed. New York: McGraw-Hill/Irwin; 2005. 1396 p.
- 9. Gandossi L., Annis C. *Probability of Detection Curves: Statistical Best-Practices. ENIQ report.* No. 41. Luxembourg: Publications Office of the European Union; 2010. 72 p.
- Schneider C.R.A., Rudlin J.R. Review of statistical methods used in quantifying NDT reliability. *Insight – Non-Destructive Testing and Condition Monitoring*. 2004;46(2):77–79. https://doi.org/10.1784/ insi.46.2.77.55549
- 11. Berens A.P., Hovey P.W. Evaluation of NDE reliability characterization. AFWAL-TR-81-4160. V. 1. Dayton: Air Force Wright-Aeronautical Laboratories, Wright-Patterson Air Force Base; 1981.

## СПИСОК ЛИТЕРАТУРЫ

- 1. Berens A.P. Probability of Detection (PoD) Analysis for the Advanced Retirement for Cause (RFC). Engine Structural Integrity Program (ENSIP) Nondestructive Evaluation (NDE) System Development. V. 1. PoD Analysis. Technical Report. Dayton: University of Dayton, Research Institute; 2000. 88 p.
- 2. Berens A.P. NDE reliability data analysis. In: *ASM Metals Handbook*. V. 17. *Non-Destructive Evaluation and Quality Control: Qualitative Non-Destructive Evaluation*. 1989:17:689–701.
- 3. Subair S.M., Balasubramaniama K., Rajagopala P., Kumar A., Rao B.P., Jayakumar T. Finite element simulations to predict probability of detection (PoD) curves for ultrasonic inspection of nuclear components. *Procedia Engineering: 1st International Conference on Structural Integrity.* 2014;86:461–468. https://doi.org/10.1016/j.proeng.2014.11.059
- 4. Филинов В.В., Микаева С.А., Родюков М.С., Филинова А.В. Разработка средств неразрушающего контроля изделий из ферромагнитных сталей на основе использования магнитных шумов. *Russ. Technol. J.* 2017;5(3): 114–123. https://doi.org/10.32362/2500-316X-2017-5-3-114-123
- Link R., Riess N. Non-Destructive Material Testing: Surface Crack Detection. V. 1. Hamburg: Helling GmbH; 2014.
- 6. Александров А.Е., Аждер Т.Б., Степанова И.В. Вероятностная модель расчета трубопроводов по механизму вязкого и хрупкого разрушения. *Информационные технологии*. 2020;26(8):443–450. https://doi.org/10.17587/it.26.443-450
- 7. Casella G., Berger R. *Statistical inference*. 2nd ed. Duxbury Press; 2007. 650 p.
- 8. Kutner M.H., Nachtsheim C.I., Neter J., Li W. *Applied Linear Statistical Models*. 5th ed. New York: McGraw-Hill/Irwin; 2005. 1396 p.
- Gandossi L., Annis C. Probability of Detection Curves: Statistical Best-Practices. ENIQ report. No. 41. Luxembourg: Publications Office of the European Union; 2010. 72 p.
- Schneider C.R.A., Rudlin J.R. Review of statistical methods used in quantifying NDT reliability. *Insight – Non-Destructive Testing and Condition Monitoring*. 2004;46(2):77–79. https://doi.org/10.1784/ insi.46.2.77.55549
- 11. Berens A.P., Hovey P.W. Evaluation of NDE reliability characterization. AFWAL-TR-81-4160. V. 1. Dayton: Air Force Wright-Aeronautical Laboratories, Wright-Patterson Air Force Base; 1981.

- Alain S., Badeau N. Using passive-axis focusing wedges to decrease inspection reject rates. FOCUS The NDT Technician. 2021;20(3):1–5. Available from URL: https://ndtlibrary.asnt.org/2021/UsingPassiveAxisFocusingWedgestoDecreaseInspectionRejectRates (accessed December 15, 2022).
- Berens A.P., Hovey P.W. Flaw detection reliability criteria. V. 1. Methods and results. AD-A142 001. Final technical report. Dayton: University of Dayton, Research Institute; 1984. 175 p. Available from URL: https:// archive.org/details/DTIC\_ADA142001
- Getman A.F., Kozin Yu.N. Nerazrushayushchii kontrol' ibezopasnost'ekspluatatsiisosudovitruboprovodovdavleniya (Non-Destructive Testing and Safety of Operation of Pressure Vessels and Pipelines). Moscow: Energoatomizdat; 1997. 288 p. (in Russ.). ISBN 5-283-03151-9
- 15. Annis C., Aldrin J.C., Sabbagh H.A. What is missing in nondestructive testing capability evaluation? *Mater. Eval.* 2015;73(1):1–11.
- Aleksandrov A.E. Evaluation of the reliability of metal testing results based on an alternative algorithm. Informatsionnye Tekhnologii = Information Technologies. 2018;8(24):529–537 (in Russ.). https://doi.org/10.17587/it.24.529-537
- 17. Montgomery D.C. Design and Analysis of Experiments. 10th ed. Wiley; 2020. 688 p. ISBN 978-1-119-72210-6
- Annis C., Gandossi L., Martin O. Optimal sample size for probability of detection curves. *Nucl. Eng. Des.* 2013;262: 98–105. https://doi.org/10.1016/j.nucengdes.2013.03.059
- 19. Tikhonov A.N., Kal'ner V.D., Glasko V.B. Matematicheskoe modelirovanie i metod obratnykh zadach v mashinostroenii (Mathematical Modeling and Method of Inverse Problems in Mechanical Engineering). Moscow: Mashinostroenie; 1990. 264 p. (in Russ.).
- Aldrin J.C., Shell E.B., Oneida E.K., Sabbagh H.A., Sabbagh E., Murphy R.K., Mazdiyasni S., Lindgren E.A. Model-based inverse methods for sizing surface-breaking discontinuities with eddy current probe variability. *AIP Conference Proceedings*. 2016;1706(1):090002\_1-090002\_10. https://doi.org/10.1063/1.4940539
- Aldrin J.C., Oneida E.K., Shell E.B., Sabbagh H.A., Sabbagh E., Murphy R.K., Mazdiyasni S., Lindgren E.A., Mooers R.D. Model-based probe state estimation and crack inverse methods addressing eddy current probe variability. *AIP Conference Proceedings*. 2017;1806(1):110013\_1-110013\_11. https://doi.org/10.1063/1.4974691
- 22. Bertovic M., Given J., Rentala V.M., Lehleitner J., Kanzler D., Heckel T., Tkachenko V. Human Factors in der POD ist das möglich? *e-Journal of Nondestructive Testing (eJNDT)*. https://www.ndt.net/article/dgzfp2022/papers/mo.3.b.3.pdf
- 23. Yusa N., Knopp J.S. Evaluation of probability of detection (POD) studies with multiple explanatory variables. *J. Nucl. Sci. Technol.* 2015;53(4):574–579. Available from URL: https://doi.org/10.1080/00223131.2015.1064332
- Schneider C.R.A., Sanderson R.M., Carpentier C., Zhao L., Nageswaran C. Estimation of probability of detection curves based on theoretical simulation of the inspection process. *Annual Br. Conf. on NDT*. 2012. 12 p. Available from URL: https://www.bindt.org/downloads/ NDT2012\_5C1.pdf

- 12. Alain S., Badeau N. Using passive-axis focusing wedges to decrease inspection reject rates. FOCUS The NDT Technician. 2021;20(3). 5 p. URL: https://ndtlibrary.asnt.org/2021/UsingPassiveAxisFocusingWedgestoDecrease InspectionRejectRates (дата обращения 15.12.2022).
- Berens A.P., Hovey P.W. Flaw detection reliability criteria. V. 1. Methods and results. AD-A142 001. Final technical report. Dayton: University of Dayton, Research Institute; 1984. 175 p. URL: https://archive.org/details/ DTIC ADA142001
- 14. Гетман А.Ф., Козин Ю.Н. *Неразрушающий контроль* и безопасность эксплуатации сосудов и трубопроводов давления. М.: Энергоатомиздат; 1997. 288 с. ISBN 5-283-03151-9
- 15. Annis C., Aldrin J.C., Sabbagh H.A. What is missing in nondestructive testing capability evaluation? *Mater. Eval.* 2015;73(1):1–11.
- 16. Александров А.Е. Оценка достоверности результатов контроля металла на основе альтернативного метода. *Информационные технологии*. 2018;8(24):529–537. https://doi.org/10.17587/it.24.529-537
- 17. Montgomery D.C. *Design and Analysis of Experiments*. 10th ed. Wiley; 2020. 688 p. ISBN 978-1-119-72210-6
- Annis C., Gandossi L., Martin O. Optimal sample size for probability of detection curves. *Nucl. Eng. Des.* 2013;262: 98–105. https://doi.org/10.1016/j.nucengdes.2013.03.059
- 19. Тихонов А.Н., Кальнер В.Д., Гласко В.Б. *Математическое моделирование и метод обратных задач в машиностроении*. М.: Машиностроение; 1990. 264 с.
- Aldrin J.C., Shell E.B., Oneida E.K., Sabbagh H.A., Sabbagh E., Murphy R.K., Mazdiyasni S., Lindgren E.A. Model-based inverse methods for sizing surface-breaking discontinuities with eddy current probe variability. *AIP Conference Proceedings*. 2016;1706(1):090002\_1-090002\_10. https://doi.org/10.1063/1.4940539
- Aldrin J.C., Oneida E.K., Shell E.B., Sabbagh H.A., Sabbagh E., Murphy R.K., Mazdiyasni S., Lindgren E.A., Mooers R.D. Model-based probe state estimation and crack inverse methods addressing eddy current probe variability. *AIP Conference Proceedings*. 2017;1806(1):110013\_1-110013\_11. https://doi.org/10.1063/1.4974691
- Bertovic M., Given J., Rentala V.M., Lehleitner J., Kanzler D., Heckel T., Tkachenko V. Human factors in der POD ist das möglich? *e-Journal of Nondestructive Testing* (*eJNDT*): *DGZfP-Jahrestagung*. 2022;7.
   p. (in Deutsch). URL: https://www.ndt.net/article/dgzfp2022/papers/mo.3.b.3.pdf
- 23. Yusa N., Knopp J.S. Evaluation of probability of detection (POD) studies with multiple explanatory variables. *J. Nucl. Sci. Technol.* 2015;53(4):574–579. https://doi.org/10.1080/00223131.2015.1064332
- Schneider C.R.A., Sanderson R.M., Carpentier C., Zhao L., Nageswaran C. Estimation of probability of detection curves based on theoretical simulation of the inspection process. *Annual Br. Conf. on NDT*. 2012. 12 p. URL: https://www.bindt.org/downloads/NDT2012 5C1.pdf
- Aldrin J.C., Annis C., Sabbagh H.A., Knopp J.S., Lindgren E.A. Assessing the reliability of nondestructive evaluation methods for damage characterization. *AIP Conference Proceedings*. 2014;1581(1):2071–2078. https://doi.org/10.1063/1.4865078

- Aldrin J.C., Annis C., Sabbagh H.A., Knopp J.S., Lindgren E.A. Assessing the reliability of nondestructive evaluation methods for damage characterization. *AIP Conference Proceedings*. 2014;1581(1):2071–2078. https://doi.org/10.1063/1.4865078
- Alexandrov A.E., Azhder T.B., Bunina L.V., Bikovsky S.S., Titov A.P. Computer program for calculating pipelines destruction probability. In: Silhavy R., Silhavy P., Prokopova Z. (Eds.). Proceedings of the Computational Methods in Systems and Software. CoMeSySo: Data Science and Intelligent Systems. Ser. Lecture Notes in Networks and Systems. 2021. V. 231. P. 718–733. https:// doi.org/10.1007/978-3-030-90321-3\_59
- Alexandrov A.E., Azhder T.B., Bunina L.V., Bikovsky S.S., Titov A.P. Computer program for calculating pipelines destruction probability. In: Silhavy R., Silhavy P., Prokopova Z. (Eds.). Proceedings of the Computational Methods in Systems and Software. CoMeSySo: Data Science and Intelligent Systems. Ser. Lecture Notes in Networks and Systems. 2021. V. 231. P. 718–733. https:// doi.org/10.1007/978-3-030-90321-3

## **About the authors**

**Alexander E. Alexandrov,** Dr. Sci. (Eng.), Professor, Department of Hardware Software and Mathematical Support of Computing System, Institute for Cybersecurity and Digital Technologies, MIREA – Russian Technological University (20, Stromynka ul., Moscow, 107996 Russia). E-mail: femsystem@yandex.ru. Scopus Author ID 57364491800, RSCI SPIN-code 6121-3825, https://orcid.org/0000-0002-6104-6227

**Sergey P. Borisov,** Senior Lecturer, Department of Hardware Software and Mathematical Support of Computing System, Institute for Cybersecurity and Digital Technologies, MIREA – Russian Technological University (20, Stromynka ul., Moscow, 107996 Russia). E-mail: bsp345@gmail.com. RSCI SPIN-code 4045-6550, https://orcid.org/0000-0002-6043-9547

**Ludmila V. Bunina,** Senior Lecturer, Department of Hardware Software and Mathematical Support of Computing System, Institute for Cybersecurity and Digital Technologies, MIREA – Russian Technological University (20, Stromynka ul., Moscow, 107996 Russia). E-mail: ludmilabunina@mail.ru. Scopus Author ID 57218190491, RSCI SPIN-code 1629-1700, https://orcid.org/0000-0002-3392-6569

**Sergey S. Bikovsky,** Senior Lecturer, Department of Hardware Software and Mathematical Support of Computing System, Institute for Cybersecurity and Digital Technologies, MIREA – Russian Technological University (20, Stromynka ul., Moscow, 107996 Russia). E-mail: bykovskij@mirea.ru. Scopus Author ID 57363858400, RSCI SPIN-code 1450-2101, https://orcid.org/0000-0002-3645-3808

Irina V. Stepanova, Cand. Sci. (Geol.-Mineral.), Associate Professor, Department of Hardware Software and Mathematical Support of Computing System, Institute for Cybersecurity and Digital Technologies, MIREA – Russian Technological University (20, Stromynka ul., Moscow, 107996 Russia). E-mail: ivs\_rrr@mail.ru. Scopus Author ID 57213161230, RSCI SPIN-code 7065-5203, https://orcid.org/0000-0002-0944-3989

Andrey P. Titov, Cand. Sci. (Eng.), Associate Professor, Department of Hardware Software and Mathematical Support of Computing System, Institute for Cybersecurity and Digital Technologies, MIREA – Russian Technological University (20, Stromynka ul., Moscow, 107996 Russia). E-mail: titov\_and@mail.ru. Scopus Author ID 57363858500, RSCI SPIN-code 3872-9708, https://orcid.org/0000-0001-8823-2524

## Об авторах

**Александров Александр Евгеньевич,** д.т.н. профессор, кафедра «Аппаратное, программное и математическое обеспечение вычислительных систем» Института кибербезопасности и цифровых технологий ФГБОУ ВО «МИРЭА – Российский технологический университет» (107996, Россия, Москва, ул. Стромынка, д. 20). E-mail: femsystem@yandex.ru. Scopus Author ID 57364491800, SPIN-код РИНЦ 6121-3825, https://orcid.org/0000-0002-6104-6227

**Борисов Сергей Петрович,** старший преподаватель, кафедра «Аппаратное, программное и математическое обеспечение вычислительных систем» Института кибербезопасности и цифровых технологий ФГБОУ ВО «МИРЭА – Российский технологический университет» (107996, Россия, Москва, ул. Стромынка, д. 20). E-mail: bsp345@gmail.com. SPIN-код РИНЦ 4045-6550, https://orcid.org/0000-0002-6043-9547

**Бунина Людмила Владимировна,** старший преподаватель, кафедра «Аппаратное, программное и математическое обеспечение вычислительных систем» Института кибербезопасности и цифровых технологий ФГБОУ ВО «МИРЭА – Российский технологический университет» (107996, Россия, Москва, ул. Стромынка, д. 20). E-mail: ludmilabunina@mail.ru. Scopus Author ID 57218190491, SPIN-код РИНЦ 1629-1700, https://orcid.org/0000-0002-3392-6569

**Быковский Сергей Сергеевич,** старший преподаватель, кафедра «Аппаратное, программное и математическое обеспечение вычислительных систем» Института кибербезопасности и цифровых технологий ФГБОУ ВО «МИРЭА – Российский технологический университет» (107996, Россия, Москва, ул. Стромынка, д. 20). E-mail: bykovskij@mirea.ru. Scopus Author ID 57363858400, SPIN-код РИНЦ 1450-2101, https://orcid.org/0000-0002-3645-3808

Степанова Ирина Владимировна, к.г.-м.н., доцент, кафедра «Аппаратное, программное и математическое обеспечение вычислительных систем» Института кибербезопасности и цифровых технологий ФГБОУ ВО «МИРЭА – Российский технологический университет» (107996, Россия, Москва, ул. Стромынка, д. 20). E-mail: ivs rrr@mail.ru. Scopus Author ID 57213161230, SPIN-код РИНЦ 7065-5203, https://orcid.org/0000-0002-0944-3989

**Титов Андрей Петрович,** к.т.н., доцент, кафедра «Аппаратное, программное и математическое обеспечение вычислительных систем» Института кибербезопасности и цифровых технологий ФГБОУ ВО «МИРЭА – Российский технологический университет» (107996, Россия, Москва, ул. Стромынка, д. 20). E-mail: titov\_and@mail.ru. Scopus Author ID 57363858500, SPIN-код РИНЦ 3872-9708, https://orcid.org/0000-0001-8823-2524

Translated from Russian into English by Vladislav V. Glyanchenko Edited for English language and spelling by Thomas A. Beavitt

## **Mathematical modeling**

## Математическое моделирование

UDC 539.3 https://doi.org/10.32362/2500-316X-2023-11-3-70-85



RESEARCH ARTICLE

## Developing generalized model representations of thermal shock for local non-equilibrium heat transfer processes

## Eduard M. Kartashov @

MIREA – Russian Technological University, Moscow, 119454 Russia <sup>®</sup> Corresponding author, e-mail: professor.kartashov@gmail.com

## Abstract

Objectives. Processes of energy transfer in solids and resultant thermal loads are widespread in nature and technology. This explains the scientific and practical significance of constructing a theory of these processes, as well as developing effective methods for studying the modeled concepts developed on this basis. The purpose of such studies is to determine basic flux patterns of complex processes occurring especially under conditions of powerful energy impacts in various technological operations. These include plasma-chemical processing of materials, their processing in infrared furnaces and solar plants, intense heating of materials carried out by laser or electron beams, and the use of powerful radiation emitters for thermal hardening and hardening of the surface of products. In these cases, the phenomenon of thermal shock arises, forming one of the central topics in thermomechanics and strength physics of solids. The present work considers an open theoretical problem of thermal shock in terms of a generalized model of dynamic thermoelasticity under conditions of a locally nonequilibrium heat transfer process. Depending on the type and curvature of the boundary surface of the considered massive body, the model can be used to study the problem in three coordinate systems: cartesian coordinates—a massive body bounded by a flat surface; spherical coordinates—a massive body with an internal spherical cavity; cylindrical coordinates—a massive body with an internal cylindrical cavity. Three types of intensive heating are considered: temperature heating, thermal heating, and heating by medium. Following the development of an analytical solution, the results of conducted numerical experiments are presented along with their physical analysis.

Methods. The study applies methods and theorems of operational calculus according to the theory of special functions.

**Results.** Generalized model representations of thermal shock are developed in terms of dynamic thermoelasticity for locally nonequilibrium heat transfer processes simultaneously in three coordinate systems: Cartesian, spherical, and cylindrical. The presence of curvature of the boundary surface of the thermal shock area substantiates the initial statement of the dynamic problem in displacements using the proposed corresponding "compatibility" equation.

**Conclusions.** A generalized dynamic model of the thermal reaction of massive bodies with internal cavities simultaneously in Cartesian, spherical, and cylindrical coordinate systems under conditions of intense temperature heating, thermal heating, and heating by medium is proposed. The model is considered in terms of displacements based on local nonequilibrium heat transfer. A numerical experiment carried out according to the obtained analytical solution for stresses forms a basis for a description of the wave nature of the propagation of a thermoelastic wave. A comparison with the classical solution is made without taking into account local nonequilibrium. The calculation of engineering relations carried out on the basis of the operational solution of the problem is important in practical terms for the upper estimate of the maximum thermal stresses.

Keywords: heat stroke, generalized dynamic model, analytical solution, thermal stresses

• Submitted: 24.06.2022 • Revised: 16.12.2022 • Accepted: 03.03.2023

**For citation:** Kartashov E.M. Developing generalized model representations of thermal shock for local non-equilibrium heat transfer processes. *Russ. Technol. J.* 2023;11(3):70–85. https://doi.org/10.32362/2500-316X-2023-11-3-70-85

Financial disclosure: The author has no a financial or property interest in any material or method mentioned.

The author declares no conflicts of interest.

НАУЧНАЯ СТАТЬЯ

# Развитие обобщенных модельных представлений теплового удара для локально-неравновесных процессов переноса теплоты

## Э.М. Карташов <sup>®</sup>

МИРЭА – Российский технологический университет, Москва, 119454 Россия <sup>®</sup> Автор для переписки, e-mail: professor.kartashov@gmail.com

## Резюме

Цели. Процессы переноса энергии в твердых телах и вызываемые ими тепловые нагрузки имеют широкое распространение в природе и технике. Этим объясняется исключительно важное научное и практическое значение построения теории указанных процессов, создание эффективных методов исследования развиваемых при этом модельных представлений. Цель этих исследований - установление основных закономерностей протекания достаточно сложных процессов, особенно в условиях мощных энергетических воздействий в различного рода технологических операциях. К ним можно отнести плазмохимическую обработку материалов, обработку в инфракрасных печах и гелиоустановках, интенсивный нагрев материалов лазерными или электронными лучами, применение мощных радиационных излучателей для термической закалки и упрочнения поверхности изделий. В этих случаях возникает так называемый термический удар – одна из центральных тем в термомеханике и физике прочности твердых тел, имеющая важное научное и практическое значение. Цель работы - рассмотреть открытую проблему теории теплового удара в терминах обобщенной модели динамической термоупругости в условиях локально-неравновесного процесса переноса теплоты. Модель (в зависимости от вида и кривизны граничной поверхности рассматриваемого массивного тела) позволяет исследовать проблему в трех системах координат: декартовы координаты - массивное тело, ограниченное плоской поверхностью; сферические координаты - массивное тело с внутренней сферической полостью; цилиндрические координаты – массивное тело с внутренней цилиндрической полостью. Рассматриваются три вида интенсивного нагрева: температурный, тепловой, нагрев средой. Ставится задача: получить аналитическое решение, провести численные эксперименты и дать их физический анализ.

Методы. Использованы методы и теоремы операционного исчисления, теория специальных функций.

**Результаты.** Развиты обобщенные модельные представления теплового удара в терминах динамической термоупругости для локально-неравновесных процессов переноса теплоты одновременно в трех системах координат: декартовой, сферической и цилиндрической. Наличие кривизны граничной поверхности области теплового удара обосновывает исходную постановку динамической задачи в перемещениях с использованием предложенного соответствующего уравнения «совместности».

**Выводы.** Предложена обобщенная динамическая модель термической реакции массивных тел с внутренними полостями одновременно в декартовой, сферической и цилиндрической системах координат в условиях интенсивного температурного нагрева, теплового нагрева, нагрева средой. Модель рассмотрена в перемещениях на основе локально-неравновесного теплопереноса. Получено аналитическое решение для напряжений, проведен численный эксперимент; описан волновой характер распространения термоупругой волны.

Проведено сравнение с классическим решением без учета локальной неравновесности. На основе операционного решения задачи предложены важные в практическом отношении расчетные инженерные соотношения для верхней оценки максимума термических напряжений.

**Ключевые слова:** тепловой удар, обобщенная динамическая модель, аналитическое решение, термические напряжения

• Поступила: 24.06.2022 • Доработана: 16.12.2022 • Принята к опубликованию: 03.03.2023

**Для цитирования:** Карташов Э.М. Развитие обобщенных модельных представлений теплового удара для локально-неравновесных процессов переноса теплоты. *Russ. Technol. J.* 2023;11(3):70–85. https://doi.org/10.32362/2500-316X-2023-11-3-70-85

**Прозрачность финансовой деятельности:** Автор не имеет финансовой заинтересованности в представленных материалах или методах.

Автор заявляет об отсутствии конфликта интересов.

#### INTRODUCTION

The present work continues the author's earlier research described in [1,2]. Within the generalized model of dynamic thermoelasticity, the open problem of the thermal response to heating of a massive body bounded from the inside either by a flat surface (an elastic half-space in the Cartesian coordinate system), or a cylindrical surface (an elastic space in the cylindrical coordinate system with an inner cylindrical cavity), or a spherical surface (an elastic space in the spherical coordinate system with an inner spherical cavity), is studied. Three cases of intense heating of the body (region) boundary are considered: temperature heating, thermal heating, and heating by medium.

The development of generalized models involving numerous practical applications is one of the insufficiently studied directions in thermal shock theory. The specificity of such research lies, on the one hand, in the relative simplicity of initial mathematical models, and on the other, in computational difficulties in obtaining the desired result. Moreover, the obtained relations have obvious relevance for solving numerous practical situations.

The study is conducted under the conditions of locally nonequilibrium heat transfer processes [3–8]. Two circumstances are considered. During high-intensity heating of solids causing thermal shock, heat fluxes  $\overline{q}(M,t)$ ,—where t is time in region  $\Omega = \{M(x,y,z) \in D, t>0\}$  describing a real solid body—lag behind the temperature gradient T(M,t) by a value proportional to relaxation time  $\tau_r$  related to the heat propagation rate  $v_T$  by relation  $v_T = \sqrt{a/\tau_r}$ ; here, a is temperature conductivity [9–15]:

$$\overline{q}(M,t) = -\lambda_{\mathrm{T}} \operatorname{grad} T(M,t) - \tau_{\mathrm{r}} \frac{\partial \overline{q}(M,t)}{\partial t},$$
 (1)

where  $\lambda_T$  is the thermal conductivity.

The combination of the energy equation for isotropic solids  $c\rho^* \partial T(M,t) / \partial t = \text{div} \overline{q}(M,t)$ , where c is specific heat capacity while  $\rho^*$  is the density, and Eq. (1) result in the following hyperbolic transfer equation [16, 17]:

$$\frac{\partial T(M,t)}{\partial t} = a\Delta T(M,t) - \tau_{\rm r} \frac{\partial^2 T(M,t)}{\partial t^2},\tag{2}$$

containing not only the first, but also the second derivative of the temperature over time. As a consequence, Eq. (2) describes wave processes—in this case, wave heat transfer. While issues of correct formulation of boundary value problems for Eq. (2) have been considered relatively recently [16], a number of issues related to associated thermal problems require further study.

### DEFINING RELATIONS OF DYNAMIC THERMOELASTICITY

Let D be the finite or partially bounded convex region of space M(x, y, z) describing the real solid body and being in the thermally stressed state; S be the piecewise smooth surface bounding region D;  $\overline{n} = (n_1, n_2, n_3)$  be the external normal to S (the vector continuous on S); T(M, t) be the temperature distribution in region D at t > 0;  $T_0$  be the initial temperature at which the region is in the unstrained and unstressed state. Let  $\sigma_{ij}(M, t)$ ,  $\varepsilon_{ij}(M, t)$ , and  $U_i(M, t)$  be the components of the stress tensor, strain tensor, and displacement vector, respectively, satisfying basic equations of (uncoupled) thermoelasticity (in index notation) [17]:

$$\sigma_{ii}(M, t) + F_i(M, t) = \rho^* U_i(M, t),$$
 (3)

$$\varepsilon_{ij}(M, t) = (1/2)[U_{i,j}(M, t) + U_{j,i}(M, t)],$$
 (4)

$$\sigma_{ij}(M, t) = 2\mu\varepsilon_{ij}(M, t) + [\lambda\varepsilon_{ii}(M, t) -$$

$$-(3\lambda + 2\mu)\alpha_{T}(T(M, t) - T_{0})]\delta_{ij}, M \in D, t > 0, \quad (5)$$

where  $\rho^*$  is density;  $\lambda$ ,  $\mu$  are isothermal Lame coefficients; G is the shear modulus;  $\lambda = 2Gv/(1-2v)$ ;  $\nu$  is the Poisson's ratio, with  $2G(1+\nu)=E$ , where E is the Young's modulus;  $\alpha_T$  is the linear thermal expansion coefficient;  $\delta_{ij}$  is the Kronecker symbol;  $F_i(M,t)$  are components of volume force;  $\overline{e}(M,t)=U_{i,i}(M,t)=\varepsilon_{ii}(M,t)$  is the volume strain, which is related to the sum of normal stresses  $\overline{\sigma}(M,t)=\sigma_{nn}(M,t), n=x,y,z$  by the following relation:

$$\overline{e}(M,t) = \frac{1-2\nu}{E}\overline{\sigma}(M,t) + 3\alpha_{\mathrm{T}} \left[ T(M,t) - T_0 \right]. \quad (6)$$

The thermal stress state of region D at t > 0 may arise under various modes of thermal effect on boundary S, creating a thermal shock. These may include the most common in practice cases:

· temperature heating

$$T(M, t) = T_c(t), M \in S, t > 0 \ (T_c(t) > T_0, t \ge 0);$$
 (7)

· thermal heating

$$\frac{1}{\tau_{\rm r}} \int_{0}^{t} \frac{\partial T(M, \tau)}{\partial n} \Big|_{M \in S} \exp\left(-\frac{t - \tau}{\tau_{\rm r}}\right) d\tau = 
= -\frac{1}{\lambda_{\rm T}} q(t) S_{+}(t), t \ge 0;$$
(8)

• heating by medium

$$\frac{1}{\tau_{\rm r}} \int_{0}^{t} \frac{\partial T(M,\tau)}{\partial n} \Big|_{M \in S} \exp\left(-\frac{t-\tau}{\tau_{\rm r}}\right) d\tau = 
= h \Big\{ T(M,t) \Big|_{M \in S} - \Big[ T_0 + S_+(t) (T_{\rm c} - T_0) \Big] \Big\}, t \ge 0,$$
(9)

as well as under the action of internal heat sources. Here,  $\lambda_{\rm T}$  is the thermal conductivity of the material; q(t) is the heat flux; h is the relative heat transfer coefficient;  $T_{\rm c}$  is

the ambient temperature; 
$$S_{+}(t) = \begin{cases} 1, t > 0, \\ 0, t \le 0. \end{cases}$$

Also, the cases of solid cooling can be equally considered.

The temperature function T(M, t) included in (5) is found from the solution of the boundary-value problem of unsteady thermal conductivity for Eq. (2) with boundary conditions (7)–(9). Relations (3)–(6) are general relations of dynamic thermoelasticity linking stresses, strains, displacements, and temperature. When passing to specific cases, it is necessary to transform (3)–(6) into the so-called compatibility equations either in stresses or in displacements and to write the corresponding problem of dynamic thermoelasticity for these equations. For the case considered in the paper, it is necessary to take into account the effect of the solid boundary surface curvature

on the temperature and the corresponding temperature stresses. Here, the more convenient mathematical model is the "compatibility" equation in displacements covering the cylindrical, spherical, and Cartesian coordinate systems, simultaneously.

Substituting the right parts of (5) into (3) (without volume forces) and using further (4) and (6), the following three equations may be written after a number of long transformations:

$$\begin{split} \Delta U_{i}(M,t) + & \frac{1}{(1-2\nu)} \cdot \frac{\partial \overline{e}(M,t)}{\partial i} - (\rho^{*}/G) \frac{\partial^{2} U_{i}(M,t)}{\partial t^{2}} = \\ & = \frac{2(1+\nu)\alpha_{\mathrm{T}}}{(1-2\nu)} \cdot \frac{\partial \left[T(M,t) - T_{0}\right]}{\partial i}, \ i = x,y,z, \end{split}$$

which formally can be written in the following form of vector equality:

$$\Delta \overline{U}(M,t) + \frac{1}{(1-2\nu)} \operatorname{grad} \left[ \operatorname{div} \overline{U}(M,t) \right] -$$

$$- (\rho^*/G) \frac{\partial^2 \overline{U}(M,t)}{\partial t^2} =$$

$$= \frac{2(1+\nu)}{(1-2\nu)} \alpha_{\mathrm{T}} \operatorname{grad} \left[ T(M,t) - T_0 \right], M \in D, t > 0.$$
(10)

It should be noted that it is necessary to equate the corresponding components in the vector record of the left and right parts in (10) in the inverse transition.

Let us further consider practical cases of dynamic thermoelasticity based on Eq. (10). In the first case, in Cartesian coordinates (x, y, z), region z > R, t > 0 bounded by the flat surface whose temperature state is described by function  $T_i(z, t)$ , i = 1, 2, 3 is considered; thus,  $U_x = U_y = 0$ ,  $U_z = U_z(z, t)$ , and Eq. (10) may be written as follows:

$$\frac{\partial^{2} U_{z}(z,t)}{\partial z^{2}} - \frac{1}{v_{p}^{2}} \cdot \frac{\partial^{2} U_{z}(z,t)}{\partial t^{2}} =$$

$$= \frac{1+v}{1-v} \cdot \alpha_{T} \frac{\partial [T_{i}(z,t) - T_{0}]}{\partial z}, z > R, t > 0.$$
(11)

Here, 
$$v_{\rm p} = \sqrt{\frac{2G(1-v)}{\rho^*(1-2v)}} = \sqrt{(\lambda + 2\mu)/\rho^*}$$
 is the

speed of expansion wave propagation in elastic medium, which is close to the speed of sound.

The desired stress component  $\sigma_{zz}(z, t)$  is related to displacement by the following relation:

$$\sigma_{zz}(z,t) = 2G \left\{ \frac{1-\nu}{1-2\nu} \cdot \frac{\partial U_z(z,t)}{\partial z} - \frac{1+\nu}{1-2\nu} \cdot \alpha_T \left[ T_i(z,t) - T_0 \right] \right\}.$$
(12)

The temperature function satisfies three heating conditions

$$\frac{\partial T_i(z,t)}{\partial t} = a \frac{\partial^2 T_i(z,t)}{\partial z^2} - \tau_r \frac{\partial^2 T_i(z,t)}{\partial t^2},$$

$$z > R, t > 0.$$
(13)

$$T_{i}(z,t)|_{t=0} = T_{0}, \quad \frac{\partial T_{i}(z,t)}{\partial t}\Big|_{t=0} = 0,$$

$$z \ge R, |T_{i}(z,t)| < \infty, \ z \ge R, \ t \ge 0,$$
(14)

$$T_i(z,t)\big|_{z=R} = T_c, t > 0,$$
 (15)

$$\frac{1}{\tau_{\rm r}} \int_{0}^{t} \frac{\partial T_2(z,\tau)}{\partial z} \bigg|_{z=R} \exp\left(-\frac{t-\tau}{\tau_{\rm r}}\right) d\tau = -\frac{1}{\lambda_{\rm T}} q_0, \ t > 0, \ (16)$$

$$\frac{1}{\tau_{\rm r}} \int_{0}^{t} \frac{\partial T_3(z,\tau)}{\partial z} \Big|_{z=R} \exp\left(-\frac{t-\tau}{\tau_{\rm r}}\right) d\tau =$$

$$= h \Big[ T_3(z,t) \Big|_{z=R} - T_{\rm c} \Big], t > 0.$$
(17)

In the second case, in spherical coordinates  $(\rho, \varphi, \theta)$ , region  $\rho > R$ , t > 0 with inner spherical cavity when heated under conditions of central symmetry  $T_i = T_i(\rho, t)$ is considered; thus,  $U_{\varphi} = U_{\theta} = 0$ ,  $U_{\rho} = U_{\rho}(\rho, t)$ , and (12) may be written in the following form:

$$\frac{\partial U_{\rho}(\rho,t)}{\partial \rho^{2}} + \frac{2}{\rho} \cdot \frac{\partial U_{\rho}(\rho,t)}{\partial \rho} - \frac{2}{\rho^{2}} \cdot U_{\rho}(\rho,t) - \frac{1}{v_{p}^{2}} \cdot \frac{\partial^{2} U_{\rho}(\rho,t)}{\partial t^{2}} = (18)$$

$$= \frac{1+\nu}{1-\nu} \cdot \alpha_{T} \cdot \frac{\partial [T_{i}(\rho,t) - T_{0}]}{\partial \rho}, \rho > R, t > 0.$$

Here,

$$\sigma_{\rho\rho}(\rho,t) = 2G \left\{ \frac{1-\nu}{1-2\nu} \cdot \frac{\partial U_{\rho}(\rho,t)}{\partial \rho} + \frac{2\nu}{1-2\nu} \cdot \frac{1}{\rho} \times U_{\rho}(\rho,t) - \frac{1+\nu}{1-2\nu} \cdot \alpha_{T} \left[ T_{i}(\rho,t) - T_{0} \right] \right\},$$
(19)

$$\frac{\partial T_{i}(\rho,t)}{\partial t} = a \left( \frac{\partial^{2} T_{i}(\rho,t)}{\partial \rho^{2}} + \frac{2}{\rho} \cdot \frac{\partial T_{i}(\rho,t)}{\partial \rho} \right) - \\
- \tau_{r} \cdot \frac{\partial^{2} T_{i}(\rho,t)}{\partial t^{2}}, \, \rho > R, \, t > 0, \tag{20}$$

$$T_{i}(\rho,t)|_{t=0} = T_{0}, \frac{\partial T_{i}(\rho,t)}{\partial t}\Big|_{t=0} = 0,$$

$$\rho \ge R, |T_{i}(\rho,t)| < \infty, \rho \ge R, t \ge 0,$$
(21)

$$T_i(\rho, t)\Big|_{\rho=R} = T_c, t > 0,$$
 (22)

$$\frac{\partial T_i(z,t)}{\partial t} = a \frac{\partial^2 T_i(z,t)}{\partial z^2} - \tau_r \frac{\partial^2 T_i(z,t)}{\partial t^2}, \qquad (13) \qquad \frac{1}{\tau_r} \int_0^t \frac{\partial T_2(\rho,\tau)}{\partial \rho} \bigg|_{\rho=R} \exp\bigg(-\frac{t-\tau}{\tau_r}\bigg) d\tau = -\frac{1}{\lambda_T} q_0, \, t > 0, \quad (23)$$

$$\frac{1}{\tau_{\rm r}} \int_{0}^{t} \frac{\partial T_3(\rho, \tau)}{\partial \rho} \bigg|_{\rho = R} \exp\left(-\frac{t - \tau}{\tau_{\rm r}}\right) d\tau = 
= h \left[ T_3(\rho, t) \bigg|_{\rho = R} - T_{\rm c} \right], t > 0.$$
(24)

In the third case, in cylindrical coordinates  $(r, \varphi, z)$ , region r > R, t > 0 with inner cylindrical cavity under radial temperature conditions  $T_i = T_i(r, t)$  is considered; thus,  $U_{\varphi} = U_{z} = 0$ ,  $U_{r} = U_{r}(r, t)$ , and Eq. (10) may be written in the following form:

$$\frac{\partial^{2}U_{r}(r,t)}{\partial r^{2}} + \frac{1}{r} \cdot \frac{\partial U_{r}(r,t)}{\partial r} - \frac{1}{r^{2}} \cdot U_{r}(r,t) - \frac{1}{v_{p}^{2}} \cdot \frac{\partial^{2}U_{r}(r,t)}{\partial t^{2}} = (25)$$

$$= \frac{1+v}{1-v} \cdot \alpha_{T} \cdot \frac{\partial \left[T_{i}(r,t) - T_{0}\right]}{\partial r}, r > R, t > 0.$$

Then,

$$\sigma_{rr}(r,t) = 2G \left\{ \frac{1-\nu}{1-2\nu} \cdot \frac{\partial U_r(r,t)}{\partial r} + \frac{\nu}{1-2\nu} \times \frac{1}{r} U_r(r,t) - \frac{1+\nu}{1-2\nu} \cdot \alpha_T \left[ T_i(r,t) - T_0 \right] \right\},$$
(26)

$$\frac{\partial T_{i}(r,t)}{\partial t} = a \left( \frac{\partial^{2} T_{i}(r,t)}{\partial r^{2}} + \frac{1}{r} \cdot \frac{\partial T_{i}(r,t)}{\partial r} \right) - \tau_{r} \cdot \frac{\partial^{2} T_{i}(r,t)}{\partial t^{2}}, \ r > R, \ t > 0, \tag{27}$$

$$T_{i}(r,t)|_{t=0} = T_{0}, r \ge R, \frac{\partial T_{i}(r,t)}{\partial t}\Big|_{t=0} = 0,$$

$$r \ge R, |T_{i}(r,t)| < \infty, r \ge R, t \ge 0,$$
(28)

$$T_{i}(r,t)\Big|_{r=R} = T_{c}, t > 0,$$

$$\frac{1}{\tau_{r}} \int_{0}^{t} \frac{\partial T_{2}(r,\tau)}{\partial r} \Big|_{r=R} \exp\left(-\frac{t-\tau}{\tau_{r}}\right) d\tau = -\frac{1}{\lambda_{T}} q_{0}, t > 0, \tag{29}$$

$$\frac{1}{\tau_{r}} \int_{0}^{t} \frac{\partial T_{3}(r,\tau)}{\partial r} \bigg|_{r=R} \exp\left(-\frac{t-\tau}{\tau_{r}}\right) d\tau =$$

$$= h \left[ T_{3}(r,t) \right]_{r=R} - T_{c} \right] t > 0.$$
(30)

Such cases of intense heating of the surface area (real body) are of considerable practical interest, for example, in the following cases: surface dielectric heating; calculation of thermal stresses in the cylinder walls of steam machines and internal combustion engines; in the theory of automatic temperature control systems; in the studying the sound frequency region of metals at high or very low surface temperatures; numerous cases

of abrupt change in the surface temperature of space and aviation objects; in the mechanical engineering industry when working at various experimental facilities to determine the temperature state of samples; etc. [6]. Of undoubted practical importance for the theory of thermal shock is representing all three cases simultaneously in three coordinate systems within the framework of the generalized model.

The following dimensionless variables may be introduced to avoid unnecessary inconvenience. In region z > R, t > 0:

$$\xi = \frac{v_{p}z}{a}, \ \tau = \frac{v_{p}^{2}t}{a}, \ \xi_{0} = \frac{v_{p}R}{a}, \ \beta = \frac{v_{p}}{v_{T}}, \ Bi^{*} = \frac{ha}{v_{p}}, \ S_{T} = \frac{2G\alpha_{T}(1+v)}{1-2v},$$

$$W_{i}(\xi,\tau) = \frac{T_{i}(z,t) - T_{0}}{T_{c} - T_{0}}, \ i = 1, \ 3; \ W_{2}(\xi,\tau) = \frac{T_{2}(z,t) - T_{0}}{(q_{0}/\lambda_{T})(a/v_{p})}, \ i = 2,$$

$$\sigma_{\xi\xi}(\xi,\tau) = \frac{\sigma_{zz}(z,t)}{S_{T}(T_{c} - T_{0})}, \ i = 1, \ 3; \ \sigma_{\xi\xi}(\xi,\tau) = \frac{\sigma_{zz}(z,t)}{S_{T}(q_{0}/\lambda_{T})(a/v_{p})}, \ i = 2,$$

$$U_{i}(\xi,\tau) = \frac{(1-v)U_{z}(z,t)}{(1+v)\alpha_{T}(T_{c} - T_{0})(a/v_{p})}, \ i = 1, \ 3,$$

$$U_{2}(\xi,\tau) = \frac{(1-v)U_{z}(z,t)}{(1+v)\alpha_{T}(q_{0}/\lambda_{T})(a/v_{p})^{2}}, \ i = 2.$$

$$(31)$$

In region  $\rho > R$ , t > 0:

$$\xi = \frac{v_{p}\rho}{a}, \ \tau = \frac{v_{p}^{2}t}{a}, \ \xi_{0} = \frac{v_{p}R}{a}, \ \beta = \frac{v_{p}}{v_{T}}, \ Bi^{*} = \frac{ha}{v_{p}}, \ S_{T} = \frac{2G\alpha_{T}(1+v)}{1-2v},$$

$$W_{i}(\xi,\tau) = \frac{T_{i}(\rho,t) - T_{0}}{T_{c} - T_{0}}, \ i = 1, \ 3; \ W_{2}(\xi,\tau) = \frac{T_{2}(\rho,t) - T_{0}}{(q_{0}/\lambda_{T})(a/v_{p})}, \ i = 2,$$

$$\sigma_{\xi\xi}(\xi,\tau) = \frac{\sigma_{\rho\rho}(\rho,t)}{S_{T}(T_{c} - T_{0})}, \ i = 1, \ 3; \ \sigma_{\xi\xi}(\xi,\tau) = \frac{\sigma_{\rho\rho}(\rho,t)}{S_{T}(q_{0}/\lambda_{T})(a/v_{p})}, \ i = 2,$$

$$U_{i}(\xi,\tau) = \frac{(1-v)U_{\rho}(\rho,t)}{(1+v)\alpha_{T}(T_{c} - T_{0})(a/v_{p})}, \ i = 1, \ 3,$$

$$U_{2}(\xi,\tau) = \frac{(1-v)U_{\rho}(\rho,t)}{(1+v)\alpha_{T}(q_{0}/\lambda_{T})(a/v_{p})^{2}}, \ i = 2.$$

$$(32)$$

In region r > R, t > 0:

$$\xi = \frac{v_{p}r}{a}, \ \tau = \frac{v_{p}^{2}t}{a}, \ \xi_{0} = \frac{v_{p}R}{a}, \ \beta = \frac{v_{p}}{v_{T}}, \ Bi^{*} = \frac{ha}{v_{p}}, \ S_{T} = \frac{2G\alpha_{T}(1+v)}{1-2v},$$

$$W_{i}(\xi,\tau) = \frac{T_{i}(r,t) - T_{0}}{T_{c} - T_{0}}, \ i = 1, \ 3; \ W_{2}(\xi,\tau) = \frac{T_{2}(r,t) - T_{0}}{(q_{0} / \lambda_{T})(a / v_{p})}, \ i = 2,$$

$$\sigma_{\xi\xi}(\xi,\tau) = \frac{\sigma_{rr}(r,t)}{S_{T}(T_{c} - T_{0})}, \ i = 1, \ 3; \ \sigma_{\xi\xi}(\xi,\tau) = \frac{\sigma_{rr}(r,t)}{S_{T}(q_{0} / \lambda_{T})(a / v_{p})}, \ i = 2,$$

$$U_{i}(\xi,\tau) = \frac{(1-v)U_{r}(r,t)}{(1+v)\alpha_{T}(T_{c} - T_{0})(a / v_{p})}, \ i = 1, \ 3,$$

$$U_{2}(\xi,\tau) = \frac{(1-v)U_{r}(r,t)}{(1+v)\alpha_{T}(q_{0} / \lambda_{T})(a / v_{p})^{2}}, \ i = 2.$$
(33)

## GENERALIZED MATHEMATICAL MODEL OF THE PROBLEM AND ITS ANALYTICAL SOLUTION

Assuming the boundaries of the region free of stresses, the generalized model of the problem may be written as follows:

$$\frac{\partial^{2}U_{i}(\xi,\tau)}{\partial\xi^{2}} + \frac{2m+1}{\xi} \left[ \frac{\partial U_{i}(\xi,\tau)}{\partial\xi} - \frac{U_{i}(\xi,\tau)}{\xi} \right] - \frac{\partial^{2}U_{i}(\xi,\tau)}{\partial\tau^{2}} = \frac{\partial W_{i}(\xi,\tau)}{\partial\xi}, \; \xi > \xi_{0}, \; \tau > 0. \tag{34}$$

$$\begin{aligned} &U_{i}(\xi,\tau)\big|_{\tau=0} = \frac{\partial U_{i}(\xi,\tau)}{\partial \tau}\bigg|_{\tau=0} = 0,\\ &\xi \geq \xi_{0}, \ \left|U_{i}(\xi,\tau)\right| < \infty, \ \xi \geq \xi_{0}, \ \tau \geq 0. \end{aligned} \tag{35}$$

$$\left[\frac{\partial U_{i}(\xi,\tau)}{\partial \xi} + \frac{(2m+1)\nu}{1-\nu} \cdot \frac{1}{\xi} U_{i}(\xi,\tau)\right]_{\xi=\xi_{0}} =$$

$$= W_{i}(\xi,\tau)\Big|_{\xi=\xi_{0}}, \ \tau > 0. \tag{36}$$

$$\frac{\partial W_i(\xi, \tau)}{\partial \tau} = \frac{\partial^2 W_i(\xi, \tau)}{\partial \xi^2} + \xi \frac{\partial W_i(\xi, \tau)}{\partial \xi} - \beta^2 \frac{\partial^2 W_i(\xi, \tau)}{\partial \tau^2} = 0, \ \xi > \xi_0, \ \tau > 0.$$
(37)

$$W_{i}(\xi,\tau)|_{\tau=0} = 0, \ \xi \ge \xi_{0}, \ \frac{\partial W_{i}(\xi,\tau)}{\partial \tau}\Big|_{\tau=0} = 0;$$

$$|W_{i}(\xi,\tau)| < \infty, \ \xi \ge \xi_{o}, \ \tau \ge 0.$$
(38)

$$W_1(\xi, \tau)\Big|_{\xi=\xi_0} = 1, \ \tau > 0.$$
 (39)

$$\frac{1}{\beta^2} \int_0^{\tau} \frac{\partial W_2(\xi, \tau')}{\partial \xi} \bigg|_{\xi = \xi_0} \exp\left(-\frac{\tau - \tau'}{\beta^2}\right) d\tau' = -1, \ \tau > 0. \quad (40)$$

$$\begin{split} \frac{1}{\beta^2} \int_0^{\tau} \frac{\partial W_3(\xi, \tau')}{\partial \xi} \bigg|_{\xi = \xi_0} \exp \left( -\frac{\tau - \tau'}{\beta^2} \right) d\tau' = \\ &= Bi^* \bigg[ W_3(\xi, \tau) \bigg|_{\xi = \xi_0} = -1 \bigg], \ \tau > 0. \end{split} \tag{41}$$

Here, i = 1 at m = -0.5, i = 2 at m = 0.5, and i = 3 at m = 0. It should be noted that the desired stress  $\sigma_{\xi\xi}(\xi, \tau)$  in all three cases is related to displacement  $U_i(\xi, \tau)$  by the following relation:

$$\sigma_{\xi\xi}(\xi,\tau) = \frac{\partial U_i(\xi,\tau)}{\partial \xi} + \frac{(2m+1)\nu}{(1-\nu)} \times \frac{1}{\xi} \cdot U_i(\xi,\tau) - W_i(\xi,\tau).$$
(42)

The solution of the generalized problem (34)–(42) in order to study, for example, the impact of the region geometry on the kinetics of corresponding thermoelastic stresses is an open problem of thermal shock theory. Its solution is given below.

According to Laplace, in the image space

$$\overline{W}_{i}(\xi, p) = \int_{0}^{\infty} W_{i}(\xi, \tau) \exp(-p\tau) d\tau,$$

$$\overline{U}_{i}(\xi, p) = \int_{0}^{\infty} U_{i}(\xi, \tau) \exp(-p\tau) d\tau,$$

$$\overline{\sigma}_{\xi\xi}(\xi, p) = \int_{0}^{\infty} \sigma_{\xi\xi}(\xi, \tau) \exp(-p\tau) d\tau,$$
(43)

the solution of the thermal problem (37)–(41) may be written in the following form:

$$\overline{W}_{i}(\xi, p) = \overline{f}_{i}(\xi_{0}, p)(\xi_{0} / \xi)^{m} K_{m} [\xi \overline{\mu}(p)],$$
$$(\overline{\mu}(p) = \sqrt{\beta^{2} p^{2} + p}),$$

where

$$\begin{split} \overline{f}_{i}(\xi_{0},p) &= \\ &= \begin{cases} \frac{1}{pK_{m}[\xi_{0}\overline{\mu}(p)]}, & i = 1, \\ \frac{\overline{\mu}(p)}{p^{2}K_{m+1}[\xi_{0}\overline{\mu}(p)]}, & i = 2, \\ \frac{Bi^{*}\overline{\mu}(p)}{p\{pK_{m+1}[\xi_{0}\overline{\mu}(p)] + Bi^{*}\overline{\mu}(p)K_{m}[\xi_{0}\overline{\mu}(p)]\}}, & i = 3. \end{cases} \end{split}$$

Here,  $K_m(z)$  is the modified Bessel function. We shall transform relations (34)–(36) into the image space (43):

$$\frac{d^{2}\overline{U}_{i}(\xi,p)}{d\xi^{2}} + \frac{2m+1}{\xi} \cdot \frac{d\overline{U}_{i}(\xi,p)}{d\xi} - \left(p^{2} + \frac{2m+1}{\xi^{2}}\right)\overline{U}_{i}(\xi,p) = \frac{d\overline{W}_{i}(\xi,p)}{d\xi}, \, \xi > \xi_{0}.$$
(44)

$$\left[ \frac{d\overline{U}_{i}(\xi,p)}{d\xi} + \frac{(2m+1)\nu}{(1-\nu)} \cdot \frac{1}{\xi} \cdot \overline{U_{i}}(\xi,p) \right]_{\xi=\xi_{0}} =$$

$$= \overline{W}_{i}(\xi,p) \Big|_{\xi=\xi_{0}}.$$
(45)

$$\left|\overline{U}_{i}(\xi,p)\right| < \infty, \ \xi \ge \xi_{0}.$$
 (46)

The general solution of equation (44) consists of the general solution of homogeneous equation and the partial solution of inhomogeneous equation:

$$\overline{U}_{i}(\xi, p) = \frac{1}{\xi^{m}} \left[ C_{1} K_{m+1}(\xi p) + C_{2} I_{m+1}(\xi p) \right] + \overline{U}_{i\text{part}}(\xi, p).$$
(47)

Finding a partial solution of Eq. (44) requires a separate consideration. We have:

$$\frac{d}{d\xi}(\Delta \overline{U}_i) = \Delta \left(\frac{d\overline{U}_i}{d\xi}\right) - \frac{2m+1}{\xi^2} \cdot \frac{d\overline{U}_i}{d\xi}.$$
 (48)

Here,

$$\Delta \overline{U}_{i} = \frac{d^{2}\overline{U}_{i}}{d\xi^{2}} + \frac{2m+1}{\xi} \cdot \frac{d\overline{U}_{i}}{d\xi},$$

$$\Delta \overline{W}_{i} = (\beta^{2}p^{2} + p)\overline{W}_{i}.$$
(49)

The partial solution in (47) is found in the form  $\overline{U}_{i\text{part}}(\xi,p) = A\frac{d\overline{W}_i}{d\xi}$ , where constant A is to be found. Substituting this expression into (44) and using (48)–(49),  $A = \frac{1}{p^2(\beta^2 - 1) + p}$  is found. Thus, the general solution of Eq. (44) with allowance for boundary condition (46) may be written in the following form:

$$\overline{U}_{i}(\xi, p) = C \left[ \frac{1}{\xi^{m}} K_{m+1}(\xi p) \right] - \\
-\overline{\varphi}_{i}(\xi_{0}, p) (\xi_{0} / \xi)^{m} K_{m+1} \left[ \xi \overline{\mu}(p) \right], \tag{50}$$

where

$$\begin{split} & \phi_i(\xi_0, p) = \\ & = \begin{cases} \frac{\overline{\mu}(p)}{p^2[p(\beta^2 - 1) + 1]K_m[\xi_0\overline{\mu}(p)]}, & i = 1, \\ & \frac{\overline{\mu}^2(p)}{p^3[p(\beta^2 - 1) + 1]K_{m+1}[\xi_0\overline{\mu}(p)]}, & i = 2, \\ & \frac{Bi^*\overline{\mu}^2(p)}{p^2[p(\beta^2 - 1) + 1][pK_{m+1}(\xi_0\overline{\mu}(p)) + Bi^*\overline{\mu}(p)K_m(\xi_0\overline{\mu}(p))]}, & i = 3. \end{cases} \end{split}$$

The following relation is used here:

$$\frac{d}{d\xi} \Big[ \xi^{-m} K_m(\xi \overline{\mu}(p)) \Big] = -\overline{\mu}(p) \xi^{-m} K_{m+1} \Big[ \xi \overline{\mu}(p) \Big].$$

Using the properties of Bessel functions, the following important relation being of fundamental importance for finding an analytical solution of the generalized problem (34)–(42) is found after transformations:

$$\frac{d}{d\xi} \left[ \frac{1}{\xi^m} K_{m+1}(\xi p) \right] + \frac{(2m+1)\nu}{(1-\nu)} \times \frac{1}{\xi^{m+1}} \cdot K_{m+1}(\xi p) = -\frac{1}{\xi^{m+1}} \overline{\Theta}(\xi p), \tag{51}$$

where

$$\overline{\Theta}(\xi p) = \xi p K_m(\xi p) + (2m+1) \frac{(1-2\nu)}{(1-\nu)} K_{m+1}(\xi p).$$
 (52)

Relations (59)–(60) and the boundary condition (50) allow determining the constant in (55) along with the desired displacement. We find:

$$\begin{split} \overline{U}_{i}(\xi,p) &= \frac{(\xi_{0} / \xi)^{m} \overline{\Theta} \left[ \xi_{0} \mu(p) \right] K_{m+1}(\xi p) \overline{\varphi}_{i}(\xi_{0} p)}{\overline{\Theta}(\xi_{0} p)} - \\ &- \frac{(\xi_{0} / \xi)^{m} K_{m} \left[ \xi_{0} \overline{\mu}(p) \right] K_{m+1}(\xi p) \overline{f}_{i}(\xi_{0},p)}{\xi_{0}^{-1} \overline{\Theta}(\xi_{0} p)} - \\ &- (\xi_{0} / \xi)^{m} \overline{\varphi}_{i}(\xi_{0},p) K_{m+1} \left[ \xi \overline{\mu}(p) \right]. \end{split}$$

The desired stress is found, as follows:

$$\begin{split} &\frac{\overline{\sigma}_{\xi\xi}(\xi,p)}{(\xi_0\,/\,\xi)^m} = \frac{(\xi_0\,/\,\xi)\overline{\Theta}(\xi p)K_m\Big[\,\xi_0\overline{\mu}(p)\,\Big]\overline{f}_i(\xi_0,p)}{\overline{\Theta}(\xi_0\,p)} \,+\\ &+ \frac{\overline{\phi}_i(\xi_0,p)\overline{\Theta}\Big[\xi\overline{\mu}(p)\Big]}{\xi} - \frac{\overline{\phi}_i(\xi_0,p)\overline{\Theta}\Big[\xi_0\overline{\mu}(p)\Big]\overline{\Theta}(\xi p)}{\xi\overline{\Theta}(\xi_0\,p)} \,-\\ &- \overline{f}_i(\xi_0,p)K_m\Big[\xi\overline{\mu}(p)\big]. \end{split}$$

The following operational relations for stresses for all three types of heating may be written:

• temperature heating (i = 1)

$$\frac{\overline{\sigma}_{\xi\xi}(\xi,p)}{(\xi_{0}/\xi)^{m}} = \frac{(\xi_{0}/\xi)\Theta(\xi p)}{p\overline{\Theta}(\xi_{0}p)} + \frac{\overline{\mu}(p)\overline{\Theta}[\xi\overline{\mu}(p)]}{\xi p^{2}[p(\beta^{2}-1)+1]K_{m}[\xi_{0}\overline{\mu}(p)]} - \frac{K_{m}[\xi\overline{\mu}(p)]}{pK_{m}[\xi_{0}\overline{\mu}(p)]} - \frac{\overline{\mu}(p)\overline{\Theta}[\xi_{0}\overline{\mu}(p)]}{\xi p^{2}[p(\beta^{2}-1)+1]K_{m}[\xi_{0}\overline{\mu}(p)]\overline{\Theta}(\xi p)};$$
(53)

• thermal heating (i = 2)

$$\begin{split} & \frac{\overline{\sigma}_{\xi\xi}(\xi,p)}{(\xi_{0}/\xi)^{m}} = \frac{(\xi_{0}/\xi)\overline{\mu}(p)\overline{\Theta}(\xi p)K_{m}[\xi_{0}\overline{\mu}(p)]}{p^{2}\overline{\Theta}(\xi_{0}p)K_{m+1}[\xi_{0}\overline{\mu}(p)]} + \\ & + \frac{\overline{\mu}^{2}(p)\overline{\Theta}(\xi\overline{\mu}(p))}{\xi p^{3}[p(\beta^{2}-1)+1]K_{m+1}[\xi_{0}\overline{\mu}(p)]} - \\ & - \frac{\overline{\mu}(p)K_{m}[\xi_{0}\overline{\mu}(p)]}{p^{2}K_{m+1}[\xi_{0}\overline{\mu}(p)]} - \\ & - \frac{\overline{\mu}^{2}(p)\overline{\Theta}(\xi p)\overline{\Theta}[\xi_{0}\overline{\mu}(p)]}{\xi p^{3}[p(\beta^{2}-1)+1]\overline{\Theta}(\xi_{0}p)K_{m+1}[\xi_{0}\overline{\mu}(p)]}; \end{split}$$
(54)

• heating by medium (i = 3)

$$\frac{\overline{\sigma}_{\xi\xi}(\xi,p)}{(\xi_{0}/\xi)^{m}} = \frac{(\xi_{0}/\xi)\overline{\Theta}(\xi p)}{p\overline{\Theta}(\xi_{0}p)} \times \frac{K_{m}[\xi_{0}\overline{\mu}(p)]Bi^{*}\overline{\mu}(p)}{p\overline{\Theta}(\xi_{0}p)} \times \frac{K_{m}[\xi_{0}\overline{\mu}(p)]Bi^{*}\overline{\mu}(p)}{[pK_{m+1}(\xi_{0}\overline{\mu}(p))+Bi^{*}\overline{\mu}(p)K_{m}(\xi_{0}\overline{\mu}(p))]\overline{\mu}} + \frac{Bi^{*}\overline{\mu}^{2}(p)}{\xi p^{2}[p(\beta^{2}-1)+1]} \times \frac{\overline{\Theta}[\xi_{0}\overline{\mu}(p)]}{[pK_{m+1}(\xi_{0}\overline{\mu}(p))+Bi^{*}\overline{\mu}(p)K_{m}(\xi_{0}\overline{\mu}(p))]} - \frac{Bi^{*}\overline{\mu}^{2}(p)}{\xi p^{2}[p(\beta^{2}-1)+1]} \times \frac{\overline{\Theta}[\xi_{0}\overline{\mu}(p)]\overline{\Theta}(\xi p)}{[pK_{m+1}(\xi_{0}\overline{\mu}(p))+Bi^{*}\overline{\mu}(p)K_{m}(\xi_{0}\overline{\mu}(p))]\overline{\Theta}(\xi_{0}p)} - \frac{Bi^{*}\overline{\mu}(p)K_{m}(\xi_{0}\overline{\mu}(p))}{[pK_{m+1}(\xi_{0}\overline{\mu}(p))+Bi^{*}\overline{\mu}(p)K_{m}(\xi_{0}\overline{\mu}(p))]}.$$
(55)

The inverse transformation in (53)–(55) turns out to be rather cumbersome resulting in the complex and hard to see expressions. But if inertial effects of a microsecond duration [17] during which stresses  $\sigma_{\xi\xi}(\xi, \tau)$  just reach maximum values are considered in formulating problem (34)–(42), then short times  $\tau$  corresponding to large p in images, that is immediately after the thermal shock, may be considered. For this, the asymptotic representation of cylindrical functions for large p is used in (53)–(55), as follows:

$$K_{v}(p) = \frac{\sqrt{\pi/2}}{\sqrt{p}} \exp(-p), v \ge 0,$$

where  $K_{v}$  is the modified Bessel function.

The following notations are introduced then:

$$A_m(\xi) = \frac{(2m+1)(1-2\nu)}{(1-\nu)\xi}, \ \gamma = \frac{1}{1-\beta^2}.$$

We shall also introduce a function for this class of problems that is the Kartashov function

$$\overline{\chi}_m(\xi, p) = \frac{p + A_m(\xi)}{(p - \gamma)[p + A_m(\xi_0)]},$$

which is used in finding the originals of found images. The original of this function may be written in the following form:

$$\begin{split} \chi_m(\xi,\tau) &= \frac{\gamma + A_m(\xi)}{\gamma + A_m(\xi_0)} \times \\ &\times \left[ \frac{A_m(\xi_0) - A_m(\xi)}{\gamma + A_m(\xi)} \exp(-A_m(\xi_0)\tau) + \exp(\gamma\tau) \right]. \end{split}$$

After transformations, we find:

$$\frac{\overline{\sigma}_{\xi\xi}(\xi, p)}{(\xi_0 / \xi)^{m+1/2}} = -\overline{\Psi}_1(\xi, p) \exp\left[-(\xi - \xi_0)\overline{\mu}(p)\right] + 
+\overline{\Psi}_2(\xi, p) \exp\left[-(\xi - \xi_0)p\right],$$
(56)

where at temperature heating (i = 1):

$$\overline{\Psi}_1(\xi, p) = \left\{ \frac{\gamma \overline{\mu}(p) [\overline{\mu}(p) + A_m(\xi)]}{p^2 (p - \gamma)} + \frac{1}{p} \right\}, \quad (57)$$

$$\overline{\Psi}_{2}(\xi, p) = \left\{ \frac{p - \gamma}{p} \overline{\chi}_{m}(\xi, p) + \frac{\gamma \overline{\mu}(p) \left[ \overline{\mu}(p) + A_{m}(\xi_{0}) \right] \overline{\chi}_{m}(\xi, p)}{p^{2}} \right\};$$
(58)

at thermal heating (i = 2):

$$\overline{\Psi}_{1}(\xi, p) = \left\{ \frac{\gamma \overline{\mu}^{2}(p) [\overline{\mu}(p) + A_{m}(\xi)]}{p^{3}(p - \gamma)} + \frac{\overline{\mu}^{2}(p)}{p^{2}} \right\}, (59)$$

$$\overline{\Psi}_{2}(\xi,p) = \left\{ \frac{\overline{\mu}(p)(p-\gamma)\overline{\chi}_{m}(\xi,p)}{p^{2}} + \frac{\gamma\overline{\mu}^{2}(p)[\overline{\mu}(p) + A_{m}(\xi_{0})]\overline{\chi}_{m}(\xi,p)}{p^{3}} \right\};$$
(60)

at heating by medium (i = 3):

$$\overline{\Psi}_{1}(\xi, p) =$$

$$= \left\{ \frac{\gamma B i^{*} \overline{\mu}^{2}(p) [\overline{\mu}(p) + A_{m}(\xi)]}{p^{2}(p - \gamma) [p + B i^{*} \overline{\mu}(p)]} + \frac{B i^{*} \overline{\mu}(p)}{p [p + B i^{*} \overline{\mu}(p)]} \right\},$$
(61)

$$\overline{\Psi}_{2}(\xi, p) = \left\{ \frac{Bi^{*}\overline{\mu}(p)(p-\gamma)\overline{\chi}_{m}(\xi, p)}{p[p+Bi^{*}\overline{\mu}(p)]} + \frac{\gamma Bi^{*}\overline{\mu}^{2}(p)[\overline{\mu}(p) + A_{m}(\xi_{0})]\overline{\chi}_{m}(\xi, p)}{p^{2}[p+Bi^{*}\overline{\mu}(p)]} \right\}.$$
(62)

When finding the originals in (56)–(62), attention should be paid to the value of parameter  $\beta=\nu_p/\nu_T$ . Thus,  $\beta=0.4$  for organic glass and  $\beta=0.7$  for quartz and silicon, that is  $\beta<1$ ;  $\beta=3.4$  for steel and  $\beta=1.8$  for crystals and aluminum, that is  $\beta>1$ . The value of parameter  $\beta$  plays the determining role in writing stress intervals  $\sigma_{\xi\xi}(\xi,\tau)$ . The following is found for stresses:

at  $\beta < 1$ : at  $\beta > 1$ :

$$\frac{\sigma_{\xi\xi}(\xi,\tau)}{(\xi_{0}/\xi)^{m+1/2}} = \frac{\sigma_{\xi\xi}(\xi,\tau)}{(\xi_{0}/\xi)^{m+1/2}} = \begin{cases}
0, & \tau < (\xi - \xi_{0})\beta, \\
-\sigma_{\xi\xi}^{(1)}(\xi,\tau), & (\xi - \xi_{0})\beta < \tau < (\xi - \xi_{0}), \\
-\sigma_{\xi\xi}^{(1)}(\xi,\tau) + \sigma_{\xi\xi}^{(2)}(\xi,\tau), & \tau > (\xi - \xi_{0});
\end{cases}$$

$$\frac{\sigma_{\xi\xi}(\xi,\tau)}{(\xi_{0}/\xi)^{m+1/2}} = \begin{cases}
0, & \tau < (\xi - \xi_{0}), \\
\sigma_{\xi\xi}^{(2)}(\xi,\tau), & (\xi - \xi_{0}) < \tau < (\xi - \xi_{0})\beta, \\
-\sigma_{\xi\xi}^{(1)}(\xi,\tau) + \sigma_{\xi\xi}^{(2)}(\xi,\tau), & \tau > \beta(\xi - \xi_{0}).
\end{cases}$$
(64)

Here,  $\sigma_{\xi\xi}^{(1)}(\xi,\tau)$  is the original mage

$$\overline{\Psi}_{1}(\xi, p) \exp \left[ -(\xi - \xi_{0}) \beta \sqrt{p^{2} + p / \beta^{2}} \right], \ \sigma_{\xi\xi}^{(2)}(\xi, \tau) = \Psi_{2}[\xi, \tau - (\xi - \xi_{0})]$$

Turning to the originals, the following analytical relations for stresses in all three cases of heating may be written:

• temperature heating (i = 1)

$$\sigma_{\xi\xi}^{(1)}(\xi,\tau) = \gamma \left\langle \exp\{\gamma[\tau - (\xi - \xi_0)\beta] - (\xi - \xi_0)/2\beta\} + \frac{\xi - \xi_0}{2\beta} \int_{(\xi - \xi_0)\beta}^{\tau} \exp[\gamma(\tau - \tau') - (1/2\beta^2)\tau'] \frac{I_1\Big((1/2\beta^2)\sqrt{(\tau')^2 - (\xi - \xi_0)^2\beta^2}\Big)}{\sqrt{(\tau')^2 - (\xi - \xi_0)^2\beta^2}} d\tau' \right\rangle \times \eta[\tau - (\xi - \xi_0)\beta] + \frac{\gamma A_m(\xi)}{\beta} \left\{ \int_{(\xi - \xi_0)\beta}^{\tau} \exp\Big[\gamma(\tau - \tau') - (1/2\beta^2)\tau'\Big] I_0\Big((1/2\beta^2)\sqrt{(\tau')^2 - (\xi - \xi_0)^2\beta^2}\Big) d\tau' \right\} \times \eta[\tau - (\xi - \xi_0)\beta] - \frac{A_m(\xi)}{\beta} \left\{ \int_{(\xi - \xi_0)\beta}^{\tau} \exp[-(1/2\beta^2)\tau'] I_0\Big((1/2\beta^2)\sqrt{(\tau')^2 - (\xi - \xi_0)^2\beta^2}\Big) d\tau' \right\} \times \eta[\tau - (\xi - \xi_0)\beta].$$
(65)

$$\sigma_{\xi\xi}^{(2)}(\xi,\tau) = \Psi_2[\xi,\tau - (\xi - \xi_0)],\tag{66}$$

where

$$\Psi_{2}(\xi,\tau) = \gamma \chi_{m}(\xi,\tau) + A_{m}(\xi_{0}) \left[ 2\beta \int_{0}^{\tau} \chi_{m}(\xi,\tau') d\tau' \right] - \beta \int_{0}^{\tau} \exp[-(1/2\beta^{2})(\tau-\tau')] \chi_{m}(\xi,\tau') d\tau'; \tag{67}$$

• thermal heating (i = 2)

$$\begin{split} \sigma_{\xi\xi}^{(1)}(\xi,\tau) &= \gamma\beta \exp[-(1/2\beta^2)\tau] I_0 \left( (1/2\beta^2) \sqrt{\tau^2 - (\xi - \xi_0)^2 \beta^2} \right) \eta[\tau - (\xi - \xi_0)\beta] + \\ &+ \frac{\gamma^2}{\beta} \left\{ \int_{(\xi - \xi_0)\beta}^{\tau} \exp[\gamma(\tau - \tau') - (1/2\beta^2)\tau'] I_0 \left( (1/2\beta^2) \sqrt{(\tau')^2 - (\xi - \xi_0)^2 \beta^2} \right) d\tau' \right\} \times \eta[\tau - (\xi - \xi_0)\beta] + \\ &+ A_m(\xi) \left\langle \left\{ \exp\gamma[\tau - (\xi - \xi_0)\beta] - 1 - [\tau - (\xi - \xi_0)\beta] \right\} \exp(-1/2\beta^2)\tau + \right. \\ &+ \frac{\xi - \xi_0}{2\beta} \int_{(\xi - \xi_0)\beta}^{\tau} \left[ \exp\gamma(\tau - \tau') - 1 - (\tau - \tau') \right] \exp[-(1/2\beta^2)] \times \\ &\times \frac{I_1 \left( (1/2\beta^2) \sqrt{(\tau')^2 - (\xi - \xi_0)^2 \beta^2} \right)}{\sqrt{(\tau')^2 - (\xi - \xi_0)^2 \beta^2}} d\tau' \right\rangle \eta[\tau - (\xi - \xi_0)\beta]. \end{split}$$

$$\Psi_{2}(\xi,\tau) = \gamma \beta \chi_{m}(\xi,\tau) + \frac{\gamma [1 + 2\beta^{3} A_{m}(\xi_{0})]}{2\beta} \int_{0}^{\tau} \chi_{m}(\xi,\tau') d\tau' + \gamma A_{m}(\xi_{0}) \int_{0}^{\tau} (\tau - \tau') \chi_{m}(\xi,\tau') d\tau'; \tag{69}$$

• heating by medium (i = 3). For this case, decomposition of the image  $\overline{\mu}(p) = \beta p[1 + 1/(\beta^2 p)]^{1/2}$  into the binominal series is used in finding the original. We shall also introduce the following number of notations:

$$\begin{split} \gamma = & 1 + \gamma \beta^2; \, \gamma_1 = \frac{1}{1 + Bi^*\beta}; \, \gamma_2 = \frac{Bi^*}{2\beta(1 + Bi^*\beta)}; \\ A_1 = & \gamma - \frac{\gamma_1[\gamma^2 + (\gamma - 1)Bi^*A_m(\xi)]}{\gamma + \gamma_2}; \\ A_2 = & \frac{\gamma_1[\gamma^2 + (\gamma - 1)Bi^*A_m(\xi)]}{\gamma + \gamma_2} - \gamma \gamma_1 + 2\beta A_m(\xi); \, A_3 = -2\beta A_m(\xi); \\ A_4 = & [\gamma\gamma_1(1 + \gamma_2) - \gamma_1\gamma_2 - \gamma(1 + \gamma_1)\beta A_m(\xi_0)]. \end{split}$$

The desired originals are found, as follows:

$$\begin{split} \Psi_{1}(\xi,\tau) &= A_{1} \left\{ \exp[\gamma(\tau - (\xi - \xi_{0})\beta) - (\xi - \xi_{0})/2\beta] \right\} + \\ &+ \frac{A_{1}(\xi - \xi_{0})}{2\beta} \int_{(\xi - \xi_{0})\beta}^{\tau} \exp\left[\gamma(\tau - \tau') - (1/2\beta^{2})\tau'\right] \frac{I_{1}\left((1/2\beta^{2})\sqrt{(\tau')^{2} - (\xi - \xi_{0})^{2}\beta^{2}}\right)}{\sqrt{(\tau')^{2} - (\xi - \xi_{0})^{2}\beta^{2}}} d\tau' \times \eta[\tau - (\xi - \xi_{0})\beta] + \\ &+ A_{2} \left\langle \exp[-\gamma_{2}(\tau - (\xi - \xi_{0})\beta)) - (\xi - \xi_{0}/2\beta] + \frac{\xi - \xi_{0}}{2\beta} \int_{(\xi - \xi_{0})\beta}^{\tau} \exp[-\gamma_{2}(\tau - \tau') - (1/2\beta^{2})\tau'] \times \right. \\ &\times \frac{I_{1}\left((1/2\beta^{2})\sqrt{(\tau')^{2} - (\xi - \xi_{0})^{2}\beta^{2}}\right)}{\sqrt{(\tau')^{2} - (\xi - \xi_{0})^{2}\beta^{2}}} d\tau' \right\rangle \times \eta[\tau - (\xi - \xi_{0})\beta] + \\ &+ A_{3} \times \left\{ \exp[-(1/2\beta)(\xi - \xi_{0})] + \frac{\xi - \xi_{0}}{2\beta} \int_{(\xi - \xi_{0})\beta}^{\tau} \exp[-(1/2\beta^{2})\tau'] \frac{I_{1}\left((1/2\beta^{2})\sqrt{(\tau')^{2} - (\xi - \xi_{0})^{2}\beta^{2}}\right)}{\sqrt{(\tau')^{2} - (\xi - \xi_{0})^{2}\beta^{2}}} d\tau' \right\} \times \\ &\times \eta[\tau - (\xi - \xi_{0})\beta]; \end{split}$$

$$\Psi_{2}(\xi,\tau) = \gamma(1-\gamma_{1})\chi_{m}(\xi,\tau) + 2\beta A_{m}(\xi_{0})\int_{0}^{\tau}\chi_{m}(\xi,\tau')d\tau' + A_{4}\int_{0}^{\tau}\exp\left[-\gamma_{2}(\tau-\tau')\right]\chi_{m}(\xi,\tau')d\tau'. \tag{71}$$

Thus, the resulted relations (63)–(71) complete solving the practically important problem on the thermal reaction of the massive body with internal cavities. In addition to the developed approach, the highly effective method of estimating the value of thermal stresses practically not applied earlier in the theory of thermal shock may be specified.

As follows from the operational solution of the dynamic problem, the presence of term  $\overline{\Psi}_2(\xi,p)\exp\left[-(\xi-\xi_0)p\right]$  in (56) shows the possibility of proposing the computational engineering formula for the upper-bound estimate of the temperature stress through the stress jump in (70) at the front of the thermoelastic wave. For this, the lag theorem [6] is used in the following form:

$$\begin{cases} \overline{\Psi}(\xi,p) \exp\Bigl[-(\xi-\xi_0)p\Bigr] \leftarrow 0, & \tau < \xi - \xi_0, \\ \Psi_2\Bigl[\xi,\tau - (\xi-\xi_0)\Bigr], & \tau > \xi - \xi_0, \end{cases}$$

wherefrom it is seen that at point  $(\xi - \xi_0)$ , a jump of function  $\Psi_2(\xi, \tau)$  occurs, whose value is calculated by the following equation:

$$\begin{split} & \left| \Delta \right| = \lim_{\tau \to (\xi - \xi_0) + 0} \Psi_2 \left[ \xi, \tau - (\xi - \xi_0) \right] = \\ & = \lim_{\tau \to 0+} \Psi_2 (\xi, \tau) = \lim p_{p \to \infty} \overline{\Psi}_2 (\xi, p). \end{split}$$

We shall first find the jump value for stresses  $\sigma_{\xi\xi}(\xi,\,\tau)$  in coordinates  $(\xi,\,\tau)$ , then we pass to initial

stresses in initial regions (11)–(30) using transfer equations (31)–(33). As a result, the following is found for temperature heating (58):

$$|\Delta| = |\sigma_{zz}; \sigma_{\rho\rho}; \sigma_{rr}|_{\text{max}} =$$

$$= \begin{cases} \frac{2G\gamma(1+\nu)\alpha_{\text{T}} |T_{\text{c}} - T_{0}|}{(1-2\nu)}, & m = -1/2; \\ \frac{(R/\rho)2G\gamma(1+\nu)\alpha_{\text{T}} |T_{\text{c}} - T_{0}|}{(1-2\nu)}, & m = 1/2; \end{cases}$$

$$\frac{\sqrt{R/r} 2G\gamma(1+\nu)\alpha_{\text{T}} |T_{\text{c}} - T_{0}|}{(1-2\nu)}, & m = 0.$$
(72)

The estimates (72) are valid both for intense heating  $(T_{\rm c} > T_0)$  when compressive stresses occur in the fixed cross-section  $\xi = {\rm const} > \xi_0$ , and for cooling  $(T_{\rm c} < T_0)$  when more dangerous tensile stresses occur.

#### PHYSICAL ANALYSIS OF THE SOLUTION

Figure 1 shows the stress (63), (65)–(67) (temperature heating) vs. time curves in the fixed cross section  $\xi = 1$  with  $\xi_0 = 0.1$ , v = 0.3,  $\beta = 0.4$  for m = -0.5; 0; 0.5. The curves for stresses (temperature heating) under the same data but for  $\beta = 0$ , i.e., for the case of classical Fourier phenomenology based on parabolic type equations, are shown in Fig. 2.

It would be of interest to compare these two approaches, namely to describe the effect of hyperbolicity of the dynamic problem (i.e., the effect of local disequilibrium in the system) on the value of temperature stresses. We shall write out the solution of the "parabolic" problem of thermal shock under temperature heating for all three areas described above, considering that this part of the research is also of great practical interest and is also an open problem so far.

$$\frac{\sigma_{\xi\xi}(\xi,\tau)}{(\xi_0/\xi)^{m+1/2}} = \sigma_{\xi\xi}^{(1)}(\xi,\tau) + \begin{cases} 0, & \tau < \xi - \xi_0, \\ \sigma_{\xi\xi}^{(2)}(\xi,\tau), & \tau > \xi - \xi_0, \end{cases} (73)$$

where

$$\sigma_{\xi\xi}^{(1)}(\xi,\tau) = -\Psi_1^*(\xi,\tau); \quad \sigma_{\xi\xi}^{(2)}(\xi,\tau) = \Psi_2^*[\xi,\tau - (\xi - \xi_0)];$$

$$\begin{split} \Psi_1^*(\xi,\tau) &= \frac{1}{2} \left\{ \exp\left[\tau - (\xi - \xi_0)\right] \Phi^* \left(\frac{\xi - \xi_0}{2\sqrt{\tau}} - \sqrt{\tau}\right) + \right. \\ &\quad + \exp\left[\tau + (\xi - \xi_0)\right] \Phi^* \left(\frac{\xi - \xi_0}{2\sqrt{\tau}} + \sqrt{\tau}\right) \right\} + \\ &\quad + A_m(\xi) \left\langle \frac{1}{2} \left[ \exp(\tau - (\xi - \xi_0)) \Phi^* \left(\frac{\xi - \xi_0}{2\sqrt{\tau}} - \sqrt{\tau}\right) - \right. \right. \\ &\quad - \exp(\tau + (\xi - \xi_0)) \Phi^* \left(\frac{\xi - \xi_0}{2\sqrt{\tau}} + \sqrt{\tau}\right) \right] - \\ &\quad - \frac{2\sqrt{\tau}}{\sqrt{\pi}} \exp\left[ -\frac{(\xi - \xi_0)^2}{4\tau} \right] + (\xi - \xi_0) \Phi^* \left(\frac{\xi - \xi_0}{2\sqrt{\tau}}\right) \right\rangle; \end{split}$$

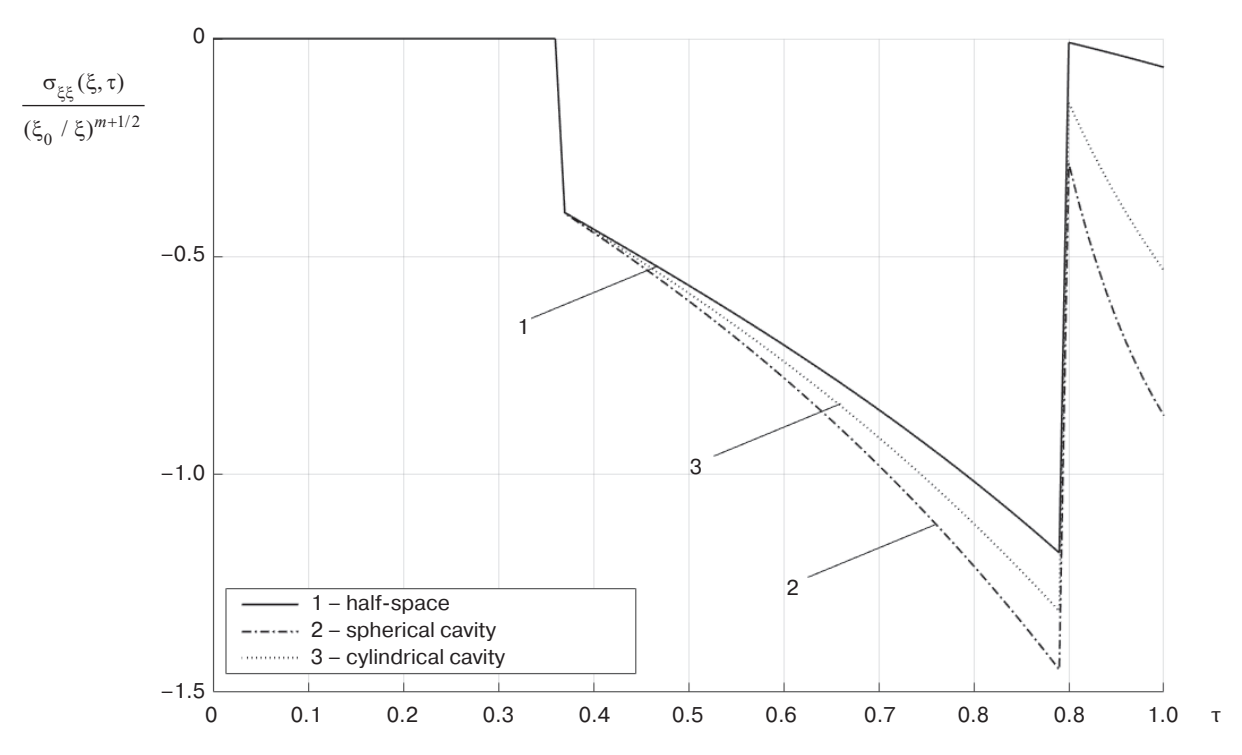


**Fig. 1.** Stress–time dependence in section  $\xi = 1$  at  $\xi_0 = 0.1$ , v = 0.3, and  $\beta = 0.4$ . Calculated by equations (63), (65)–(67) for m = -0.5 (curve 1), m = 0.5 (curve 2), and m = 0 (curve 3)

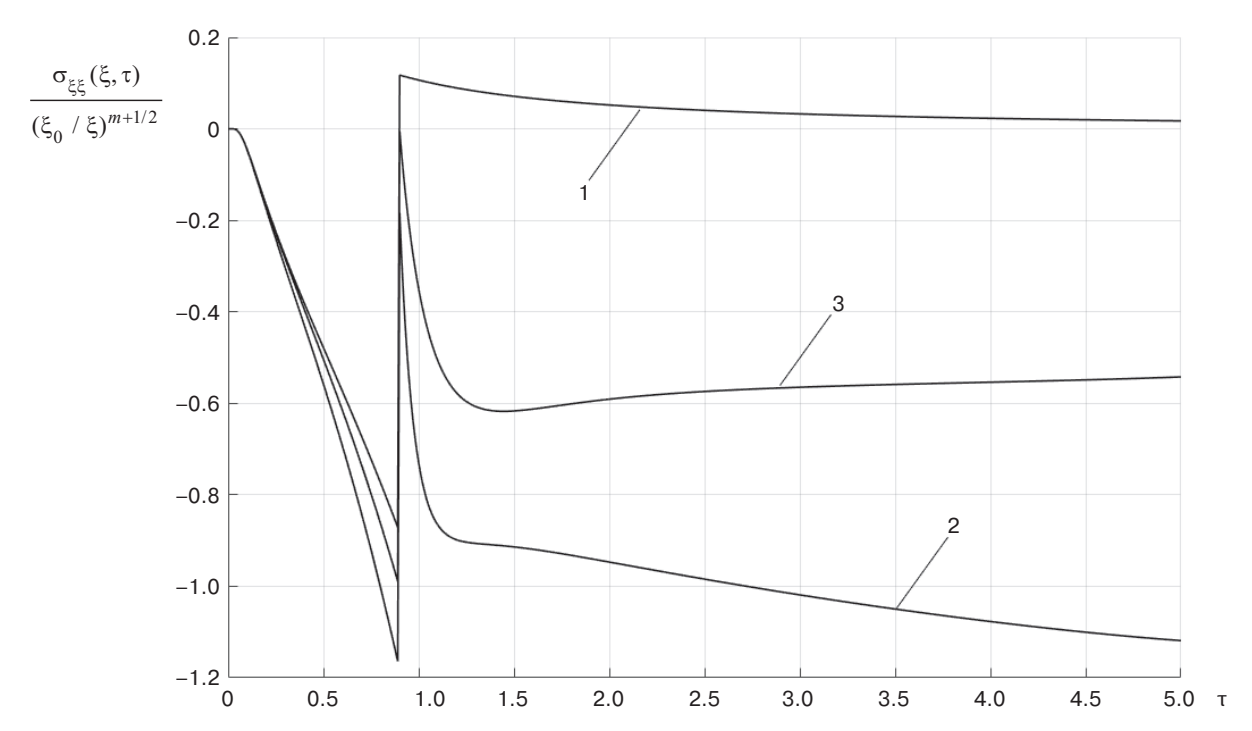


**Fig. 2.** Stress–time dependence in section  $\xi = 1$  at  $\xi_0 = 0.1$ , v = 0.3, and  $(\beta = 0)$ . Calculated by equations (73)–(75) for m = -0.5 (curve 1), m = 0.5 (curve 2), and m = 0 (curve 3)

$$\Psi_2^*(\xi,\tau) = \chi_m(\xi,\tau) + \frac{2A_m(\xi_0)}{\sqrt{\pi}} \int_0^{\tau} \sqrt{\tau - \tau'} \cdot \chi_m(\xi,\tau') d\tau'.$$
 (75)

Here,

$$\Phi^*(z) = 1 - \Phi(z), \ \Phi(z) = (2 / \sqrt{\pi}) \int_0^z \exp(-y^2) dy$$

is the Laplace function.

As it follows from the graphs, considering the finite speed of heat propagation results in a significant change in the pattern of dynamic temperature stresses compared to the data in Fig. 2. In contrast to (73), relation (63) shows the presence of two stress jumps, one occurring at the front of the heat wave and the other occurring at the front of the elastic wave moving at speeds  $v_{\rm T}$  and  $v_{\rm p}$ , respectively.

Let us consider the fixed cross-section inside region  $\xi > \xi_0$ . At  $\beta < 1$ , stresses in the cross-section are zero at the beginning. At the moment  $\tau = \beta(\xi - \xi_0)$ , the thermal stress wave arrives at this cross-section with its front moving at speed  $v_T$ ; the compressive stress occurs jumping and increases further. At the moment  $\xi - \xi_0$ , the longitudinal elastic wave approaches the cross-section, thus causing a jump change in the stress and its further decrease.

The curves in Fig. 1 also show another interesting result: the most "vulnerable" (in terms of thermal reaction) is the region with inner spherical cavity. In all

three cases (m = -0.5; 0; 0.5) the resulting stresses are compressive. Estimates (72) clearly show that the near-surface layers (near the boundary of the body (region)) are most susceptible to thermal shock. As for the thermal shock in the classical case (Fig. 2), the highest compression stresses are characteristic of the massive body bounded by flat surface (m = -0.5). In this case, after passing the expansion wave (due to function  $\sigma_{\xi\xi}^{(2)}(\xi,\tau)$  in (72)), the stress passes into the region of positive (tensile) values and then rapidly decreases reaching quasi-static values.

#### **CONCLUSIONS**

The developed generalized model represents thermal shock in terms of dynamic thermoelasticity to describe locally nonequilibrium processes of heat transfer. An analytical solution of the (open) generalized problem of the thermal reaction of massive bodies with internal cavities simultaneously in Cartesian, cylindrical, and spherical coordinate systems under temperature heating, thermal heating, and heating the boundary of solid by medium is obtained. Numerical experiments showing the effect of local nonequilibrium on the kinetics of temperature stresses (compared to the classical Fourier phenomenology) have been carried out. The calculated engineering relations for the upper boundary of temperature stresses during intense temperature heating have important practical applications.

#### **REFERENCES**

- 1. Kartashov E.M. Model representations of heat shock in terms of dynamic thermal elasticity. *Russ. Technol. J.* 2020;8(2):85–108 (in Russ.). https://doi.org/10.32362/2500-316X-2020-8-2-85-108
- 2. Kartashov E.M. New operational relations for mathematical models of local nonequilibrium heat transfer. *Russ. Technol. J.* 2022;10(1):68–79 (in Russ.). https://doi.org/10.32362/2500-316X-2022-10-1-68-79
- 3. Kudinov I.V., Kudinov V.A. Mathematical simulation of the locally nonequilibrium heat transfer in a body with account for its nonlocality in space and time. *J. Eng. Phys. Thermophy.* 2015;88(2):406–422. https://doi.org/10.1007/s10891-015-1206-6
  [Original Russian Text: Kudinov I.V., Kudinov V.A. Mathematical simulation of the locally nonequilibrium heat transfer in a body with account for its nonlocality in space and time. *Inzhenerno-Fizicheskii Zhurnal.* 2015;88(2):393–408 (in Russ.).]
- 4. Kudinov V.A., Eremin A.V., Kudinov I.V. The development and investigation of a strongly non-equilibrium model of heat transfer in fluid with allowance for the spatial and temporal non-locality and energy dissipation. *Thermophys. Aeromech.* 2017;24(6):901–907. https://doi. org/10.1134/S0869864317060087
  [Original Russian Text: Kudinov V.A., Eremin A.V., Kudinov I.V. The development and investigation of a strongly non-equilibrium model of heat transfer in fluid with allowance for the spatial and temporal non-locality and energy dissipation. *Teplofizika i Aeromekhanika*. 2017;24(6):929–935 (in Russ.).]
- 5. Kirsanov Yu.A., Kirsanov A.Yu. About measuring the thermal relaxation time of solid body. *Izvestiya RAN. Energetika*. 2015;1:113–122 (in Russ.).
- Kartashov E.M., Kudinov V.A. Analiticheskie metody teorii teploprovodnosti i ee prilozhenii (Analytical Methods of the Theory of Heat Conduction and its Applications). Moscow: URSS; 2012. 1080 p. (in Russ.). ISBN 978-5-9710-4994-4
- Sobolev S.L. Transportprocesses and traveling waves in systems with local nonequilibrium. Sov. Phys. Usp. 1991;34:217. https://doi.org/10.1070/PU1991v034n03ABEH002348
  [Original Russian Text: Sobolev S.L. Transport processes and traveling waves in systems with local nonequilibrium. Uspekhi Fizicheskikh Nauk. 1991;161(3):5–29 (in Russ.). https://doi.org/10.3367/UFNr.0161.199103b.0005]
- Sobolev S.L. Local non-equilibrium transport models. Phys. Usp. 1997;40(10):1043. https://doi.org/10.1070/ PU1997v040n10ABEH000292
   [Original Russian Text: Sobolev S.L. Local non-equilibrium transport models. Uspekhi Fizicheskikh Nauk. 1997;167(10):1095–1106 (in Russ.). https://doi.org/10.3367/UFNr.0167.199710f.1095]
- Kudinov I.V., Kotova E.V., Kudinov V.A. A method for obtaining analytical solutions to boundary value problems by defining additional boundary conditions and additional sought-for functions. *Numer. Analys. Appl.* 2019;12(2):126–136. https://doi.org/10.1134/ S1995423919020034

#### СПИСОК ЛИТЕРАТУРЫ

- 1. Карташов Э.М. Модельные представления теплового удара в динамической термоупругости. *Russ. Technol. J.* 2020;8(2):85–108. https://doi.org/10.32362/2500-316X-2020-8-2-85-108
- Карташов Э.М. Новые операционные соотношения для математических моделей локально-неравновесного теплообмена. Russ. Technol. J. 2022;10(1):68–79. https://doi.org/10.32362/2500-316X-2022-10-1-68-79
- 3. Кудинов И.В., Кудинов В.А. Математическая модель локально-неравновесного теплопереноса с учетом пространственно-временной нелокальности. *Инженерно-физический журнал.* 2015;88(2):393–408.
- 4. Кудинов В.А., Еремин А.В., Кудинов И.В. Разработка и исследование сильно неравновесной модели теплообмена в жидкости с учетом пространственновременной нелокальности и диссипации энергии. *Теплофизика и аэромеханика*. 2017;24(6):929–935.
- 5. Кирсанов Ю.А., Кирсанов А.Ю. Об измерении времени тепловой релаксации твердых тел. *Изв. РАН. Энергетика*. 2015;1:113–122.
- 6. Карташов Э.М., Кудинов В.А. *Аналитические мето- ды теории теплопроводности и ее приложений*. М.: URSS; 2012. 1080 с. ISBN 978-5-9710-4994-4
- 7. Соболев С.Л. Процессы переноса и бегущие волны в локально-неравновесных системах. *Успехи физ. наук.* 1991;161(3):5–29. https://doi.org/10.3367/UFNr.0161.199103b.0005
- Соболев С.Л. Локально-неравновесные модели процессов переноса. Успехи физ. наук. 1997;167(10): 1095–1106. https://doi.org/10.3367/UFNr.0167.199710f.1095
- 9. Кудинов И.В., Котова Е.В., Кудинов В.А. Метод получения аналитических решений краевых задач на основе определения дополнительных граничных условий и дополнительных искомых функций. Сиб. журн. вычисл. математ. 2019;22(2):153–165. https://doi.org/10.15372/SJNM20190203
- 10. Кудинов В.А., Еремин А.В., Кудинов И.В., Жуков В.В. Исследование сильнонеравновесной модели теплового воспламенения с учетом пространственно-временной нелокальности. *Физика горения и взрыва*. 2018;54(6):25–29. https://doi.org/10.15372/FGV20180603
- 11. Формалев В.Ф. *Уравнения математической физики*. М.: URSS; 2021. 648 с. ISBN 978-5-9710-8380-1
- Kudinov I.V., Eremin A.V., Kudinov V.A., Dovgallo A.I., Zhukov V.V. Mathematical model of damped elastic rod oscillations with dual-phase-lag. *Int. J. Solids Struct.* 2020; 200–201:231–241. https://doi.org/10.1016/j.ijsolstr.2020.05.018
- 13. Zhukov V.V. Study of analytical solution of the thermal conductivity equation considering relaxation phenomena under the third class boundary conditions. *J. Phys.: Conf. Ser.* 2021;1889:022027. https://doi.org/10.1088/1742-6596/1889/2/022027
- Zhukov V.V., Kudinov I.V., Kutsev N.M., Mikheeva G.V., Klebleev R.M. Determination of quasi-static and residual stresses in the course of the thermoplastic hardening in a boundary layer of the material. *IOP Conf. Ser.: Mater. Sci. Eng.* 2020;709(3):033078. https://doi.org/10.1088/1757-899X/709/3/033078

- [Original Russian Text: Kudinov I.V., Kotova E.V., Kudinov V.A. Amethod for obtaining analytical solutions to boundary value problems by defining additional boundary conditions and additional sought-for functions. *Sibirskii Zhurnal Vychislitel 'noi Matematiki*. 2019;22(2):153–165. https://doi.org/10.15372/SJNM20190203]
- Kudinov V.A., Eremin A.V., Kudinov I.V., Zhukov V.V. Strongly nonequilibrium model of thermal ignition with account for space–time nonlocality. *Combust. Explos. Shock Waves.* 2018;54(6):649–653. https://doi.org/10.1134/S0010508218060035
   [Original Russian Text: Kudinov V.A., Eremin A.V., Kudinov I.V., Zhukov V.V. Strongly nonequilibrium model of thermal ignition with account for space–time nonlocality. *Fizika Goreniya i Vzryva.* 2018;54(6):25–29 (in Russ.). https://doi.org/10.15372/FGV20180603]
- 11. Formalev V.F. *Uravneniya matematicheskoi fiziki* (*Equations of mathematical physics*). Moscow: URSS; 2021. 648 p. (in Russ.). ISBN 978-5-9710-8380-1
- Kudinov I.V., Eremin A.V., Kudinov V.A., Dovgallo A.I., Zhukov V.V. Mathematical model of damped elastic rod oscillations with dual-phase-lag. *Int. J. Solids Struct.* 2020; 200–201:231–241. https://doi.org/10.1016/j.ijsolstr.2020.05.018
- 13. Zhukov V.V. Study of analytical solution of the thermal conductivity equation considering relaxation phenomena under the third class boundary conditions. *J. Phys.: Conf. Ser.* 2021;1889:022027. https://doi.org/10.1088/1742-6596/1889/2/022027
- Zhukov V.V., Kudinov I.V., Kutsev N.M., Mikheeva G.V., Klebleev R.M. Determination of quasi-static and residual stresses in the course of the thermoplastic hardening in a boundary layer of the material. *IOP Conf. Ser.: Mater. Sci. Eng.* 2020;709(3):033078. https://doi.org/10.1088/1757-899X/709/3/033078
- Eremin A.V., Kudinov V.A., Kudinov I.V., Zhukov V.V., Trubitsyn K.V. Mathematical model of fuel heat ignition considering space-time nonlocality. *IOP Conf.* Ser.: Mater. Sci. Eng. 2019;552(1):012003. https://doi. org/10.1088/1757-899X/552/1/012003
- Kartashov É.M. Analytical solutions of hyperbolic heat-conduction models. J. Eng. Phys. Thermophy. 2014;87(5):1116–1125. https://doi.org/10.1007/s10891-014-1113-2
   [Original Russian Text: Kartashov E.M. Analytical solutions of hyperbolic heat-conduction models. Inzhenerno-Fizicheskii Zhurnal. 2014;87(5):1072–1081
- 17. Kartashov E.M., Kudinov V.A. Analiticheskaya teoriya teploprovodnosti i prikladnoi termouprugosti (Analytical theory of thermal conductivity and applied thermoelasticity). Moscow: URSS; 2012. 670 p. (in Russ.). ISBN 978-5-397-02750-2

- Eremin A.V., Kudinov V.A., Kudinov I.V., Zhukov V.V., Trubitsyn K.V. Mathematical model of fuel heat ignition considering space-time nonlocality. *IOP Conf. Ser.: Mater. Sci. Eng.* 2019;552(1):012003. https://doi. org/10.1088/1757-899X/552/1/012003
- 16. Карташов Э.М. Аналитические решения гиперболических моделей теплопроводности. *Инженерно-физ.* журн. 2014;87(5):1072–1081.
- 17. Карташов Э.М., Кудинов В.А. *Аналитическая теория теплопроводности и прикладной термоупругости*. M.: URSS; 2012. 670 с. ISBN 978-5-397-02750-2

(in Russ.).]

#### About the author

**Eduard M. Kartashov,** Dr. Sci. (Phys.-Math.), Honored Scientist of the Russian Federation, Honorary Worker of Higher Professional Education of the Russian Federation, Honorary Worker of Science and Technology of the Russian Federation, Honorary Professor of the Lomonosov Moscow State University of Fine Chemical Technology, Laureate of the Golden Medal of the Academy of Sciences of Belarus in Thermophysics, Professor, Department of Higher and Applied Mathematics, M.V. Lomonosov Institute of Fine Chemical Technologies, MIREA – Russian Technological University (86, Vernadskogo pr., Moscow, 119571 Russia). E-mail: professor.kartashov@gmail.com. Scopus Author ID 7004134344, ResearcherID Q-9572-2016, https://orcid.org/0000-0002-7808-4246

#### Об авторе

**Карташов Эдуард Михайлович,** д.ф.-м.н., Заслуженный деятель науки РФ, Почетный работник высшего профессионального образования РФ, Почетный работник науки и техники РФ, Почетный профессор МИТХТ им. М.В. Ломоносова, Лауреат Золотой медали АН Беларуси по теплофизике, профессор, кафедра высшей и прикладной математики Института тонких химических технологий им. М.В. Ломоносова ФГБОУ ВО «МИРЭА – Российский технологический университет» (119571, Россия, Москва, пр-т Вернадского, д. 86). E-mail: professor.kartashov@gmail.com. Scopus Author ID 7004134344, ResearcherID Q-9572-2016, https://orcid.org/0000-0002-7808-4246

Translated from Russian into English by Kirill V. Nazarov Edited for English language and spelling by Thomas A. Beavitt

#### **Mathematical modeling**

#### Математическое моделирование

UDC 539.3 https://doi.org/10.32362/2500-316X-2023-11-3-86-103



**REVIEW ARTICLE** 

# Mathematical modeling of experiments on the interaction of a high-power ultraviolet laser pulse with condensed targets

#### Ivan G. Lebo @

MIREA – Russian Technological University, Moscow, 119454 Russia

© Corresponding author, e-mail: lebo@mirea.ru

#### **Abstract**

**Objectives.** The paper aimed to review and analyze the results of works devoted to numerical modeling of experiments on the interaction of high-power ultraviolet (UV) laser pulses with condensed targets. The experiments were carried out at GARPUN, the powerful KrF-laser facility at the P.N. Lebedev Physical Institute of the Russian Academy of Sciences (Moscow). The relevance of the research is related to the use of excimer UV lasers as a driver for a thermonuclear reactor. Physical aspects of laser–plasma interaction, including those related to the possibility of using two-sided cone target in a fission–fusion reactor, are discussed.

Methods. The research is based on physico-mathematical models, including Euler and Lagrange.

**Results.** The mathematical modeling of three types of natural experiments is presented: (1) burning through different thicknesses of Al foils by high-power UV laser; (2) studying hydrodynamic instability development at the UV laser acceleration of thin polymer films and features of turbulent zone formation; (3) interaction of high-power UV laser pulses with two-layer targets (Al + Plexiglas) and study of fine structures. Numerical modeling showed that a hybrid reactor with UV laser driver can use targets in the form of two-sided counter cones.

**Conclusions.** Physico-mathematical models are developed along with 2D codes in Lagrangian and Eulerian coordinates as confirmed in the results of natural experiments. The models can be used to describe the physics of high-power UV laser pulses interacting with various targets and forecast the results of reactor-scale experiments.

Keywords: numerical modeling, high-power UV laser pulse interaction with plasma, hybrid reactor with laser initiation

• Submitted: 22.06.2022 • Revised: 07.12.2022 • Accepted: 12.03.2023

**For citation:** Lebo I.G. Mathematical modeling of experiments on the interaction of a high-power ultraviolet laser pulse with condensed targets. *Russ. Technol. J.* 2023;11(3):86–103. https://doi.org/10.32362/2500-316X-2023-11-3-86-103

Financial disclosure: The author has no a financial or property interest in any material or method mentioned.

The author declares no conflicts of interest.

**ОБЗОР** 

# Численное моделирование экспериментов по взаимодействию мощных ультрафиолетовых лазерных импульсов с конденсированными мишенями

#### И.Г. Лебо <sup>®</sup>

МИРЭА – Российский технологический университет, Москва, 119454 Россия <sup>®</sup> Автор для переписки, e-mail: lebo@mirea.ru

#### Резюме

**Цели.** Цель исследования – обзор и анализ результатов работ, посвященных численному моделированию экспериментов по взаимодействию мощных ультрафиолетовых (УФ) лазерных импульсов с конденсированными мишенями. Натурные эксперименты были выполнены в Физическом институте им. П.Н. Лебедева РАН на мощном криптон-фтор (KrF) лазере «ГАРПУН». Актуальность исследований связана с тем, что эксимерные УФ-лазеры являются одним из основных претендентов на драйвер в термоядерном реакторе. Физика взаимодействия такого излучения с плазмой имеет свою специфику. Обсуждается возможность использования мишеней в виде встречных конусов в таком ядерно-термоядерном реакторе.

Методы. Для моделирования лазер-плазменных процессов используются физико-математические модели, лагранжевы и эйлеровы методики, двумерные программы в цилиндрических и сферических координатах. Результаты. Представлены результаты численного моделирования трех типов экспериментов: а) прожигание УФ-лазером алюминиевых фольг различной толщины; б) изучение развития гидродинамической неустойчивости при ускорении тонких полимерных пленок мощным УФ-импульсом и особенностей формирования турбулентного слоя; в) взаимодействие мощных УФ-импульсов с двухслойными мишенями (алюминий + оргстекло) и исследование «тонких» структур, формирующихся в веществе. На основании численных расчетов показано, что в гибридном реакторе с УФ-лазерным драйвером могут применяться мишени в виде двухсторонних встречных конусов. Выводы. Развиты физико-математические модели и апробированы двумерные программы в эйлеровых и лагранжевых координатах на натурных экспериментах, позволяющие описывать физику взаимодействия мощных УФ-лазерных импульсов с мишенями различной конструкции. Это дает возможность прогнозировать эксперименты реакторного масштаба.

**Ключевые слова:** численное моделирование, взаимодействие мощных УФ-лазеров с плазмой, гибридные реакторы с лазерным инициированием

• Поступила: 22.06.2022 • Доработана: 07.12.2022 • Принята к опубликованию: 12.03.2023

**Для цитирования:** Лебо И.Г. Численное моделирование экспериментов по взаимодействию мощных ультрафиолетовых лазерных импульсов с конденсированными мишенями. *Russ. Technol. J.* 2023;11(3):86–103. https://doi.org/10.32362/2500-316X-2023-11-3-86-103

**Прозрачность финансовой деятельности:** Автор не имеет финансовой заинтересованности в представленных материалах или методах.

Автор заявляет об отсутствии конфликта интересов.

#### INTRODUCTION

Laser thermonuclear fusion (LTF) research has been conducted in Russia and abroad since the 1960s [1]. Using powerful laser pulses, targets containing a deuterium-tritium (DT) mixture are heated and compressed. As a result, fusion reactions occur in the compressed fuel (for more details on the physics of laser fusion, see [2, 3]).

A number of important requirements are imposed on the laser ("driver"): the energy in the pulse should be equal to a few megajoules; the radiation intensity on the target surface should be  $10^{15}$ – $10^{16}$  W/cm<sup>2</sup> in the visible or ultraviolet wavelength range; the laser pulse of 10–100 ns duration should have a given temporal intensity "profiling"; and the target must be exposed to good uniformity to reduce instability during fuel

compression. To create a fusion reactor, along with high fusion flare efficiency (gain factor  $G = E_{\rm f}/E_{\rm las} >> 1$ , where  $E_{\rm f}$  is released fusion energy and  $E_{\rm las}$  is absorbed plasma energy of the laser pulse) requires that the driver can operate in the frequency mode (1–10 Hz) with a large resource and high efficiency ( $\eta \approx 1$ –10%).

In Russia [4] and abroad<sup>1</sup> [5–11], powerful laser facilities are being built to initiate thermonuclear microbursts and conduct research in this field of knowledge. The NIF (National Ignition Facility, Lawrence Livermore National Laboratory, USA) laser facility built for LTF purposes has been in operation since 2012. A record fusion neutron yield  $Y_n = (4-5) \cdot 10^{17}$  corresponding to  $\approx 0.7G$  was achieved at this facility in August 2021 [6]<sup>2</sup>. As well as NIF, facilities under construction (UFL-2M, Russian Federal Nuclear Center - All-Russian Research Institute of Experimental Physics (RFNC-VNIIEF), Russia; Laser Mégajoule<sup>3</sup>, France; Shen Guang<sup>4</sup>, China) are based on solid-state Nd lasers<sup>5</sup>, which currently appear to be the most promising in terms of demonstrating single thermonuclear microbursts. However, this type of laser has serious disadvantages in terms of creating a driver for a thermonuclear reactor. While gas excimer lasers offer a number of advantages, such as functioning directly in the ultraviolet wavelength range, the ability to operate with a pulse repetition rate greater than 1 Hz, as well as a wide generation frequency bandwidth, these types of lasers also have disadvantages.

Due to the high cost (in the region of \$10 bn), systematic research is required to support the right decisions when deciding to build the driver for a fission reactor. The GARPUN facility hosted at the P.N. Lebedev Physical Institute of the Russian Academy of Sciences (FIAN) serves to produce a hot dense plasma. This is based on an excimer KrF-laser with pulse energy  $E_{\rm L}\approx 100$  J, pulse duration  $\tau=100$  ns, and wavelength  $\lambda=0.248~\mu{\rm m}$ . For interpreting experimental data, physico-mathematical models and programs have been developed to solve problems involved in interaction of powerful laser pulses with condensed and gaseous targets, as well as predicting new LTF target designs. Below is the review of studies on the mathematical

modeling of three series of experiments performed at the GARPUN facility, as well as the study of targets in the form of counter cones being promising for LTS purposes.

## BRIEF DESCRIPTION OF THE PHYSICO-MATHEMATICAL MODELS AND TWO-DIMENSIONAL PROGRAMS ATLANT AND NUTCY

The *Atlant* software package [12] consists of programs simulating the dynamics and energy transfer in laser plasma in spherical (*Atlant\_Sp* version: coordinates  $\check{r}$  is radius-vector module;  $\theta$ , t is time) and cylindrical (*Atlant\_C* version: coordinates r, z, t is time) geometries.

The equations describing the evolution of the laser target in the two-temperature approximation may be written as follows:

$$\frac{d\rho}{dt} = -\rho \operatorname{div} \overline{\mathbf{u}},\tag{1}$$

$$\rho \frac{d\overline{\mathbf{u}}}{dt} = -\rho \operatorname{grad} P, \tag{2}$$

$$\left(\frac{\overline{9}}{|9|}, \nabla\right)\overline{9} = K\overline{9},\tag{3}$$

$$\rho \frac{d\varepsilon_{\rm e}}{dt} = -P_{\rm e} \operatorname{div} \overline{\mathbf{u}} + \operatorname{div} W_{\rm e} - Q - R_{\rm self} + \operatorname{div} \overline{\boldsymbol{\vartheta}}, \quad (4)$$

$$\rho \frac{d\varepsilon_{i}}{dt} = -P_{i} \operatorname{div} \overline{\mathbf{u}} + \operatorname{div} W_{i} + Q, \tag{5}$$

$$W_e = \alpha_e \operatorname{grad} T_e,$$
 (6)

$$W_i = \alpha_i \operatorname{grad} T_i,$$
 (7)

$$Q = Q_0 \frac{T_e - T_i}{T_e^{3/2}} \rho^2,$$
 (8)

$$P_{e} = P_{e}(\rho, T_{e}), P_{i} = P_{i}(\rho, T_{i}),$$
 (9)

$$\frac{dZ_{i}}{dt} = Z_{i} \cdot (\varphi_{i} - \varphi_{r} - \varphi_{fr}), \tag{10}$$

$$\varepsilon_{e} = \varepsilon_{e}(\rho, T_{e}), \ \varepsilon_{i} = \varepsilon_{i}(\rho, T_{i}),$$

$$R_{\text{self}} = R_{\text{self}}(\rho, T_{e}), P = P_{i} + P_{e}, \tag{11}$$

$$\mathfrak{X}_{0} = \mathfrak{X}_{0}(\rho, T_{0}), \, \mathfrak{X}_{0} = \mathfrak{X}_{0}(\rho, T_{0}), \, K = K(\rho, T_{0}), \, Q_{0} = Q_{0}(\rho, T_{0}),$$

where  $P_{\rm e}$ ,  $P_{\rm i}$ ,  $T_{\rm e}$ ,  $T_{\rm i}$  are electron and ion pressures and temperatures;  $\rho$  is matter density;  $\overline{\bf u}$  is the hydrodynamic velocity vector; P is the total pressure;  $P_{\rm e}$ ,  $P_{\rm i}$  are electron and ion pressures;  $\varepsilon_{\rm e}$ ,  $\varepsilon_{\rm i}$  are electron and ion specific internal energies;  $\varepsilon_{\rm e}$ ,  $\varepsilon_{\rm i}$  are electron and ion thermal

<sup>&</sup>lt;sup>1</sup> Kritcher A. and HIBRYD-E ICF team. Initial results from HYBRID-E DT experiment N210808 with >1.3 MJ yield. *IFSA Virtual Meeting*. September 2021. LLNL-PRES-826367. P. 16. https://www.aps.org/units/maspg/meetings/upload/obenschain-11172021.pdf. Accessed February 07, 2023.

<sup>&</sup>lt;sup>2</sup> In December 2022, reports appeared on the Internet that  $G \approx 1.5$  was obtained at the NIF facility in the United States!

<sup>&</sup>lt;sup>3</sup> https://www-lmj.cea.fr/. Accessed February 07, 2023.

<sup>&</sup>lt;sup>4</sup> https://lssf.cas.cn/en/facilities-view.jsp?id=ff8080814ff565 99014ff5a31abb004a. Accessed February 07, 2023.

 $<sup>^5</sup>$  The Nd-laser generates radiation in the infrared range  $\lambda=1.06~\mu m,$  and expensive complex devices are required to convert to 2nd and 3rd harmonics.

conductivity coefficients;  $\overline{9}$  is the laser radiation flux; K is the absorption coefficient; Q is the exchange term;  $R_{\text{self}}$  is the energy sink due to the plasma self-radiation;  $Z_{\text{i}}$  is the ion charge average in the Lagrangian cell;  $\varphi_{\text{i}}$ ,  $\varphi_{\text{r}}$ ,  $\varphi_{\text{fr}}$  are rates of ternary ionization, ternary recombination, and photorecombination.

The pressure and zero heat flux are set at the outer boundary, while heat fluxes and zero velocity components in the direction normal to the boundary are set on the axis of rotation ( $\theta = 0$  in the spherical coordinate system, r = 0 in the cylindrical one) and zero symmetry planes. The initial conditions can be arbitrary.

The solution of equations (1)–(11) is performed numerically using additive accounting schemes for physical processes.

The *Atlant* program suite, which has been developed during the last four decades, consists of several programs with the following features: (1) the physical model is based on the dense high-temperature laser plasma; (2) a two-dimensional Lagrangian coordinate system is used; (3) the modular principle of program writing; (4) all programs are written in FORTRAN language. More detailed information on the *Atlant* software package can be found in [12, 13].

The *NUTCY* software [12] allows solving numerically gas dynamics equations in two-dimensional cylindrical (*r*, *z*, *t* is time) geometry in Eulerian coordinates [12]:

$$\begin{split} \frac{\partial \rho}{\partial t} + \frac{1}{r} \cdot \frac{\partial r \rho u}{\partial r} + \frac{\partial \rho \omega}{\partial z} &= 0, \\ \frac{\partial \rho u}{\partial t} + \frac{1}{r} \cdot \frac{\partial r \rho u^2}{\partial r} + \frac{\partial \rho u \omega}{\partial z} + \frac{\partial \rho}{\partial r} &= 0, \end{split} \tag{12}$$
$$\frac{\partial \rho \omega}{\partial t} + \frac{1}{r} \cdot \frac{\partial r u \omega}{\partial r} + \frac{\partial \rho u \omega}{\partial z} + \frac{\partial \rho}{\partial z} &= 0, \\ \frac{\partial e}{\partial t} + \frac{1}{r} \cdot \frac{\partial r u (e + p)}{\partial r} + \frac{\partial (e + p) \omega}{\partial z} &= -div \ q_{\mathrm{T}} - div \ q_{\mathrm{L}}. \end{split}$$

Here,  $\rho$  is density; p is pressure;  $V_r = u$ ,  $V_z = \omega$  are components of the velocity vector  $\mathbf{V}$ ;  $e = \rho \left( \varepsilon + \frac{\mathbf{V}^2}{2} \right)$  is the total energy;  $q_T = -\omega_e$  grad T is the flux of electronic heat conductivity;  $q_L$  is the flux of laser radiation.

A one-temperature approximation is used, i.e., it is assumed that the relaxation time between the electronic and ionic components is short compared to the typical time of change in the basic thermodynamic quantities. The system of equations (12) is supplemented by the equation of state  $p = (\gamma - 1)\rho\epsilon$ , where  $\epsilon$  is the specific internal energy,  $\gamma$  is the adiabatic index, and the continuity equation for each gas component (n components in total):

$$\frac{\partial \rho_i}{\partial t} = \operatorname{div} \rho_i \mathbf{V} = 0, \text{ where } i = \overline{1, n-1}.$$
 (13)

If the gas contains two components, it would be convenient to solve the continuity equation for the mixture (the upper equation of the system (12)) and then the equation for one of the components (13). Then, the first component concentration C is determined, while the second component concentration is equal to (1 - C).

This program also uses the modular (block) principle for writing the program using the FORTRAN programming language.

For solving equations (12), (13), total variation diminishing differential schemes of increased approximation order (gas dynamics block) and implicit schemes for taking into account electronic thermal conductivity are used [13]. Methods for solving such problems have been developed at the Institute of Mathematical Modeling and the Keldysh Institute of Applied Mathematics of the Russian Academy of Sciences [12, 14, and 15] with direct participation of the author.

#### MODELING EXPERIMENTS ON BURNING FOIL

Experiments on burning through aluminum foils were carried out at the GARPUN facility [16]. The intensity of the radiation incident on the target was  $I \approx 6 \cdot 10^{12}$  W/cm<sup>2</sup>, while the plasma interaction efficiency parameter  $(I \cdot \lambda^2) \approx 3.4 \cdot 10^{13}$  (W/cm<sup>2</sup>)·µm<sup>2</sup>.

At fixed parameters of incident laser flux on the aluminum foil (target), the thickness of this foil is varied. After placing a screen behind the foil, the time delay between the appearance of glow on the screen and the time of the appearance of plasma glow on the front surface of the target is measured (Fig. 1).

In the experiments, burning through aluminum foils down to  $300~\mu m$  is observed during the laser pulse duration

Figure 2a shows the temporal shape of the laser pulse and compares the results of numerical calculations performed using the *NUTCY* program (solid curves) with experimental data (vertical red bars). The yellow curve shows quasi-dimensional calculations (when the distribution of radiation intensity in the transverse direction is set as a constant value). The blue line shows the results of fully two-dimensional calculations where the intensity is set in the following way:  $I(r,t) = I_1(t) \cdot I_r(r)$  with the transverse intensity distribution having the form  $I_r = C_0/\exp(r/R_{\rm f})^2$ . Here,  $C_0$  is the normalization constant such that  $2\pi \int_0^{R_0} I_r r dr = 1$ ,  $R_0$  is the transverse radius of the calculated region,  $R_{\rm f} = 49~\mu{\rm m}$ . In both variants, the laser intensity averaged over the focusing spot is the

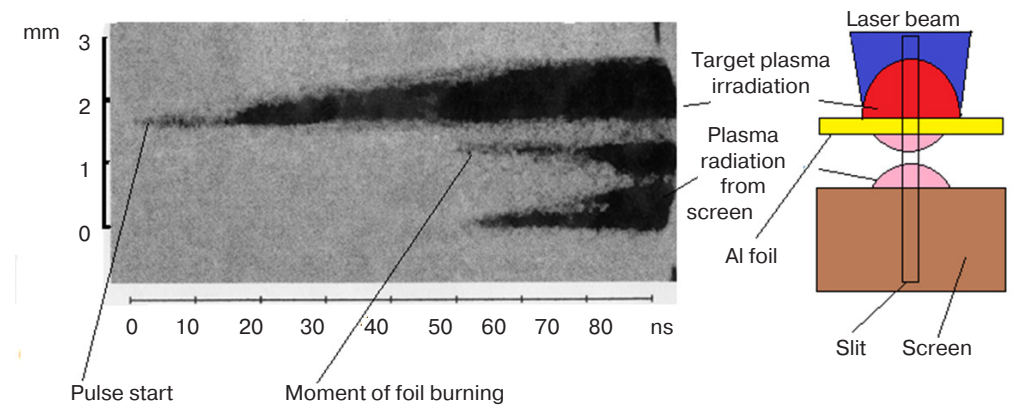


**Fig. 1.** Plasma glow obtained through a slit using the photoelectronic recorder as a function of time (left); scheme of the experiment (right) [12]

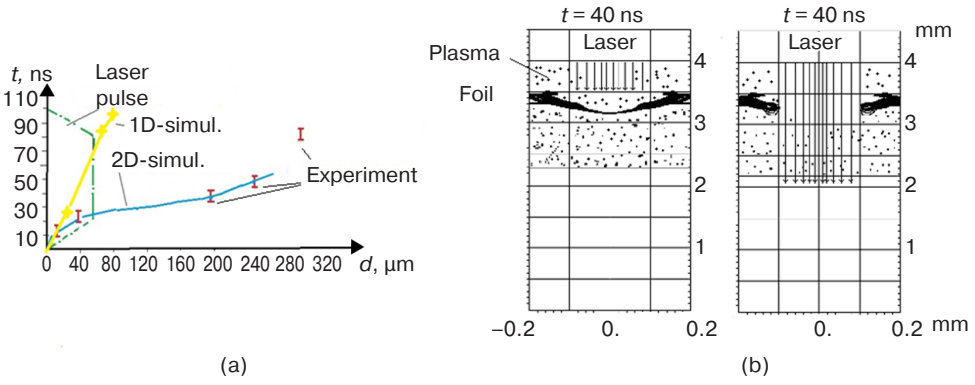


**Fig. 2.** Laser pulse time shape and the results of one-dimensional (1D) and two-dimensional (2D) calculations and experimental data (a); density isolines at time moments t = 40 ns (up to the moment of foil burning through) and t = 45 ns (moment of burning through) (b) [12]

same.  $I_1$  is time dependence of the laser pulse, which has a trapezoid shape with time moments at tops  $t_1 = 0$  ns,  $t_2 = 20$  ns,  $t_3 = 80$  ns, and  $t_4 = 100$  ns.  $\int_0^\infty I_1(t)dt = E_{\text{las}}$  is absorbed laser energy.

The foil density isolines are shown in Fig. 2b. In this calculation, the initial thickness of the aluminum foil is 200  $\mu$ m (initial density  $\rho = 2.7 \text{ g/cm}^3$ ).

Figure 2a shows good agreement between two-dimensional calculations and the experimental data on the "penetration time", but a significant discrepancy with the results of one-dimensional calculations. Along with the evaporation of outer layers towards the incident radiation (directly connected with the burning-through process), the most likely explanation for this is the effect of diverging cone-shaped shock waves (SWs) formed near the crater apex, which plays an important role in such foil "drilling". These "move apart" cold dense layers to increase the penetration depth of laser radiation [16].

In this case, the distance  $L_{\rm SW}$  that the SW travels during the laser pulse duration (SW velocity  $V_{\rm SW}\sim 5$  km/s,  $t\sim 100$  ns, then  $L_{\rm SW}\sim 500$  µm) is much larger than the focus spot size  $(2R_{\rm f}\approx 100$  µm).

## MODELING EXPERIMENTS ON TURBULENT LAYER DEVELOPMENT DURING LASER ACCELERATION OF THIN FILMS

The Richtmyer–Meshkov instability that develops when SWs pass through the contact surfaces of two gases or plasma results in the rapid evolution of initially small perturbations of interface surface of two media to the formation and the development of a turbulent layer [17, 18]. Studying the laws of turbulence development in the physics of extreme state of matter is an extremely important task in inertial thermonuclear fusion in cosmology and astrophysics [2].

Using powerful laser pulses, it is possible to accelerate dense unevaporated layers to velocities of  $\sim 10-100$  km/s. It has been proposed to accelerate such layers in special transparent cells filled with a gas or two gases separated by a thin film. The development features of hydrodynamic instabilities of the contact boundary perturbations and transition into the turbulent state may be studied in such "laser shock tubes" [19].

In the second series of experiments, the development of the turbulent layer during laser acceleration of thin Lavsan<sup>TM</sup> films with a thickness of 1–50 μm is studied

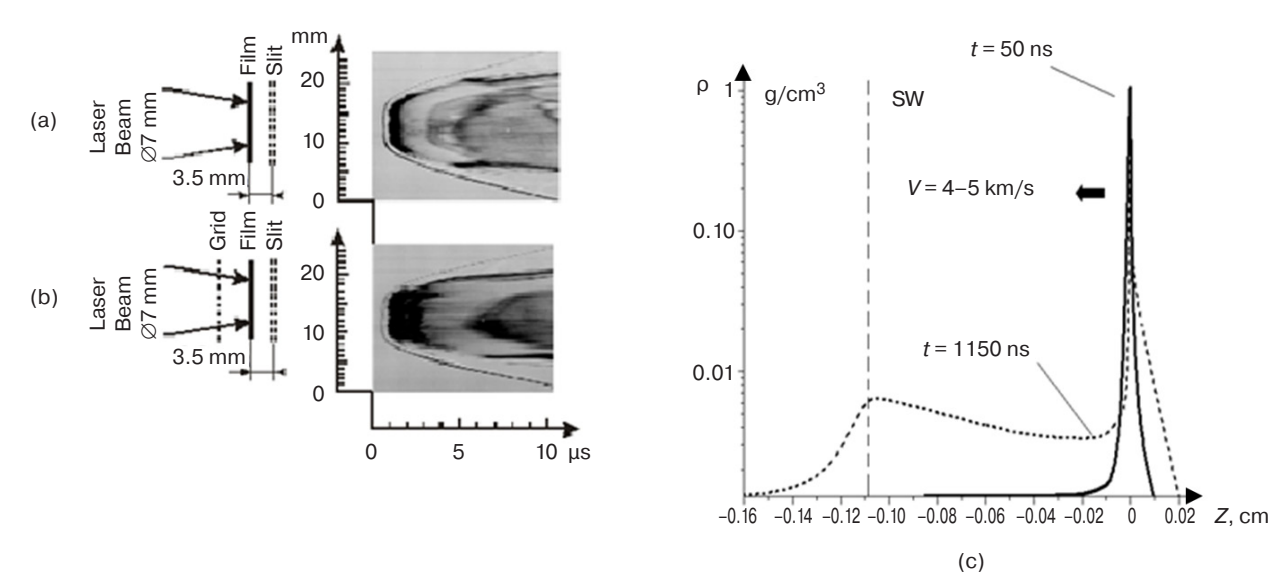


Fig. 3. Schematic of experiments (left) and images of the accelerated layer obtained with slit sweep in the case of uniform (a) and nonuniform (b) irradiation,  $\emptyset$  is a side of a square-shaped laser beam; numerical calculation results of the density distribution along the OZ axis at time moments t = 50 ns and t = 1150 ns (c) [20]

at the GARPUN facility. The targets are placed inside a vacuum chamber filled with air or argon with initial pressure of 0.0002-1.0 bar. Laser radiation is focused into the  $7 \times 7$  mm<sup>2</sup> square spot using a prism raster, thus ensuring irradiation uniformity not worse than 1–2%. The intensity of laser radiation on the target surface is varied  $I=0.1-1.0\,\mathrm{GW/cm^2}$  by attenuating the power of the incident light beam. The slit of the electron photochronograph is parallel to the film surface and is located at different distances behind it. The "registograms" of a film with initial thickness  $d = 5 \mu m$  irradiated by laser with intensity  $I = 0.55 - 0.65 \text{ GW/cm}^2$  in the air at atmospheric pressure are shown in Figs. 3a and 3b. The slit is placed at the distance of 3.5 mm behind the initial position of the film. In Fig. 3a, homogeneous radiation falls on the target surface, while in Fig. 3b, the radiation passes through the wire mesh with a mesh size of  $0.7 \times 0.7 \text{ mm}^2$  placed in front of the film at the distance of  $\sim 1$  cm. This provides a given scale of the intensity nonuniformity. In the second case, the thickness of the dense layer flying past the slit is 3–4 times greater than in the first case. The density profiles obtained in numerical calculations at time moments t = 50 ns and t = 1150 ns are shown in Fig. 3c. The density maxima are combined in one point for easy comparison. The vertical dashed line is the shock front at time moment t = 1150 ns.

The process of laser acceleration of the film is simulated using the cylindrical version of the *Atlant* software package. It is shown that numerical calculations accurately reproduce the dynamics of the film flight. The velocity is ~3–4 km/s at the moment when the dense layer flies past the slit.<sup>6</sup> The initial density

of the film is 1 g/cm<sup>3</sup>. During flight, the layer density should be noted to decrease with time due to thermal expansion, as well as due to the purely geometrical factor of increasing the surface of the layer boundary. By the moment t = 1150 ns (when the layer reaches a distance of 3.5 mm from the initial position), the density maximum is 0.1 g/cm<sup>3</sup>. By this point, the width of the dense layer has increased compared to the initial one (Fig. 3c). The development of turbulent mixing during laser acceleration and braking of the layer by the surrounding air results in an additional increase in the film thickness. Thus, at a layer flight velocity of ~3 km/s and time of flight past the slit of  $\sim 0.5 \mu s$ , the layer width is 1.5 mm, while in the calculation with no allowance for turbulent mixing, it is an order of magnitude smaller (Fig. 3c). In the experiments with the perturbed laser flux (Fig. 3b), the layer thickness is 3-5 times greater.

For modeling turbulence, the turbulent mixing model described in [21, 22] is used. In this model it is assumed that the turbulent layer develops according to the laws of diffusion, but with empirical coefficients obtained from natural experiments. Thus, the turbulent diffusion equation may be written as follows:

$$\frac{\partial \rho}{\partial t} = \frac{\partial}{\partial z} \left( D_{\rm m} \frac{\partial \rho}{\partial z} \right), \tag{14}$$

where  $\rho$  is density and  $D_{\rm m}$  is the turbulent mixing coefficient,

$$D_{\rm m} = l_{\rm p}^2 \omega_{\rm t}, \, \omega_{\rm t} = \left(\frac{\partial \ln \rho}{\partial z} \cdot \frac{1}{\rho} \cdot \frac{\partial P}{\partial z}\right)^{0.5}. \tag{15}$$

 $<sup>^6</sup>$  By the time t= 50 ns, the boundary of the air–CH layer accelerated to 4–5 m/s. Then the dense layer moved by inertia, gradually expanding and transferring part of the energy to the environment.

Here,  $\omega_l$  is the increment of hydrodynamic instability development derived in [22],  $L_{\rho} = 1 / \frac{\partial \ln \rho}{\partial z}$  is the density gradient scale, and  $l_{\rm p}(xl)$  is the turbulent pulsation size and depends on the width of the turbulence zone xl.

The authors of [21] suggest that

$$l_{p} = \alpha L_{\text{mix}}, \tag{16}$$

where  $L_{\rm mix}$  is the current size of the turbulent zone ( $L_{\rm mix} \approx xl$  in the experiment in Fig. 3a), while the value of  $\alpha$  should be given *a priori*.

A program has been written that allows equation (14), (15) to be solved making allowance for (16).

The averaged values of layer acceleration  $g=-\frac{1}{\rho}\cdot\frac{\partial P}{\partial z}$  and  $L_{\rho}$  are taken from the numerical calculation results using the  $Atlant\_C$  software.

It should be noted that the estimate  $L_{\rm mix} \approx \alpha^4 \ln(\rho_1/\rho_2) gt^2$  is made in [21] for the case of contact between two incompressible media  $(\rho_1 \text{ and } \rho_2)$  in the field of constant acceleration g (the acceleration is directed from the less dense medium toward the more dense one).

There are two stages of film acceleration: (1) when exposed to a laser pulse, the layer is accelerated due to reactive and thermal pressure from the vaporized plasma side,  $g = +(3-4) \cdot 10^{12}$  cm/c<sup>2</sup> on the front side; (2) the layer is decelerated in the atmosphere,  $g = -(1-2) \cdot 10^{11}$  cm/c<sup>2</sup> on the back side of the layer. The data are taken from numerical calculations in the *Atlant C* software.

In numerical calculations, the value of  $\alpha$  (alfa) is varied so that by the time the dense layer is flying past the slit, its width  $\Delta L$  (delta\_L) is equal to the value measured in the experiment [20].

The "broadening" due to turbulent mixing of the layers accelerated by the laser pulse in the case of the first and second types of film irradiation is shown in Fig. 4. The time moment t = 1150 ns when the layer is "seen" through the slit is given.

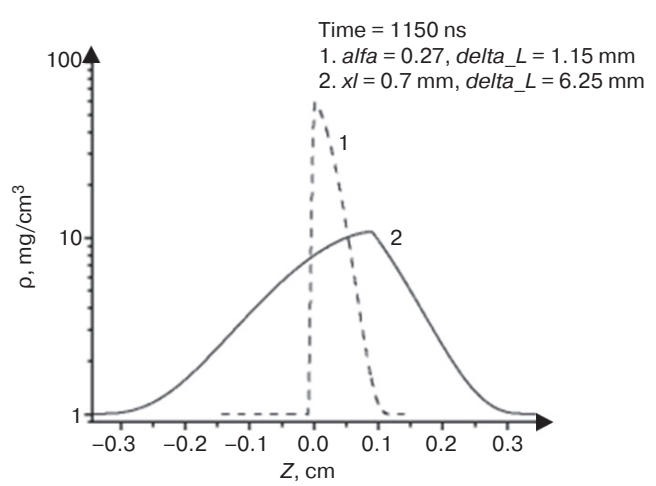


**Fig. 4.** Density of the accelerated layers obtained in calculations: 1—film is irradiated by a laser flux without flux perturbation, 2—introducing flux perturbation by dint of the grid, xl is a grid cell size,  $l_p = xl$  [20]

## MODELING EXPERIMENTS ON IRRADIATION OF TWO-LAYER TARGETS AND FORMATION OF FINE STRUCTURES

In the third series of experiments, two-layer targets are irradiated in the form of a 100  $\mu$ m aluminum layer followed by a ~5 mm plexiglass layer. The laser beam is incident on the aluminum side. The focus spot radius on the target surface is 50–70  $\mu$ m. In the plexiglass, extended craters about 1 mm long are observed, while one or two narrow channels over 100–600  $\mu$ m long are formed near its top (Fig. 5) [16, 23].

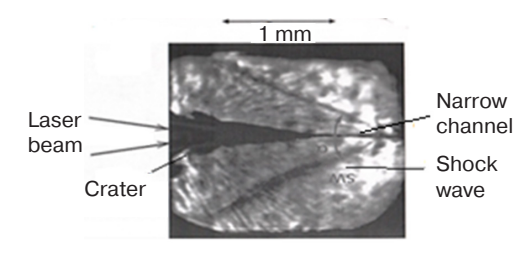


**Fig. 5.** Two-layer target after laser irradiation. The incident laser beam is shown on the left [23]

Calculations of the interacting laser pulses with targets are performed using the *NUTCY* software. In the calculated area, laser beams propagate strictly along the *OZ* axis, while refraction and self-focusing of light beams are not considered. The problem statement for modeling experiments is shown in Fig. 6.

The following parameters are used: focus spot radius  $R_{\rm f} = 50~\mu{\rm m}$  at Gaussian intensity distribution in the spot; the absorbed laser pulse energy 40 J; aluminum foil 100  $\mu{\rm m}$  thick and having initial density 2.7 g/cm<sup>3</sup> with plexiglass having initial density 1.19 g/cm<sup>3</sup> behind it; calculation area is a cylinder having radius  $R_0 = 0.5~{\rm mm}$  and length  $OZ = 1.5~{\rm cm}$ .

The two-dimensional distributions of density and temperature of the matter obtained in calculations in the *NUTCY* software are shown in Fig. 7. The length scale (R and Z) is given in units of  $10^{-2}$  cm. The temperature scale is given in units of 100 eV. The corresponding density and temperature intervals are shown in the tables on the right and are represented as tonality in the figure (white–gray–black).

The plasma density and temperature distribution along the OZ axis as well as the density distribution along the radius at  $Z_0 = 1$  cm (the initial position of the condensed matter-plasma boundary) is shown in Fig. 8.

Calculations in the *NUTCY* software allow modeling processes of forming the flaring plasma and extended crater in the condensed target. However, additional considerations and the development of a physical and mathematical model are required to explain the appearance of narrow channels in plexiglass.

The primary reason for the formation of narrow channels in plexiglass is the development of selffocusing of the laser beam in the plasma due to the

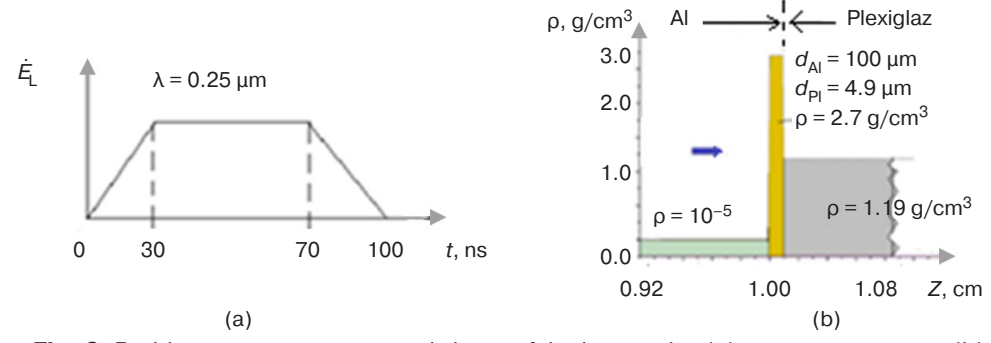
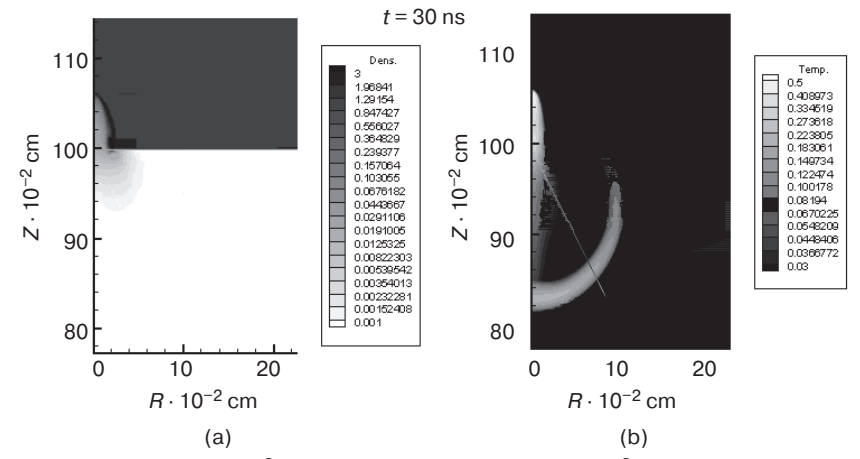
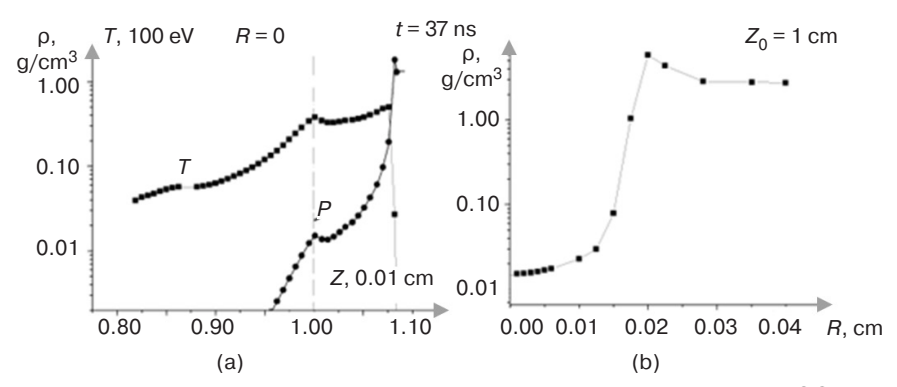


Fig. 6. Problem statement: temporal shape of the laser pulse (a); target parameters (b) [23]



**Fig. 7.** Density  $\rho(R, Z)$ , g/cm<sup>3</sup> (a) and temperature T(R, Z),  $10^2$  eV (b) fields calculated for time moment t = 30 ns [23]



**Fig. 8.** Distribution of density  $\rho$  and temperature T in the plasma along the axis  $OO_1$  (R = 0) at time moment t = 37 ns (a); dependence of density  $\rho$  on radius R at this moment at  $Z_0 = 1$  cm (b) [23]

thermal mechanism. In the presence of the extended plasma, due to small perturbations of the laser beam intensity near the axis, the region of high temperature arises, thus resulting in "squeezing" of the plasma in the transverse direction. Due to refraction, beams gather toward the axis, in turn resulting in further formation of the low-density channel in the plasma. In case of small perturbations, an estimate of the threshold intensity  $I_{\rm th}$  for the thermal mechanism (in units of  $10^{14}$  W/cm²) is given in [24], as follows:

$$I_{\rm th} \ge 2 \cdot 10^5 \, (\rho_{\rm cr}/\rho)^3 \, \frac{T^5 \lambda^2}{Z_{\rm i}^2 L_{\rm pl}^2}.$$
 (17)

Here, temperature T is given in keV units (~11.6 mln degrees), the plasma longitudinal channel scale  $L_{\rm pl}$  and emission wavelength  $\lambda$  are given in  $\mu$ m, while  $Z_{\rm i}$  is the average ion charge. The typical plasma parameters for conditions of the discussed experiments are the following:  $Z_{\rm i} = 4$ –6,  $L_{\rm pl} = 1000~\mu$ m,  $T = 0.1~{\rm keV}$  and  $\lambda = 0.25~\mu$ m, whence  $I_{\rm th} \ge 2 \cdot 10^{10}~{\rm W/cm^2}$ .

It is also possible to use a strictional (ponderomotive) mechanism of self-focusing, where the channel of reduced density is formed due to the action of ponderomotive force in the plasma in which beams are focused. However, the intensity perturbation threshold in this case is two orders of magnitude greater than in the case of thermal self-focusing.

In order to more accurately account for the abovementioned effects in nonuniform plasma, it is necessary to use mathematical modeling methods involving the development of new programs to calculate the plasma dynamics equations together with nonlinear Maxwell equations<sup>7</sup>.

The results of numerical modeling of laser beam self-focusing according to the simplified model of laser beam evolution in the conducting medium are given in [26]. This model implies the Gaussian distribution of radiation intensity in cylindrical beam

$$E^{2}(r,z) = E_{0}^{2} \cdot \exp\left(-\frac{r^{2}}{a^{2}(z)}\right)$$
, where E is electric

intensity in the laser beam, a(z) is effective radius changing as the radiation propagates along the OZ axis.

Assuming that the permittivity depends on the law (paraxial approximation):

$$\varepsilon(z,r) = \varepsilon_0(z) + \beta(z) \cdot r^2, \quad \beta = \frac{\partial \varepsilon}{\partial (r^2)} \Big|_{r=0}$$
 (18)

the following equation for describing the dimensionless beam radius  $f = \frac{a(z)}{a_0}$  may be written as (see more details in [27, 28]):

$$\varepsilon_0 \frac{df}{dz^2} + \frac{1}{2} \frac{d\varepsilon_0}{dz} \frac{df}{dz} = \frac{c^2}{\omega^2 a_0^4 f^3} - \beta(z) f.$$
 (19)

The first term on the right in equation (19) describes beam diffraction, while the second term describes selffocusing.

In case of strictional (or ponderomotive) mechanism:

$$\beta(z) = \left(\frac{\omega_p}{\omega}\right)^2 \frac{\alpha I_0}{f^2 a_0^2} e^{-\alpha I_0},$$

$$\alpha = \frac{e^2}{8m_e \cdot \omega^2 T_e}, \qquad I_0 = E_0^2 \sqrt{\frac{\varepsilon_0(0)}{\varepsilon_0(z)}}.$$
(20)

In case of a thermal mechanism:

$$\beta(z) = \left(\frac{\omega_p}{\omega}\right)^2 \cdot \frac{\sigma E_0^2}{8\chi_0 T_e^{3.5}} \cdot \sqrt{\frac{\varepsilon_0(0)}{\varepsilon_0(z)}} \cdot \frac{1}{f^2} =$$

$$= \frac{9}{16} \cdot \frac{v_{ei}^2}{\omega^2 T_e^2} \cdot I_0,$$
(21)

where  $\sigma$  is high-frequency electrical conductivity;  $v_{ei}$  is the effective frequency of electron-ion collisions.

Equations (18)–(21) are solved numerically on the given density profiles  $\rho(z)$  and the fixed value of electronic temperature T(z).

The laser radiation and plasma parameters are taken from [23]:  $I = 5 \cdot 10^{12}$  W/cm<sup>2</sup>,  $\rho_{\rm cr} = 0.1354$  g/cm<sup>3</sup>, T(z) = 0.1 keV, ion charge  $Z_{\rm i} = 6$ , and plasma length  $0 \le z \le 0.1$  cm. The exponential density profile is given:  $\rho = \rho_{\rm cr} \cdot \exp(-B(0.1-z))$ , B = 40 cm<sup>-1</sup>.

The evolution of the dimensionless radius of beam  $f_{\rm th}$  along the OZ axis for initial beam  $a_0 = 35$  (1) and 100 µm (2) is shown in Fig. 9a. In both cases, self-focusing of light beams is observed due to the thermal mechanism. The strictional mechanism does not appear  $(f_{\rm str} > 1)$ .

The beam having initial radius 100  $\mu$ m has decreased to dimensions  $f < 10^{-3}$ . The calculation is discontinued. The beam with initial radius 35  $\mu$ m begins to increase in cross section after reaching the minimum value of  $f = 2 \cdot 10^{-3}$ . The first focus occurs at plasma density  $\rho = 0.00243$  g/cm<sup>3</sup>, i.e.,  $\rho/\rho_{cr} \approx 0.2$ .

The development of thermal self-focusing of the laser beam in the crater plasma formed during irradiation of the condensed target by the high-power laser results in increasing intensity by 2–3 orders of magnitude. Further, the strictional mechanism near the critical surface may already dominate.

The beam evolution in the case of the ponderomotive (strictional) self-focusing development is shown in Fig. 9b. The initial beam radius  $a_0 = 10 \, \mu \text{m}$ ,  $I = 5 \cdot 10^{16} \, \text{W/cm}^2$ . In this calculation series,  $\rho_{\rm cr} = 0.0677 \, \text{g/cm}^3$ ;  $T(z) = 1 \, \text{keV}$ ; and ion charge  $Z_{\rm i} = 12$ . In this case, it can be seen that the self-focusing increases much faster due to the strictional mechanism (red line) than due to the thermal mechanism (blue line).

When condition  $I \cdot \lambda^2 > 10^{14} \, (\text{W/cm}^2) \cdot \mu \text{m}^2$  is fulfilled, "hot spots" arise near the critical surface where fluxes of above-thermal electrons are formed [2, 3]. These electrons penetrate deep into the cold condensed matter whose trace is observed in the discussed experiments near the crater top (Fig. 5).

The physico-mathematical models and numerical programs described above, which have been tested in experiments carried out using the powerful KrF-laser facility at GARPUN, reproduce the experimental data at a good level of accuracy with different types of targets and under various conditions of natural experiments. These circumstances allow the predictive mathematical modeling results of planned large-scale experiments (at the level of absorbed laser energy ~1 MJ) to be treated with confidence.

 $<sup>^7</sup>$  The numerical modeling results of thermal self-focusing of the laser beam in plasma at the 3rd harmonic of Nd-laser ( $\lambda=0.35~\mu m$ ) are given in [25] where the geometric optics model is used for describing the propagation of laser beams in a weakly heterogeneous medium ( $\lambda << L_{\rho}$ ), but without paraxial approximation and hypothesis of the beam quasi-stationarity.

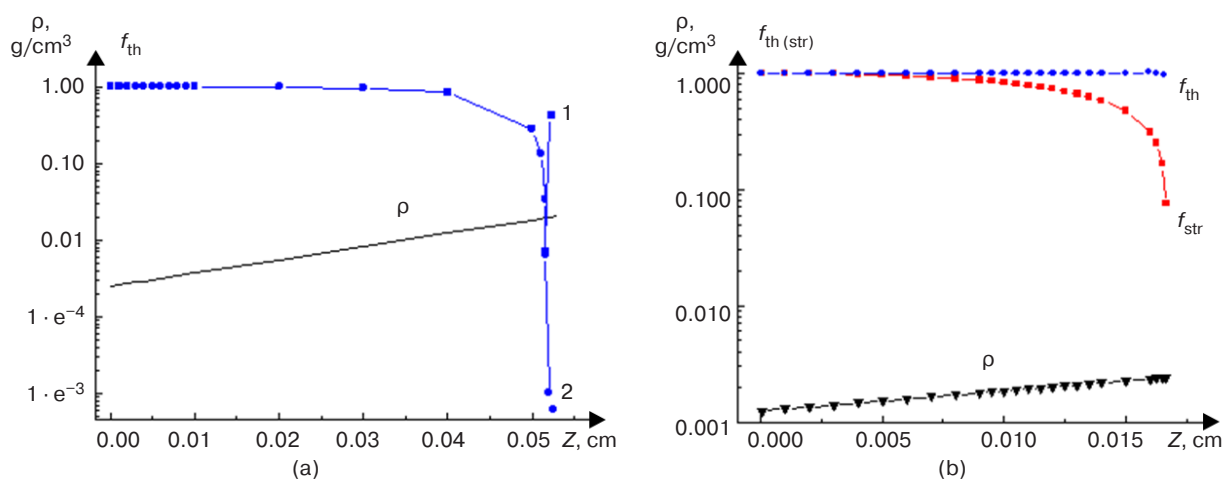


Fig. 9. Changing dimensionless beam radius on exponential plasma density profile: blue lines denote thermal mechanism; red line denotes strictional mechanism; and black line denotes density profile.

(a)  $I = 5 \cdot 10^{12} \text{ W/cm}^2$ , (b)  $I = 5 \cdot 10^{16} \text{ W/cm}^2$  [26]

## ON POSSIBLE TARGET DESIGN IN THE FORM OF A DOUBLE-SIDED CONE FOR AN EXCIMER DRIVER

It is conditionally possible to distinguish four main directions of promising applications of thermonuclear microbursts initiated by laser pulses. These are: (1) modeling substance behavior in laboratory conditions at very high energy concentrations and consequences of nuclear explosions, testing of corresponding numerical programs, as well as other applied tasks; (2) nuclear power engineering and development of new reactor types; (3) modeling astrophysical phenomena; and (4) development of rocket engines for interplanetary flights [2]. Generally speaking, the driver requirements for each of these directions can differ significantly. In the present paper, only the second direction is discussed.

It was stated in the introduction that, to date, no final choice has been made regarding the type of driver for the laser fusion reactor. At the first stage, the reactor function according to a hybrid scheme when the main energy is apparently obtained through the fission of heavy element nuclei (uranium), with this process being controlled by neutron fluxes from thermonuclear microbursts initiated by laser flares [29, 30]. This type of reactor is safer than those based on nuclear fission reactions only, since its "assemblies" are subcritical; moreover, the frequency of laser shots can decrease as fissile elements accumulate in blankets. The fuel of such reactors does not require pre-enrichment of uranium, since its power cycle can start with natural uranium U<sup>238</sup>. Since the driver itself can be placed in an adjacent building at the distance of about 10 m from the reactor, the fission chain reactions can be quickly silenced by turning off the laser. It is possible to organize the fissile element production regime in such a way that the retrieval of the reactions would be an extremely rare

procedure carried out directly on the plant premises or in another specially equipped location. In this way, the probability of terrorist takeover of these resources would be minimized, and the rooms where the radioactive elements are stored would be reliably protected from potential bomb blasts.

Nuclear reactions produce unique elementary particles including neutrinos and positrons. External magnetic fields allow the selection of charged particles and their temporary storage [2].

As mentioned above, the solid-state Nd-laser is planned to achieve high gain factors in a single thermonuclear microburst  $(G \gg 1 \text{ is "ignition"}).$ To achieve large values of G, it is necessary to compress the fuel to densities 1000 times greater than the density of the liquid DT mixture in order to initiate the fusion combustion wave. Due to development of hydrodynamic instability and mixing [2], such conditions have not yet been achieved in inertial thermonuclear fusion targets. On the other hand, achieving  $G \sim 1$  is an independent goal of practical importance. Indeed, Fig. 10 shows a schematic of the nuclear-thermonuclear power plant with laser excitation of fusion microbursts [30]. Here,  $\eta$  is the laser efficiency;  $\beta$  is the conversion efficiency of thermal energy into electrical energy; φ is the fraction of energy providing reactor operation; f is the frequency of laser shots;  $E_{\rm L}$  is the energy in the laser pulse;  $W_t = fKE_L$  is the thermal power generated in the reactor;  $W_n$  is the power, which a consumer gets (nettopower); K = (0.2 + 0.8M)G is the reactor energy gain factor; M is the energy multiplication factor in the reactor uranium blanket;  $(1/\eta - 1)fE_1$  is the laser pumping energy loss. In order to "close" the energy cycle, the following inequality should be fulfilled:

$$(1 - \phi)\beta(0.2 + 0.8M)G > 1/\eta. \tag{22}$$

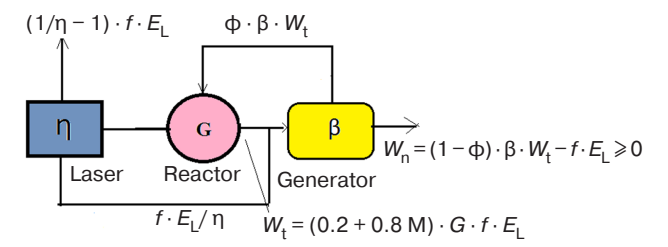


**Fig. 10.** Structural diagram of the hybrid nuclear-thermonuclear station [32, 33]

It follows from (22) that the gain factor should be  $G \ge 1$  at  $\phi = 0.2$ ,  $\beta = 0.4$ ,  $\eta = 0.05$ , and M = 60. The use of a conical target and KrF-laser as the hybrid reactor driver is proposed in [31]. The laser pulse would consist of two long parts (accelerating) pulse with  $\tau_1 \approx 100$  ns and a series of short pulses with  $\tau_2 \approx 0.01-0.1$  ns. Due to the deformation of cone walls by strong SWs formed near its apex, it is virtually impossible to achieve compression of the fuel to densities significantly exceeding the normal wall density (i.e., 10-20 g/cm<sup>3</sup>) in such a target design; however, this is not required for achieving gain factors  $G \sim 1$ . Short laser pulses injected through special holes near the cone apex would carry out local retention and additional heating of the compressed fuel.

The schematic of the two-sided conical target and its irradiation with laser beams taken from [32, 33] is shown in Fig. 11. The upper part of Fig. 11a shows an axial section of the target. The trigger (outer radius  $R_0$ ) consists of polymer material 2 and a low-density substance (foam, aerogel) 3 required for "smoothing out" ablative pressure disturbances at the initial stage of the trigger acceleration. The low-density layer reduces the impact of small-scale disturbances of the laser flux, which can develop in the extended plasma due to self-focusing and forced Brillouin-Mandelstam scattering (BLS) and affect the stability of the flight. Next is a thin layer of gold 4, followed by vacuum 5 and 6 comprising a layer of condensed DT fuel. The thin gold layer in the trigger increases the fuel compression ratio (in one-dimensional calculations). Using cryogenic DT fuel also allows the compression ratio to be increased<sup>8</sup>.

The general scheme of the target in the form of counter cones is shown in Fig. 11b, while its central part is shown separately in Fig. 11c. The layer of low-density substance (foam in Fig. 11c) for "smoothing out" perturbations of ablative pressure of short pulses is located at the cone apex between the thin inner gold layer and the target outer chamber.

To achieve the level  $G \sim 1$ , it is sufficient to compress the condensed fuel by 30–50 times compared to the density of the liquid DT mixture. The entire compression process occurs mainly on the incident and reflected SW;

under these conditions, it may be expected that mixing would not result in a catastrophic situation (i.e., in a decrease in the neutron yield by orders of magnitude compared to the results of one-dimensional calculations).

The calculation results performed in the spherical version of the *Atlant\_Sp* software are given in [32], while those carried out in *SND* program developed at RFNC–VNIIEF [34, 35] are given in [33]. It should be noted that the comparative calculations carried out earlier using the *Atlant\_Sp* and *SND* programs show close results at the same formulation of physical problems [36].

Numerical calculations show that thermonuclear yield  $G \sim 1$  can be achieved in such a target design using pulses in the "long + short" mode at the level of absorbed laser energy  $\sim 1$  MJ.

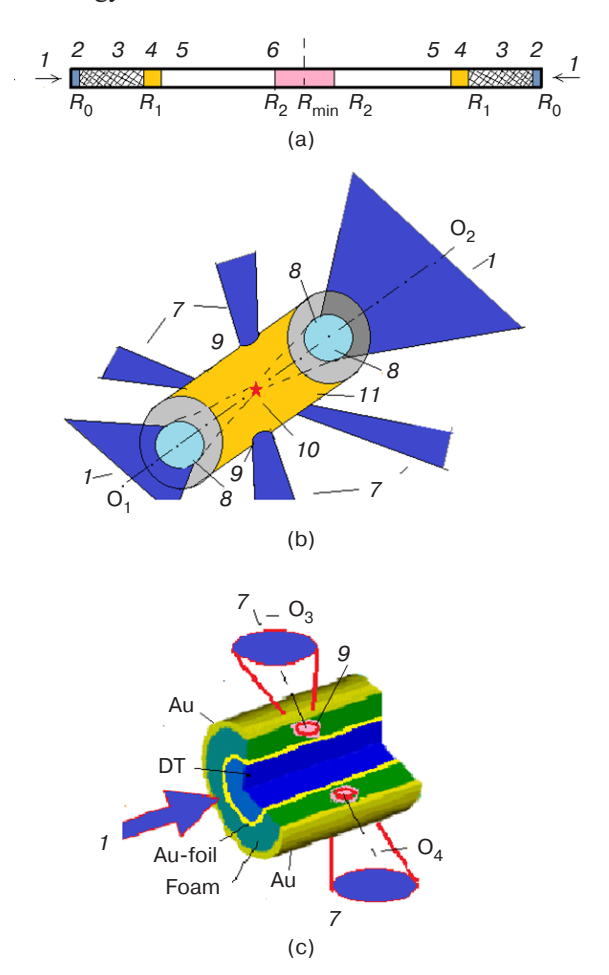


Fig. 11. Scheme of the two-sided conical target (a) and its irradiation by long + short laser pulses, O<sub>1</sub>O<sub>2</sub> is the symmetry axis (b); (c) central part of the conical target. 1 is laser beams (long pulses) accelerating the trigger, 2 is the trigger dense layer, 3 is the foam layer, 4 is the thin gold layer, 5 is the vacuum gap, 6 is the cryogenic DT fuel layer, 7 is short laser pulses, 8 is the shell-trigger, 9 is holes for short pulses, 10 is the thermonuclear microburst, 11 is the gold target chamber with conical channels along the O<sub>1</sub>O<sub>2</sub> axis, and O<sub>3</sub>O<sub>4</sub> is the axis passing through target center in the plane perpendicular to symmetry axis O<sub>1</sub>O<sub>2</sub> [32, 33]

<sup>&</sup>lt;sup>8</sup> The impact of the development of self-focusing and hydrodynamic instabilities is not considered directly in calculations.

The calculations assume that cone walls are absolutely elastic and heat-resistant. The formation of the "shell-wall" boundary layer is not considered there. The problem has perfect symmetry with respect to the top of the truncated cone (the O<sub>3</sub>O<sub>4</sub> axis through which the symmetry plane perpendicular to the O<sub>1</sub>O<sub>2</sub> axis passes is shown in Fig. 11c). The process of compression and initiation of thermonuclear reactions in such targets may be conventionally divided into two stages. At the first stage, a long laser pulse accelerates the trigger that moves to the top of the cone and compresses the DT fuel. When the SW reaches the apex of the truncated cone and is reflected there, a series of short pulses (total duration about ~0.1 ns, total energy ~10% of the main heating pulse) is injected through the holes into the target in the plane perpendicular to the O1O2 axis. The purpose of these pulses is to ensure the dynamic retention of the compressed fuel and its additional heating (second stage).

The following two series of calculations of the target compression by a long pulse of KrF-laser of various time shapes are performed: (1) in the form of a triangle with time moments at tops  $t_1=0,\ t_2=100$  ns, and  $t_3=101$  ns; (2) in the form of a curved trapezoid with the tightened front smoothly rising  $(t_2-t_1=12$  ns) and with a subsequent rectangular pulse  $(t_3-t_2=10$  ns). The targets have the form of truncated cones with aspect ratios  $R_0/R_{\rm min}=10$ –20 (Fig. 11a). The gain factor G>1.

Thus, using UV laser pulses with energies of  $\approx$ 2 MJ and targets in the form of counter truncated cones allows providing the "thermonuclear flare"<sup>9</sup>.

### DISCUSSION OF RESULTS AND CONCLUSIONS

The main elements of the scheme discussed in the paper are individually tested in small-scale natural and numerical experiments.

Experiments with conical laser targets performed at the Prokhorov General Physics Institute of the RAS on a solid-state infrared laser are described in the review [37].

The amplification of picosecond pulses generated by the Ti:sapphire laser together with long UV pulse is tested at the GARPUN-MTV facility (FIAN, Russia) [38, 39].

The impact of hydrodynamic instability and interaction with the wall during laser acceleration of the trigger in the conical channel remain insufficiently studied; this is also the case with the development of self-focusing and BLS in the extended plasma. Semiempirical physico-mathematical models and software packages are developed based on numerical calculations and natural experiments carried out

on various laboratory benches [40–44]. Direct mathematical modeling of these phenomena requires the use of high-performance supercomputers and parallel computing algorithms. Such work is being carried out, in particular, at the MIREA – Russian Technological University [45].

In the USA, the *ELECTRA* program for constructing a powerful KrF-laser-based LTF research facility operating in frequency mode has been announced [46–51].

The physico-mathematical models and programs, which adequately describe the model data from experiments performed at the GARPUN laser facility, provide a basis for target designs for future large-scale reactor-scale experiments.

Figure 12 shows the proposed scenario for the development of laser fusion research as applied to the creation of a power plant: the first stage is research and development (R&D), while the second stage is the experimental and technological development (ETD), the third stage is the development of a pilot and experimental reactor (DPER), and the fourth stage is the development of a commercial reactor (DCR). The abscissa axis shows the estimated costs of overcoming these stages.

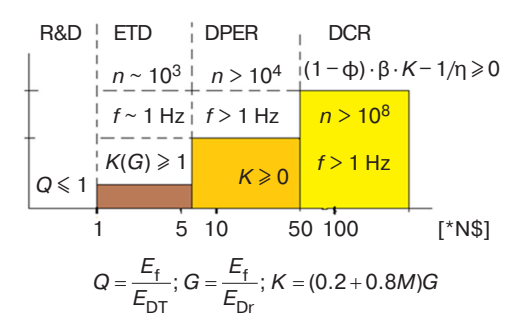


**Fig. 12.** Assumed scenario for the development of inertial fusion research (drawn by the Author). n—resource, f—frequency of microbursts, \*N\$—capital expenditure, N = 1—expenditure of R&D stage (footstep),  $E_{\rm Dr}$ —driver energy, and  $E_{\rm L}$ —laser pulse energy.  $E_{\rm Dr}$  =  $E_{\rm L}$ 

There are several criteria for characterizing fusion efficiency:

- 1)  $Q = E_f / E_{DT} = 1$  is the "physical threshold of fusion reactions," when the released fusion energy  $E_f$  equals the energy invested in the DT plasma from the third-party source  $E_T$ ;
- 2)  $G = E_f E_{Dr}$ , "gain" is gain or "flash criterion." As a rule, this coefficient is an order of magnitude smaller than Q at the same  $E_f$ , since a significant part of the energy is "lost" with the vaporized inert material of the target and does not get into the compressed fuel:
- 3)  $K = (0.2 + 0.8M) \cdot G$  is the reactor gain factor allowing also for the energy gain M due to fission reactions;

<sup>&</sup>lt;sup>9</sup> We shall mean G = 2-3 by "flash."

4)  $C_E = (1 - \phi)\beta K - 1/\eta$  is the "plant energy efficiency" parameter.

At the R&D stage, the main challenge is the physical threshold of thermonuclear reactions. American scientists have managed to achieve this  $^{10}$  [7] to approach the value  $G \sim 1$  at the NIF facility. On this basis, it can be said that they are ready to move to the second stage, i.e., ETD.

Overcoming this stage requires a repetition frequency of laser pulses at the level of  $f \sim 1$  Hz and the consequent feeding of targets into the focus of laser beams at the same frequency, as well as providing "resource n," i.e., uninterrupted operation of the entire system at least for an hour ( $n \sim 10^3$ ).

At the ETD stage, it is necessary to provide  $K(G) \ge 1$ , i.e., to check the possibility of the blanket functioning in the frequency mode of loads, as well as "some

resource"  $n \sim 10^3$ , i.e., ensuring the functioning of the whole reactor for a certain period of time without stopping or interrupting operations.

At the DPER stage, it is necessary to reach the level of "closing" the reactor power cycle ( $C_{\rm E} > 0$ ) and ensuring resource  $n > 10^4$ , i.e., the uninterrupted operation of such an experimental reactor for several hours (possibly even days).

The final stage is the development of a commercial reactor. Such a reactor could operate non-stop for several decades and would be economically viable compared to other sources of energy.

#### **ACKNOWLEDGMENTS**

The study was performed within the National Center for Physics and Mathematics, Gas Dynamics and Explosion Physics Program on the topic "Investigation of Physical Processes during Controlled Thermonuclear Fusion and in Stellar Systems."

#### **REFERENCES**

- 1. Basov N.G., Krokhin O.N. Conditions for heating up of a plasma by the radiation from an optical generator. *Sov. Phys. JETP.* 1964;19(1):123–126. Available from URL: http://www.jetp.ras.ru/cgi-bin/dn/e\_019\_01\_0123.pdf
- 2. Basov N.G., Lebo I.G., Rozanov V.B. Fizika lazernogo termoyadernogo sinteza (Physics of Laser Thermonuclear Fusion). Moscow: Znanie; 1988. 172 p. (in Russ.).
- 3. Atzeni S. Laser driven inertial fusion: The physical basis of current and recently proposed ignition experiments. *Plasma Phys. Control Fusion*. 2009;51(12):124029. https://doi.org/10.1088/0741-3335/51/12/124029
- Garanin S.G., Bel'kov S.A., Bondarenko C.V. The concept of building a laser installation UFL-2M. In: Doklady 39 Mezhdunarodnoi (Zvenigorodskoi) konferentsii po fizike plazmy i upravlyaemomu termoyadernomu sintezu (Proc. 39th Intern. (Zvenigorod) Conf. on Plasma Physics and Control. Thermonuclear Fusion). Zvenigorod; 2012. P. 17 (in Russ.).
- 5. Moses E.I. and NIC Collaboration. The National Ignition Campaign: status and progress. *Nucl. Fusion*. 2013;53(10):104020. https://doi.org/10.1088/0029-5515/53/10/104020

#### СПИСОК ЛИТЕРАТУРЫ

- 1. Басов Н.Г., Крохин О.Н. Условия разогрева плазмы излучением оптического генератора. *ЖЭТФ*. 1964;46(1):171–175.
- 2. Басов Н.Г., Лебо И.Г., Розанов В.Б. *Физика лазерного термоядерного синтеза*. М.: Знание: 1988. 176 с.
- 3. Atzeni S. Laser driven inertial fusion: The physical basis of current and recently proposed ignition experiments. *Plasma Phys. Control Fusion*. 2009;51(12):124029. https://doi.org/10.1088/0741-3335/51/12/124029
- 4. Гаранин С.Г., Бельков С.В., Бондаренко С.В. Концепция построения лазерной установки УФЛ-2М. В сб.: Доклады XXXIX Международной (Звенигородской) конференции по физике плазмы и управляемому термоядерному синтезу. Звенигород; 2012. С. 17.
- 5. Moses E.I. and NIC Collaboration. The National Ignition Campaign: status and progress. *Nucl. Fusion*. 2013;53(10):104020. https://doi.org/10.1088/0029-5515/53/10/104020
- Ebrardt J., Chapt J.M. LMJ on its way to fusion. *J. Phys: Conf. Ser:* 2010;244(3):032017. https://doi.org/10.1088/1742-6596/244/3/032017

<sup>&</sup>lt;sup>10</sup> Kritcher A. and HIBRYD-E ICF team. Initial results from HYBRID-E DT experiment N210808 with >1.3 MJ yield. *IFSA Virtual Meeting*. September 2021. LLNL-PRES-826367. P. 16. https://www.aps.org/units/maspg/meetings/upload/obenschain-11172021.pdf. Accessed February 07, 2023.

- Ebrardt J., Chapt J.M. LMJ on its way to fusion. *J. Phys: Conf. Ser:* 2010;244(3):032017. https://doi.org/10.1088/1742-6596/244/3/032017
- 7. Le P.S., Hopkins B.L.F., Divol L., et. al. Fusion energy output greater than the kinetic energy of an imploding shell at the National Ignition Facility. *Phys. Rev. Lett.* 2018;120(24):245003. https://doi.org/10.1103/PhysRevLett.120.245003
- Clery D. Laser-powered fusion effort near 'ignition'. Science. 2021;373(6557):841. https://doi.org/10.1126/ science.373.6557.841
- Clark D.S., Casey D.T., Weber C.R., et al. Exploring implosion designs for increased compression on the National Ignition Facility using high density carbon ablation. *Phys. Plasmas*. 2022;29(5):052710. https://doi. org/10.1063/5.0087052
- 10. He X.T., Zhang W.Y., and Chinese ICF Team. Advances in the national inertial fusion program in China. *EPJ Web of Conference*. 2013;59:001009. https://doi.org/10.1051/epjconf/20135901009
- 11. Zhen W., Wei X., Zhu Q., Jing F., et al. Laser performance of the SG-III laser facility. *High Power Laser. Sci. Eng.* 2016;4:e21. https://doi.org/10.1017/hpl.2016.20
- 12. Lebo I.G., Tishkin V.F. Issledovanie gidrodinamicheskoi neustoichivosti v zadachakh lazernogo termoyadernogo sinteza (Investigation of Hydrodynamic Instability in Problems of Laser Thermonuclear Synthesis). Moscow: Fizmatlit; 2006. 304 p. (in Russ.). ISBN 5-9221-0683-X
- 13. Kuzenov V.V., Lebo A.I., Lebo I.G., Ryzhkov S.V. Fiziko-matematicheskie modeli i metody rascheta vozdeistviya moshchnykh lazernykh i plazmennykh impul'sov na kondensirovannye i gazovye sredy (Physical-Mathematical Models and Numerical Methods of Simulation of High Power laser and Plasma Pulses Interaction with Condense and Gas Medias). Moscow: BMSTU; 2015. 327 p. (in Russ.). ISBN 978-5-7038-4183-9
- Samarskii A.A. Teoriya raznostnykh skhem (Difference Scheme Theory). Moscow: Nauka; 1990. 616 p. (in Russ.). ISBN 5-02-014576-9
- 15. Samarskii A.A., Popov Yu.P. Raznostnye metody resheniya zadach gazovoi dinamiki (Difference methods for solving problems of gas dynamics). Moscow: Nauka; 1992. 422 p. (in Russ.). ISBN 5-02-014577-7
- Zvorykin V.D., Lebo I.G. Laser and target experiments on KrF GARPUN laser installation at FIAN. *Laser Part. Beams*. 1999;17(1):69–88. https://doi.org/10.1017/ S0263034699171064
- Richmyer R.D. Taylor instability in shock acceleration of compressible fluids. *Commun. Pure Appl. Math.* 1960;13(2):297–319. https://doi.org/10.1002/cpa.3160130207
- 18. Meshkov E.E. The instability of two gases surface, which accelerated by shock wave. *Izvestiya AN SSSR. Ser. Mekhanika Zhidkosti i Gaza.* 1969;5:151–158 (in Russ.). Available from URL: https://mzg.ipmnet.ru/ru/get/1969/5/151-158
- Zvorykin V.D., Lebo I.G. Application of a high power KrF laser for the study of supersonic gas flows and the development of hydrodynamic instability in layered media. *Quantum Electron*. 2000;30(6):540–544. https:// doi.org/10.1070/QE2000v030n06ABEH001761

- Le P.S., Hopkins B.L.F., Divol L., et. al. Fusion energy output greater than the kinetic energy of an imploding shell at the National Ignition Facility. *Phys. Rev. Lett.* 2018;120(24):245003. https://doi.org/10.1103/ PhysRevLett.120.245003
- 8. Clery D. Laser-powered fusion effort near 'ignition'. *Science*. 2021;373(6557):841. https://doi.org/10.1126/science.373.6557.841
- Clark D.S., Casey D.T., Weber C.R., et al. Exploring implosion designs for increased compression on the National Ignition Facility using high density carbon ablation. *Phys. Plasmas*. 2022;29(5):052710. https://doi. org/10.1063/5.0087052
- He X.T., Zhang W.Y., and Chinese ICF Team. Advances in the national inertial fusion program in China. *EPJ Web* of Conference. 2013;59:001009. https://doi.org/10.1051/ epjconf/20135901009
- 11. Zhen W., Wei X., Zhu Q., Jing F., et al. Laser performance of the SG-III laser facility. *High Power Laser. Sci. Eng.* 2016;4:e21. https://doi.org/10.1017/hpl.2016.20
- 12. Лебо И.Г., Тишкин В.Ф. Исследование гидродинамической неустойчивости в задачах лазерного термоядерного синтеза. М.: Физматлит; 2006. 304 с. ISBN 5-9221-0683-X
- 13. Кузенов В.В., Лебо А.И., Лебо И.Г., Рыжков С.В. Физико-математические модели и методы расчета воздействия мощных лазерных и плазменных импульсов на конденсированные и газовые среды. М.: Изд-во МГТУ им. Н.Э. Баумана; 2015. 327 с. ISBN 978-5-7038-4183-9
- 14. Самарский А.А. *Теория разностных схем*. М.: Наука; 1990. 616 с. ISBN 5-02-014576-9
- 15. Самарский А.А., Попов Ю.П. *Разностные методы решения задач газовой динамики*. М.: Наука; 1992. 422 с. ISBN 5-02-014577-7
- Zvorykin V.D., Lebo I.G. Laser and target experiments on KrF GARPUN laser installation at FIAN. *Laser Part. Beams*. 1999;17(1):69–88. https://doi.org/10.1017/ S0263034699171064
- 17. Richmyer R.D. Taylor instability in shock acceleration of compressible fluids. *Commun. Pure Appl. Math.* 1960;13(2):297–319. https://doi.org/10.1002/cpa. 3160130207
- 18. Мешков Е.Е. Неустойчивость границы раздела двух газов, ускоряемой ударной волной. *Известия АН СССР. Сер. Механика жидкости и газа.* 1969;5:151–158. URL: https://mzg.ipmnet.ru/ru/get/1969/5/151-158
- 19. Зворыкин В.Д., Лебо И.Г. Применение мощного KrF-лазера для исследования сверхзвуковых течений газа и развития гидродинамических неустойчивостей в слоистых средах. Квантовая электроника. 2000;30(6):540–544.
- Lebo I.G., Zvorykin V.D. The study of turbulent mixing zone development in laser shock tube experiments. *Phys. Scr.* 2008;2008(T132):014018. https://doi.org/10.1088/0031-8949/2008/T132/014018
- 21. Беленький С.З., Фрадкин Е.С. Теория турбулентного перемешивания. *Труды ФИАН*. 1965;29:207–233.
- 22. Фрадкин Е.С. Исследование устойчивости произвольного одномерного гидродинамического течения. *Труды ФИАН*. 1965;29:250–256.

- [Original Russian Text: Zvorykin V.D., Lebo I.G. Application of a high power KrF laser for the study of supersonic gas flows and the development of hydrodynamic instability in layered media. *Kvantovaya Elektronika*. 2000;30(6):540–544 (in Russ.).]
- Lebo I.G., Zvorykin V.D. The study of turbulent mixing zone development in laser shock tube experiments. *Phys. Scr.* 2008;2008(T132):014018. https://doi. org/10.1088/0031-8949/2008/T132/014018
- 21. Belen'kii S.Z., Fradkin E.S. Theory of turbulent mixing. *Trudy FIAN = Proceedings of the Lebedev Physics Institute*. 1965;29:207–233 (in Russ.).
- 22. Fradkin E.S. The investigation of the arbitrary 1D hydrodynamic flow stability. *Trudy FIAN = Proceedings of the Lebedev Physics Institute*.1965;29:250–256 (in Russ.).
- Zvorykin V., Lebo I., Shutov A., Ustinovskii N. Self-focusing of UV radiation in 1 mm scale plasma in a deep ablative crater produced by 100 ns, 1 GW KrF laser pulse in the context of the ICF. *Matter Radiat. Extremes*. 2020;5(30):03540. https://doi.org/10.1063/1.5142361
- Craxton R.S., Anderson K.S., Boehly T.R., et al. Direct drive inertial confinement fusion: A review. *Phys. Plasmas*. 2015;22(1):110501. https://doi.org/10.1063/1.4934714
- 25. Craxton R.S., McCrory R.L. Hydrodynamics of thermal self-focusing in laser plasmas. *J. Appl. Phys.* 1984;56(1):108. https://doi.org/10.1063/1.333742
- 26. Lebo I.G. About the modeling of light beam self-focusing in plasma at the irradiation of the target by power UV laser. *Russ. Technol. J.* 2021;9(1):79–86 (in Russ.). https://doi.org/10.32362/2500-316X-2021-9-1-79-86
- 27. Akhmanov S.A., Sukhorukov A.P., Khohlov R.V. Self-focusing and diffraction of light in nonlinear medium. Sov. Phys. Usp. 1968;10(3):609–636. https://doi.org/10.1070/PU1968v010n05ABEH005849 [Original Russian Text: Akhmanov S.A., Sukhorukov A.P., Khohlov R.V. Self-focusing and diffraction of light in nonlinear medium. Uspekhi Fizicheskikh Nauk. 1967;93(1):19–70 (in Russ.). https://doi.org/10.3367/UFNr.0093.196709c.0019]
- Sodha M.S., Tripathi V.K. Nonlinear penetration of an inhomogeneous laser beam in an overdense plasma. *Phys. Rev. A.* 1977;16(5):2101–2104. https://doi.org/10.1103/PhysRevA.16.2101
- Basov N.G., Subbotin V.I., Feoktistov L.P. Nuclear reactor with laser fusion neutron source. Vestnik Rossiiskoi Akademii Nauk = Bulletin of the Russian Academy of Sciences. 1993;63(10):787–884 (in Russ.).
- Basov N.G., Belousov N.I., Grishunin P.A., et al. Hybrid reactor based on laser thermonuclear fusion. Sov. J. Quantum Electronics. 1987;17(10):1324–1332. https://doi.org/10.1070/QE1987v017n10ABEH010765
   [Original Russian Text: Basov N.G., Belousov N.I., Grishunin P.A., Kalmykov Yu.K., Lebo I.G., Rozanov V.B., Sklizkov G.V., Subbotin V.I., Finkel'shtein K.I., Kharitonov V.V., Sherstnev K.B. Hybrid reactor based on laser thermonuclear fusion. Kvantovaya Elektronika. 1987;14(10):2068–2081 (in Russ.).]
- 31. Zvorykin V.D., Lebo I.G., Rozanov V.B. On the feasibility of the production of a source of the thermonuclear neutrons on the basis of a KrF laser. *Bulletin of the Lebedev Physical Institute*. 1997;9:15–22.

- 23. Zvorykin V., Lebo I., Shutov A., Ustinovskii N. Self-focusing of UV radiation in 1 mm scale plasma in a deep ablative crater produced by 100 ns, 1 GW KrF laser pulse in the context of the ICF. *Matter Radiat. Extremes*. 2020;5(30):03540. https://doi.org/10.1063/1.5142361
- 24. Craxton R.S., Anderson K.S., Boehly T.R., et al. Direct drive inertial confinement fusion: A review. *Phys. Plasmas*. 2015;22(1):110501. https://doi.org/10.1063/1.4934714
- 25. Craxton R.S., McCrory R.L. Hydrodynamics of thermal self-focusing in laser plasmas. *J. Appl. Phys.* 1984;56(1):108. https://doi.org/10.1063/1.333742
- 26. Лебо И.Г. О моделировании самофокусировки светового пучка в плазме при облучении мишеней мощным ультрафиолетовым лазером. *Russ. Technol. J.* 2021;9(1): 79–86. https://doi.org/10.32362/2500-316X-2021-9-1-79-86
- 27. Ахманов С.А., Сухоруков А.П., Хохлов Р.В. Самофокусировка и дифракция света в нелинейной среде. *УФН*. 1967;93(1):19–70. https://doi.org/10.3367/UFNr.0093.196709c.0019
- Sodha M.S., Tripathi V.K. Nonlinear penetration of an inhomogeneous laser beam in an overdense plasma. *Phys. Rev. A.* 1977;16(5):2101–2104. https://doi.org/10.1103/PhysRevA.16.2101
- 29. Басов Н.Г., Субботин В.И., Феоктистов Л.П. Ядерный реактор с лазерным термоядерным источником нейтронов. *Вестник Российской академии наук*. 1993:63(10):787–884.
- 30. Басов Н.Г., Белоусов Н.И., Гришунин П.А., Калмыков Ю.К., Лебо И.Г., Розанов В.Б., Склизков Г.В., Субботин В.И., Финкельштейн К.И., Харитонов В.В., Шерстнев К.Б. Гибридный реактор на основе лазерного термоядерного синтеза. Квантовая электроника. 1987;14(10):2068–2081.
- 31. Зворыкин В.Д., Лебо И.Г., Розанов В.Б. О возможности создания источника термоядерных нейтронов на основе KrF-лазера. *Краткие сообщения по физике*. 1997;(9–10):20–29.
- 32. Лебо И.Г., Исаев Е.А., Лебо А.И. Двухсторонняя лазерная коническая мишень для нейтронного источника ядерно-термоядерного реактора. *Квантовая электроника*. 2017;47(2):106–110.
- Долголева Г.В., Лебо И.Г. К вопросу о разработке нейтронного источника для ядерно-термоядерного реактора с лазерным возбуждением. Квантовая электроника. 2019;49(8):796–800.
- 34. Долголева Г.В. Методы расчета движения двухтемпературного излучающего газа. Вопросы атомной науки и техники. Сер. Методики и программы численного решения задач математической физики. 1983;2(13):29–33.
- 35. Бельков С.А., Долголева Г.В. Модель среднего иона для расчета кинетики ионизации, населенностей возбужденных уровней и спектральных коэффициентов переноса излучения в программе СНДП. Вопросы атомной науки и техники. Сер. Методики и программы численного решения задач математической физики. 1992;1:59–61.
- 36. Долголева Г.В., Лебо А.И., Лебо И.Г. Моделирование сжатия термоядерных мишеней на уровне энергии лазера порядка 1 МДж. *Матем. моделирование*. 2016;28(1):23–32.

- [Original Russian Text: Zvorykin V.D., Lebo I.G., Rozanov V.B. On the feasibility of the production of a source of the thermonuclear neutrons on the basis of a KrF laser. *Kratkie Soobshcheniya po Fizike*. 1997;(9–10):20–29 (in Russ.).]
- 32. Lebo I.G., Isaev E.A., Lebo A.I. Two-sided conical laser target for a neutron source of a hybrid nuclear-thermonuclear reactor. *Quantum Electronics*. 2017;47(2):106–110. https://doi.org/10.1070/QEL16277 [Original Russian Text: Lebo I.G., Isaev E.A., Lebo A.I. Two-sided conical laser target for a neutron source of a hybrid nuclear-thermonuclear reactor. *Kvantovaya Elektronika*. 2017;47(2):106–110 (in Russ.).]
- 33. Dolgoleva G.V., Lebo I.G. On the issue of neutron source development for a nuclear-thermonuclear reactor. *Quantum Electronics*. 2019;49(8):796–800. https://doi.org/10.1070/QEL16953
  [Original Russian Text: Dolgoleva G.V., Lebo I.G. On the issue of neutron source development for a nuclear-thermonuclear reactor. *Kvantovaya Elektronika*. 2019;49(8):796–800 (in Russ.).]
- 34. Dolgoleva G.V. Methods of simulation of two temperature irradiated gas. *Voprosy Atomnoi Nauki i Tekhniki. Ser. Metodiki i Programmy Chislennogo Resheniya Zadach Matematicheskoi Fiziki.* 1983;2(13):29–33 (in Russ.).
- 35. Bel'kov S.A., Dolgoleva G.V. The model of average ion for the simulation of ionization kinetics, excited levels and spectral radiation transfer coefficients in SNDP program. *Voprosy Atomnoi Nauki i Tekhniki. Ser. Metodiki i Programmy Chislennogo Resheniya Zadach Matematicheskoi Fiziki.* 1992;1:59–61 (in Russ.).
- 36. Dolgoleva G.V., Lebo A.I., Lebo I.G. Simulation of a thermonuclear target drive at the 1 MJ laser energy level. *Math. Models Comput. Simul.* 2016;8(4):438–445. https://doi.org/10.1134/S2070048216040062
  [Original Russian Text: Dolgoleva G.V., Lebo A.I., Lebo I.G. Simulation of a thermonuclear target drive at the 1 MJ laser energy level. *Matematicheskoe Modelirovanie*. 2016;28(1):23–32 (in Russ.).]
- Krasyuk I.K., Semenov A.Yu., Charakhch'yan A.A. Use a conic targets in Inertial confinement fusion. *Quantum Electronics*. 2005;35(9):769–777. https://doi.org/10.1070/QE2005v035n09ABEH006128
   [Original Russian Text: Krasyuk I.K., Semenov A.Yu., Charakhch'yan A.A. Use a conic targets in Inertial confinement fusion. *Kvantovaya Elektronika*. 2005;35(9):769–777 (in Russ.).]
- Zvorykin V.D., Didenko N.V., Ionin A.A., et al. GARPUN-MTW: A hybrid Ti:Sapphire/KrF laser facility for simultaneous amplification of subpicosecond/nanosecond pulses relevant to fast-ignition ICF concept. *Laser Part. Beams*. 2007;25(3): 435–451. https://doi.org/10.1017/S0263034607000559
- Zvorykin V.D., Levchenko A.O., Ustinovskii N.N. Amplification of subpico second UV pulses in the multistage GARPUN-MTW Ti:sapphire–KrF-laser system. *Quantum Electronics*. 2010;40(5):381–385. https://doi.org/10.1070/QE2010v040n05ABEH014241 [Original Russian Text: Zvorykin V.D., Levchenko A.O., Ustinovskii N.N. Amplification of subpico second UV pulses in the multistage GARPUN-MTW Ti:sapphire–KrF-laser system. *Kvantovaya Elektronika*. 2010;40(5): 381–385 (in Russ.).]

- Красюк И.К., Семенов А.Ю., Чарахчьян А.А. Использование конических мишеней в исследованиях по инерциальному термоядерному синтезу. Квантовая электроника. 2005;35(9):769–777. URL: https://www. mathnet.ru/links/a64472a2c6918f95785286b47b113907/ qe6128.pdf
- Zvorykin V.D., Didenko N.V., Ionin A.A., et al. GARPUN-MTW:
   A hybrid Ti:Sapphire/KrF laser facility for simultaneous amplification of subpicosecond/nanosecond pulses relevant to fast-ignition ICF concept. *Laser Part. Beams.* 2007;25(3): 435–451. https://doi.org/10.1017/S0263034607000559
- 39. Зворыкин В.Д., Левченко А.О., Устиновский Н.Н. Усиление субпикосекундных УФ импульсов в многокаскадной лазерной Ті:сапфир–КrF-системе ГАРПУН-МТВ. Квантовая электроника. 2010;40(5):381–385.
- 40. Неуважаев В.Е. *Математическое моделирование турбу*лентного перемешивания. Снежинск: РФЯЦ-ВНИИТФ; 2007. 160 c. URL: https://math.csu.ru/new\_files/students/ lectures/ur mat fiz/neyvajaev mat model.pdf
- 41. Невмержицкий Н.В. Гидродинамические неустойчивости и турбулентное перемешивание веществ. Лабораторное моделирование. Саров: РФЯЦ-ВНИИЭФ; 2018. 245 с. ISBN 978-5-9515-0377-0
- 42. Янилкин Ю.В., Стаценко В.П., Козлов В.И. *Математическое моделирование турбулентного перемешивания в сжимаемых средах:* в 2-х т. Т. 1. Саров: РФЯЦ-ВНИИЭФ; 2019. 357 с. ISBN 978-5-9515-0421-0
- 43. Янилкин Ю.В., Стаценко В.П., Козлов В.И. *Математическое моделирование турбулентного перемешивания в сжимаемых средах:* в 2-х т. Т. 2. Саров: РФЯЦ-ВНИИЭФ; 2020. 407 с. ISBN 978-5-9515-0458-6
- 44. Разин А.Н. *Моделирование турбулентного перемешивания в газовых слойках*. Саров: РФЯЦ-ВНИИЭФ; 2020. 290 с. ISBN 978-5-9515-0434-0
- 45. Лебо И.Г., Обручев И.В. Моделирование двумерных вихревых течений в цилиндрическом канале с помощью параллельных вычислений на суперкомпьютере. *Russ. Technol. J.* 2022;10(1):60–67. https://doi.org/10.32362/2500-316X-2022-10-1-60-67
- Obenschain S., Lehmlerg R., Kehne D., et al. Highenergy krypton-fluoride laser for inertial fusion. *Appl. Opt.* 2015;54(31):F103–F122. http://dx.doi.org/10.1364/ AO.54.00F103
- 47. Sethian J., Obenschain S. Fusion energy with krypton fluoride lasers and direct drive targets. *Fusion Sci. Technol.* 2012;61(1T):41–46. https://doi.org/10.13182/FST12-A13394
- 48. Wolford M.F., Sethian J.D., Myers M.C., Hegeler F., Giuliani J.L., Obenschain S.P. Krypton fluoride (KrF) laser for inertial fusion energy. *Fusion Sci. Technol.* 2013;64(2):179–186. https://doi.org/10.13182/FST12-502
- 49. Bodner S.E. The path to electrical energy using laser fusion. *High Power Laser Science and Engineering*. 2019;7:e63. https://doi.org/10.1017/hpl.2019.51
- Schmitt A.J., Obenschain S.P. The importance of laser wavelength for driving inertial confinement fusion targets.
   Basic physics. *Phys. Plasmas*. 2023;30(1):012701. https://doi.org/10.1063/5.0118080
- Schmitt A.J., Obenschain S.P. The importance of laser wavelength for driving inertial confinement fusion targets.
   II. Target design. *Phys. Plasmas*. 2023;30(1):012702. https://doi.org/10.1063/5.0118093

- 40. Neuvazhaev V.E. *Matematicheskoe modelirovanie turbulentnogo peremeshivaniya* (*The mathematical modeling of turbulent mixing*). Snezhinsk; 2007. 160 p. (in Russ.). Available from URL: https://math.csu.ru/new\_files/students/lectures/ur mat fiz/neyvajaev mat model.pdf
- 41. Nevmerzhitskii N.V. Gidrodinamicheskie neustoichivosti i turbulentnoe peremeshivanie veshchestv. Laboratornoe modelirovanie (Hydrodynamic instability and turbulent mixing of matters. The laboratory modeling). Sarov; 2018. 245 p. (in Russ.). ISBN 978-5-9515-0377-0
- 42. Yanilkin Yu.V., Statsenko V.P., Kozlov V.I. Matematicheskoe modelirovanie turbulentnogo peremeshivaniya v szhimaemykh sredakh (The mathematical modeling of turbulent mixing in compressed matters): in 2 v. V. 1. Sarov; 2019. 357 p. (in Russ.). ISBN 978-5-9515-0421-0
- 43. Yanilkin Yu. V., Statsenko V.P., Kozlov V.I. Matematicheskoe modelirovanie turbulentnogo peremeshivaniya v szhimaemykh sredakh (The mathematical modeling of turbulent mixing in compressed matters): in 2 v. V. 2. Sarov; 2020. 407 p. (in Russ.). ISBN 978-5-9515-0458-6
- Razin A.N. Modelirovanie turbulentnogo peremeshivaniya v gazovykh sloikakh (The modeling of turbulent mixing in gas layers). Sarov; 2020. 290 p. (in Russ.). ISBN 978-5-9515-0434-0
- 45. Lebo I.G., Obruchev I.V. The modeling of two-dimensional vortex flows in a cylindrical channel using parallel calculation on a supercomputer. *Russ. Technol. J.* 2022;10(1):60–67 (in Russ.). https://doi.org/10.32362/2500-316X-2022-10-1-60-67
- Obenschain S., Lehmlerg R., Kehne D., et al. Highenergy krypton-fluoride laser for inertial fusion. *Appl. Opt.* 2015;54(31):F103–F122. http://dx.doi.org/10.1364/ AO.54.00F103
- 47. Sethian J., Obenschain S. Fusion energy with krypton fluoride lasers and direct drive targets. *Fusion Sci. Technol.* 2012;61(1T):41–46. https://doi.org/10.13182/FST12-A13394
- Wolford M.F., Sethian J.D., Myers M.C., Hegeler F., Giuliani J.L., Obenschain S.P. Krypton fluoride (KrF) laser for inertial fusion energy. *Fusion Sci. Technol*. 2013;64(2):179–186. https://doi.org/10.13182/FST12-502
- Bodner S.E. The path to electrical energy using laser fusion. *High Power Laser Science and Engineering*. 2019;7:e63. https://doi.org/10.1017/hpl.2019.51
- Schmitt A.J., Obenschain S.P. The importance of laser wavelength for driving inertial confinement fusion targets.
   I. Basic physics. *Phys. Plasmas*. 2023;30(1):012701. https://doi.org/10.1063/5.0118080
- Schmitt A.J., Obenschain S.P. The importance of laser wavelength for driving inertial confinement fusion targets.
   II. Target design. *Phys. Plasmas*. 2023;30(1):012702. https://doi.org/10.1063/5.0118093

#### **About the author**

**Ivan G. Lebo,** Dr. Sci. (Phys.-Math.), Professor, Department of Higher Mathematics, Institute of Artificial Intelligence, MIREA – Russian Technological University (78, Vernadskogo pr., Moscow, 119454 Russia). E-mail: lebo@mirea.ru. RSCI SPIN-code 9416-5542, https://orcid.org/0000-0001-8341-9453

#### Об авторе

**Лебо Иван Германович,** д.ф.-м.н., профессор, кафедра высшей математики Института искусственного интеллекта ФГБОУ ВО «МИРЭА – Российский технологический университет» (119454, Россия, Москва, пр-т Вернадского, д. 78). E-mail: lebo@mirea.ru. SPIN-код РИНЦ 9416-5542, https://orcid.org/0000-0001-8341-9453

Translated from Russian into English by Kirill V. Nazarov Edited for English language and spelling by Thomas A. Beavitt

#### Philosophical foundations of technology and society Мировоззренческие основы технологии и общества

UDC 378.147:372.881.1 https://doi.org/10.32362/2500-316X-2023-11-3-104-116



**REVIEW ARTICLE** 

# Technology for determining non-humanities university students' cognitive-and-psychological characteristics

## Nadezhda I. Chernova <sup>®</sup>, Ekaterina A. Ivanova, Nadezhda B. Bogush, Nataliya V. Katakhova

MIREA – Russian Technological University, Moscow, 119454 Russia <sup>®</sup> Corresponding author, e-mail: chernova@mirea.ru

#### **Abstract**

**Objectives.** The purpose of this work was to create a special entrance test for first-year students starting to learn a new foreign language. To achieve the research objective, the study analyzed data on testing language/linguistic proficiency and motivation for learning a foreign language. A range of test parameters identifying both abilities and motivation to learn a foreign language in general, but not related to learning a specific language, were highlighted. The identified parameters were used to inform a questionnaire tested on a group of students, whose level of abilities and motivation had already been ascertained. The findings about students were compared with the already known empirical data to support the improvement of test items.

**Methods.** To describe a special entrance test for first-year students starting to learn a new foreign language in a non-humanities higher education institution, a test technology for identifying certain cognitive, psychological, intellectual, motivational characteristics of a student's language personality was created. The developed test parameters served as the basis for constructing several heterogeneous test blocks.

**Results.** The initial version of the test obtained was verified by pilot testing first-semester-first-year students. Expert assessments of the foreign language potential learning on the part of students were used to evaluate the reliability and validity of the test. A subsequent correction of tasks and responses was carried out in light of the verification results.

**Conclusions.** A recommendation to conduct this kind of testing prior to the first semester with the aim of forecasting the success of foreign-language educational activities of students enrolled in the foreign language study group from the "starter" level is formulated. The results of such diagnostics can be used to draw up personified adaptive training programs within the educational process.

Keywords: testing, entrance test, learning a foreign language from scratch, language skills, abilities

• Submitted: 21.11.2022 • Revised: 09.12.2022 • Accepted: 09.03.2023

**For citation:** Chernova N.I., Ivanova E.A., Bogush N.B., Katakhova N.V. Technology for determining non-humanities university students' cognitive-and-psychological characteristics. *Russ. Technol. J.* 2023;11(3):104–116. https://doi.org/10.32362/2500-316X-2023-11-3-104-116

**Financial disclosure:** The authors have no a financial or property interest in any material or method mentioned.

The authors declare no conflicts of interest.

#### НАУЧНАЯ СТАТЬЯ

# Технология определения когнитивно-психологических особенностей студентов негуманитарного вуза

### Н.И. Чернова<sup>®</sup>, Е.А. Иванова, Н.Б. Богуш, Н.В. Катахова

МИРЭА – Российский технологический университет, Москва, 119454 Россия <sup>®</sup> Автор для переписки, e-mail: chernova@mirea.ru

#### Резюме

**Цель.** Цель исследования – разработка специального входного теста для студентов-первокурсников, начинающих изучать новый для них иностранный язык. Для достижения этой цели был проведен анализ научных работ по проблемам, касающимся тестирования языковых/лингвистических способностей, мотивации к обучению иностранному языку; очерчен круг параметров тестирования, не связанных с изучением конкретного языка, однако дифференцирующих способности и мотивацию к его изучению; составлен вопросник на основе выявленных параметров. Полученный тест апробирован в группе студентов, уровень способностей и мотивированности которых определен. По итогам результатов тестирования и уже известных эмпирических знаний о студентах скорректированы тестовые задания, верифицированные по уровню и направлению подготовки обучающихся.

**Методы.** Для описания специального входного теста для студентов-первокурсников, приступающих к изучению нового иностранного языка в негуманитарном вузе, создана тестовая технология выявления когнитивных, психологических, интеллектуальных, мотивационных характеристик языковой личности обучающихся, на основании которой разработаны параметры тестирования, созданы вариативные разноуровневые блоки вводного теста.

**Результаты.** В логике заявленного эксперимента проведена верификация исходного варианта теста, его апробация в группах студентов-первокурсников по окончании обучения в первом семестре. Оценивание их потенциала в изучении иностранных языков рассматривалось в качестве экспертной оценки для определения надежности и валидности теста. С учетом верификации проведена последующая коррекция как самих тестовых заданий, так и ответов на них.

**Выводы.** При прогнозировании успешности иноязычной учебной деятельности студентов, зачисленных в группы по изучению иностранного языка с нулевого уровня, считаем целесообразным и продуктивным проведение подобного рода тестирования перед началом первого семестра. По итогам предложенной диагностики весьма актуальной представляется разработка персонифицированных адаптивных программ иноязычной подготовки таких студентов в неязыковом вузе.

Ключевые слова: тестирование, входной тест, изучение иностранного языка с нуля, языковые способности

• Поступила: 21.11.2022 • Доработана: 09.12.2022 • Принята к опубликованию: 09.03.2023

**Для цитирования:** Chernova N.I., Ivanova E.A., Bogush N.B., Katakhova N.V. Technology for determining non-humanities university students' cognitive-and-psychological characteristics. *Russ. Technol. J.* 2023;11(3):104–116. https://doi.org/10.32362/2500-316X-2023-11-3-104-116

**Прозрачность финансовой деятельности:** Авторы не имеют финансовой заинтересованности в представленных материалах или методах.

Авторы заявляют об отсутствии конфликта интересов.

#### 1. INTRODUCTION

Traditional methods for foreign language teaching at non-humanities universities do not always produce the necessary results to support the future professional activity of students. One common problem faced by teachers is the need to establish a basic level of knowledge, skills and abilities of a number of students in order to bring them to the level required for their subsequent advancement through the curriculum, which greatly complicates the educational process of teaching a foreign language.

Currently, numerous studies aimed at developing innovative technologies in the field of foreign language training of students are being carried out. Adaptive, personalized technologies for teaching foreign languages are being introduced [1–3]. Since each applicant has a different initial knowledge base and background, opportunities for mastering educational material vary considerably. Therefore, there is a need to focus on a student's personal characteristics, helping him or her to build an individual trajectory for successful language acquisition [4, 5]. At the same time, this approach need not violate the boundaries of an integral system of educational standards, curricula, and learning objectives.

In order to determine the initial level of foreign language proficiency of those entering a university, some kind of entrance lingua-didactic testing is typically carried out to form language groups having the corresponding level of language preparation. Along with the various test forms (input, current, intermediate, final) to determine the level of students' knowledge, there is a considerable amount of published scientific literature on the issue [6–9].

For this reason, entrance testing becomes an important initial stage in the formation of a student's portfolio, forming the basis on which their further educational activities can be planned. In the pedagogical literature, however, the question of how entrance tests are used to determine the initial level of language training obtained in a secondary school is still under discussion [10–14].

The practice of teaching a foreign language at a technical university demonstrates that students entering a university with existing knowledge of one foreign language sometimes have to learn another foreign language from scratch. In this context, existing entry tests are not applicable. In order to implement an adaptive approach, it is necessary to divide the groups of students into subgroups in accordance with their potential for learning a foreign language. Thus, there is a need to develop a special test within the framework of adaptive technologies that cover the most important personal characteristics: psychological, cognitive and linguistic along with the level of motivation in language learning.

To date, a relatively small number of researchers are developing the issue from the above-described perspective. The following studies are closest to the matter under consideration [15–17]. Some researchers recommend that the testing of language abilities should be carried out in the process of foreign language activity, that is, if a student does not know the basics of foreign language acquisition, then the identification of his or her innate language abilities becomes problematic [18–20]. However, other researchers consider that linguistic understanding is formed prior to targeted language acquisition [21, 22], on which the existing psychological tests for identifying language abilities are based [23–30]. In this work, we use such described tests as a section of the questionnaire.

The purpose of the present study was to create a special entrance test for first-year students who are beginning to learn a new foreign language. To achieve the goal of the study, the following theoretical research methods were applied and the subsequent problems were solved:

- 1) analyze the scientific literature on the issues related to testing linguistic abilities and motivation to learn a foreign language;
- 2) outline a range of testing parameters, which are not related to the study of a particular language, but instead reveal the ability and motivation to study it;
- 3) design a questionnaire based on the identified parameters;
- 4) try out the obtained test on a group of students, whose level of abilities and motivation is already known, in order to compare test results with already known empirical (expert) knowledge about the students;
- 5) adjust test items if necessary.

In investigating the psychological, personal, psychophysiological characteristics of applicants, the present work considered the entrance testing of students prior to enrolling them in a group for studying a foreign language from scratch. The theoretical significance of this work is due to the lack of a single test relating to the lingua-didactic type for applicants' preliminary testing. The practical relevance of the work is determined by the need to obtain certain preliminary personalized data about students who begin to learn a foreign language from scratch.

#### 2. MATERIAL AND METHODS

The study was carried out within the scope of an adaptive approach, requiring the development of technologies for individualization of learning. The material for this comprised a special entrance test designed for diagnosing

<sup>&</sup>lt;sup>1</sup> As well as: Tarasova E. *Test na lingvisticheskuyu intuitsiyu* (*Linguistic intuition test*). https://subscribe.ru/group/obo-vsyomponemnogu/15246393/. Accessed January 31, 2022 (in Russ.).

the particular cognitive, psychological, linguistic and motivational characteristics of students setting out to learn a new foreign language at a non-linguistic university. As part of the experimental methodology, the test was tried out on the first-year students whose language abilities had already been assessed by teachers. The methodology included a comparison of the results of the entrance test with the expert assessments of students' knowledge and capabilities to serve as a basis for adjusting test tasks and interpreting answers to them.

#### 3. THEORETICAL BACKGROUND

### 3.1. Individual psychological characteristics and their diagnosis

In addition to tests examining the level of students' knowledge in terms of their foreign language competence, tests are used to determine the general level of language proficiency and speech activity, as well as to identify linguistic abilities [6, 8, 10, 21, 31, 32]. Within the framework of adaptive technologies, the development of tests aimed at identifying applicants' individual psychological characteristics, [33, 34] namely memory, attention, motivation, thought processes, and emotional states, are of great importance.

Many tests have been developed and designed to investigate human cognitive abilities related to language learning. However, a number of researchers point to various inadequacies in the available tests, which cannot be used to evaluate intellectual abilities in general, but only some intellectual skills and thinking features (in the epistemological sense [35]) formed at the time of testing.

Tests for "the success of the verbal functioning of an individual in the society" include the following questions:

- firstly, on general intelligence ("the ability to logical reasoning, planning, problem solving, abstract thinking, the ability to understand complex ideas, the speed of learning and the ability to benefit from the experience gained," linguistic, spatial abilities);
- secondly, on verbal abilities (definition of concepts, mental analysis and synthesis in verbal form, the establishment of verbal similarities and differences) [36, p. 127].

Also of interest in this connection are the Wexler scales to detect mental abilities, including verbal and nonverbal, which are used to define various features of memory, thinking, attention, and visual perception [33, 37].

The tests developed by John B. Carroll and Stanley Sapon aimed at identifying special cognitive abilities—mechanical associative memory (rote associational memory), the ability to recognize and derive rules (inductive ability), phonetic coding ability, and the perception of grammatical relations (grammatical sensitivity)—are also relevant [23, 24].

Tests for studying the motivational sphere of personality [38–40] have also been created. However, such tests, which are mainly designed for schoolchildren and job seekers, are underapplied to university students [41].

#### 3.2. Language abilities and their diagnostics

The issue of determining linguistic abilities and giftedness has been repeatedly raised in the psycholinguistic literature [18, 23, 36, 42–46]. However, while various indicators of the general giftedness of learners [20, 33, 47, etc.] and conditions for assessing linguistic abilities [19, 31, 48, 49] have been described in detail, a universal common approach is yet to be developed.

Linguistic ability/giftedness is also diagnosed by the following verbal-semantic methods: free associative experiment [50], associative-translation method<sup>2</sup> [20], the word semantics method [15, 16, 51], and the remote associates test<sup>3</sup> [52, 53].

Linguistic tasks for new interpreters [17] combine linguistic, mathematical and logical methods of language research in one task that allows a subject's understanding of the language structure and the laws of its functioning to be evaluated. This collection of tests determines linguistic abilities along with the ability to apply logical reasoning and linguistic thinking.

Paul Pimsleur's language aptitude battery [28] is aimed at identifying potentially underperforming students before they start learning foreign languages. Pimsleur highlights three factors that determine the success of mastering foreign languages: (1) the level of speech development, determined by using the "Vocabulary" test (individual lexicon in one's native language); (2) motivation and interest in learning a foreign language; (3) sound difference and quasi-signal-based communication.

L.A. Khokhlova's complex psychological and diagnostic approach to the study of students' language abilities is based on the hypothesis of M.M. Gohlerner and G.V. Eiger [21], showing that speech transformations, interverbal connections, and generalizations are formed faster and easier in the presence of linguistic talent [21, 54].

There is also a psychophysiological instrumental method for determining linguistic talent (using functional magnetic resonance imaging along with neurolinguistic programming), which has its own specifics [31, 54].

<sup>&</sup>lt;sup>2</sup> As well as: Romanovskaya N.V. Yazykovaya sposobnost' kak determinanta ponimaniya inoyazychnogo teksta (Language ability as a determinant of understanding a foreign language text). Abstract of thesis. Tver; 2004 (in Russ.).

<sup>&</sup>lt;sup>3</sup> Remote Associates Test (RAT) test as adapted by T.V. Galkina, L.G. Alekseeva, L.G. Khusnutdinova; for adults, by A.N. Voronin.

Thus, the tests available today are typically used to diagnose a person's characteristics from only one point of view, which means that they are homogeneous. As such, there is still no unified multi-component test for preliminary testing of applicants enrolling in a group for beginner learners of a foreign language. In their work when developing the test, the present authors have analyzed and taken into account achievements of domestic and foreign researchers who have studied various aspects of the linguistic personality.

#### 4. STUDY AND RESULTS

The development stages of the test considered in this paper correlate with the standard stages of any professional test compilation [55–57]:

- 1. **Determination of the testing goals,** i.e., diagnosing the linguistic potential of an applicant who enrolled in a group for learning a foreign language from scratch.
- 2. Selection of the educational material content. For this purpose, an analysis of the cognitive, psychological, motivational, some intellectual and individual characteristics of a student's personality, needed for the successful mastering a foreign language was carried out.
- 3. Compilation and assignment of test items. Test examination—the compiled test is heterogeneous; the developed tasks are assembled into several blocks referring to various aspects of the applicant's linguistic and intellectual abilities; an independent expertise is carried out by the teachers of the Foreign Languages Department of the RTU MIREA to evaluate the qualitative characteristics of the test items in accordance with certain parameters.
- 4. **Approbation of test tasks**, i.e., after the design of the developed test tasks, a single multi-component test was offered to first-year students.
- 5. Determination and calculation of quality indicators for the test items, which implies testological investigation of both individual test items and the test as a whole, statistical processing of approbation results, establishing quantitative values of the characteristics of the tasks proposed and the definition of a normal distribution.
- 6. Task rejection and preparation of the test— tasks that caused severe difficulties for the majority of subjects or, on the contrary, were successfully and quickly passed by all the test takers, were replaced by other ones or excluded from the test.
- 7. Second approbation and preparation of the final version of the test.

The content of the developed test corresponds to the scheme of any closed-type test and includes:

- 1) instruction for test takers, which includes information about the number of questions and time to complete the test, score per each answer, etc.;
- 2) test questions;
- 3) correct answers (at the teacher's disposal);
- 4) evaluation parameters.

When developing the test, the authors sought to comply with the necessary requirements for the test, such as:

- 1) validity;
- 2) sufficient reliability;
- 3) compactness.

When writing the test, attention was paid to the possibility of conducting it under certain conditions. An important component in the content of the test was a system for objective evaluation in scoring, as well as considering the test's rationality and complexity.

The developed test is aimed at identifying the psychological and cognitive characteristics of a student, on which basis a model is then created in the individual trajectory of each student learning the foreign language from scratch [58].

The questionnaire consists of several blocks affecting various aspects of the linguistic personality and general learning competence of students. The included questions are aimed at defining:

- 1) level of development of language abilities;
- 2) responsiveness to a given practical task;
- 3) ability to analyze, synthesize, generalize and compare, establish logical relationships, select elements from a whole;
- 4) individual memory features required for language learning;
- 5) level of student's motivation in language learning.

The amount of time to complete the test has also to be taken into account.

The first block contains tasks aimed at identifying the ability to work with linguistic signs and concepts, for example, decipher anagrams, find synonyms and antonyms for the given words, and fill in gaps in words, in texts, and proverbs. Despite the fact that the test questions relate to the Russian language, the correctness of the answers to them demonstrates general linguistic abilities.

#### Here are some examples.

*Fill in the missing words in the text:* 

For centuries, people have been sure that a magnet must be a metal. Even a quarter ... ago, hardly ... could assume that such ... can ... others ... They ... did not think about it—they do not exist in nature. Moreover, the idea to synthesize magnets ... be ... fantastic.

Ferromagnetic substances can ... into magnetically soft and magnetically hard ones, depending on how they ... or retain their magnetic properties.

A soft magnetic substance is the substance made of ferromagnetic material, which ... in that it loses its magnetic properties after magnetization and ... from the external magnetic field. Magnetically soft material requires pure iron and low carbon steel.

A hard magnetic substance is the substance ... of ferromagnetic material, which differs in that after ... it retains its magnetic properties for a long time after removal from the external magnetic field of the magnet. Hard magnetic materials are, for example, permanent magnets (Sm—samarium, Nd—neodymium).

Solve the anagrams and eliminate the extra word: ALETB ECGINLI RHCIA DRAWOBRE

The second block contains tasks that test the lexical potential of a particular student, including his ability to put the right word in a certain context. These tasks include identifying an extra concept, selecting suitable words, hyponyms, and hypernyms, defining concepts, and describing polysemantic words. For example, a task like this:

Replace the dots with a word that would mean the same as the words outside the brackets:

Kind of sport (...) a container

Find the word that is different in meaning from the rest:

Laurel

Triumph

Vertex

Fiasco

Choose synonyms or antonyms for the words: amorphous—reduced / defined / limited / hostile Which series has a negative value?

- 1) hell, angry, illegal, ex-president
- 2) importance, antimony, invisible, reduction
- 3) encourage, uncertain, inversion, indifferent
- 4) countertops, irrigation, unpaid, demilitarize

Generalize and restrict concepts, i.e., find a more general concept (hypernym) and a more specific one (hyponym) for each given concept:

Adverb (part of speech; syntax; adverb measures; speech; verb)

In the following tasks, analyze the concepts, i.e., identify essential and random features:

Human anatomy (academic subject, science, boring lesson, complex science, studies a person, part of natural science)

The word 'garden' is given and the words in parentheses (plants, gardener, dog, fence, land). From the words in brackets, you need to choose words that denote the main features (without which a given concept cannot exist).

Find pairs of concepts that are in causal relationships with each other:

Ice formation, north, frost, weather, snow

For each concept, select such concepts that are in a functional relationship with it:

Drawing  $- \dots$ ; lake  $- \dots$ ; bee  $- \dots$ ; number  $- \dots$ ; task  $- \dots$ .

The third block presents in our opinion the most characteristic tasks to a certain extent reflecting some intellectual abilities of a subject. This included tasks for establishing logical connections, determining common semantic and lexical and grammatical characteristics between words, identifying errors, establishing language patterns, etc.

After analyzing the chain of letters, you need to find the missing letter:

After analyzing the chain of letters, you need to insert the missing letter:

A	D	G
D	Н	L
Н	M	?

*Insert the missing word:* 

BOOKS (KIDS) DIG

SIEGE ( ... ) MAY

Which series consists of internationalism words?

- 1) revolution, sport, science, nation
- 2) electric, ferment, molecule, experiment
- 3) exhibition, atom, today, actor
- 4) insert, automobile, computer, word

Which of the following statements represents a point of view?

Life has a beginning and an end.

Cucumber is 90% water.

Artificial fibres worsen our lives.

The oceans cover two-thirds of the Earth's surface.

Which word does not refer to the other two?

think, see, hear

When developing questions regarding the definition of memory features, we relied on the methods available in psychological science.

In particular, simple introspective questions were asked, such as *Do you have a good memory? Do you memorize poems easily? After reading a one-page story, can you retell it in detail?* 

We used the method of preliminary diagnosing short-term memory by the known method of ten words, as well as memorizing sentences related and unrelated to each other for 15–30 s.

Long-term memory was diagnosed using the same 10 words and sentences, but written by the subjects after 40–60 min of testing on other tasks and without repeating them.

The fifth block of questions concerned the applicants' motivation in foreign language learning. This block included introspective questions such as: what is more important for you grades or knowledge?, Specific questions about the personal goal of language learning—I will need French: 1) for traveling and / or communicating with French-speaking friends;

2) in the future profession; 3) to be an educated person; 4) speak another language is just great; 5) I do not think I will need it, I have no choice, I have to study a foreign language at the university, otherwise I won't get a diploma; 6) Maybe I do not need French, but I just got tired of learning a foreign language that I had at school; 7) ... I may not need it, but I really like French; 8) I need a foreign language because I prefer to watch foreign films and read books in the original).

General questions were asked in a veiled form to affect the latent character traits, but relate to the motivational aspects of the subject's behaviour.

(In my behaviour at my future job, I need to follow the principles:

1) I need to move up the career ladder; 2) Work is a forced necessity in order to live; 3) The most important thing is gaining credibility and recognition; 4) It is necessary to strive to comfortable environment; 5) It is important to find something exciting at work; 6) One should constantly improve in his work).

The amount of time spent by a subject to complete the test is not a separate block, but is included in the study and evaluated using a scoring system. Here, it is hypothesized that the faster and more successfully a test is passed by the subject, the higher that subject's linguistic potential; the more time spent on passing the test when it was not very successful, the less the linguistic potential. There are cases of successful test completion by subjects who spent more time than was allocated. The explanations for such results can include natural slowness, search for information from extraneous sources due to an inability to do the test from memory, increased distraction and attention deficit.

While the listed factors do not contribute to the successful acquisition of a foreign language within the narrow framework of the curriculum at a technological university, they affect the number of points received.

There are examples of quick but unsuccessful completions of a test, which can be explained by a student's frivolous attitude to the matter at hand, which also does not contribute to the success of learning of a foreign language.

All five blocks of the test are combined into a single test presented to students. The amount of time spent on its execution is measured. Points are summed up. For a single entrance test, one can get up to 100 points: those who score 70–100 points go to the advanced subgroup of the experimental group, those who score 55–69 points go to the middle subgroup, and those who score less than 55 points join the third subgroup for weak students.

#### 5. DISCUSSION

The predictive test under consideration was constructed by teachers of English and French for the preliminary diagnosis of the psychological and

cognitive potential of students who had just entered RTU MIREA (Institute of Information Technologies, Institute of Artificial Intelligence, Institute for Advanced Technologies and Industrial Programming, Institute of Management Technologies, Institute of Radio Electronics and Informatics). This contingent of students was enrolled to study a foreign language from the starting level. At the time of admission to the university and the beginning of classes, teachers know neither the students' cognitive and psychological characteristics nor their linguistic abilities. For the successful language mastering, it is advisable to conduct preliminary diagnostic of a linguistic personality.

Prior to testing applicants, the final version of the developed test was tested on first-year students at the end of the first semester, when the level of their language potential becomes obvious.

The test was offered to 71 first-year students of RTU MIREA. 22 students received high scores, 32—average scores, while 17 were awarded low scores.

In order to process the results and determine the validity of the test for its further use among applicants, the differentiating power of test items was analyzed based on the correlation coefficient of each item with the final score obtained for the entire test. This coefficient, if it is more than 0.5, distinguishes between *advanced* and *lagging* students.

Having compared and analyzed the results of testing and the abilities of students demonstrated in foreign language classes, we can conclude that, in general, the diagnostic results were to be expected. However, there were some discrepancies—the number of students who studied well turned out to be slightly larger than the number of students who received higher test scores. This can be explained by the fact that applicants who studied the foreign language at the institute for two or three years had enrolled to study it from scratch. This contingent of students mastered the program faster and more successfully. This can be explained by the fact that students of non-linguistic universities are subject to different language proficiency requirements than those for students of language universities.

We would like to pay special attention to the block of the test concerning motivation. The test results showed that the motivation to learn a foreign language is often determined by pragmatic social factors: getting a higher education, obtaining good employment, etc. In such cases, a student's progress in learning activities at various stages of language learning will obviously be less successful.

Diagnostics of some intellectual abilities of RTU MIREA first-year students under testing shows that, in general, students have a normal and sometimes a reduced level of development of linguistic and general intelligence.

#### 6. CONCLUSIONS

The created diagnostic technology for studying the general intellectual, linguistic, and motivational components of a first-year student's linguistic personality is aimed at predicting the success of foreign language learning activities, developing and implementing personalized adaptive training programs and using them in the educational process based on diagnostic results.

Statistical calculations were carried out with respect to the normal distribution, standard deviation, variance, degree of difficulty and correctness of tasks and answers to them, as well as correlations and homogeneity within individual test blocks, considering the reliability and validity of each block. The initial version of the test was adjusted in accordance with the results of calculations. Thus, the results of the conducted research support the belief that the final version of the test, aimed at preliminary diagnosis of linguistic abilities and motivation of applicants, was sufficiently accurate to reflect the characteristics of the linguistic personality in order to adequately distribute the students by rank. This means that the obtained test results can be used to personify foreign language teaching from starter level at a non-linguistic university.

Alongside the actual practice of conducting classes in such groups, the test results demonstrate that the language learning process is greatly facilitated by the presence of at least minimal existing knowledge, skills and abilities on the part of a student studying a foreign language from scratch. On this basis, we believe that when forming student groups, it is advisable to determine both the subject's score for predictive testing and the presence of at least minimal knowledge, abilities and skills in a chosen foreign language. If an

applicant has certain knowledge, abilities and skills, but received an average score on the main test, he or she should, nevertheless, be taken in the strong student group. If a student receives a low score for testing, it is necessary to conduct diagnostics in the corresponding foreign language in order to determine the level of his knowledge, abilities, and skills. This fact is important, since it is known from teaching experience that the level of foreign language proficiency remains quite low even after ten years of learning a foreign language, never mind a period of two-three years of language learning in a secondary school.

The results of the pre-diagnostic testing in the framework of the adaptive learning technologies at the very initial stage of teaching a foreign language to non-linguistic students support certain conclusions on the organization of further language learning. Although the results cannot be claimed to comprise an absolute criterion of effectiveness in mastering the foreign language, carrying out such assessments of the psychological and cognitive characteristics of future students in terms of their personal potential and motivation to learn a language will certainly contribute to the improved quality of foreign language teaching at a technological university starting from the first semester.

#### **Authors' contributions**

- **N.I. Chernova**—justification for the study concept, research findings synthesis.
- **E.A. Ivanova**—analysis and synthesis of the literature, drafting the manuscript.
- **N.B. Bogush**—study of domestic and foreign publications on the issue, developing the experimental work algorithm.
- **N.V. Katakhova**—formulation of the conclusions, interpretation of the study results.

#### **REFERENCES**

- 1. Baeva I.V. Adaptive and integrative approach in foreign higher education. *Molodoi Uchenyi = Young Scientist*. 2020;13(303):207–210 (in Russ.). Available from URL: https://moluch.ru/archive/303/68412/ (accessed February 28, 2021).
- Vilkova K.A., Lebedev D.V. Adaptivnoe obuchenie v vysshem obrazovanii: za i protiv (Adaptive Learning in Higher Education: Pros and Ons). Moscow: National Research University Higher School of Economics, Institute of Education; 2020. 36 p. (Series: Modern Analytics of Education. 2020;7(37)7) (in Russ.).
- 3. Krechetov I.A., Romanenko V.V. Implementing the adaptive learning techniques. *Voprosy obrazovaniya = Educational Studies*. 2020;2:252–277 (in Russ.). https://doi.org/10.17323/1814-9545-2020-2-252-277

#### СПИСОК ЛИТЕРАТУРЫ

- 1. Баева И.В. Адаптивно-интегративный подход в высшем иноязычном образовании. *Молодой ученый*. 2020;13(303):207–210. URL: https://moluch.ru/ archive/303/68412/ (дата обращения 28.02.2022).
- 2. Вилкова К.А., Лебедев Д.В. Адаптивное обучение в высшем образовании: за и против. М.: Национальный исследовательский университет «Высшая школа экономики», Институт образования; 2020. 36 с. (Серия: Современная аналитика образования. 2020;7(37)7).
- 3. Кречетов И.А., Романенко В.В. Реализация методов адаптивного обучения. *Вопросы образования* = *Educational Studies*. 2020;2:252–277. https://doi.org/10.17323/1814-9545-2020-2-252-277

- 4. Kudzh S.A., Golovanova N.B. On improving training mechanisms teaching staff and prospects for targeted learning in the interests of universities. *Russ. Technol. J.* 2020;8(4):112–128 (in Russ.). https://doi.org/10.32362/2500-316X-2020-8-4-112-128
- 5. Savka O.G. Influence of the humanitarian environment on improving the quality of training of specialists in a technical university. *Russ. Technol. J.* 2021;9(5):95–101 (in Russ.). https://doi.org/10.32362/2500-316X-2021-9-5-95-101
- 6. Kokkota V.A. *Lingvodidakticheskoe testirovanie* (*Linguodidactic testing*). Moscow: Vysshaya shkola; 1989. 130 p. (in Russ.). ISBN 5-06-000219-5
- 7. Lerner I.Ya. Indicators of the system of educational and cognitive tasks. *Novye issledovaniya v pedagogicheskikh naukakh* = *New Research in Educational Sciences*. 1990;2(56):3–74 (in Russ.).
- 8. Ershova O.N. University linguo-didactic testing: Theoretical and methodological review. In: *Problemy upravleniyav sotsial 'no-gumanitarnykh, ekonomicheskikh i tekhnicheskikh sistemakh: materialy Vserossiiskoi (zaochnoi) nauchno-prakticheskoi konferentsii (Problems of Management in Social, Humanitarian, Economic and Technical Systems: Materials of the All-Russian (Correspondence) Scientific and Practical Conference).* In 2 v. Tver: TSTU; 2016. V. 2. P. 179–186 (in Russ.).
- 9. Rusinova E.A. Input control as a mechanism for managing pedagogical systems (based on the materials of the discipline "Foreign languages"). Vestnik Voronezhskogo gosudarstvennogo universiteta. Seriya: Problemy vysshego obrazovaniya = Bulletin of the Voronezh State University. Series: Problems of Higher Education. 2002;2:39–40 (in Russ.). Available from URL: https://rucont.ru/efd/518533 (accessed December 19, 2021),
- 10. Avanesov V.S. The problem of connection of learning and testing. *Narodnoe obrazovanie = National Education*. 2016;(7–8):32–140 (in Russ.).
- 11. Batunova I.V. Testing as one of the most effective methods of control in students training process among students of non-linguistic specialties. *Mezhdunarodnyi nauchno-issledovatel'skii zhurnal = International Research Journal*. 2017;05(59):8–10 (in Russ.). https://doi.org/10.23670/IRJ.2017.59.005
- Mineeva O.A., Klopova Yu.V., Oladyshkina A.A. Test control in English in the non-linguistic high school. *Gumanitarnye nauchnye issledovaniya = Humanities Scientific Research*. 2017;2 (in Russ.). Available from URL: https://human.snauka.ru/2017/02/20723 (accessed February 25, 2022).
- 13. Scrivener J. *Learning teaching*. Oxford: Macmillan; 2005. 418 p. ISBN 978-3190-125-760
- 14. Tatarnitseva S.N., Konoplyuk N.V. Entrance testing in English for students of non-linguistic specialties as a factor in improving the effectiveness of training. *Vektor* nauki Tol'yattinskogo gosudarstvennogo universiteta. Seriya: Pedagogika, psikhologiya = Science Vector of Togliatti State University. Series: Pedagogy, Psychology. 2017;2:53–58 (in Russ.). https://doi.org/10.18323/2221-5662-2017-2-53-58
- 15. Mandrikova G.M. Lexical lacunarity as an indicator of the level of development of the language personality of the applicant. *Filosofiya obrazovaniya = Philosophy of Education*. 2005;3:237–247 (in Russ.).

- 4. Кудж С.А., Голованова Н.Б. О совершенствовании механизмов подготовки научно-педагогических кадров и перспективы целевого обучения в интересах вузов. *Russ. Technol. J.* 2020;8(4):112–128. https://doi.org/10.32362/2500-316X-2020-8-4-112-128
- 5. Савка О.Г. Влияние гуманитарной среды на повышение качества подготовки специалистов в техническом вузе. *Russ. Technol. J.* 2021;9(5):95–101. https://doi.org/10.32362/2500-316X-2021-9-5-95-101
- Коккота В.А. Лингводидактическое тестирование.
   М.: Высшая школа; 1989. 130 с. ISBN 5-06-000219-5
- 7. Лернер И.Я. Показатели системы учебно-познавательных заданий. *Новые исследования в педагогических науках*. 1990;2(56):3–74.
- 8. Ершова О.Н. Лингводидактическое тестирование в вузе: теоретико-методологический обзор. Проблемы управления в социально-гуманитарных, экономических и технических системах: материалы Всероссийской (заочной) научно-практической конференции; под общ. ред. И.И. Павлова. В 2 ч. Тверь: ТГТУ; 2016. Ч. 2. С. 179–186.
- 9. Русинова Е.А. Входной контроль как механизм управления педагогическими системами (на материалах дисциплины «Иностранные языки»). Вестник Воронежского государственного университета. Серия: Проблемы высшего образования. 2002;2:39–40. URL: https://rucont.ru/efd/518533 (дата обращения 19.12.2021).
- 10. Аванесов В.С. Проблема соединения тестирования с обучением. *Народное образование*. 2016;(7–8): 132–140.
- 11. Батунова И.В. Тестирование как один из наиболее эффективных методов контроля при обучении студентов неязыковых специальностей иностранному языку. Международный научно-исследовательский журнал. 2017;05(59):8–10. https://doi.org/10.23670/IRJ.2017.59.005
- 12. Минеева О.А., Клопова Ю.В., Оладышкина А.А. Тестовый контроль по дисциплине «Английский язык» в неязыковом вузе. *Гуманитарные научные исследования*. 2017;2. URL: https://human.snauka.ru/2017/02/20723 (дата обращения 25.02.2022).
- 13. Scrivener J. *Learning teaching*. Oxford: Macmillan; 2005. 418 p. ISBN 978-3190-125-760
- 14. Татарницева С.Н., Коноплюк Н.В. Входное тестирование по английскому языку студентов неязыковых специальностей как фактор повышения эффективности обучения. Вектор науки Тольяттинского государственного университета. Серия: Педагогика, психология. 2017;2:53–58. https://doi.org/10.18323/2221-5662-2017-2-53-58
- 15. Мандрикова Г.М. Лексическая лакунарность как показатель уровня развития языковой личности абитуриента. *Философия образования*. 2005;3:237–241.
- 16. Лукашевич Е.В. Диагностика состояния семантического уровня языковой способности современного школьника. Естественная письменная русская речь: исследовательский и образовательный аспекты. Ч. 1. Проблемы письменной речи и развития языкового чувства: Материалы конференции. Барнаул: Алтайский университет, 2002. С. 27–36.

- 16. Lukashevich E.V. Diagnostics of the state of the semantic level of the language ability of a modern student. Estestvennaya pis 'mennaya russkaya rech': issledovatel'skii i obrazovatel'nyi aspekty. Ch. 1. Problemy pis 'mennoi rechi i razvitiya yazykovogo chuvstva: Materialy konferentsii (Natural Written Russian Speech: Research and Educational Aspects. Part 1. Problems of Written Speech and the Development of Language Sense: Materials of the conference). Barnaul: AltGU; 2002. P. 27–36 (in Russ.).
- 17. Shimanovskaya L.A. Lingvisticheskie zadachi dlya nachinayushchikh perevodchikov (Linguistic Tasks for Beginner Translators). Kazan: KGTU; 2005. 47 p. (in Russ.). Available from URL: https://rucont.ru/efd/292519 (accessed April 12, 2022).
- 18. Igna O.N. Approaches to the identification of linguistic talent and ability to foreign languages. *Vestnik Tomskogo gosudarstvennogo pedagogicheskogo universiteta (Vestnik TGPU) = Tomsk State Pedagogical University Bulletin (TSPU Bulletin)*. 2013;3(131):115–119 (in Russ.). Available from URL: https://vestnik.tspu.edu.ru/files/vestnik/PDF/articles/igna\_o\_n.\_115\_119\_3\_131\_2013. pdf (accessed April 12, 2022).
- 19. Shcherbatykh L.N. Theoretical and applied aspects of the identifying linguistically gifted pupils. *Nauka i shkola* = *Science and School*. 2013;4:36–39 (in Russ.).
- Yakovchenko E.V. Experimental study of the language ability formation (based on metaphor). In: Aktual'nye problemy issledovaniya yazyka: teoriya, metodika, praktika obucheniya: Mezhvuzovskii sbornik nauchnykh trudov. Kursk: Kursk State University; 2003. P. 60–61 (in Russ.).
- 21. Gohlerner M.M., Eiger G.V. The psychological mechanism of the language sense. *Voprosy Psikhologii*. 1983;4:137–142 (in Russ.).
- 22. Teplov B.M. Ability and talent. Vestnik moskovskogo universiteta. Seriya 20: Pedagogicheskoe obrazovanie = Bulletin of Moscow University. Ser. 20: Pedagogical Education. 2014;4:99–105 (in Russ.).
- 23. Carroll J.B. Psychometric approaches to the study of language abilities. In: Fillmore C.J., Kempler D., Wang W.S.-Y. (Eds.). *Individual Differences in Language Ability and Language Behavior*. New York, San-Francisco, London: Academic Press; 1979. P. 13–32. https://doi.org/10.1016/B978-0-12-255950-1.50008-1
- 24. Carroll J.B., Sapon S.M. *The modern language aptitude test (MLAT)*. San Antonio, TX: Psychological Corporation; 1959. 27 p.
- 25. Cattell R.B., Eber H.W., Tatsuoka M.M. *Handbook of the Sixteen Personality Factor Questionnaire* (*16 PF*). Champaign: Institute for Personality and Ability Testing; 1970. 388 p.
- 26. Eysenck H.J. *Prover'te svoi sposobnosti (Test your IQ)*. St. Petersburg: Lan', Soyuz; 1996. 158 p. (in Russ.).
- Patitina V.N. Diagnostics of abilities to foreign languages. Vestnik Vostochno-Sibirskoi Otkrytoi Akademii.
   2013;7:12–16 (in Russ.). Available from URL: http://vsoa.esrae.ru/pdf/2013/7/723.pdf (accessed February 25, 2022).
- 28. Pimsleur P.A. Language aptitude testing. In: Davies A. (Ed.). Language Testing Symposium: A Psycholinguistic Approach. London: Oxford University Press; 1968. P. 98–106.
- 29. Siewert H. *Vash koeffitsient intellekta. Testy.* (*Your IQ. Tests*): transl. from Germ. Moscow: Interekspert; 1997. 138 p. (in Russ.).

- 17. Шимановская Л. А. *Лингвистические задачи для начинающих переводчиков*. Казань: КГТУ4; 2005. 47 с. URL: https://rucont.ru/efd/292519 (дата обращения 12.04.2022).
- 18. Игна О.Н. Подходы к выявлению лингвистической одаренности и способностей к иностранным языкам. Вестник Томского государственного педагогического университета (TSPU Bulletin). 2013;3(131): 115–119. URL: https://vestnik.tspu.edu.ru/files/vestnik/PDF/articles/igna\_o.\_n.\_115\_119\_3\_131\_2013.pdf (дата обращения 12.04.2022).
- 19. Щербатых Л.Н. Теоретические и прикладные аспекты выявления лингвистически одаренных школьников. *Наука и школа*. 2013;4:36–39.
- 20. Яковченко Е.В. Экспериментальное исследование формирования языковой способности (на материале метафоры). Актуальные проблемы исследования языка: теория, методика, практика обучения: Межвузовский сборник научных трудов. Курск: Изд-во Курск. гос. ун-та; 2003. С. 60–61.
- 21. Гохлернер М.М., Ейгер Г.В. Психологический механизм чувства языка. *Вопросы психологии*. 1983;4: 137–142.
- 22. Теплов Б.М. Способности и одаренность. Вестник московского университета. Серия 20: Педагогическое образование. 2014;4:99–105.
- 23. Carroll J.B. Psychometric approaches to the study of language abilities. In: Fillmore C.J., Kempler D., Wang W.S.-Y. (Eds.). *Individual Differences in Language Ability and Language Behavior*. New York, San-Francisco, London: Academic Press; 1979. P. 13–32. https://doi.org/10.1016/B978-0-12-255950-1.50008-1
- 24. Carroll J.B., Sapon S.M. *The modern language aptitude test (MLAT)*. San Antonio, TX: Psychological Corporation; 1959. 27 p.
- Cattell R.B., Eber H.W., Tatsuoka M.M. Handbook of the Sixteen Personality Factor Questionnaire (16 PF). Champaign: Institute for Personality and Ability Testing; 1970. 388 p.
- 26. Айзенк Г.Ю. *Проверьте свои способности*: пер. с англ. СПб.: Лань, Союз; 1996. 158 с.
- 27. Патитина В.Н. Диагностика способностей к иностранным языкам. *Вестник Восточно-Сибирской открытой академии*. 2013;7:12–16. URL: http://vsoa.esrae.ru/pdf/2013/7/723.pdf (дата обращения 12.04.2022).
- Pimsleur P.A. Language aptitude testing. In: Davies A. (Ed.). Language Testing Symposium: A Psycholinguistic Approach. London: Oxford University Press; 1968. P. 98–106.
- 29. Зиверт Х. Ваш коэффициент интеллекта. Тесты: пер. с нем. М.: АО Интерэксперт; 1997. 138 с.
- 30. Туник Е.Е. Тест интеллекта Амтхауэра. Анализ и интерпретация данных. СПб.: Речь; 2009. 96 с.
- 31. Кабардов М.К. Языковые способности: психология, психофизиология, педагогика. М.: Смысл; 2013. 400 с.
- 32. Kormos J. New conceptualizations of language aptitude in second language attainment. In: Granena G., Long M. (Eds.). *Sensitive periods, language aptitude, and ultimate L2 attainment.* Amsterdam, Philadelphia: John Benjamins; 2013. P. 131–152. https://doi.org/10.1075/lllt.35.05kor

- 30. Tunik E.E. *Test intellekta Amtkhauera. Analiz i interpretatsiya dannykh (Amthauer's intelligence test. data analysis and interpretation)*. St. Petersburg: Rech'; 2009. 96 p. (in Russ.).
- 31. Kabardov M.K. *Yazykovye sposobnosti: psikhologiya, psikhofiziologiya, pedagogika (Language Abilities: Psychology, Psychophysiology, Pedagogy).* Moscow: Smysl; 2013. 400 p. (in Russ.).
- 32. Kormos J. New conceptualizations of language aptitude in second language attainment. In: Granena G., Long M. (Eds.). *Sensitive periods, language aptitude, and ultimate L2 attainment*. Amsterdam, Philadelphia: John Benjamins; 2013. P. 131–152. https://doi.org/10.1075/lllt.35.05kor
- 33. Chan E., Skehan P., Gong G. Working memory, phonemic coding ability and foreign language aptitude: Potential for construction of specific language aptitude tests the case of Cantonese. *A Journal of English Language, Literature in English and Cultural Studies*. 2011;1(60):45–73. https://doi.org/10.5007/2175-8026.2011n60p045
- 34. Khokhlova L.A., Deryagina L.E. Influence of individual psychological peculiarities in successful languages mastering. *Rossiiskii mediko-biologicheskii vestnik imeni akademika I.P. Pavlova = I.P. Pavlov Russian Medical Biological Herald.* 2010;18(1):124–130 (in Russ.).
- 35. Molchanov K.V. The dialectic study of the English language in the light of the work "Science of logic" by Hegel: New Dialectic Cognition, Dialectical Programming, and the Processes of Thinking. *Russ. Technol. J.* 2019;7(2):74–82 (in Russ.). https://doi.org/10.32362/2500-316X-2019-7-2-74-82
- 36. Voronin A.N., Kochkina O.M. Discursive and linguistic abilities in the structure of human intelligence. *Psikhologiya. Zhurnal Vysshei shkoly ekonomiki = Psychology. Journal of the Higher School of Economics.* 2008;5(2):124–132 (in Russ.).
- 37. Vladimirova S.G. David Wechsler's scale: Present and future in solving the problem of intelligence measurement. *Yaroslavskii pedagogicheskii vestnik* = *Yaroslavl Pedagogical Bulletin*. 2016;2:122–126 (in Russ.). Available from URL: http://vestnik.yspu.org/releases/2016\_2/24.pdf (accessed February 25, 2022).
- 38. Milman V.E. Method for studying the motivational sphere of personality. In: *Praktikum po psikhodiagnostike*. *Psikhodiagnostika motivatsii i samoregulyatsii (Workshop on Psychodiagnostics. Psychodiagnostics of Motivation and Self-regulation)*. Moscow: MSU; 1990. P. 23–43 (in Russ.).
- Pakulina S.A., Ketko S.M. Diagnostics method of learning motivation in pedagogical university students. Psikhologicheskaya nauka i obrazovanie = Psychological Science and Education. 2010;2(1) (in Russ.). Available from URL: https://psyjournals.ru/journals/psyedu/archive/2010\_n1/psyedu\_2010\_n1\_26655.pdf (accessed February 25, 2022).
- 40. Rukhlova T.S. Some ways to determine the level of motivation of teenagers to learn a foreign language. Psikhologiya i pedagogika: metodika i problemy prakticheskogo primeneniya = Psychology and Pedagogy: Methods and Problems of Practical Application. 2012;28:315–317 (in Russ.).
- 41. Emel'yanova N.A. Motivatsiya ovladeniya inostrannym yazykom: struktura i formirovanie (Motivation for mastering a foreign language: structure and formation). Nizhnii Novgorod: HSE; 2013. 145 p. (in Russ.).

- 33. Chan E., Skehan P., Gong G. Working memory, phonemic coding ability and foreign language aptitude: Potential for construction of specific language aptitude tests the case of Cantonese. *A Journal of English Language, Literature in English and Cultural Studies*. 2011;1(60):45–73. https://doi.org/10.5007/2175-8026.2011n60p045
- Хохлова Л.А., Дерягина Л.Е. Влияние индивидуально-психологических особенностей на успешность в овладении иностранными языками. Российский медико-биологический вестник имени академика И.П. Павлова. 2010;18(1):124–130.
- Молчанов К.В. Диалектическое изучение английского языка в свете труда «Наука логики» Гегеля: новодиалектическое познание, диалектическое программирование и процессы мышления. Russ. Technol. J. 2019;7(2):74–82. https://doi.org/10.32362/2500-316X-2019-7-2-74-82
- 36. Воронин А.Н., Кочкина О.М. Дискурсивные и лингвистические способности в структуре интеллекта человека. *Психология*. *Журнал Высшей школы экономики*. 2008;5(2):124–132.
- 37. Владимирова С.Г. Шкала Давида Векслера: настоящее и будущее в решении проблемы измерения интеллекта. *Ярославский педагогический вестник*. 2016;2: 122–126. URL: http://vestnik.yspu.org/releases/2016\_2/24. pdf (дата обращения 25.02.2022).
- 38. Мильман В.Э. Метод изучения мотивационной сферы личности. *Практикум по психодиагностике*. *Психодиагностика мотивации и саморегуляции*. М.: МГУ; 1990. С. 23–43.
- 39. Пакулина С.А., Кетько С.М. Методика диагностики мотивации учения студентов педагогического вуза. *Психологическая наука и образование*. 2010;2(1). URL: https://psyjournals.ru/journals/psyedu/archive/2010\_n1/psyedu\_2010\_n1\_26655.pdf (дата обращения 25.02.2022).
- 40. Рухлова Т.С. Некоторые способы определения уровня мотивации подростков к изучению иностранного языка. Психология и педагогика: методика и проблемы практического применения. 2012;28:315–317.
- 41. Емельянова Н.А. *Мотивация овладения иностранным языком: структура и формирование: монография*. Нижний Новгород: Издательский дом Высшей школы экономики; 2013. 145 с.
- 42. Ансимова О.К. Языковая способность: теоретические основы изучения. В кн.: *Наука и образование: современные тренды: коллективная монография*. Чебоксары: ЦНС «Интерактив плюс»; 2015. С. 7–29. URL: https://interactive-plus.ru/e-articles/124/Action124-11081.pdf (дата обращения 19.12.2021).
- 43. Гаврилова Е.В. Лингвистические способности и их когнитивные детерминанты: современные перспективы исследований. *Современная зарубежная психология*. 2015;4(4):30–38. https://doi.org/10.17759/jmfp.2015040405
- 44. Хохлова Л.А. Психолого-диагностический подход к исследованию языковых способностей. Современные исследования социальных проблем. 2012;1(09): 790–799. URL: https://cyberleninka.ru/article/n/psihologodiagnosticheskiy-podhod-k-issledovaniyu-yazykovyhsposobnostey (дата обращения 25.02.2023).

- 42. Ansimova O.K. Language ability: the theoretical foundations of learning. Science and education: modern trends. In: *Nauka i obrazovanie: sovremennye trendy: kollektivnaya monografiya*. Cheboksary: Interactive Plus; 2015. P. 7–29 (in Russ.). Available from URL: https://interactive-plus.ru/e-articles/124/Action124-11081.pdf (accessed December 19, 2021).
- 43. Gavrilova E.V. Linguistic abilities and its cognitive determinants: contemporary research perspectives. *Sovremennaya zarubezhnaya psikhologiya = J. Modern Foreign Psychology*. 2015;4(4):30–38 (in Russ.). https://doi.org/10.17759/jmfp.2015040405
- 44. Khokhlova L.A. Psychological approach to the investigation of foreign language abilities. Sovremennye issledovaniya sotsial'nykh problem = Modern Research of Social Problems. 2012;1(09):790–799 (in Russ.). Available from URL: https://cyberleninka.ru/article/n/psihologo-diagnosticheskiy-podhod-k-issledovaniyu-yazykovyh-sposobnostey (accessed February 25, 2022).
- 45. Ushakova T.N. Duality of human language ability nature. *Psikhologicheskii zhurnal = Psychological Journal*. 2004;25(2):5–16 (in Russ.).
- 46. Voronova N.G. Language ability in the context of psychology of abilities. *Vestnik Bashkirskogo universiteta* = *Bulletin of Bashkir University.* 2014;19(4):1407–1412 (in Russ.). Available from URL: http://bulletin-bsu.com/arch/files/2014/4/54\_4670\_Voronova\_1407-1412.pdf (accessed February 25, 2022).
- 47. Matyushkin A.M. Creative giftedness concept. *Voprosy Psihologii*. 1989;6:29–33 (in Russ.). Available from URL: http://www.voppsy.ru/issues/1989/896/896029.htm (accessed February 25, 2022).
- 48. Khovanskaya E.A. Study of the language ability: Psycho-pedagogical and methodological aspects. *Vestnik Kemerovskogo gosudarstvennogo universiteta = Bulletin of Kemerovo State University*. 2014;(3–1):184–188 (in Russ.).
- 49. Kudinova I.M. Conceptual provisions and a model of linguistic gift assessment. *Chelovecheskii capital = Human Capital*. 2020;3(135):149–155 (in Russ.).
- 50. Lukashevich E.V. Teoriya yazykovogo razvitiya v kognitivno-diskursivnoi paradigme (Theory of Language Development in the Cognitive-Discursive Paradigm). Barnaul: Altai State University; 2006. 39 p. (in Russ.).
- 51. Lukashevich E.V. Language ability of the student in aspect of cognitive and communicative activity. In: Russkii yazyk i kul'tura rechi kak distsiplina gosudarstvennykh obrazovatel'nykh standartov vysshego professional'nogo obrazovaniya: opyt, problemy, perspektivy (Russian language and culture of speech as a discipline of state educational standards of higher professional education: Experience, problems, prospects). Barnaul: Altai State University; 2003. P. 105–117 (in Russ.).
- 52. Mednick S.A. The remote associates test. *Journal of creative behavior*. 1968;2(3):213–214. https://doi.org/10.1002/j.2162-6057.1968.tb00104.x
- 53. Bowden E.M., Jung-Beeman M. Normative data for 144 compound remote associate problems. *Behavior Research Methods, Instrumentation, and Computer.* 2003;35(4): 634–639. https://doi.org/10.3758/BF03195543

- 45. Ушакова Т.Н. Двойственность природы речеязыковой способности человека. *Психологический журнал*. 2004;25(2):5–16.
- 46. Воронова Н.Г. Языковая способность в контексте психологии способностей. Вестини Башкирского университета. 2014;19(4):1407–1412. URL: http://bulletin-bsu.com/arch/files/2014/4/54\_4670\_Voronova 1407-1412.pdf (дата обращения 25.02.2022).
- 47. Матюшкин А.М. Концепция творческой одаренности. *Вопросы психологии*. 1989;6:29–33. URL: http://www.voppsy.ru/issues/1989/896/896029.htm (дата обращения 25.02.2022).
- 48. Хованская Е.А. Исследование языковой способности: психолого-педагогический и методические аспекты. Вестник Кемеровского государственного университета. 2014;(3–1):184–188.
- 49. Кудинова И.М. Концептуальные положения и модель оценки лингвистической одаренности. *Человеческий капитал.* 2020;3(135):149–155.
- 50. Лукашевич Е.В. *Теория языкового развития в когнитивно-дискурсивной парадигме*. Барнаул: Издательство Алт. гос. университета; 2006. 39 с.
- 51. Лукашевич Е.В. Языковая способность студента в аспекте когнитивной и коммуникативной деятельности. Русский язык и культура речи как дисциплина государственных образовательных стандартов высшего профессионального образования: опыт, проблемы, перспективы. Барнаул: Издательство Алт. гос. университета; 2003. Р. 105—117.
- 52. Mednick S.A. The remote associates test. *Journal of Creative Behavior*: 1968;2(3):213–214. https://doi.org/10.1002/j.2162-6057.1968.tb00104.x
- Bowden E.M., Jung-Beeman M. Normative data for 144 compound remote associate problems. *Behavior Research Methods, Instrumentation, and Computer.* 2003;35(4): 634–639. https://doi.org/10.3758/BF03195543
- 54. Хохлова Л.А. *Психофизиологические связи в структу-* ре иноязычно-речевых способностей. СПб.: Изд-во 7 СТУДИЯ РИК; 2014. 255 с.
- 55. Челышкова М.Б. *Теория и практика конструирования педагогических тестов*. М.: Логос; 2002. 432 с.
- 56. Майоров А.Н. *Теория и практика создания тестов* для системы образования. М.: Интеллект-Центр; 2002. 352 с.
- 57. McNamara T. *Language testing*. Oxford: Oxford University Press; 2000. 140 p.
- Martin F., Markant D. Adaptive learning modules. In: David M.E., Amey M.J. (Eds.). *The SAGE Encyclopedia of Higher Education*. London: Sage; 2020. P. 2–4. http://dx.doi.org/10.4135/9781529714395.n31

- 54. Khokhlova L.A. *Psikhofiziologicheskie svyazi v* strukture inoyazychno-rechevykh sposobnostei (*Psychophysiological connections in the structure of foreign language and speech abilities*). St.-Petersburg: 7 STUDIYa RIK; 2014. 255 p. (in Russ.).
- 55. Chelyshkova M.B. *Teoriya i praktika konstruirovaniya pedagogicheskikh testov (Theory and practice of designing pedagogical tests)*. Moscow: Logos; 2002. 432 p. (in Russ.).
- 56. Maiorov A.N. Teoriya i praktika sozdaniya testov dlya sistemy obrazovaniya (Theory and practice of creating tests for the education system). Moscow: Intellekt-Tsentr; 2002. 352 p. (in Russ.).
- 57. McNamara T. *Language testing*. Oxford: Oxford University Press; 2000. 140 p.
- 58. Martin F., Markant D. Adaptive learning modules. In: David M.E., Amey M.J. (Eds.). *The SAGE Encyclopedia of Higher Education*. London: Sage; 2020. P. 2–4. http://doi.org/10.4135/9781529714395.n31

#### **About the authors**

**Nadezhda I. Chernova,** Dr. Sci. (Pedagog.), Professor, Head of Foreign Languages Department, Institute of Radio Electronics and Informatics, MIREA – Russian Technological University (78, Vernadskogo pr., Moscow, 119454 Russia). E-mail: chernova@mirea.ru. Scopus Author ID 57194042371, RSCI SPIN-code 7391-4040, https://orcid.org/0000-0002-5685-9733

**Ekaterina A. Ivanova,** Cand. Sci. (Philolog.), Assistant Professor, Foreign Languages Department, Institute of Radio Electronics and Informatics, MIREA – Russian Technological University (78, Vernadskogo pr., Moscow, 119454 Russia). E-mail: ivanova@mirea.ru. Scopus ID 57216646627, RSCI SPIN-code 8980-5591, https://orcid.org/0000-0001-6891-4966

**Nadezhda B. Bogush,** Cand. Sci. (Philolog.), Assistant Professor, Foreign Languages Department, Institute of Radio Electronics and Informatics, MIREA – Russian Technological University (78, Vernadskogo pr., Moscow, 119454 Russia). E-mail: bogouchn@mirea.ru. RSCI SPIN-code 9258-6672, https://orcid.org/0000-0003-0332-1136

**Nataliya V. Katakhova**, Cand. Sci. (Pedagog.), Associate Professor, Foreign Languages Department, Institute of Radio Electronics and Informatics, MIREA – Russian Technological University (78, Vernadskogo pr., Moscow, 119454 Russia). E-mail: katakhova@mirea.ru. Scopus Author ID 57204175929, RSCI SPIN-code 2552-5380, https://orcid.org/0000-0002-9416-5011

#### Об авторах

**Чернова Надежда Ивановна,** д.пед.н., профессор, заведующий кафедрой иностранных языков Института радиоэлектроники и информатики ФГБОУ ВО «МИРЭА – Российский технологический университет» (119454, Россия, Москва, пр-т Вернадского, д. 78). E-mail: chernova@mirea.ru. Scopus Author ID 57194042371, SPIN-код РИНЦ 7391-4040, https://orcid.org/0000-0002-5685-9733

**Иванова Екатерина Александровна,** к.филол.н, доцент, кафедра иностранных языков Института радиоэлектроники и информатики ФГБОУ ВО «МИРЭА – Российский технологический университет» (119454, Россия, Москва, пр-т Вернадского, д. 78). E-mail: ivanova@mirea.ru. Scopus ID 57216646627, SPIN-код РИНЦ 8980-5591, https://orcid.org/0000-0001-6891-4966

**Богуш Надежда Борисовна,** к.филол.н, доцент, кафедра иностранных языков Института радиоэлектроники и информатики ФГБОУ ВО «МИРЭА – Российский технологический университет» (119454, Россия, Москва, пр-т Вернадского, д. 78). E-mail: bogouchn@mirea.ru. SPIN-код РИНЦ 9258-6672, https:// orcid.org/0000-0003-0332-1136

**Катахова Наталия Владимировна,** к.пед.н., доцент, кафедра иностранных языков Института радиоэлектроники и информатики ФГБОУ ВО «МИРЭА – Российский технологический университет» (119454, Россия, Москва, пр-т Вернадского, д. 78). E-mail: E-mail: katakhova@mirea.ru. Scopus Author ID 57204175929, SPIN-код РИНЦ 2552-5380, https://orcid.org/0000-0002-9416-5011

The text was submitted by the authors in English Edited for English language and spelling by Thomas A. Beavitt

MIREA – Russian Technological University.
78, Vernadskogo pr., Moscow, 119454 Russian
Federation.
Publication date May 31, 2023.
Not for sale.

МИРЭА – Российский технологический университет.

119454, РФ, г. Москва, пр-т Вернадского, д. 78.

Дата опубликования 31.05.2023 г.

Не для продажи.

